Planar Topological Defects in Unconventional Superconductors

by

Michelle Przedborski

BSc (Honours Physics) Department of Physics,
Brock University, Canada

A THESIS SUBMITTED IN PARTIAL FULFILMENT OF
THE REQUIREMENTS FOR THE DEGREE OF
MASTER OF SCIENCE

in

The Faculty of Mathematics and Science
Department of Physics

BROCK UNIVERSITY
September 11, 2013
2013 © Michelle Przedborski

Abstract

In this work, we consider the properties of planar topological defects in unconventional superconductors. Specifically, we calculate microscopically the interaction energy of domain walls separating degenerate ground states in a chiral p-wave fermionic superfluid. The interaction is mediated by the quasiparticles experiencing Andreev scattering at the domain walls. As a by-product, we derive a useful general expression for the free energy of an arbitrary nonuniform texture of the order parameter in terms of the quasiparticle scattering matrix.

The thesis is structured as follows. We begin with a historical review of the theories of superconductivity (Sec. 1.1), which led the way to the celebrated Bardeen-Cooper-Schrieffer (BCS) theory (Sec. 1.3). Then we proceed to the treatment of superconductors with so-called "unconventional pairing" in Sec. 1.4, and in Sec. 1.5 we introduce the specific case of chiral p-wave superconductivity. After introducing in Sec. 2 the domain wall (DW) model that will be considered throughout the work, we derive the Bogoliubov-de Gennes (BdG) equations in Sec. 3.1, which determine the quasiparticle excitation spectrum for a nonuniform superconductor. In this work, we use the semiclassical (Andreev) approximation, and solve the Andreev equations (which are a particular case of the BdG equations) in Sec. 4 to determine the quasiparticle spectrum for both the single- and two-DW textures. The Andreev equations are derived in Sec. 3.2, and the formal properties of the Andreev scattering coefficients are discussed in the following subsection. In Sec. 5, we use the transfer matrix method to relate the interaction energy of the DWs to the scattering matrix of the Bogoliubov quasiparticles. This facilitates the derivation of an analytical expression for the interaction energy between the two DWs in Sec. 5.3. Finally, to illustrate the general applicability our method, we apply it in Sec. 6 to the interaction between phase solitons in a two-band s-wave superconductor.

Acknowledgements

I take great pride in presenting this thesis in partial fulfillment of my MSc degree requirements in Theoretical Physics. I am unquantifiably grateful for all of the help and support I have received from my family, my supervisory committee, and my peers over the course of my studies. I would specifically like to thank my supervisor, Dr. Samokhin, for his patience and inspirational instruction over the past two years, as well as the other members of my supervisory committee, Dr. Mitrović and Dr. Reedyk, for their continued guidance and support. I would also like to extend my gratitude to the Physics Department at Brock University for giving me the opportunity to conduct a research project in such a stimulating and gratifying field.

I have grown not only as a student and a researcher during my time at the Physics Department, but also as a mentor and a person. I am tremendously excited to be continuing my studies at this department to pursue a PhD in Theoretical Physics as a Vanier Scholar. I cannot express how thankful I am to those involved in the scholarship application process, who took the time to write the reference letters which strengthened my successful application (Dr. Samokhin, Dr. Mitrović, Jill Brindle, Elizabeth Ilnicki-Stone).

This section would not be complete if I did not give individual thanks to my mother, Sandra Lane. She has been my inspiration and driving force over the course of my academic career, and for all of her support, I am truly grateful. It is pleasing to know that she is so proud of my accomplishments, and so I would like to dedicate this newest accomplishment, my thesis, to her. Thank you for being such a stable role model in my life. I can only hope that I am capable of providing the same support through this difficult time, and that one day we will look back with marvel at the strength we amassed to carry forward.

When life throws one challenges, they must rise up, and uncover strengths untold. One cannot prosper in life without determination, and one cannot be determined without belief. While life may present obstacles, one can choose to have the faith to push on.

Contents

1 Introduction 1

1.1 A tour through the history . . . 1

1.2 Cooper pairs . . . 16

1.3 The BCS theory . . . 24

1.4 Unconventional pairing . . . 41

1.5 Chiral p-wave superconductivity . . . 46

2 The model 53

3 Derivation of the BdG and Andreev equations 56

3.1 Derivation of BdG equations . . . 56

3.2 Semiclassical (Andreev) approximation . . . 76

3.2.1 Formal properties of the Andreev scattering states . . . 78

4 Quasiparticle properties of DWs 83

4.1 Quasiparticle spectrum for a single DW . . . 83

4.1.1 ABS energies for a DW . . . 83

4.1.2 Andreev scattering states for a DW . . . 84

4.2 Quasiparticle spectrum for two DWs . . . 86

4.2.1 Scattering matrix for the two DWs . . . 86

4.2.2 Reflection and transmission coefficients from direct Andreev calculation . . . 90

4.2.3 Bound state spectrum from the scattering matrix . . . 92

4.2.4 Bound states from the direct Andreev solution . . . 93

5 Interaction between DWs 98

5.1 Relating the determinants . . . 101

5.2 Calculation of the Fredholm determinant . . . 113

5.3 Interaction energy . . . 115

6 Phase solitons in two-band superconductors 117

6.1 Quasiparticle spectrum in the two-soliton texture . . . 119

6.1.1 Scattering states for the two-soliton texture . . . 120

6.2 Interaction between solitons . . . 122

6.2.1 Interaction energy . . . 123

7 Conclusions 126

7.1 Future work 126

A Ginzburg-Landau description of a domain wall 128

B Ginzburg-Landau description of a phase soliton 131

List of Figures

1 The resistance as a function of temperature for a normal metal and a superconductor. Reproduced from Ref. [4]. 2

2 The Meissner effect in a superconducting material, reproduced from Ref. [5]. Above T_c, a SC behaves like a normal metal, while below T_c, it expels the magnetic field from its interior, as in the image on the right. In contrast, a normal metal preserves the initial flux at all temperatures. . . 2

3 Phase diagram of a type-I superconductor. Reproduced from Ref. [6]. . . 4

4 Phase diagram of a type-II SC [6], illustrating the lower and upper critical fields. 4

5 Abrikosov vortices in the mixed state, retrieved from Ref. [8]. The magnetic field (red) penetrates the normal cores, and the circulating supercurrent (yellow) screens the bulk of the sample. The screening currents from different vortices interact with each other and this leads to forces between the vortices, as illustrated by the black arrows. 5

6 The tetragonal crystal structure of $\mathrm{Sr_2RuO_4}$ compared to that of LBCO. Image reproduced from Ref. [31]. 50

7 The electron pairing state in superconducting $\mathrm{Sr_2RuO_4}$. The large arrow denotes the direction of $\hat{\boldsymbol{\ell}}$, and the small arrows the spins of the electrons in a pair. The spins lie in the xy plane, and all $\hat{\boldsymbol{\ell}}$ lie along the z-axis. Image reproduced from Ref. [31]. 50

8 Isotropic excitation energy gap on a cylindrical Fermi surface [31]. 51

9 Alternating chirality states in the two-DW model. 54

10 The relative phase between the order parameter components for two sharp DWs separated by distance L. 55

11 The ABS energy for a sharp DW as a function of the direction of the quasiparticle propagation θ, for selected values of the phase difference across the DW: $\chi = \pi$ (top), $\chi = \pi/4$ (middle), and $\chi = 0$ (bottom). 85

12 Bound state energy for the sharp two-DW model with $\chi = \pi$, for varying dimensionless DW separation $\tilde{L} = L/\xi$. From the top: $\tilde{L} = 5$, 1, 0.5. . . . 94

13 The order parameter phase in the ath band for two sharp solitons with a fixed separation L. 119

Abbreviations

1) SC- superconductor
2) DW- domain wall
3) NMR- nuclear magnetic resonance
4) MRI- magnetic resonance imaging
5) BCS- Bardeen-Cooper-Schrieffer
6) GL- Ginzburg-Landau
7) BdG- Bogoliubov-de Gennes
8) IREP- irreducible representation
9) ABM- Anderson-Brinkman-Morel
10) TRS- time reversal symmetry
11) SQUID- superconducting quantum interference device
12) MF- mean field
13) ABS- Andreev bound state

1 Introduction

In this section, we provide the reader with a brief introduction into the important aspects of superconductivity. We investigate the basic experimental behaviour of superconducting materials; as well as a give an overview of the proposed theories that led the way to our current understanding, the shortcomings of these theories, and the challenges faced at the time by the physicists who pioneered the field. This section is not a complete overview of the field of superconductivity, and should be taken solely as an introduction to the concepts therein.

1.1 A tour through the history

Superconductors (SCs) were first discovered by Dutch physicist H. Kamerlingh Onnes in 1911 [1], and amazingly about a dozen Nobel Prizes in physics have been awarded in this field alone since. These materials currently have many useful physical applications, and in particular, they are vital in the function of nuclear magnetic resonance (NMR) spectrometers, magnetic resonance imaging (MRI), and particle accelerators. They also have wonderful potential applications, which include high-speed magnetic levitating trains, as well as possibly reducing the world's electrical power consumption. Since they are electrically more efficient than the current materials in use, if SCs could cost-effectively be implemented into the world's electrical power grid, power could potentially be sent long distances without the large losses due to heat dissipation, helping to sustain the world's increasing power needs.

Superconductors are a class of materials in which quantum mechanics manifests itself in spectacular electric and magnetic properties on the macroscopic scale. In contrast to normal metals, which have a finite electrical resistance even at zero temperature, Kamerlingh Onnes discovered that superconductors behave like metals at high temperatures, but exhibit the onset of zero electrical resistivity below a certain critical temperature, T_c, as illustrated in Fig. 1. Experimentally, typical values of the resistivity of materials in the superconducting state are $\rho < 10^{-23}$ Ohm·cm [2], which is orders of magnitude smaller than the resistivity in normal metals.

SCs also exhibit perfect diamagnetism through a phenomenon known as the Meissner effect, discovered in 1933 by Meissner and Ochsenfeld [3]. A normal metal preserves the initial magnetic flux when an external field is held constant and the temperature is lowered (Fig. 2). In contrast, once the transition temperature is reached in a superconductor, the magnetic field is completely expelled from the bulk of the material via the formation of dissipationless screening currents. Since the magnetic induction $\boldsymbol{B} = 0$ in

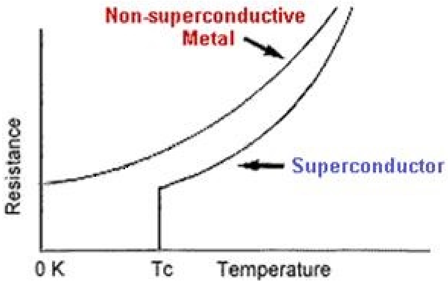

Figure 1: The resistance as a function of temperature for a normal metal and a superconductor. Reproduced from Ref. [4].

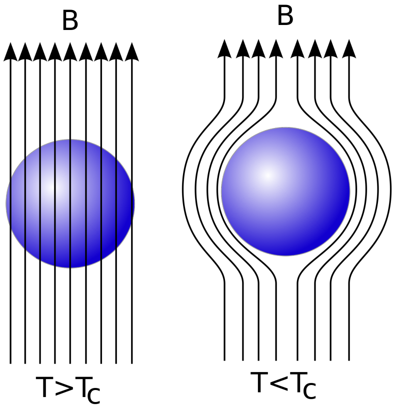

Figure 2: The Meissner effect in a superconducting material, reproduced from Ref. [5]. Above T_c, a SC behaves like a normal metal, while below T_c, it expels the magnetic field from its interior, as in the image on the right. In contrast, a normal metal preserves the initial flux at all temperatures.

the interior of the SC, it follows from the Maxwell equation that the supercurrent is also zero in the bulk of the sample, and thus the screening currents only flow near the surface.

A superconductor is not just an ideal conductor, and this becomes clear by considering in detail the magnetic response of an ideal conductor. Since the resistivity $\rho = 0$, it follows from Ohm's law, $\boldsymbol{j} = (1/\rho)\boldsymbol{E}$, that $\boldsymbol{E} = 0$. From the Maxwell equation, one has $\partial\boldsymbol{B}/\partial t = 0 \rightarrow \boldsymbol{B}(t) = \boldsymbol{B}(0)$, and consequently, if one fixes the temperature while altering the external magnetic field, an ideal conductor will preserve the initial flux. In a material which is in the superconducting state, the magnetic induction is zero in the interior of the SC, regardless of the initial flux.

The experiments also show that there is a maximum external magnetic field, known as the critical field H_c, beyond which superconductivity is destroyed. This idea can be understood by considering the following argument: according to the microscopic theory of superconductivity proposed by Bardeen, Cooper, and Schrieffer (BCS theory), which is described below, superconductivity is associated with the effective formation of pairs of electrons, known as Cooper pairs. The screening supercurrent is generated by these Cooper pairs, which create an opposing field to cancel the interior flux. There is a maximum supercurrent which can be sustained because there is a maximum velocity at which the Cooper pairs can remain correlated. We see that the maximum velocity is therefore connected to the maximum strength of the Meissner screening field that is created. Beyond this velocity, the pairs “break up”, and thus there is a maximum external field at which superconductivity can be maintained.

There is a compelling energy reason why materials should enter the superconducting state, i.e. it is the thermodynamically advantageous state of the system. To formally illustrate this, one introduces the condensation energy $E_{cond}(T)$, which is the energy gained per unit volume when the system enters the superconducting state. In terms of the free energies (per unit volume) of the normal and superconducting states, the condensation energy is given by:

$$E_{cond}(T) = f_n(T, \boldsymbol{H} = 0) - f_s(T, \boldsymbol{H} = 0),$$

and we expect this quantity to be greater than zero for $T < T_c$. One can relate the condensation energy to the critical field H_c at which the superconductivity is destroyed, since, by definition, this is the field at which the normal and superconducting free energy densities are equal: $f_n(T, H_c) = f_s(T, H_c)$. Therefore the condensation energy takes the following form:

$$E_{cond} = \frac{H_c^2(T)}{8\pi}. \tag{1.1}$$

We see that one can directly probe the energy gain at the transition into the superconducting state simply by measuring the critical field.

Depending on the details of the response to an applied magnetic field, superconductors fall into two distinct categories. Type-I SCs are materials which exhibit the complete Meissner effect, as explained above, as well as a first order transition into the superconducting state at nonzero magnetic field. The phase diagram of a type-I SC is given in Fig. 3. The latent heat in this first order transition is related to the condensation energy, and since $H_c = 0$ at $T = T_c$, it follows that $E_{cond} = 0$, and the phase transition becomes second order (or continuous) at the critical temperature. The materials that were primarily studied in the 1920’s and 1930’s, such as Hg, Pb, and Sn, are type-I SCs. It turns out, however, that these materials are rather an exception to the world of superconductivity,

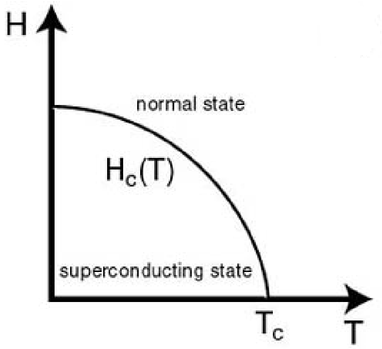

Figure 3: Phase diagram of a type-I superconductor. Reproduced from Ref. [6].

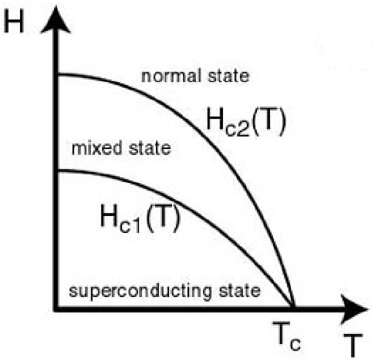

Figure 4: Phase diagram of a type-II SC [6], illustrating the lower and upper critical fields.

and that this type of response is observed mostly in “clean” elemental metals (excluding Nb). The vast majority of SCs, including all superconducting alloys, exhibit a type-II response below T_c.

The phase diagram of a typical type-II SC is presented in Fig. 4. Unlike in the type-I case, there are two transition lines, which separate three distinct phases of the material. The upper critical field H_{c2} separates the normal state from an unusual superconducting state called the mixed, or Abrikosov, state; the lower critical field H_{c1} separates the mixed state from the Meissner state, where the complete Meissner effect is observed. There is no latent heat associated with the transition from either the normal state to the mixed state, or from the mixed state to the complete Meissner state, i.e. both transitions are continuous in both zero and nonzero magnetic field.

In the mixed state, the incomplete Meissner effect is observed, and thus $\boldsymbol{B} \neq 0$ in the interior of the SC. In fact, the magnetic field penetrates the bulk of the sample by forming a periodic array of normal cores (Abrikosov vortices [7]), which is typically in a

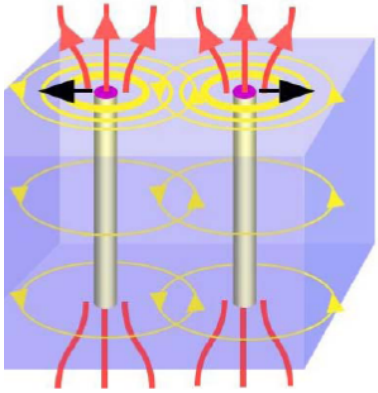

Figure 5: Abrikosov vortices in the mixed state, retrieved from Ref. [8]. The magnetic field (red) penetrates the normal cores, and the circulating supercurrent (yellow) screens the bulk of the sample. The screening currents from different vortices interact with each other and this leads to forces between the vortices, as illustrated by the black arrows.

hexagonal pattern. The superconductivity is destroyed at the cores, which are surrounded by a dissipationless circulating current that screens the magnetic field, as illustrated in Fig. 5. This results in a magnetic induction which is maximum near the core and decays exponentially away from it.

Abrikosov developed the theoretical idea of this mixed state in the early 1950's, well before the microscopic BCS theory was developed. He published his work in 1957, around the same time the BCS theory emerged, and after his work was experimentally confirmed, he was awarded the Nobel Prize in physics in 2003.

Before introducing the BCS theory, we give an overview of some other concepts that helped lead to our current understanding of the field of superconductivity. It is useful for the reader to keep in mind that in the late 1930's physicists didn't know anything about Cooper pairs and could not fathom the microscopic nature of superconductivity. Over the years, various models were proposed to explain the mechanisms behind this phenomenon, but it wasn't until the BCS theory arrived in 1957 that we had a truly microscopic theory which explained the physical properties of SCs.

The London model [9], proposed in 1935 by F. and H. London, was purely phenomenological (i.e. it was designed to explain experiments without microscopically justifying all of the concepts or parameters in the theory). The basic assumption in this theory is that there are two types of charge carriers in a superconductor, in contrast to the electron quasiparticles in a normal metal. In a superconductor, it was assumed that "normal" electrons are responsible for the dissipative normal current, which is proportional to the electric field according to Ohm's law: $\boldsymbol{j}_n = en_n\boldsymbol{v}_n = \sigma\boldsymbol{E}$. Here e is the electron charge, $\boldsymbol{v}_n$ is the velocity of normal electrons, $\sigma = 1/\rho$ is the conductivity, $\boldsymbol{E}$ is the electric field, and n_n is the density of the normal electrons.

In contrast, the "superconducting" electrons were assumed to respond to the external magnetic field and create persistent screening currents given by the expression $\boldsymbol{j}_s = en_s\boldsymbol{v}_s$, where n_s is the number density and $\boldsymbol{v}_s$ is the velocity of the superconducting electrons. The total density of electrons is then given by $n = n_n + n_s$. It is important to note that in this theory, n_s is a phenomenological parameter that cannot be derived from first principles. It is possible for both n_n and n_s to be non-uniform, and it is assumed that $n_s = 0$ in the normal state. On the contrary, in the absence of an electric field, it follows that the total contribution to the current is the supercurrent $\boldsymbol{j}_s$.

The key assumption in the London theory is that the contribution to the free energy associated with the motion of the superconducting electrons can be written in the following way:

$$E_{current} = \frac{1}{2}\int d^3\boldsymbol{r}\, n_s m\boldsymbol{v}_s^2,$$

where m is the electron mass, and n_s and $\boldsymbol{v}_s$ were introduced above. Physically, $E_{current}$ takes place against the background of the Fermi distribution, i.e. it is the "extra" energy that comes from the motion of the superconducting electrons as a whole. Using the London expression for the supercurrent above, we have the following formula for the kinetic energy associated with the supercurrent:

$$E_{current} = \frac{1}{2}\frac{m}{e^2 n_s}\int d^3\boldsymbol{r}\, \boldsymbol{j}_s^2.$$

By invoking the Maxwell equation $\boldsymbol{\nabla}\times\boldsymbol{B} = (4\pi/c)\boldsymbol{j}_s$, and after variational minimization of the total free energy with respect to the magnetic induction, one arrives at the London equation:

$$\boldsymbol{\nabla}^2\boldsymbol{B} = \frac{1}{\lambda_L^2}\boldsymbol{B}. \tag{1.2}$$

In this last expression, the magnetic induction satisfies the boundary condition $\boldsymbol{B} = \boldsymbol{H}$ far away from the superconductor, and $\lambda_L = (mc^2/4\pi e^2 n_s)^{1/2}$ is the London penetration depth. In the normal state, $n_s = 0$ and thus $\lambda_L = \infty$, or $\boldsymbol{B} = \boldsymbol{H}$ everywhere, as expected.

By appropriately manipulating the London equation, one can relate the supercurrent to the vector potential $\boldsymbol{A}$, where $\boldsymbol{B} = \boldsymbol{\nabla}\times\boldsymbol{A}$, as follows:

$$\boldsymbol{j}_s(\boldsymbol{r}) = -\frac{e^2 n_s}{mc}\boldsymbol{A}(\boldsymbol{r}). \tag{1.3}$$

This linear dependence on the vector potential is different from what we see in a normal metal, where $\boldsymbol{j} = \sigma \boldsymbol{E} = -(\sigma/c)\partial \boldsymbol{A}/\partial t$. This is one of the defining features of superconductivity.

We consider the solution to the London equation (1.2) for the simplest geometry, which is a planar normal-superconducting interface (taken to be in the yz-plane, i.e. perpendicular to the x-axis), in the presence of an external magnetic field parallel to the interface, i.e. $\boldsymbol{H} = H\hat{z}$. It follows from Eq. (1.2), along with the boundary condition $\boldsymbol{B}(x) = \boldsymbol{H}$ far from the SC, that $B(x) = He^{-x/\lambda_L}$ in the superconducting material. Furthermore, it follows from the Maxwell equation that the supercurrent $\boldsymbol{j}_s$ has the same exponential dependence as the magnetic induction, and thus the magnetic response of the SC is limited to a region of thickness λ_L. In other words, $B(x)$ falls to $1/e$ of its original value at the depth λ_L into the sample. In the more general case, a quick inspection of the London equation reveals that the latter lends itself to some sort of exponentially-dependent solution, which is indeed consistent with the Meissner effect. The magnetic field falls off exponentially into the sample, characterized by the magnetic penetration depth, λ_L. It follows that the screening current also falls off exponentially and thus the current only flows near the surface. Consequently, the magnetic induction is zero in the bulk of the superconductor as expected.

While the London theory does reproduce the Meissner effect, one of the shortcomings of this theory is that the value of n_s remains undefined (though a natural upper limit is n, the total density of conduction electrons). Alleviating this problem requires a full microscopic theory. This ambiguity becomes particularly important when comparing calculations with measurements of the penetration depths in superconducting materials. Experimentally, the temperature dependence of the penetration depth is given by

$$\lambda(T) \simeq \lambda(0)[1 - (T/T_c)^4]^{-1/2}.$$

We see that this expression diverges at the critical temperature T_c; however, comparisons of radio frequency penetration depths of samples in the normal and superconducting states have shown that the superconducting penetration depths are always larger than λ_L, even after an extrapolation of the data to $T = 0$ [10]. In order to quantitatively address this excess penetration depth, Pippard developed a nonlocal generalization of the London theory, wherein another characteristic length scale of superconductors, the coherence length, was introduced [11].

The most general relation between the supercurrent and the vector potential is indeed a nonlocal one, and it was proposed by Pippard that the ith component of the supercurrent can be expressed in the following form:

$$j_i(\boldsymbol{r}) = -\int d^3\boldsymbol{r}'\, Q_{ij}(\boldsymbol{r}-\boldsymbol{r}')A_j(\boldsymbol{r}'), \tag{1.4}$$

where Q_{ij} is the current-response kernel. We note that the current at point $\boldsymbol{r}$ is still linear in $\boldsymbol{A}$, but it is now determined by $\boldsymbol{A}$ at various other points $\boldsymbol{r}'$. One can recover the local (London) relation for the supercurrent in the limit $Q_{ij}(\boldsymbol{R}) = (e^2 n_s/mc)\delta_{ij}\delta(\boldsymbol{R})$, where $\boldsymbol{R} = \boldsymbol{r} - \boldsymbol{r}'$.

Pippard argued that, since the sample goes superconducting, there must be a characteristic temperature scale set by T_c, and consequently there is an energy scale set by $k_B T_c$, where k_B is the Boltzmann constant. He pointed out that since T_c is small, this energy scale is much less than the Fermi energy ϵ_F in metals, and thus only electrons near the Fermi surface (within a thin shell of thickness $k_B T_c$) can play a major role in superconductivity. The thickness of this shell in momentum space is given by $\Delta p \sim k_B T_c/v_F$, where v_F is the Fermi speed. Pippard further argued that the superconducting wavefunction should have a characteristic dimension, which could be estimated by uncertainty principle arguments. It follows from the Heisenberg uncertainty relation $\Delta x \Delta p \sim \hbar$ that $\Delta x \sim \hbar v_F / k_B T_c$. This allows one to introduce the coherence length

$$\xi_0 = a\frac{\hbar v_F}{k_B T_c}, \tag{1.5}$$

where $a \sim 1$ is a dimensionless constant. Typical values of the Pippard coherence length are of the order of $10^{-5} - 10^{-7}$ cm [12], which is much larger than the interelectron distance $n^{-1/3}$.

Below we will show that ξ_0 physically corresponds to the size of a Cooper pair, i.e. to the size of the wavepacket of the paired charge carriers in superconductors. As a result, one would expect a weakened supercurrent response to a vector potential $\boldsymbol{A}(\boldsymbol{r})$ which decreases over a volume of radius ξ_0 about the point of interest. Because of this, ξ_0 plays a role analogous to the mean free path ℓ in the nonlocal electrodynamics of normal metals [10]. If the ordinary mean free path is less than ξ_0, we would expect an even more weakened response to an applied field. By collecting these ideas together, Pippard used the following expression for the current response kernel:

$$Q_{ij}(\boldsymbol{R}) = \frac{3 n_s e^2}{4\pi m c \xi_0}\frac{R_i R_j}{R^4} e^{-R/\xi}. \tag{1.6}$$

In this last expression, ξ is the coherence length in the presence of scattering, which is given by

$$\frac{1}{\xi} = \frac{1}{\xi_0} + \frac{1}{\ell}. \tag{1.7}$$

Using Eq. (1.6) in the nonlocal relation for the supercurrent, Eq. (1.4), Pippard was able to fit experimental data for Sn and Al with the choice of the single parameter $a = 0.15$ in Eq. (1.5) [13]. With the development of the BCS theory, it was microscopically determined that this is indeed the correct form, with $a \simeq 0.18$ [10].

To conclude the Pippard theory, we remark on the fact that one can characterize superconducting materials based on the ratio of their penetration depth λ to the coherence length. Since the vector potential changes on the scale of the penetration depth, and the size of the Cooper pairs is characterized by ξ_0, it follows that if $\lambda \gg \xi_0$, then this is a local response and the London theory applies. As a result, these types of superconductors are coined “London SCs”, and $\lambda = \lambda_L$. On the other hand, if $\lambda \ll \xi_0$, which is the case in clean materials, electrons are correlated over large distances and feel the effects of other electrons, leading to a non-local response. Consequently the London theory fails here, and these types of materials are called “Pippard SCs”. One can show that in this case $\lambda = \lambda_P \simeq \text{const}(\xi_0 \lambda_L^2)^{1/3} \gg \lambda_L$, see Ref. [10]. If $\xi_0 \ll \lambda(T = 0)$, one will have a London SC at all temperatures, but since the Pippard penetration depth λ_P diverges at the critical temperature due to its dependence on n_s, a Pippard SC will become a London SC close to $T = T_c$. Therefore all SCs become London SCs close to the transition temperature. If one introduces impurities into the system, the coherence length decreases as the mean free path decreases, see Eq. (1.7), and eventually $\xi \ll \lambda$ and one will have a London SC. This classification is not to be confused with type-I and type-II SCs, which depend on the material and not the temperature.

While the Pippard nonlocal relation for the supercurrent addresses the excess penetration depth that is not accounted for in the London theory, there are additional shortcomings of the latter that are not solved by the Pippard model alone. In particular, the linear relation between the supercurrent and the vector potential, see Eq. (1.4), poses a complication since it should be gauge-invariant, but is evidently not. Fortunately, this issue can be fixed using a quantum-mechanical generalization of the London theory, which was done by Ginzburg and Landau in 1950 [14].

In the Ginzburg-Landau (GL) theory, one works with the wavefunction of the superconducting charge carriers in a system. Essentially, Ginzburg and Landau applied the Landau theory of continuous phase transitions to SCs, and the central idea in this theory is that there is an order parameter which is zero in the normal state and nonzero in the superconducting state. One takes the order parameter in this system to be the wavefunction, $\psi(\boldsymbol{r})$, of the superconducting electrons and the assumption is that $n_s(\boldsymbol{r}) = \gamma|\psi(\boldsymbol{r})|^2$, where γ is a coefficient. Since the wavefunction is complex, we have $\psi(\boldsymbol{r}) = |\psi(\boldsymbol{r})|e^{i\varphi(\boldsymbol{r})}$, and this additional degree of freedom resulting from the phase $\varphi(\boldsymbol{r})$ allows one to fix the gauge invariance of the supercurrent.

In this approach, one obtains the supercurrent by taking the variational derivative of the energy with respect to the vector potential:

$$\boldsymbol{j}_s(\boldsymbol{r}) = -c\frac{\delta E}{\delta \boldsymbol{A}(\boldsymbol{r})}.$$

The energy $E = \langle \hat{H} \rangle$ is a functional of the vector potential, i.e. $E = \int d^3\boldsymbol{r}\, \psi^* \hat{H} \psi$, where we take the Hamiltonian to have the form:

$$\hat{H} = \frac{1}{2M}\left(\hat{\boldsymbol{p}} - \frac{q}{c}\boldsymbol{A}\right)^2.$$

In this last expression, M is the mass of the superconducting carriers of charge q, and $\hat{\boldsymbol{p}} = -i\hbar\boldsymbol{\nabla}$ is the canonical momentum. It then follows that the supercurrent has the following form:

$$\boldsymbol{j}_s = \frac{i\hbar q}{2M}\left[(\boldsymbol{\nabla}\psi^*)\psi - \psi^*(\boldsymbol{\nabla}\psi)\right] - \frac{q^2}{Mc}\boldsymbol{A}|\psi|^2,$$

which is similar to the usual quantum-mechanical expression for the current density. Using the amplitude-phase representation for the wavefunction, we have:

$$\boldsymbol{j}_s = \frac{n_s}{\gamma}\frac{q^2}{Mc}\left(\frac{\hbar c}{q}\frac{\partial\varphi}{\partial\boldsymbol{r}} - \boldsymbol{A}\right), \tag{1.8}$$

where we have used the GL assumption that $\gamma|\psi|^2 = n_s$ in this last equality. In the uniform case, Eq. (1.8) reduces to $\boldsymbol{j}_s = -(n_s q^2/\gamma Mc)\boldsymbol{A}$.

Since the energy cannot change in a gauge transformation $\boldsymbol{A} \to \boldsymbol{A} + \boldsymbol{\nabla} f$, where f is a scalar function, it follows from the Schrödinger equation that in such a transformation, the phase of the wavefunction must be twisted: $\psi(\boldsymbol{r}) \to \psi(\boldsymbol{r})\exp(iqf/\hbar c)$. Because of this phase-twisting, one can easily check that the gauge invariance of the supercurrent is restored in Eq. (1.8). While we have seemingly sorted out most of the kinks in the London theory, we should note that one still cannot calculate q and M from first principles, and the remaining parameters of the theory must be obtained from experiments.

The flux quantization experiments [15] were performed in 1961 and provided, in addition to profound results, a confirmation for the BCS theory that was developed four years prior. As we shall see, the results of these experiments can be directly derived from the GL theory, if the superconducting carriers are Cooper pairs. A typical experiment involved a large superconductor with a cylindrical hole in it, in the presence of an external magnetic field oriented parallel to the cylindrical axis. The field was turned on at $T > T_c$, and then the system was cooled in constant field to $T < T_c$, where the sample becomes superconducting, exhibiting the Meissner effect. Measurements of the flux trapped inside the cavity revealed that it is quantized: $|\Phi/n\Phi_0| = 1$, i.e. $\Phi = n\Phi_0$, where n is an integer, and $\Phi_0 = hc/2e \simeq 2.07 \times 10^{-7}$ G/cm^2 is the superconducting magnetic flux quantum. We note that throughout the GL theory, e will denote the absolute value of the electron charge.

To provide a theoretical foundation for the results of the flux quantization experiments, one can calculate the flux Φ that is captured in the cylindrical cavity when the sample goes superconducting. We begin by integrating the circulation of supercurrent around an arbitrarily large loop, C, enclosing the normal cavity, and from Eq. (1.8), we have:

$$\oint_C \boldsymbol{j}_s \cdot d\boldsymbol{\ell} = \frac{n_s e^2}{mc} \oint_C d\boldsymbol{\ell} \cdot \left(\frac{\hbar c}{q} \frac{\partial \varphi}{\partial \boldsymbol{r}} - \boldsymbol{A} \right). \tag{1.9}$$

Since we are free to choose the contour, we can take it to be far outside the penetration depth, where $\boldsymbol{j}_s = 0$. On the other hand, $\oint_C \boldsymbol{A} \cdot d\boldsymbol{\ell} = \int_S \boldsymbol{B} \cdot d\boldsymbol{S} = \Phi$, where S is the surface whose boundary is C. It follows from Eq. (1.9) that the flux trapped inside the cavity takes the following form:

$$\Phi = \frac{\hbar c}{q} \oint_C d\boldsymbol{\ell} \cdot \boldsymbol{\nabla} \varphi. \tag{1.10}$$

Since ψ is a single-valued function, when you wind the function around a loop and return to the same point, ψ must stay the same. This can only happen if the phase φ changes by multiples of 2π as you wind the wavefunction. Consequently, we must have $\oint_C d\boldsymbol{\ell} \cdot \boldsymbol{\nabla}\varphi = \varphi(\boldsymbol{r}_2) - \varphi(\boldsymbol{r}_1) = 2\pi n$, where n is an integer, and $\boldsymbol{r}_2 = \boldsymbol{r}_1$. We see that while ψ must be the same, φ is free to vary as explained, and this is one of the first topological arguments in theoretical physics, i.e. that the topology of ψ may be non-trivial. It follows from these arguments that the flux is indeed quantized:

$$\Phi = \frac{nhc}{q} = n\Phi_0 \frac{2e}{q}. \tag{1.11}$$

Since we know from the flux quantization experiments that $|\Phi/n\Phi_0| = 1$, we must have $|q| = 2e$, where e is the absolute value of the electron charge. Furthermore, because the current is carried by electrons, it directly follows that $q = -2e$. It is natural to assume if $q = -2e$ that $M = 2m$, where m is the single electron mass, and this is precisely the result one would expect from the microscopic BCS theory. We can then calculate the constant γ from the GL assumption, and we find that $\gamma = 2$, and thus $n_s = 2|\psi|^2$. When Ginzburg and Landau first developed this theory, nearly seven years before the emergence of the BCS theory, they did not know about the existence of Cooper pairs. Like other physicists at the time, they could only fathom that the charge carriers in SCs were single electrons, and consequently they assumed that $q = -e$, $M = m$ and therefore $\gamma = 1 \Rightarrow |\psi|^2 = n_s$. We now know from the BCS theory that the correct choice for the parameters is as described above.

When the GL theory was first proposed, its importance was not generally appreciated in the Western literature because it appeared to be of a purely phenomenological nature [10]. It wasn't until Gor'kov derived it microscopically from the BCS model in 1959 that the GL theory started to gain wide acceptance [16]. In general, the power of the GL theory manifests itself in the way it simplifies the understanding of nonuniform systems.

To determine the order parameter in this theory, one expands the free energy in powers of ψ, taking into account the symmetry requirements of the system. Since it is assumed in this theory that T is close to T_c, ψ is assumed to be small, and one can neglect higher-order terms in the expansion. In the simplest case of singlet s-wave order parameter (the precise definition will be introduced below) in zero magnetic field, the GL free energy can be written as $F = \int d^3\boldsymbol{r}\, f_s$, where the free energy density is given by the following expression:

$$f_s = f_n + \alpha|\psi|^2 + \frac{\beta}{2}|\psi|^4 + K|\boldsymbol{\nabla}\psi|^2. \tag{1.12}$$

Here f_n is the free energy density in the normal state, $\alpha = a(T - T_c)$ with $a > 0$, and both β and K are positive constants. We note that $K = \hbar^2/2M$, where $M = 2m$ is the mass of Cooper pairs, and so the last term in expression (1.12) has the form of the kinetic energy associated with the wavefunction ψ. As we will show later in this section, it is possible for a superconducting system to have a multi-component order parameter. We will address the free energy expansions in more detail for these cases, particularly, for the chiral p-wave pairing in Appendix A, and for the two-band singlet s-wave order parameter in Appendix B.

In a uniform superconductor, the last term in Eq. (1.12) is zero, and thus f_s does not depend on the phase of the wavefunction. Consequently, the superconducting free energy has an infinite degeneracy with respect to the phase. One can determine the magnitude of the order parameter through variational minimization of the free energy with respect to $|\psi|$. In this case, one finds that the minimum in the free energy corresponds to $|\psi| = \psi_0 = \sqrt{a(T_c - T)/\beta}$, and the free energy difference between the normal and superconducting states then takes the form:

$$\Delta f = f_s - f_n = -\frac{a^2(T-T_c)^2}{2\beta}, \tag{1.13}$$

which is evidently less than zero, as expected. The expression above is nothing other than the condensation energy, and from the definition of the latter, see Eq. (1.1), it follows that one can relate the critical field to the parameters in expression (1.13) as follows:

$$H_c(T) = \sqrt{\frac{4\pi a^2}{\beta}}(T_c - T). \tag{1.14}$$

We note that this linear dependence is valid at least for the type-I materials near the critical temperature. Furthermore, we should note that the results from the GL theory are valid only near the critical temperature, where the order parameter is small, as it grows continuously from zero at $T > T_c$ to a finite value at $T < T_c$.

One can differentiate expression (1.13) with respect to temperature to easily reproduce the jump in the specific heat at $T = T_c$. In this way, we find:

$$\Delta C = (C_s - C_n)|_{T=T_c} = \frac{a^2}{\beta}T_c. \tag{1.15}$$

As we shall see in Sec. 1.3, the BCS model leads to the same result, but after a much more laborious calculation.

The real power of the GL theory comes into effect in the nonuniform systems, i.e. $\psi = \psi(\boldsymbol{r})$, and this is the topic we now address. In the general case, one can also include a magnetic field into the GL theory by making the replacement $-i\hbar\boldsymbol{\nabla} \rightarrow -i\hbar\boldsymbol{\nabla} + (2e/c)\boldsymbol{A}$, and adding the magnetic field energy to Eq. (1.12). After variational minimization of the resulting expression (the general GL functional) with respect to the wavefunction ψ, one obtains the following nonlinear differential equation, known as the GL equation:

$$\alpha\psi + \beta|\psi|^2\psi - K\boldsymbol{D}^2\psi = 0. \tag{1.16}$$

In this last expression, $\boldsymbol{D} = \boldsymbol{\nabla} + i(2e/\hbar c)\boldsymbol{A}$ is the long derivative. One can obtain a solution for the pair wavefunction by solving the GL equation, subject to the appropriate boundary conditions (see, for example, Ref. [10]).

Through the variational minimization of the general GL functional with respect to the vector potential, one can recover the Maxwell equation $\boldsymbol{\nabla} \times \boldsymbol{B} = (4\pi/c)\boldsymbol{j}_s$, where the supercurrent is given by the following expression:

$$\boldsymbol{j}_s = -\frac{2e}{\hbar} K \left\{ i \left[(\boldsymbol{\nabla}\psi^*)\psi - \psi^*(\boldsymbol{\nabla}\psi) \right] + \frac{4e}{\hbar c}|\psi|^2 \boldsymbol{A} \right\}. \tag{1.17}$$

We see that this last expression has the identical form for the supercurrent calculated earlier in this section. We note also that the total contribution to the current is indeed only the supercurrent since excitations do not play a role in the GL theory, and it is the excitations which are responsible for the normal current. One can recover the London supercurrent, see Eq. (1.3), by using the phase-amplitude form for the wavefunction $\psi = |\psi(\boldsymbol{r})|e^{i\phi(\boldsymbol{r})}$, and taking $|\psi(\boldsymbol{r})| = \psi_0$, where ψ_0 is defined above. Furthermore, neglecting the variation in ϕ, we find that the supercurrents have the same form if $n_s = 2\psi_0^2$.

To gain more insight into the structure of the GL equation, it is useful to introduce its dimensionless form. This is accomplished by defining the dimensionless order parameter $f(\boldsymbol{r}) = \psi(\boldsymbol{r})/\psi_0$, where $\psi_0 = \sqrt{|\alpha|/\beta}$ is the order parameter in the uniform state introduced above. In this way, we can rewrite the GL equation (1.16) in the following dimensionless form:

$$-\xi^2 \left(\boldsymbol{\nabla} + i\frac{2e}{\hbar c}\boldsymbol{A} \right)^2 f - f + |f|^2 f = 0, \tag{1.18}$$

where

$$\xi(T) = \sqrt{\frac{K}{|\alpha|}} = \sqrt{\frac{K}{a(T_c - T)}}, \tag{1.19}$$

is the GL correlation length. We note that, despite a similar notation, ξ is not the same as the Pippard coherence length ξ_0. This can be understood by considering the fact that ξ is temperature-dependent, while the size of a Cooper pair is essentially temperature-independent. It does turn out, however, that $\xi(T) \approx \xi_0$ for pure materials in the limit $T \ll T_c$ [10]. Physically, $\xi(T)$ characterizes the response of the wavefunction, i.e. a small disturbance of ψ from ψ_0 will decay in a characteristic length of the order of $\xi(T)$ [10]. We see from Eq. (1.19) that at the critical temperature, $\xi(T)$ diverges, which tells us that fluctuations in ψ are felt over large distances in this limit.

One can also use the dimensionless formalism to rewrite the supercurrent in Eq. (1.17) as follows:

$$\boldsymbol{j}_s = i\frac{c}{4\pi}\frac{\Phi_0}{4\pi\lambda^2}\left[f^*(\boldsymbol{D}f) - (\boldsymbol{D}f^*)f \right], \tag{1.20}$$

where

$$\lambda = \sqrt{\frac{mc^2}{8\pi e^2}\frac{\beta}{|\alpha|}} \tag{1.21}$$

is the GL penetration depth. Using the relation $n_s = 2\psi_0^2 = 2|\alpha|/\beta$, we see that one can reproduce the London penetration depth in the GL theory: $\lambda = \lambda_L = \sqrt{mc^2/4\pi e^2 n_s}$. The penetration depth characterizes the response of the supercurrent. In fact, λ is the characteristic scale over which the magnetic induction decays inside a superconducting material.

It turns out that one can use the ratio of the length scales, λ and ξ, to understand the distinction between type-I and type-II superconducting materials. We introduce the GL parameter $\kappa = \lambda/\xi$, and note that while both λ and ξ individually diverge at $T \to T_c$, κ is temperature-independent and depends only on the material parameters.

One can determine the structure of the mixed state in a type-II SC by noting that, since the phase transition is continuous at H_{c2}, the order parameter is small, which allows one to neglect the nonlinear term in Eq. (1.16) and solve it. This was done by Abrikosov in 1957, and he determined that the upper critical field H_{c2} has the following form:

$$H_{c2}(T) = \frac{\Phi_0}{2\pi\xi^2}, \tag{1.22}$$

where Φ_0 is the superconducting magnetic flux quantum introduced previously. Using the expressions (1.19) and (1.21), one can rewrite the critical field $H_c(T)$, see Eq. (1.14), in terms of the GL parameters as $H_c = \Phi_0/2\sqrt{2}\pi\xi\lambda$. Taking the ratio of this last expression with Eq. (1.22) we obtain:

$$\frac{H_{c2}}{H_c} = \sqrt{2}\kappa, \tag{1.23}$$

and so we see that if $\kappa > 1/\sqrt{2}$ then $H_{c2} > H_c$, and one will not be able to measure H_c, since the phase transition is pre-empted by H_{c2}. This allows one to make a clear distinction between the type-I and type-II SCs as follows:

$$\begin{aligned} \kappa &> \frac{1}{\sqrt{2}}, \quad \text{type-II} \\ \kappa &< \frac{1}{\sqrt{2}}, \quad \text{type-I.} \end{aligned}$$

The last topic we review before describing the BCS theory are the results of specific heat measurements on SCs. As we shall see in the next subsection, there is an energy gap Δ in the spectrum of quasiparticle excitations in SCs, which leads to an exponentially-dependent specific heat in the superconducting state, i.e. $C(T) \sim \exp(-\Delta/k_B T)$. In contrast, the specific heat of a normal metal is described by the expression $C(T) = (\pi^2 k_B T)/2T_F$, where T_F is the Fermi temperature, assuming a free electron gas with no interactions. It is very hard to separate the electronic specific heat from the lattice vibrations at finite temperatures, as one is searching for an exponentially small quantity in a huge sea of phonons. However, precise measurements of the specific heat by Corak *et al.* [17] showed that well below T_c, a good fit to the specific heat is $C(T) \sim \exp(-bT_c/T)$, where $b \sim 1.5$. Such an exponential dependence implies that $\Delta \approx 1.5k_BT_c$ is the minimum excitation energy per particle, and can in fact be interpreted as an energy gap. If the gap goes to zero at isolated points or lines on the Fermi surface (gap nodes), which is the case in some of the novel SCs, then the specific heat exhibits a power-law behaviour [18].

At around the same time of the thermodynamic measurements, the electromagnetic absorption in superconductors was measured by Glover and Tinkham [19]. They found that the Cooper pairs break up at the frequencies above the absorption edge ω_g, where $\hbar\omega_g = 2\Delta$, leading to the onset of real electromagnetic absorption. These results could be interpreted as follows: the photons destroy the bound pairs of electrons and create pairs of unbound excitations, corresponding to a minimum excitation energy of 2Δ.

We see that the spectroscopic measurement gives the total energy required to create a pair of excitations, while the thermal experiments measure the energy per one excitation [10]. As we shall see below, one of the key predicitions of the BCS theory is that there is a minimum energy $2\Delta(T)$ required to break a pair, creating two quasiparticle excitations. This agreement with the electromagnetic absorption measurements provided one of the most decisive early verifications of the BCS theory [10].

It is easy from this point for one to conclude that all of the experimental evidence we have reviewed necessarily points to the formation of coherent pairs of electrons in a superconductor. However, if this is the case, two questions immediately arise. Namely, since electrons repel each other, what could possibly be the mechanism of attractive interaction? Secondly, assuming that there is an interaction which overcomes the Coulomb repulsion, can it create bound states? Both of these questions are answered in the next subsection.

1.2 Cooper pairs

In 1956, Cooper developed an ingenious theory [20] which led the way for the fully fledged many-body BCS theory. He demonstrated that it is indeed theoretically possible for two electrons to form a bound state. It is well known in quantum mechanics that in three dimensions, there is a threshold for the strength of the attractive interaction between two particles in order for them to form a bound pair. However, Cooper realized that the pairs are formed not in a vacuum, but rather in the presence of the Fermi sea. He pictured this toy problem as a “frozen” Fermi sea, whose only purpose is to cut out some states from the momentum space, due to the Pauli exclusion principle. In this setup, all states below the Fermi momentum $p_F = \hbar k_F$ (with k_F the Fermi wavevector) are filled, and all above are empty. Cooper considered what would happen if one were to add two additional electrons which can interact only with each other. As we will see, in the presence of an arbitrarily weak attraction, the Fermi sea is unstable against the formation of bound states of electrons, or Cooper pairs.

To prove this, we consider the Schrödinger equation for a two-particle wavefunction, which has the following form:

$$-\frac{\hbar^2}{2m}\left(\frac{\partial^2}{\partial \boldsymbol{r}_1^2} + \frac{\partial^2}{\partial \boldsymbol{r}_2^2}\right)\psi + V(\boldsymbol{r}_1 - \boldsymbol{r}_2)\psi = E\psi, \tag{1.24}$$

where $V(\boldsymbol{r}_1 - \boldsymbol{r}_2)$ is an attractive interaction between particles 1 and 2. Because the two electrons can pair in different ways, there are four possible "spin channels", and the wavefunction is in general a superposition of all four of them:

$$\begin{aligned}
\psi(1,2) \equiv \psi(\boldsymbol{r}_1\sigma_1, \boldsymbol{r}_2\sigma_2) &= \psi_s(\boldsymbol{r}_1, \boldsymbol{r}_2)|S=0, S_z=0\rangle, \\
&+ \psi_t^{(+1)}(\boldsymbol{r}_1, \boldsymbol{r}_2)|S=1, S_z=1\rangle, \\
&+ \psi_t^{(0)}(\boldsymbol{r}_1, \boldsymbol{r}_2)|S=1, S_z=0\rangle, \\
&+ \psi_t^{(-1)}(\boldsymbol{r}_1, \boldsymbol{r}_2)|S=1, S_z=-1\rangle.
\end{aligned} \tag{1.25}$$

Here the subscript s corresponds to the spin-singlet state with total spin $S = 0$, and its z-projection $S_z = 0$, and subscript t denotes the triplet state with total spin $S = 1$. There are three possible z-projections for $S = 1$, i.e. $S_z = -1, 0, 1$, and the amplitudes of the triplet wavefunctions are labelled with a superscript to denote the value of S_z. The two-particle spin states can be expressed in terms of the eigenfunctions, $|\uparrow\rangle$ and $|\downarrow\rangle$, of the single-electron z-projection spin operator $\hat{s}_z$ as follows:

$$\begin{aligned}
&|S=0, S_z=0\rangle = \frac{|\uparrow\rangle_1|\downarrow\rangle_2 - |\downarrow\rangle_1|\uparrow\rangle_2}{\sqrt{2}}, \\
&|S=1, S_z=1\rangle = |\uparrow\rangle_1|\uparrow\rangle_2, \\
&|S=1, S_z=0\rangle = \frac{|\uparrow\rangle_1|\downarrow\rangle_2 + |\downarrow\rangle_1|\uparrow\rangle_2}{\sqrt{2}}, \\
&|S=1, S_z=-1\rangle = |\downarrow\rangle_1|\downarrow\rangle_2.
\end{aligned} \tag{1.26}$$

To proceed further, we use the anti-symmetrization exchange requirements for fermions, namely $\psi(1,2) = -\psi(2,1)$. Since the singlet spin state ($S = 0$) is anti-symmetric, see Eq. (1.26), it follows that the orbital part of the wavefunction is symmetric: $\psi_s(\boldsymbol{r}_1, \boldsymbol{r}_2) =$

$\psi_s(\boldsymbol{r}_2, \boldsymbol{r}_1)$. Furthermore, because the triplet spin states are symmetric with respect to spin exchange, it follows that the orbital triplet amplitudes must be antisymmetric with respect to coordinate exchange.

For simplicity, we assume that the interaction potential V is spin-independent, and also a local function of $\boldsymbol{r}_1 - \boldsymbol{r}_2$, so that it is only nonzero when the two particles are sufficiently close together. We expect the strongest interaction when $\boldsymbol{r}_1 = \boldsymbol{r}_2$, and since the triplet amplitudes are antisymmetric with respect to particle exchange, we have in this case $\psi_t^{(S_z)}(\boldsymbol{r}_1, \boldsymbol{r}_1) = -\psi_t^{(S_z)}(\boldsymbol{r}_1, \boldsymbol{r}_1)$, which can only happen if $\psi_t^{(S_z)} = 0$. Therefore it follows that only electrons in the singlet pairing state form the bound pairs. We see that the triplet pairing does not correspond to the lowest energy if the attraction is a localized one; however, nonlocal interactions do exist in real materials, and so the spin-triplet state can be realized.

In the absence of interaction between the two electrons, their minimum energy is $2\epsilon_F$, where $\epsilon_F = \hbar^2 k_F^2/2m$ is the Fermi energy. In the presence of an attractive interaction, we can write the energy of the two electrons as $E = \hbar^2 k_F^2/m + \epsilon$, where $\epsilon < 0$ since the electrons form a bound state. Because the potential depends on the difference between the two electron positions, it is natural to change into the centre-of-mass coordinate $\boldsymbol{R} = (\boldsymbol{r}_1 + \boldsymbol{r}_2)/2$, and the relative coordinate $\boldsymbol{r} = \boldsymbol{r}_1 - \boldsymbol{r}_2$. Then we can represent the wavefunction in terms of these coordinates, $\psi(\boldsymbol{r}_1, \boldsymbol{r}_2) \to \tilde{\psi}(\boldsymbol{R}, \boldsymbol{r})$, and rewrite the Schrödinger equation (1.24) as follows:

$$-\frac{\hbar^2}{4m}\frac{\partial^2\tilde{\psi}}{\partial\boldsymbol{R}^2} - \frac{\hbar^2}{m}\frac{\partial^2\tilde{\psi}}{\partial\boldsymbol{r}^2} + V(\boldsymbol{r})\tilde{\psi} = \left(\frac{\hbar^2 k_F^2}{m} + \epsilon\right)\tilde{\psi}. \tag{1.27}$$

Since there is no $\boldsymbol{R}$ dependence in the interaction, the dependence of the wavefunction on $\boldsymbol{R}$ corresponds to that of a free particle. We can therefore look for solutions of the two-particle wavefunction which have the form $\tilde{\psi}(\boldsymbol{r}, \boldsymbol{R}) = e^{i\boldsymbol{q}\cdot\boldsymbol{R}}\psi(\boldsymbol{r})$, where $\boldsymbol{q}$ is the centre-of-mass momentum of the pair. Substituting this form for $\tilde{\psi}$ into Eq. (1.27), one obtains a kinetic energy associated with the translational motion of the pair centre-of-mass, given by $\hbar^2 q^2/4m$. The lowest energy clearly corresponds to $\boldsymbol{q} = 0$, and in this case we obtain $\tilde{\psi}(\boldsymbol{r}, \boldsymbol{R}) = \psi(\boldsymbol{r})$, along with the following Schrödinger equation:

$$-\frac{\hbar^2}{m}\frac{\partial^2\psi}{\partial\boldsymbol{r}^2} + V(\boldsymbol{r})\psi = \left(\frac{\hbar^2 k_F^2}{m} + \epsilon\right)\psi. \tag{1.28}$$

Since the Fermi sea, which is a momentum-space concept, plays a major role in the theory of superconductivity, it is convenient to transform everything into the momentum representation. The coordinate-space representation of the pair wavefunction is related to the wavefunction in the momentum space, $g(\boldsymbol{k})$, as follows:

$$\psi(\boldsymbol{r}) = \int \frac{d^3\boldsymbol{k}}{(2\pi)^3} g(\boldsymbol{k}) e^{i\boldsymbol{k}\cdot\boldsymbol{r}}, \tag{1.29}$$

and the potential can be transformed in a similar manner:

$$V(\boldsymbol{r}) = \int \frac{d^3\boldsymbol{q}}{(2\pi)^3} V(\boldsymbol{q}) e^{i\boldsymbol{q}\cdot\boldsymbol{r}}. \tag{1.30}$$

Due to the Pauli exclusion principle, it follows that $g(\boldsymbol{k}) = 0$ for $|\boldsymbol{k}| < k_F$, since all of the states below the Fermi level are filled. We should point out that since $\boldsymbol{r} = \boldsymbol{r}_1 - \boldsymbol{r}_2$, Eq. (1.29) tells us that the momenta of electrons 1 and 2 are equal in magnitude and opposite in direction. Furthermore, since the pair wavefunction $\psi(\boldsymbol{r})$ must be symmetric with respect to particle exchange ($\boldsymbol{r} \to -\boldsymbol{r}$), it follows that $g(\boldsymbol{k}) = g(-\boldsymbol{k})$.

After substituting Eqs. (1.29) and (1.30) into Eq. (1.28), and manipulating the resulting expression, we find that the Schrödinger equation in the momentum space takes the following form:

$$[2\xi(\boldsymbol{k}) - \epsilon]\, g(\boldsymbol{k}) + \int \frac{d^3\boldsymbol{k}'}{(2\pi)^3} V(\boldsymbol{k} - \boldsymbol{k}') g(\boldsymbol{k}') = 0. \tag{1.31}$$

Here we have introduced a new variable

$$\xi(\boldsymbol{k}) = \frac{\hbar^2 \boldsymbol{k}^2}{2m} - \frac{\hbar^2 k_F^2}{2m},$$

which has the meaning of the kinetic energy measured from the Fermi energy.

To proceed further, we must know the analytical form of the pairing potential $V(\boldsymbol{k} - \boldsymbol{k}')$. We assume an isotropic system and then the potential can be expanded in terms of the spherical harmonics as follows:

$$V(\boldsymbol{k} - \boldsymbol{k}') = \sum_{\ell=0}^{\infty} V_\ell(k, k') \sum_{m=-\ell}^{+\ell} Y_{\ell m}(\theta, \varphi) Y^*_{\ell m}(\theta', \varphi'), \tag{1.32}$$

where $Y_{\ell m}$ are the spherical harmonics corresponding to angular momentum ℓ and its z-projection m, and θ, φ are the usual polar angles. In the anisotropic case, i.e. in the presence of a crystal lattice field, the potential is expanded slightly differently, and this is discussed in more detail in Sec. 1.4.

We substitute the expression (1.32) for the potential into the Schrödinger equation (1.31), and seek solutions for $g(\boldsymbol{k})$ of the form $g(\boldsymbol{k}) = g(k, \hat{\boldsymbol{k}}) = \sum_{\ell,m} g_{\ell m}(k) Y_{\ell m}(\hat{\boldsymbol{k}})$. The parity of the spherical harmonics is given by the relation $Y_{\ell m}(-\hat{\boldsymbol{k}}) = (-1)^{\ell} Y_{\ell m}(\hat{\boldsymbol{k}})$, and therefore, from the symmetry requirement $g(\boldsymbol{k}) = g(-\boldsymbol{k})$, it follows that ℓ must take only even values. Using this expansion for $g(\boldsymbol{k})$ in the Schrödinger equation (1.31), along with the orthonormality of the spherical harmonics, we obtain the following expression:

$$[2\xi(\boldsymbol{k}) - \epsilon]\, g_{\ell m}(k) + \frac{1}{2\pi^2}\int_0^{\infty} dk' k'^2 V_\ell(k,k') g_{\ell m}(k') = 0. \tag{1.33}$$

We see from this last equation that different ℓ channels can be considered separately. The orbital angular momentum $\ell = 0$ corresponds to the s-wave pairing, which is the case considered in the BCS theory, see the following subsection. To date, the only even orbital angular momentum states which have been found in real-life materials are the s-wave pairing, coined "conventional SCs", and the d-wave pairing, found in the high-T_c SCs.

To make analytical progress, we make the assumption, following Cooper [20], that the two electrons are attracted to each other only if they are sufficiently close to the Fermi surface, and that the interaction is constant within this thin energy shell. The pairing interaction can then be expressed as follows:

$$V_\ell(k,k') = \begin{cases} -V_\ell, & 0 < \xi(\boldsymbol{k}), \xi(\boldsymbol{k}') < \epsilon_c \\ 0, & \text{otherwise} \end{cases},$$

where $V_\ell > 0$ is a constant, and $\epsilon_c \ll \epsilon_F$ is the cutoff energy. Using this assumption, it becomes evident that the Fourier-transformed particle wavefunction has the following form:

$$g_{\ell m}(k) = g_{\ell m}\Theta(\xi_{\boldsymbol{k}})\Theta(\epsilon_c - \xi_{\boldsymbol{k}})\frac{1}{2\xi_{\boldsymbol{k}} - \epsilon}, \tag{1.34}$$

where $g_{\ell m}$ is a constant, $\Theta(x)$ is the Heaviside step function, and $\xi_{\boldsymbol{k}} = \xi(\boldsymbol{k})$. We substitute this form for $g_{\ell m}(k)$ into the Schrödinger equation (1.33), and after calculating the integrals, Eq. (1.33) yields

$$\frac{1}{N_F V_\ell} = \frac{1}{2}\ln\left(\frac{2\epsilon_c}{|\epsilon|} + 1\right), \tag{1.35}$$

where $N_F = m k_F / 2\pi^2\hbar^2$ is the density of states at the Fermi surface in three dimensions, and $\epsilon < 0$ is the energy of the bound state of the electrons measured from $2\epsilon_F$.

In the "weak-coupling approximation", the dimensionless constant $N_F V_\ell$ is small. This corresponds to a weak attraction, which happens to be an excellent approximation in most superconductors. In this limit, we can analytically solve for ϵ, and find the following result:

$$\epsilon = -2\epsilon_c e^{-2/N_F V_\ell}. \tag{1.36}$$

One can therefore conclude that there is a bound state, called a Cooper pair, at arbitrarily weak attraction, since this last equation is nonzero for any value of V_ℓ. We also note from Eq. (1.36) that the energy of the bound state is a non-analytic function of the coupling constant, i.e. its derivative at $V_\ell = 0$ is divergent. This non-analyticity means that one cannot treat the interaction as a small perturbation, and consequently it cannot be reproduced from the perturbation theory. While Cooper's theorem treats only two interacting electrons in the presence of a Fermi sea, these conclusions survive even in the more general many-body BCS theory.

We have now demonstrated that the Fermi system is unstable toward the formation of Cooper pairs. Each of the different ℓ channels corresponds to a different bound state energy, and the superconductivity is pre-empted by the channel with the strongest interactive potential. In conventional (singlet s-wave) SCs, it is V_0 which gives the largest negative bound state energy. In contrast, in the high-T_c SCs, the strongest attraction occurs in the d-wave channel.

Now that we know that electrons can form Cooper pairs, one might wonder how to quantitatively determine the spatial extent of these pairs. To estimate this quantity, one can compute the root-mean-square displacement corresponding to the ground state wavefunction $\psi(\boldsymbol{r})$ introduced above:

$$\sqrt{\langle \boldsymbol{r}^2 \rangle} = \sqrt{\frac{\int d^3\boldsymbol{r}\, \boldsymbol{r}^2 |\psi|^2}{\int d^3\boldsymbol{r} |\psi|^2}}.$$

Using the Parceval theorem in the denominator of this last expression, as well as differentiation with respect to $\boldsymbol{k}$ in the inverse Fourier transform of $\psi(\boldsymbol{r})$ in the numerator, this last relation can be written as follows:

$$\langle \boldsymbol{r}^2 \rangle = \frac{\int d^3\boldsymbol{k} \left| \frac{\partial g}{\partial \boldsymbol{k}} \right|^2}{\int d^3\boldsymbol{k} |g|^2}, \tag{1.37}$$

where $g(\boldsymbol{k})$ is defined by Eq. (1.29). Using the solution for the Fourier-transformed pair wavefunction, see Eq. (1.34), and evaluating the integrals, we find that the size of a Cooper pair is given by

$$\sqrt{\langle \boldsymbol{r}^2 \rangle} = \frac{2}{\sqrt{3}} \frac{\hbar v_F}{|\epsilon|}. \tag{1.38}$$

While the Cooper problem is not a many-body theory, it is indeed true that in the many-body system, $|\epsilon| \sim k_B T_c$. Consequenty, expression (1.38) tells us that the size of a Cooper pair is of the order $\hbar v_F / k_B T_c \sim \xi_0$, where ξ_0 is the Pippard coherence length.

One might ponder about the origin of the attractive interaction between electrons that arises in superconductors, especially because this interaction must somehow overcome the strong Coulomb repulsion between the two equivalent charges. It is important to note that when we consider electrons in a metal, we need to focus not on the properties of bare electrons, but instead on quasiparticles, or "dressed" electrons. A quasiparticle is an excitation which results from an electron moving through a surrounding exchange-correlation hole [21]. If two electrons have parallel spin, it is necessary from the Pauli exclusion principle that the probability of finding the two electrons near each other is zero, and this is known as the "exchange hole". On the other hand, the Coulomb repulsion necessitates a high energy cost associated with two electrons being near each other regardless of their spin, and this is defined as the "correlation hole". The physical manifestation of the exchange-correlation hole is that, as an electron moves through a crystal lattice, the other electrons must move out of the way.

If one considers an electron and its surrounding exchange-correlation hole in a metal, it turns out that the effective Coulomb force on the quasiparticles is greatly reduced by an exponential screening factor. While we direct the reader to standard references such as Refs. [10] or [21] for more detail, we note that one can show that the Coulomb interaction is never attractive, even in the presence of screening. This means that there must be another mechanism of attraction between the electrons in superconductors.

One such mechanism can come from the interaction of electrons with the crystal lattice vibrations (phonons), and can be understood by considering the following qualitative picture. As an electron passes through a lattice of massive positive ions, the ions are attracted to the electron's negative charge, and consequently they are displaced from their equilibrium positions. This forms a cloud of positive charge that remains long after the electron has passed through because the massive ions move slowly compared to the light electrons. When a second electron moves through the crystal lattice, these ions will still be displaced from their equilibrium positions, and the second electron will be attracted to the lingering cloud of positive charge. Since the first electron is long gone, there is no Coulomb repulsion between the two electrons, and we see that it is the retarded nature of the phonon interaction that allows for the suppression of the Coulomb repulsion.

The phonon-mediated interaction can be thought of as being accompanied by an exchange of a phonon between the two electrons. Qualitatively, the ions in a crystal lattice vibrate about their equilibrium positions in quantized modes, leading to a periodic modulation of the potential experienced by the electrons, which is characterized by wavelength $\lambda = 2\pi/|\boldsymbol{q}_{ph}|$, where $\boldsymbol{q}_{ph}$ is the wavevector of the phonon [21]. This periodic modulation of the potential causes the electrons to undergo diffraction, and so an electron is scattered from the momentum state characterized by $\boldsymbol{k}$ into one with $\boldsymbol{k}' = \boldsymbol{k} + \boldsymbol{q}_{ph}$. This extra momentum comes from the absorption of a phonon with momentum $\hbar\boldsymbol{q}_{ph}$, or from the creation of one with momentum $-\hbar\boldsymbol{q}_{ph}$, and thus one can conclude that an electron excites a phonon in a crystal lattice in this process.

Qualitatively, one of the electrons "emits" a phonon which propagates for a period of time in the solid, until another electron "absorbs" it. The net effect is to transfer momentum $\hbar\boldsymbol{q}_{ph}$ from one electron to the other. One can say that electron 1 is scattered from state $\boldsymbol{k}_1$ to $\boldsymbol{k}'_1 = \boldsymbol{k}_1 - \boldsymbol{q}_{ph}$, and the second electron is scattered from $\boldsymbol{k}_2$ to $\boldsymbol{k}'_2 = \boldsymbol{k}_2 + \boldsymbol{q}_{ph}$. The phonon is then characterized by wavevector $\boldsymbol{q}_{ph} = \boldsymbol{k}_1 - \boldsymbol{k}'_1 = \boldsymbol{k}'_2 - \boldsymbol{k}_2$, and a frequency $\omega(\boldsymbol{q})$.

While the full treatment of the effective interaction between electrons due to the phonon exchange is too complex for analytical calculation, one can make progress by using a simple approximation. Specifically, we neglect the dependence on the wavevector $\boldsymbol{q}_{ph}$ and the phonon branch, and approximate the interaction by one which effectively averages over all the wavevectors [21]. In this way, we obtain the following expression for the interaction:

$$V_{\text{eff}}(\boldsymbol{q},\omega) = |g_{\text{eff}}|^2 \frac{1}{\omega^2 - \omega_D^2}, \tag{1.39}$$

where ω_D is a typical phonon frequency, which we take to be the Debye frequency. We see that the expression (1.39) is attractive for phonon frequencies $\omega < \omega_D$, and thus the electron-phonon interaction can indeed provide the mechanism for attraction beween the two electrons.

Since only the electrons within $\pm k_B T$ of the Fermi energy play a role at low temperatures, all of the typical energy or frequency scales are much smaller than $\hbar\omega_D$. This motivates our final, simplified form for the interaction [21]:

$$V_{\text{eff}}(\boldsymbol{q},\omega) = -|g_{\text{eff}}|^2, \quad |\omega| < \omega_D. \tag{1.40}$$

As we shall see in the next section, this last expression has an equivalent form to the BCS pairing potential. In the effective Hamiltonian corresponding to the "scattering" interaction characterized by Eq. (1.40), it is important to note that one is concerned only with electrons in which all of the kinetic energies $\epsilon(\boldsymbol{k})$ lie within $\pm\hbar\omega_D$ of the Fermi energy, where the interaction is attractive.

How the idea arose that lattice vibrations may play an important role in superconductivity is an interesting topic in itself. Experiments [22] have shown that if one replaces the atoms in a SC with their isotopes, the critical temperature T_c will change with the mass of the atoms due to a phenomenon known as the "isotope effect". Since the frequency of the lattice vibrations depends on the mass of the atoms [in particular $\omega_D \sim (k/M)^{1/2}$, where k is an effective spring constant, and M is the ion mass] the presence of the isotope effect in a material suggests that phonons play an important role in the superconductivity.

While we have provided the foundation to explain many of the concepts behind superconductivity, we still do not have a complete self-consistent theory. The Cooper problem provides significant insight into the behaviour of SC electrons, but as we have mentioned many times, we require a microscopic many-body formalism which takes into account the pairing interaction and correlation between all of the electrons. This was accomplished by Bardeen, Cooper, and Schrieffer in 1957. The BCS theory [23] accurately describes the materials that belong to the conventional (singlet s-wave) superconducting class. This class includes elemental superconductors, such as Al, Nb, Pb, and their alloys, such as Nb_3Sn and Nb_3Ge (the latter had the highest critical temperature before the discovery of the high-T_c cuprates in 1986).

1.3 The BCS theory

At the heart of the BCS theory is the formation of Cooper pairs and, in fact, all of the evidence to date suggests that superconductivity is associated with the formation of pairs of electrons [24]. As we shall see, the Cooper pairs, in a sense, behave similar to bosons and condense into a coherent, many-body state. Consequently, in a qualitative picture it is sufficient to focus on a single pair of electrons, whose wavefunction maintains all of the appropriate symmetry found in the macroscopic state. Unfortunately, because the Cooper pairs overlap, this qualitative picture is slightly misleading, and we must use the many-body theory to develop a quantitative treatment of the problem.

In order to do this, it is convenient to work in the Fock space and use the occupation number representation. The Fock space for identical fermions is given by $\mathcal{F}_f = \sum_{N=1}^{\infty\oplus} \mathcal{H}_N^{(a)}$, where $\mathcal{H}_N^{(a)}$ is the antisymmetric sector of the N-particle Hilbert space. In the second-quantization formalism, single-particle operators in a many-body Hamiltonian, such as the kinetic energy $\hat{O} = \hat{\boldsymbol{p}}^2/2m$, are transformed into the Fock space as follows:

$$\sum_{i=1}^{N} \hat{O}_i \to \sum_{\ell_1,\ell_2} \langle \ell_1 | \hat{O} | \ell_2 \rangle \hat{a}_{\ell_1}^\dagger \hat{a}_{\ell_2} \tag{1.41}$$

where N is the number of particles, and $\hat{a}_\ell$ and $\hat{a}_\ell^\dagger$ are operators in the Fock space, which annihilate and create a particle in the single-particle state $|\ell\rangle$, respectively, where $\ell = \{\boldsymbol{k}, \sigma\}$, for example.

Two-particle operators, such as those corresponding to interactions, are transformed as follows:

$$\frac{1}{2}\sum_{ij}\hat{V}_{ij} \to \frac{1}{2}\sum_{\ell_1,\ell_2,\ell_3,\ell_4}\langle \ell_1\ell_2|\hat{V}|\ell_4\ell_3\rangle \hat{a}^\dagger_{\ell_1}\hat{a}^\dagger_{\ell_2}\hat{a}_{\ell_3}\hat{a}_{\ell_4}. \tag{1.42}$$

In the coordinate representation, these inner products have the following form:

$$\begin{aligned}\langle \ell_1\ell_2|\hat{V}|\ell_4\ell_3\rangle &= \sum_{s_1,s_2}\int d^3\boldsymbol{r}_1 d^3\boldsymbol{r}_2 \phi^*_{\ell_1}(\boldsymbol{r}_1, s_1)\phi^*_{\ell_2}(\boldsymbol{r}_2, s_2) \\ &\times \; V(\boldsymbol{r}_1, s_1; \boldsymbol{r}_2, s_2)\phi_{\ell_4}(\boldsymbol{r}_1, s_1)\phi_{\ell_3}(\boldsymbol{r}_2, s_2),\end{aligned} \tag{1.43}$$

where $s_{1,2} =\uparrow, \downarrow$ is the spin projection. If the single-particle basis is taken to be $\ell = \{\boldsymbol{k}, \sigma\}$, then the functions ϕ_ℓ are given by: $\phi_{\boldsymbol{k},\sigma}(\boldsymbol{r}, s) = e^{i\boldsymbol{k}\cdot\boldsymbol{r}}\delta_{s\sigma}/\sqrt{\mathcal{V}}$, where $\mathcal{V}$ is the system volume.

Using this formalism, we can rewrite a Hamiltonian of the form $\hat{H} = \hat{H}_0 + \hat{H}_{int}$, where all of the interactions are taken into account through $\hat{H}_{int}$, in terms of the Fock space operators. The free-electron part of the Hamiltonian can be written as follows:

$$\hat{H}_0 = \sum_{\boldsymbol{k},\sigma}\xi(\boldsymbol{k})\hat{a}^\dagger_{\boldsymbol{k},\sigma}\hat{a}_{\boldsymbol{k},\sigma}, \tag{1.44}$$

where $\xi(\boldsymbol{k}) = \epsilon(\boldsymbol{k}) - \mu$, with $\epsilon(\boldsymbol{k})$ the kinetic energy, and μ the chemical potential, i.e. $\hat{H}_0$ is an "extended Hamiltonian" measured from $\mu\hat{N}$, where $\hat{N} = \sum_{\boldsymbol{k},\sigma}\hat{a}^\dagger_{\boldsymbol{k},\sigma}\hat{a}_{\boldsymbol{k},\sigma}$ is the total particle number operator. We neglect the difference between the Fermi energy and the chemical potential, and do not specify the exact form for $\epsilon(\boldsymbol{k})$, because in the presence of a crystal lattice, the band dispersion can have a complicated form.

Guided by the Cooper theorem, see Sec. 1.2, we expect that the lowest energy state corresponds to the two electrons posessing equal and opposite momenta $\boldsymbol{k}, -\boldsymbol{k}$, i.e. no center-of-mass momentum. Through their interaction, the electrons are scattered into the states $\boldsymbol{k}', -\boldsymbol{k}'$, and thus we expect an interaction Hamiltonian of the form:

$$\hat{H}_{int} = \frac{1}{\mathcal{V}}\sum_{\boldsymbol{k},\boldsymbol{k}'}V(\boldsymbol{k}, \boldsymbol{k}')\hat{a}^\dagger_{\boldsymbol{k},\uparrow}\hat{a}^\dagger_{-\boldsymbol{k},\downarrow}\hat{a}_{-\boldsymbol{k}',\downarrow}\hat{a}_{\boldsymbol{k}',\uparrow}, \tag{1.45}$$

where $V(\boldsymbol{k}, \boldsymbol{k}') = \langle \boldsymbol{k}\uparrow, -\boldsymbol{k}\downarrow|\hat{V}|\boldsymbol{k}'\uparrow, -\boldsymbol{k}'\downarrow\rangle$. In the BCS theory, the matrix elements of the pairing interaction are assumed to have the following form [23]:

$$V(\boldsymbol{k},\boldsymbol{k}') = \begin{cases} -V_0, & |\xi(\boldsymbol{k})|, |\xi(\boldsymbol{k}')| \le \epsilon_c \\ 0, & \text{otherwise} \end{cases}, \tag{1.46}$$

where ϵ_c is the BCS cutoff energy. From Eq. (1.40) and the discussion thereafter, it follows that $\epsilon_c \sim \hbar\omega_D$. This interaction is indeed attractive since the coupling constant $V_0 > 0$. In contrast to the Cooper assumption, in which only two electrons in a small energy shell above the Fermi surface are involved in pairing, the BCS assumption allows all electrons, including those below the Fermi sea, to interact, as long as they are within the cutoff energy. Similar to the Cooper problem, in the BCS theory the momenta and spins of the pairing electrons must be equal and opposite, i.e. one electron with $k \equiv |\boldsymbol{k}| > k_F$ cannot interact with another which has $k < k_F$. We shall see that the Fermi surface is unstable to these interactions, and thus the ground state of the interacting system will no longer be a Fermi sphere, as in the case of a free electron gas.

To proceed with the theory, we introduce the pair creation and annihilation operators:

$$\hat{b}^\dagger_{\boldsymbol{k}} = \hat{a}^\dagger_{\boldsymbol{k}\uparrow}\hat{a}^\dagger_{-\boldsymbol{k}\downarrow}, \qquad \hat{b}_{\boldsymbol{k}} = \hat{a}_{-\boldsymbol{k}\downarrow}\hat{a}_{\boldsymbol{k}\uparrow}, \tag{1.47}$$

and then the interacting part of the Hamiltonian can be written as follows:

$$\hat{H}_{int} = \frac{1}{\mathcal{V}}\sum_{\boldsymbol{k},\boldsymbol{k}'} V(\boldsymbol{k},\boldsymbol{k}')\hat{b}^\dagger_{\boldsymbol{k}}\hat{b}_{\boldsymbol{k}'}. \tag{1.48}$$

This last form for the interacting part of the Hamiltonian is quite useful, allowing one to focus on the scattering of a pair, and not individual electrons. In this equation, one initially has a pair characterized by the momentum $\boldsymbol{k}'$, and after interacting, the pair is scattered into the state characterized by $\boldsymbol{k}$.

We now wish to find the BCS ground-state wavefunction and its associated energy. We note that in the absence of interactions, the ground state of the free electron gas can be written as follows:

$$|\Phi_0\rangle = \prod_{\substack{|\boldsymbol{k}|\le k_F \\ \sigma=\uparrow,\downarrow}} \hat{a}^\dagger_{\boldsymbol{k}\sigma}|0\rangle, \tag{1.49}$$

where $|0\rangle$ is the vacuum state, in which there are no particles present. We can see that all states below the Fermi energy are filled. It is easy to show from this last expression that the corresponding ground-state energy has the following form:

$$\epsilon_0 = \langle \Phi_0 | \hat{H}_0 | \Phi_0 \rangle = 2 \sum_{|\boldsymbol{k}| \leq k_F} \xi(\boldsymbol{k}).$$

To calculate the excitation energy, we look at the possible ways that single-particle excitations can occur. For $|\boldsymbol{k}| > k_F$, one has the electron-like excitations:

$$|\Phi_{\boldsymbol{k}\sigma}\rangle = \hat{a}^{\dagger}_{\boldsymbol{k}\sigma} |\Phi_0\rangle,$$

and for $|\boldsymbol{k}| \leq k_F$, one has the hole-like excitations:

$$|\tilde{\Phi}_{\boldsymbol{k}\sigma}\rangle = \hat{a}_{\boldsymbol{k}\sigma} |\Phi_0\rangle,$$

where $\sigma = \uparrow, \downarrow$. By calculating the energy corresponding to these excited states in the non-interacting system $\langle \Phi_{\boldsymbol{k}\sigma} | \hat{H}_0 | \Phi_{\boldsymbol{k}\sigma} \rangle$, and $\langle \tilde{\Phi}_{\boldsymbol{k}\sigma} | \hat{H}_0 | \tilde{\Phi}_{\boldsymbol{k}\sigma} \rangle$, we find that the energy of a single electron-like or hole-like excitation in the normal state is $|\xi(\boldsymbol{k})|$.

The Cooper pairs that form the superconducting condensate are often referred to as bosons in the literature because of their integer spin, and we would like to note that, technically speaking, this interpretation is not quite correct. This can be understood by checking the commutation relations of the pair creation and annihilation operators. After doing the algebra, one finds the following:

$$\begin{aligned} [\hat{b}_{\boldsymbol{k}}, \hat{b}_{\boldsymbol{k}'}] &= [\hat{b}^{\dagger}_{\boldsymbol{k}}, \hat{b}^{\dagger}_{\boldsymbol{k}'}] = 0, \\ [\hat{b}_{\boldsymbol{k}}, \hat{b}^{\dagger}_{\boldsymbol{k}'}] &= \delta_{\boldsymbol{k},\boldsymbol{k}'} (1 - \hat{n}_{\boldsymbol{k}\uparrow} - \hat{n}_{-\boldsymbol{k}\downarrow}). \end{aligned} \tag{1.50}$$

Although the first two relations are identical to the bosonic ones, the third relation is not exactly the same as the corresponding one for bosons.

We are now in a position to include the interactions into the ground-state wavefunction, to find the celebrated BCS ground state. We seek the ground-state solution of the form

$$|\Phi_0\rangle = C \prod_{\boldsymbol{k}} e^{\lambda_{\boldsymbol{k}} \hat{b}^{\dagger}_{\boldsymbol{k}}} |0\rangle, \tag{1.51}$$

where C is a normalization coefficient, $\lambda_{\boldsymbol{k}}$ is a variational parameter, which we will use to minimize the energy, and the product is taken over all values of the momentum. Expanding the exponential in a power series, one will see that the terms quadratic and higher order in $\hat{b}^{\dagger}_{\boldsymbol{k}}$ cancel because they violate the Pauli exclusion principle. Therefore the BCS ground state becomes

$$|\Phi_0\rangle = C\prod_{\boldsymbol{k}}\left(1+\lambda_{\boldsymbol{k}}\hat{b}^{\dagger}_{\boldsymbol{k}}\right)|0\rangle, \tag{1.52}$$

and we see that it is a superposition of states with arbitrary numbers of pairs. By rewriting $\lambda_{\boldsymbol{k}} = v_{\boldsymbol{k}}/u_{\boldsymbol{k}}$, where u and v are complex functions, we find that wavefunction is given by

$$|\Phi_0\rangle = \tilde{C}\prod_{\boldsymbol{k}}\left(u_{\boldsymbol{k}}+v_{\boldsymbol{k}}\hat{a}^{\dagger}_{\boldsymbol{k}\uparrow}\hat{a}^{\dagger}_{-\boldsymbol{k}\downarrow}\right)|0\rangle,$$

where $\tilde{C} = C/\Pi_{\boldsymbol{k}}u_{\boldsymbol{k}}$. From the condition $\langle\Phi_0|\Phi_0\rangle = 1$, one can show that the normalization coefficient $\tilde{C} = 1$, and thus the normalized wavefunction has the following form:

$$|\Phi_0\rangle = \prod_{\boldsymbol{k}}\left(u_{\boldsymbol{k}}+v_{\boldsymbol{k}}\hat{a}^{\dagger}_{\boldsymbol{k}\uparrow}\hat{a}^{\dagger}_{-\boldsymbol{k}\downarrow}\right)|0\rangle. \tag{1.53}$$

This last expression illustrates that $|u_{\boldsymbol{k}}|^2$ is the probability that the state with momentum $\boldsymbol{k}$ is unpaired, i.e. the pair state $(\boldsymbol{k}\uparrow, -\boldsymbol{k}\downarrow)$ is empty, and that $|v_{\boldsymbol{k}}|^2$ is the probability that the pair state is occupied. Since the state is either occupied or not, it follows that

$$|u_{\boldsymbol{k}}|^2 + |v_{\boldsymbol{k}}|^2 = 1, \tag{1.54}$$

and this gives us a constraint for the complex amplitudes $u_{\boldsymbol{k}}$ and $v_{\boldsymbol{k}}$.

To determine these amplitudes, one must use the constraint (1.54) to minimize the ground-state energy, which has the following form:

$$E_0 = \langle\Phi_0|\hat{H}|\Phi_0\rangle = \langle\Phi_0|\hat{H}_0|\Phi_0\rangle + \langle\Phi_0|\hat{H}_{int}|\Phi_0\rangle.$$

Substituting expressions (1.44), (1.48), and (1.53) into this last equation, we find that the energy of the system at $T = 0$ is a functional of $u_{\boldsymbol{k}}$ and $v_{\boldsymbol{k}}$, which is given by

$$E_0[u_{\boldsymbol{k}}, v_{\boldsymbol{k}}] = 2\sum_{\boldsymbol{k}}\xi_{\boldsymbol{k}}|v_{\boldsymbol{k}}|^2 + \frac{1}{\mathcal{V}}\sum_{\boldsymbol{k},\boldsymbol{k}'}V(\boldsymbol{k},\boldsymbol{k}')u_{\boldsymbol{k}}v^{*}_{\boldsymbol{k}}u^{*}_{\boldsymbol{k}'}v_{\boldsymbol{k}'}, \tag{1.55}$$

where $\xi_{\boldsymbol{k}} \equiv \xi(\boldsymbol{k})$.

The next step is to minimize the free energy with respect to the amplitudes $u_{\boldsymbol{k}}, v_{\boldsymbol{k}}$. We follow the original paper [23] and assume that $u_{\boldsymbol{k}}$ and $v_{\boldsymbol{k}}$ are real. Equation (1.54) suggests looking for solutions of the form

$$u_{\boldsymbol{k}} = \sin\theta_{\boldsymbol{k}}, \qquad v_{\boldsymbol{k}} = \cos\theta_{\boldsymbol{k}}, \tag{1.56}$$

and then we can minimize the ground-state energy with respect to the single parameter $\theta_{\boldsymbol{k}}$. After some lengthy but straightforward algebra, one arrives at the following non-linear integral equation for the parameter $\theta_{\boldsymbol{k}}$:

$$\tan 2\theta_{\boldsymbol{k}} = \frac{1}{2\xi_{\boldsymbol{k}}}\frac{1}{\mathcal{V}}\sum_{\boldsymbol{k}'} V(\boldsymbol{k},\boldsymbol{k}')\sin 2\theta_{\boldsymbol{k}'}. \tag{1.57}$$

This equation can be solved by introducing the zero-temperature gap function according to the following definition:

$$\Delta_{\boldsymbol{k}} = -\frac{1}{\mathcal{V}}\sum_{\boldsymbol{k}'} V(\boldsymbol{k},\boldsymbol{k}')u_{\boldsymbol{k}'}v_{\boldsymbol{k}'} = -\frac{1}{2}\frac{1}{\mathcal{V}}\sum_{\boldsymbol{k}'} V(\boldsymbol{k},\boldsymbol{k}')\sin 2\theta_{\boldsymbol{k}'}. \tag{1.58}$$

In this way, Eq. (1.57) takes the simplified form:

$$\tan 2\theta_{\boldsymbol{k}} = -\frac{\Delta_{\boldsymbol{k}}}{\xi_{\boldsymbol{k}}},$$

whose solutions are given by

$$\begin{aligned} \sin 2\theta_{\boldsymbol{k}} &= \pm\frac{\Delta_{\boldsymbol{k}}}{\sqrt{\xi_{\boldsymbol{k}}^2+\Delta_{\boldsymbol{k}}^2}}, \\ \cos 2\theta_{\boldsymbol{k}} &= \mp\frac{\xi_{\boldsymbol{k}}}{\sqrt{\xi_{\boldsymbol{k}}^2+\Delta_{\boldsymbol{k}}^2}}. \end{aligned} \tag{1.59}$$

Using Eq. (1.56), we choose the following solutions to Eq. (1.59) for $u_{\boldsymbol{k}}$ and $v_{\boldsymbol{k}}$ based upon physical arguments:

$$\begin{aligned} u_{\boldsymbol{k}} &= \frac{1}{\sqrt{2}}\left(1+\frac{\xi_{\boldsymbol{k}}}{E_{\boldsymbol{k}}}\right)^{1/2}, \\ v_{\boldsymbol{k}} &= \frac{1}{\sqrt{2}}\left(1-\frac{\xi_{\boldsymbol{k}}}{E_{\boldsymbol{k}}}\right)^{1/2}, \end{aligned} \tag{1.60}$$

where $E_{\boldsymbol{k}} = \sqrt{\xi_{\boldsymbol{k}}^2+\Delta_{\boldsymbol{k}}^2}$. Far above the Fermi surface, i.e. in the limit $\xi_{\boldsymbol{k}} \to \infty$, it follows from the above expression that $u_{\boldsymbol{k}} \to 1$ and $v_{\boldsymbol{k}} \to 0$. One indeed expects such a state to be empty since Cooper pairs exist only within a thin shell near the Fermi surface.

To find the gap function $\Delta_{\boldsymbol{k}}$, one must solve Eq. (1.58) self-consistently. By substituting the expression (1.60) into Eq. (1.58), one obtains the zero-temperature gap equation:

$$\Delta_{\boldsymbol{k}} = -\frac{1}{2}\frac{1}{\mathcal{V}}\sum_{\boldsymbol{k}'} V(\boldsymbol{k},\boldsymbol{k}')\frac{\Delta_{\boldsymbol{k}'}}{E_{\boldsymbol{k}'}}. \tag{1.61}$$

To proceed further, we use the BCS assumption about the interaction potential $V(\boldsymbol{k},\boldsymbol{k}')$, given in Eq. (1.46). In this way, one finds that the gap function can be written in the form

$$\Delta_{\boldsymbol{k}} = \Delta\Theta(\epsilon_c - |\xi_{\boldsymbol{k}}|), \tag{1.62}$$

where the constant Δ satisfies the following equation:

$$\Delta = \frac{V_0}{2}\frac{1}{\mathcal{V}}\sum_{\boldsymbol{k}'}\frac{\Delta}{\sqrt{\Delta^2+\xi^2_{\boldsymbol{k}'}}}\Theta(\epsilon_c - |\xi_{\boldsymbol{k}'}|), \tag{1.63}$$

and $\Theta(x)$ is the Heaviside step function. Taking the thermodynamic limit $\mathcal{V}\to\infty$, and introducing the density of states to rewrite the momentum sums in terms of the integrals over the energy, we arrive at the following equation for Δ:

$$\frac{1}{\Delta} = \frac{1}{\epsilon_c}\sinh\left(\frac{1}{N_F V_0}\right), \tag{1.64}$$

where N_F is the density of states at the Fermi level. In the weak-coupling approximation $N_F V_0 \ll 1$, and thus $\sinh(1/N_F V_0) \approx \exp(1/N_F V_0)/2$, so it follows that the gap has the following value:

$$\Delta = 2\epsilon_c e^{-1/N_F V_0}. \tag{1.65}$$

This last expression has the same form as the bound state energy from the Cooper theorem, see Eq. (1.36), which suggests that Δ is an energy. In fact, Δ is the binding energy of the pair of electrons. Since $\epsilon_c \sim \hbar\omega_D$, we see from Eq. (1.65) that the typical energy scale relevant to superconductivity is much less than the Debye energy. This explains why typical values of the critical temperature are much lower than other relevant energy scales in metals, such as the phonon energies or the Fermi energy [21].

One can recover the normal state with no attractive interaction, i.e. the free electron gas, by formally taking the limit $V_0 \to 0$, and thus $\Delta \to 0$. In this case, using Eq. (1.60), we obtain $u_{\boldsymbol{k}} \to \Theta(\xi_{\boldsymbol{k}})$ and $v_{\boldsymbol{k}} \to \Theta(-\xi_{\boldsymbol{k}})$, and therefore one can write the BCS ground-state wavefunction, Eq. (1.53), as follows:

$$|\Phi_0\rangle = \prod_{|\boldsymbol{k}|<k_F} \hat{a}^\dagger_{\boldsymbol{k}\uparrow}\hat{a}^\dagger_{-\boldsymbol{k}\downarrow}|0\rangle. \tag{1.66}$$

A comparison of this last expression with Eq. (1.49) reveals that this is nothing but the Fermi sea of electrons, as expected.

We make a note that from Eq. (1.60), it is evident that the quantity

$$u_{\boldsymbol{k}} v_{\boldsymbol{k}} = \frac{1}{2}\frac{|\Delta_{\boldsymbol{k}}|}{E_{\boldsymbol{k}}}$$

provides a measure of the superconductivity in the system. Furthermore, one can show from Eqs. (1.47) and (1.53) that $\langle \hat{b}^{\dagger}_{\boldsymbol{k}} \rangle = \langle \Phi_0 | \hat{b}^{\dagger}_{\boldsymbol{k}} | \Phi_0 \rangle$ is given by the following expression:

$$\langle \hat{b}^{\dagger}_{\boldsymbol{k}} \rangle = u_{\boldsymbol{k}} v^{*}_{\boldsymbol{k}} = u_{\boldsymbol{k}} v_{\boldsymbol{k}}, \tag{1.67}$$

where the second equality holds for real $v_{\boldsymbol{k}}$. One can see that $\langle \hat{b}^{\dagger}_{\boldsymbol{k}} \rangle$ can be interpreted as the pair wavefunction.

To show that the system's energy is indeed lowered in the superconducting state, we calculate the condensation energy introduced in Sec. 1.1. In order to calculate this energy change, we must first determine the ground-state energy in the BCS state. Using Eq. (1.58) in Eq. (1.55), we can write the BCS ground-state energy in terms of the gap function $\Delta_{\boldsymbol{k}}$ as follows:

$$E_0 = \sum_{\boldsymbol{k}} \left(\xi_{\boldsymbol{k}} - \frac{\xi^2_{\boldsymbol{k}}}{E_{\boldsymbol{k}}} \right) - \frac{1}{2} \sum_{\boldsymbol{k}} \frac{\Delta^2_{\boldsymbol{k}}}{E_{\boldsymbol{k}}}. \tag{1.68}$$

After summation of the second term in the last expression, and subtraction of the ground-state energy of the normal state $E_{0,n}$ (with $\Delta = 0$), we find the following relation for the energy change per unit volume when the system goes superconducting:

$$\begin{aligned} \frac{E_0 - E_{0,n}}{\mathcal{V}} &= \frac{1}{\mathcal{V}} \sum_{\boldsymbol{k}} \left(|\xi_{\boldsymbol{k}}| - \frac{\xi^2_{\boldsymbol{k}}}{E_{\boldsymbol{k}}} \right) - \frac{\Delta^2}{V_0}, \\ &= \int \frac{d^3\boldsymbol{k}}{(2\pi)^3} \left[|\xi_{\boldsymbol{k}}| - \frac{\xi^2_{\boldsymbol{k}}}{\sqrt{\xi^2_{\boldsymbol{k}} + \Delta^2}} \right] \Theta(\epsilon_c - |\xi_{\boldsymbol{k}}|) - \frac{\Delta^2}{V_0}. \end{aligned} \tag{1.69}$$

Here we have taken the thermodynamic limit $\mathcal{V} \to \infty$, and used the expression (1.62) for $\Delta_{\boldsymbol{k}}$ in the second equality. Introducing the density of states allows one to rewrite Eq. (1.69) in terms of an energy integral, and after integrating over the thin energy shell, we obtain:

$$\frac{E_0 - E_{0,n}}{\mathcal{V}} = -\frac{1}{2} N_F \Delta^2. \tag{1.70}$$

From this expression, it immediately follows that the superconducting state is lower in energy than the normal state, confirming that the superconducting state is indeed thermodynamically advantageous. The condensation energy is given by the absolute value of Eq. (1.70), and from Eq. (1.1) we can relate the condensation energy to the critical field as follows:

$$\frac{1}{2}N_F\Delta^2 = \frac{H_c^2(T=0)}{8\pi}.$$

We see that by measuring the critical field, one can determine the gap Δ.

The next step in the BCS theory is to consider the effects of finite temperatures. At a nonzero temperature, some of the Cooper pairs will be able to break up, forming excitations. Bardeen, Cooper, and Schrieffer found that it is not feasible to construct the excited states by using the BCS ground-state wavefunction acted upon by the single-particle creation operators. In order to determine the excited states, a more tractable option is to apply a mean-field decoupling of the interaction, followed by a Bogoliubov transformation on the BCS Hamiltonian.

We begin by treating the interacting part of the Hamiltonian in the mean-field approximation, in which the fourth-order term is reduced to a quadratic one. Since the Cooper pairs form a condensate, this leads to an average field and thus to an average potential experienced by the unpaired electrons. In this approximation, we make the following replacement in Eq. (1.48):

$$\hat{b}^\dagger_{\boldsymbol{k}} = \langle \hat{b}^\dagger_{\boldsymbol{k}} \rangle + \delta\hat{b}^\dagger_{\boldsymbol{k}}; \quad \hat{b}_{\boldsymbol{k}} = \langle \hat{b}_{\boldsymbol{k}} \rangle + \delta\hat{b}_{\boldsymbol{k}},$$

where $\langle \hat{b}^\dagger_{\boldsymbol{k}} \rangle$ plays the role of the wavefunction of the electron pairs that coherently propagate through the system. The matrix elements of $\delta\hat{b}^\dagger_{\boldsymbol{k}}$ ($\delta\hat{b}_{\boldsymbol{k}}$) are small in comparison to $\langle \hat{b}^\dagger_{\boldsymbol{k}} \rangle$ ($\langle \hat{b}_{\boldsymbol{k}} \rangle$), since the fluctuations away from the mean field are assumed to be small. This allows one to neglect the terms that are nonlinear in $\delta\hat{b}_{\boldsymbol{k}}$, and after a slight manipulation of the resulting expression, one obtains the mean-field interacting Hamiltonian:

$$\begin{aligned} \hat{H}^{(int)}_{MF} &= -\frac{1}{\mathcal{V}}\sum_{\boldsymbol{k},\boldsymbol{k}'} V(\boldsymbol{k},\boldsymbol{k}')\langle \hat{b}^\dagger_{\boldsymbol{k}}\rangle\langle \hat{b}_{\boldsymbol{k}'}\rangle + \frac{1}{\mathcal{V}}\sum_{\boldsymbol{k},\boldsymbol{k}'} V(\boldsymbol{k},\boldsymbol{k}')\langle \hat{b}^\dagger_{\boldsymbol{k}}\rangle \hat{b}_{\boldsymbol{k}'} \\ &\quad + \frac{1}{\mathcal{V}}\sum_{\boldsymbol{k},\boldsymbol{k}'} V(\boldsymbol{k},\boldsymbol{k}')\langle \hat{b}_{\boldsymbol{k}'}\rangle \hat{b}^\dagger_{\boldsymbol{k}}. \end{aligned} \tag{1.71}$$

To simplify this Hamiltonian, we introduce the finite-temperature gap function:

$$\Delta_{\boldsymbol{k}} = -\frac{1}{\mathcal{V}}\sum_{\boldsymbol{k}'} V(\boldsymbol{k},\boldsymbol{k}')\langle \hat{b}_{\boldsymbol{k}'}\rangle, \tag{1.72}$$

and then we can rewrite Eq. (1.71) as follows:

$$\hat{H}_{MF}^{(int)} = \sum_{\boldsymbol{k}} \Delta_{\boldsymbol{k}} \langle \hat{b}_{\boldsymbol{k}}^{\dagger} \rangle - \sum_{\boldsymbol{k}} \Delta_{\boldsymbol{k}} \hat{b}_{\boldsymbol{k}}^{\dagger} - \sum_{\boldsymbol{k}} \Delta_{\boldsymbol{k}}^{*} \hat{b}_{\boldsymbol{k}}. \tag{1.73}$$

Including the free-electron part of the Hamiltonian, see Eq. (1.44), we can write the total mean-field Hamiltonian in the following form:

$$\begin{aligned} \hat{H}_{MF} &= \sum_{\boldsymbol{k}} \xi(\boldsymbol{k}) (\hat{a}_{\boldsymbol{k}\uparrow}^{\dagger} \hat{a}_{\boldsymbol{k}\uparrow} + \hat{a}_{\boldsymbol{k}\downarrow}^{\dagger} \hat{a}_{\boldsymbol{k}\downarrow}) \\ &- \sum_{\boldsymbol{k}} (\Delta_{\boldsymbol{k}} \hat{a}_{\boldsymbol{k}\uparrow}^{\dagger} \hat{a}_{-\boldsymbol{k}\downarrow}^{\dagger} + \Delta_{\boldsymbol{k}}^{*} \hat{a}_{-\boldsymbol{k}\downarrow} \hat{a}_{\boldsymbol{k}\uparrow}) \\ &+ \sum_{\boldsymbol{k}} \Delta_{\boldsymbol{k}} \langle \hat{a}_{\boldsymbol{k}\uparrow}^{\dagger} \hat{a}_{-\boldsymbol{k}\downarrow}^{\dagger} \rangle, \end{aligned} \tag{1.74}$$

where we have replaced the pair operators with their definitions in terms of the single-particle creation (annihilation) operators. We note that while this last Hamiltonian has a quadratic form in the fermionic operators, it is not easily solved due to the fact that $\Delta_{\boldsymbol{k}}$ is not arbitrary and must be found from Eq. (1.72). The thermal average in Eq. (1.72) is calculated with respect to $\hat{H}_{MF}$, which as we see depends on $\Delta_{\boldsymbol{k}}$, and this leads to a self-consistency equation.

To simplify the Hamiltonian further, we perform a Bogoliubov transformation on the mean-field Hamiltonian (1.74). We take the set of operators $(\hat{a}_{\boldsymbol{k}\uparrow}, \hat{a}_{\boldsymbol{k}\uparrow}^{\dagger}, \hat{a}_{-\boldsymbol{k}\downarrow}, \hat{a}_{-\boldsymbol{k}\downarrow}^{\dagger})$, and represent them in terms of the new fermionic operators $(\hat{\gamma}_{\boldsymbol{k},0}, \hat{\gamma}_{\boldsymbol{k},0}^{\dagger}, \hat{\gamma}_{\boldsymbol{k},1}, \hat{\gamma}_{\boldsymbol{k},1}^{\dagger})$. As shown independently by Bogoliubov [25] and Valatin [26], in the spin-singlet case, the transformation has the following form:

$$\begin{aligned} \hat{a}_{\boldsymbol{k}\uparrow} &= u_{\boldsymbol{k}}^{*} \hat{\gamma}_{\boldsymbol{k},0} + v_{\boldsymbol{k}} \hat{\gamma}_{\boldsymbol{k},1}^{\dagger}, \\ \hat{a}_{-\boldsymbol{k}\downarrow}^{\dagger} &= -v_{\boldsymbol{k}}^{*} \hat{\gamma}_{\boldsymbol{k},0} + u_{\boldsymbol{k}} \hat{\gamma}_{\boldsymbol{k},1}^{\dagger}, \end{aligned} \tag{1.75}$$

where

$$\begin{aligned} u_{\boldsymbol{k}} &= \frac{1}{\sqrt{2}} \left(1 + \frac{\xi_{\boldsymbol{k}}}{E_{\boldsymbol{k}}} \right)^{1/2}, \\ v_{\boldsymbol{k}} &= \frac{1}{\sqrt{2}} \left(1 - \frac{\xi_{\boldsymbol{k}}}{E_{\boldsymbol{k}}} \right)^{1/2} \frac{\Delta_{\boldsymbol{k}}}{|\Delta_{\boldsymbol{k}}|}, \end{aligned} \tag{1.76}$$

and for now we relax the condition that $\Delta_{\boldsymbol{k}}$ is real. We note that the operator $\hat{\gamma}_{\boldsymbol{k},0}$ participates in destroying an electron in a state corresponding to $\boldsymbol{k}, \uparrow$, or in creating one in the state $-\boldsymbol{k}, \downarrow$. In either case, the net effect of this fermionic operator is to reduce the system's momentum by $\boldsymbol{k}$ and spin by $\hbar/2$ [10]. The operator $\hat{\gamma}^\dagger_{\boldsymbol{k},1}$ has similar properties and thus $\hat{\gamma}_{\boldsymbol{k},1}$ has the net effect of increasing the system's momentum by $\boldsymbol{k}$ and spin by $\hbar/2$. We note that these new fermionic operators do not definitely increase or decrease the number of electrons, but rather create a linear superposition of these possibilities [10].

Now we represent the Hamiltonian (1.74) in terms of the new fermionic operators using Eq. (1.75). After some straightforward manipulation, the mean-field Hamiltonian takes the form:

$$\hat{H}_{MF} = \sum_{\boldsymbol{k}} E_{\boldsymbol{k}} (\hat{\gamma}^\dagger_{\boldsymbol{k},0}\hat{\gamma}_{\boldsymbol{k},0} + \hat{\gamma}^\dagger_{\boldsymbol{k},1}\hat{\gamma}_{\boldsymbol{k},1}) + \mathcal{H}_0, \tag{1.77}$$

where

$$\mathcal{H}_0 = \sum_{\boldsymbol{k}} [\xi_{\boldsymbol{k}} - E_{\boldsymbol{k}} + \Delta_{\boldsymbol{k}} \langle \hat{a}^\dagger_{\boldsymbol{k}\uparrow}\hat{a}^\dagger_{-\boldsymbol{k}\downarrow}\rangle]$$

is just a complex number, and recall that

$$E_{\boldsymbol{k}} = \sqrt{\xi^2_{\boldsymbol{k}} + |\Delta_{\boldsymbol{k}}|^2}. \tag{1.78}$$

We see from expression (1.77) that the transformed mean-field Hamiltonian has the form of a free-fermion Hamiltonian, with two distinct species of fermionic single-particle operators $(\hat{\gamma}_{\boldsymbol{k},0}, \hat{\gamma}_{\boldsymbol{k},1})$ (and their adjoints), and the ground state energy $\mathcal{H}_0$. The fermionic operators in Eq. (1.77) create single-particle excitations above the ground state, with energies $E_{\boldsymbol{k}} > 0$. We can see that the excitations are gapped because, according to Eq. (1.78), the minimum excitation energy at the Fermi surface, i.e. at $\xi(\boldsymbol{k}) = 0$, is given by $\Delta = |\Delta_{\boldsymbol{k}}|$.

One can compute the thermal average in $\mathcal{H}_0$ by first rewriting it using the Bogoliubov transformation, see Eq. (1.75):

$$\begin{aligned} \langle \hat{a}^\dagger_{\boldsymbol{k}\uparrow}\hat{a}^\dagger_{-\boldsymbol{k}\downarrow}\rangle = & - u_{\boldsymbol{k}} v^*_{\boldsymbol{k}} \langle \hat{\gamma}^\dagger_{\boldsymbol{k},0}\hat{\gamma}_{\boldsymbol{k},0}\rangle + u^2_{\boldsymbol{k}} \langle \hat{\gamma}^\dagger_{\boldsymbol{k},0}\hat{\gamma}^\dagger_{\boldsymbol{k},1}\rangle \\ & - v^{*,2}_{\boldsymbol{k}} \langle \hat{\gamma}_{\boldsymbol{k},1}\hat{\gamma}_{\boldsymbol{k},0}\rangle + u_{\boldsymbol{k}} v^*_{\boldsymbol{k}} \langle \hat{\gamma}_{\boldsymbol{k},1}\hat{\gamma}^\dagger_{\boldsymbol{k},1}\rangle. \end{aligned} \tag{1.79}$$

Using the cyclic invariance of the trace and the anti-commutation properties of the fermionic creation and annihilation operators $\hat{\gamma}^\dagger, \hat{\gamma}$, one finds that for the Hamiltonian of the form (1.77), we have

$$\langle \hat{\gamma}^\dagger_{\boldsymbol{k},0}\hat{\gamma}_{\boldsymbol{k},0}\rangle = \langle \hat{\gamma}^\dagger_{\boldsymbol{k},1}\hat{\gamma}_{\boldsymbol{k},1}\rangle = f(E_{\boldsymbol{k}}),$$

where

$$f(E_{\boldsymbol{k}}) = \frac{1}{e^{\beta E_{\boldsymbol{k}}} + 1}$$

is the Fermi-Dirac distribution with $\beta = 1/k_B T$, and all other thermal averages in Eq. (1.79) are zero. In this way, one obtains:

$$\langle \hat{a}^{\dagger}_{\boldsymbol{k}\uparrow} \hat{a}^{\dagger}_{-\boldsymbol{k}\downarrow} \rangle = -u_{\boldsymbol{k}} v^*_{\boldsymbol{k}} f(E_{\boldsymbol{k}}) + u_{\boldsymbol{k}} v^*_{\boldsymbol{k}} (1 - f(E_{\boldsymbol{k}})), \tag{1.80}$$

which can be used to rewrite the constant $\mathcal{H}_0$ in Eq. (1.77) as follows:

$$\mathcal{H}_0 = \sum_{\boldsymbol{k}} \{\xi_{\boldsymbol{k}} - E_{\boldsymbol{k}} + \Delta_{\boldsymbol{k}} u_{\boldsymbol{k}} v^*_{\boldsymbol{k}} [1 - 2f(E_{\boldsymbol{k}})]\}. \tag{1.81}$$

At zero temperature $f(E_{\boldsymbol{k}}) = 0$ for all $\boldsymbol{k}$, and thus the mean-field Hamiltonian, Eq. (1.77), takes the following form:

$$\begin{aligned} \hat{H}_{MF} &= \sum_{\boldsymbol{k}} E_{\boldsymbol{k}} (\hat{\gamma}^{\dagger}_{\boldsymbol{k},0} \hat{\gamma}_{\boldsymbol{k},0} + \hat{\gamma}^{\dagger}_{\boldsymbol{k},1} \hat{\gamma}_{\boldsymbol{k},1}) \\ &+ \sum_{\boldsymbol{k}} (\xi_{\boldsymbol{k}} - E_{\boldsymbol{k}} + \Delta_{\boldsymbol{k}} u_{\boldsymbol{k}} v^*_{\boldsymbol{k}}). \end{aligned} \tag{1.82}$$

Since there are no excitations present at zero temperature, it follows that $\langle \hat{\gamma}^{\dagger}_{\boldsymbol{k},0} \hat{\gamma}_{\boldsymbol{k},0} \rangle = \langle \hat{\gamma}^{\dagger}_{\boldsymbol{k},1} \hat{\gamma}_{\boldsymbol{k},1} \rangle = 0$. At finite temperatures, one can create excitations by breaking up the Cooper pairs. When the temperature is high enough, these excitations will eventually kill the superconductivity.

A useful way to picture the results of the BCS theory is that at $T = 0$ all of the electrons are paired. As one increases the temperature, thermal fluctuations destroy more and more Cooper pairs, creating excitations. Above T_c, all of the Cooper pairs are broken up and the superconductivity is completely destroyed. Since the Cooper pairs break up into pairs of excitations, the minimum energy associated with this process is 2Δ, which is consistent with the optical experiments mentioned in Sec. 1.1.

We should note that the overall phase of the gap function $\Delta_{\boldsymbol{k}}$ can be rotated by an arbitrary amount since it is not measureable. In particular, it can always be made real and positive, which we assume from this point on. Furthermore, the gap function depends on temperature through the thermal average $\langle \hat{b}_{\boldsymbol{k}} \rangle$, see Eq. (1.72), which is related to the pair wavefunction, and thus one would expect that $\Delta_{\boldsymbol{k}} \to 0$ for $T > T_c$. Furthermore, one can also expect that as the temperature increases excitations are created, and thus the energy gap shrinks, making it easier to create more excitations.

We focus now on the temperature-dependent gap equation for $\Delta_{\boldsymbol{k}}$. Using Eqs. (1.47), (1.76), and (1.80), and the fact that $\langle \hat{b}_{\boldsymbol{k}} \rangle = \langle \hat{b}^{\dagger}_{\boldsymbol{k}} \rangle^{*}$, it immediately follows that

$$\langle \hat{b}_{\boldsymbol{k}} \rangle = \frac{\Delta_{\boldsymbol{k}}}{2E_{\boldsymbol{k}}} \tanh\left(\frac{\beta E_{\boldsymbol{k}}}{2}\right).$$

Using this last expression in Eq. (1.72) yields the following gap equation:

$$\Delta_{\boldsymbol{k}} = -\frac{1}{\mathcal{V}} \sum_{\boldsymbol{k}'} V(\boldsymbol{k}, \boldsymbol{k}') \frac{\Delta_{\boldsymbol{k}'}}{2E_{\boldsymbol{k}'}} \tanh\left(\frac{\beta E_{\boldsymbol{k}'}}{2}\right). \tag{1.83}$$

This is a nonlinear integral equation for $\Delta_{\boldsymbol{k}}$, which has at least one solution that is trivial, i.e. $\Delta_{\boldsymbol{k}} = 0$ at all $\boldsymbol{k}$. This solution corresponds to the normal state at all temperatures and clearly does not describe superconductivity.

We look for a nontrivial solution of Eq. (1.83), in which $\Delta_{\boldsymbol{k}} \neq 0$. To proceed further, we make the BCS assumption about the pairing potential $V(\boldsymbol{k}, \boldsymbol{k}') = -V_0 \Theta(\epsilon_c - |\xi_{\boldsymbol{k}}|)\Theta(\epsilon_c - |\xi_{\boldsymbol{k}'}|)$, which allows us to look for a solution for $\Delta_{\boldsymbol{k}}(T)$ which is a product of the same terms as in the zero-temperature case, see Eq. (1.62):

$$\Delta_{\boldsymbol{k}}(T) = \Delta(T)\Theta(\epsilon_c - |\xi_{\boldsymbol{k}}|), \tag{1.84}$$

i.e. all of the $\boldsymbol{k}$-dependence is contained in the Heaviside step function. Substituting these assumptions for $V(\boldsymbol{k}, \boldsymbol{k}')$ and $\Delta_{\boldsymbol{k}}$ into Eq. (1.83), we obtain the following nonlinear integral equation:

$$1 = \frac{V_0}{2\mathcal{V}} \sum_{\boldsymbol{k}'} \Theta(\epsilon_c - |\xi_{\boldsymbol{k}'}|) \frac{1}{E_{\boldsymbol{k}'}} \tanh\left(\frac{\beta E_{\boldsymbol{k}'}}{2}\right). \tag{1.85}$$

Taking the thermodynamic limit and introducing the Fermi level density of states, we can transform the momentum summation in this last expression into an integral over the energy, and arrive at the BCS gap equation for $\Delta(T)$:

$$\frac{1}{N_F V_0} = \int_0^{\epsilon_c} d\xi \frac{\tanh\left(\sqrt{\xi^2 + \Delta^2}/2k_B T\right)}{\sqrt{\xi^2 + \Delta^2}}. \tag{1.86}$$

Here we have used the fact that the integrand is even to change the integration limits.

We point out that the analytical solution to Eq. (1.86) is unknown. To make progress, we note that there is a temperature above which $\Delta = 0$, defined as the critical temperature T_c. We make the assumption, which is justified by the subsequent calculation, that Δ is continuous at $T = T_c$, and thus $\Delta = 0$ near the critical temperature. One can therefore evaluate the integral in Eq. (1.86) at $T = T_c$ and $\Delta = 0$ to obtain the critical temperature, and this is facilitated by making the change of variables $z = \xi/2k_BT_c$. In this way, one finds that

$$\frac{1}{N_F V_0} = \ln\left(\frac{2e^{\gamma}}{\pi}\frac{\epsilon_c}{k_B T_c}\right), \tag{1.87}$$

where $\gamma \approx 0.577\ldots$ is the Euler constant. One can see that the BCS cutoff cannot be replaced by infinity due to the logarithmic divergence of the integral in Eq. (1.86). By inverting Eq. (1.87), we obtain the following expression for the critical temperature:

$$k_B T_c = \frac{2e^{\gamma}}{\pi}\epsilon_c e^{-1/N_F V_0} \simeq 1.13\epsilon_c e^{-1/N_F V_0}, \tag{1.88}$$

which has a similar structure as the bound-state energy in Cooper's theorem, see Eq. (1.36). Both expressions are non-analytic in V_0, and thus cannot be calculated perturbatively in the pairing interaction.

We note that ϵ_c is of the order of the Debye frequency, and if the electron pairing is due to phonons, then $\epsilon_c = \hbar\omega_D \sim M^{-1/2}$, where M is the mass of the lattice ions. Thus the BCS theory reproduces the isotope effect, in particular the transition temperature varies as $T_c \sim M^{-1/2}$. We note that in the effective interaction in Eq. (1.40), one can show that the coupling constant $|g_{\text{eff}}|^2 \sim 1/(M\omega_D^2)$, which is independent of M [21]. Thus the coupling constant in the BCS theory, see Eq. (1.46), is independent of the mass of the ions, and the isotope effect arises in the BCS theory because the thickness of the energy shell around the Fermi surface is $\hbar\omega_D$, which is mass-dependent [21].

By taking the ratio of the gap function at zero temperature, Eq. (1.65), and expression (1.88), one finds

$$\frac{\Delta(T=0)}{k_B T_c} = \frac{\pi}{e^{\gamma}} \simeq 1.76. \tag{1.89}$$

This is the celebrated "universal BCS ratio", which is the same for all conventional superconductors. As discussed previously, one can experimentally measure both $\Delta(T = 0)$ and the transition temperature, and the deviation of their ratio from 1.76 tells us how "non-BCS" the superconductor is.

Although the derivation is beyond the scope of this work, we give the result for $\Delta(T)$ near the critical temperature, which has the following form [10]:

$$\frac{\Delta(T)}{\Delta(0)} \simeq \frac{e^{\gamma}}{\pi}\left(\frac{8\pi^2}{7\zeta(3)}\right)^{1/2}\left(\frac{T_c - T}{T_c}\right)^{1/2}, \tag{1.90}$$

where

$$\zeta(s) = \sum_{n=1}^{\infty}\frac{1}{n^s}$$

is the Riemann zeta function. We see that expression (1.90) is indeed a continuous function of temperature, vanishing at $T \geq T_c$.

One can use the general theory above to calculate the thermodynamic quantities. Specifically, we calculate the electronic contribution to the specific heat of a BCS superconductor. The specific heat C is related to the entropy S and temperature T of a system as follows:

$$C = T\frac{\partial S}{\partial T}. \tag{1.91}$$

Since all the pairs are condensed into the same coherent quantum state, their contribution to the entropy of the system is zero at all temperatures. The entropy is determined by thermally excitated quasiparticles, which form an ideal Fermi gas. This allows us to write the entropy of the system as follows:

$$S = -2k_B \sum_{\boldsymbol{k}} \{[1 - f(E_{\boldsymbol{k}})] \ln[1 - f(E_{\boldsymbol{k}})] + f(E_{\boldsymbol{k}}) \ln f(E_{\boldsymbol{k}})\}, \tag{1.92}$$

where the factor of 2 arises due to the fact that we have two species of fermionic excitations, see Eq. (1.77). We note that from this last expression, the total entropy at zero temperature is zero. After substitution of Eq. (1.92) into Eq. (1.91), we find that the specific heat takes the following form:

$$C = 2\sum_{\boldsymbol{k}} E_{\boldsymbol{k}} \frac{\partial f(E_{\boldsymbol{k}})}{\partial T}, \tag{1.93}$$

where $E_{\boldsymbol{k}} = \sqrt{\xi_{\boldsymbol{k}}^2 + \Delta_{\boldsymbol{k}}^2}$. Since Δ is temperature-dependent, this makes all the difference from a regular metal, in which the excitation energy does not depend on temperature. After carrying out the differentiation in Eq. (1.93), one finds the following:

$$C = 2k_B\beta \sum_{\boldsymbol{k}} \left(-\frac{\partial f}{\partial E_{\boldsymbol{k}}}\right) \left(E_{\boldsymbol{k}}^2 - T\Delta_{\boldsymbol{k}} \frac{\partial \Delta_{\boldsymbol{k}}}{\partial T}\right). \tag{1.94}$$

The second term in this last expression arises only in the superconducting state.

We first examine the specific heat in the case of low temperatures. It follows from the gap equation (1.86) that $\Delta(T)$ is nearly flat for $T \ll T_c$, which allows one to neglect the derivative of $\Delta_{\boldsymbol{k}}$ in Eq. (1.94). Furthermore, in the thermodynamic limit, we can rewrite the summation as an integral over $\boldsymbol{k}$, and introducing the density of states, as an integral over the energy as follows:

$$C(T) = \mathcal{V}\frac{N_F}{2k_BT^2}\int_{-\infty}^{+\infty} d\xi \frac{\xi^2 + \Delta^2}{\cosh^2\left(\sqrt{\xi^2+\Delta^2}/2k_BT\right)}. \tag{1.95}$$

The function $1/\cosh^2(\dots)$ is sharply peaked, and thus only energies $\sqrt{\xi^2+\Delta^2} \leq k_BT$ contribute significantly to the integral. Since $T \ll T_c \sim \Delta(0)/k_B$, see Eq. (1.89), it follows that $k_BT \ll \Delta(0)$ and we can therefore replace $E_{\boldsymbol{k}}$ with Δ in the argument of $\cosh^2(\dots)$. In this way, we arrive at the following expression for the specific heat:

$$C(T) \sim \frac{1}{T^2}e^{-\Delta/k_BT}, \tag{1.96}$$

which has the characteristic exponential dependence on the temperature, as observed in thermal experiments. We see that, while the first factor $1/T^2$ diverges at low temperatures, this divergence is cancelled by the much quicker decaying exponential function.

At the transition temperature, according to experiment, $C(T)$ is not defined because there is a jump here. This jump separates the low-temperature exponential behaviour from the normal Fermi-gas linear behaviour that occurs at $T > T_c$. We can calculate this jump by considering the specific heat immediately above and below the transition temperature.

We note that slightly above T_c, $\Delta = \partial\Delta/\partial T = 0$ and this allows one to neglect the second term in Eq. (1.94). Using Eq. (1.95) with $\Delta \to 0$, the normal-state specific heat then takes the following form:

$$\frac{C_n}{\mathcal{V}} = \frac{N_F}{2k_BT^2}\int_{-\infty}^{+\infty} d\xi \frac{\xi^2}{\cosh^2(\xi/2k_BT)} = \frac{2\pi^2}{3}k_B^2N_FT, \tag{1.97}$$

immediately above T_c. This linear dependence is exactly what we expect for the specific heat of an ideal Fermi gas.

Slightly below the critical temperature, the energy gap Δ is small, allowing one to set $\Delta = 0$, i.e. $E_{\boldsymbol{k}} \to \xi_{\boldsymbol{k}}$ in the first term in Eq. (1.94), and then this term is equivalent to the expression we obtained in Eq. (1.97). We then find that the difference in the specific heat between the normal and superconducting states is given by

$$C_s(T) - C_n(T) = -\frac{\beta}{2}\sum_{\boldsymbol{k}} \frac{1}{\cosh^2(\beta E_{\boldsymbol{k}}/2)}\Delta_{\boldsymbol{k}}\frac{\partial \Delta_{\boldsymbol{k}}}{\partial T}. \tag{1.98}$$

By observing that the jump in the specific heat comes from the derivative of the gap function [i.e. $\partial\Delta_{\boldsymbol{k}}/\partial T$ is infinite at $T = T_c$, as seen from Eq. (1.90)], one can set $\Delta = 0$ in the argument of $\cosh^2(\dots)$ in Eq. (1.98). Furthermore, we take the thermodynamic limit and change the momentum integral to one over the energy. In this way, one obtains the following expression for the jump in the specific heat:

$$\frac{C_s - C_n}{\mathcal{V}} = -\frac{\beta N_F}{4}\int_{-\epsilon_c}^{+\epsilon_c} d\xi \frac{1}{\cosh^2(\beta\xi/2)}\frac{\partial(\Delta^2)}{\partial T}. \tag{1.99}$$

Since $1/\cosh^2(\dots)$ is sharply peaked within the width $\sim k_BT$, and $\epsilon_c \gg k_BT_c$, most of the contribution comes from within the peak, which allows us to safely extend the integration limits to $\pm\infty$ in Eq. (1.99). Evaluation of the resulting integral then allows one to rewrite the jump in the specific heat as follows:

$$\frac{C_s - C_n}{\mathcal{V}} = N_F\left(-\frac{\partial\Delta^2}{\partial T}\right)\Bigg|_{T\to T_c^-}. \tag{1.100}$$

Using Eq. (1.90), we can evalulate the derivative of the energy gap, allowing one to write the jump in the specific heat in the following form:

$$\frac{\Delta C}{\mathcal{V}} = \frac{C_s - C_n}{\mathcal{V}}\Bigg|_{T\to T_c^-} = \frac{8e^{2\gamma}}{7\zeta(3)}\frac{\Delta^2(0)}{T_c}N_F. \tag{1.101}$$

Using this last expression along with Eqs. (1.89) and (1.97), we can recover another universal BCS ratio:

$$\frac{\Delta C}{C_n} = \frac{12}{7\zeta(3)} \simeq 1.43. \tag{1.102}$$

This result has been confirmed by measurements of the specific heat in many conventional superconductors [10].

The BCS model of superconductivity is a revolutionary theory because it was capable of fully describing all of the superconducting materials known at the time of its development. Bardeen, Cooper, and Schrieffer were awarded the Nobel Prize in physics in 1972 for this theory, which allowed one to finally understand what is happening in SCs at the microscopic level. The BCS theory enables one to theoretically explain the experimental properties exhibited by these so-called “conventional superconductors”, in which the electrons pair in the singlet s-wave state.

It turns out, however, that conventional SCs represent only a fraction of known superconductors, and that most newer materials belong to the class of unconventional SCs, in which the pairing is not of the singlet s-wave form. These materials include heavy-fermion SCs (UPt$_3$, CeCoIn$_5$, etc.), organic SCs, alkali-doped fullerenes (C$_{60}$), as well as the high-T_c superconductors (the copper oxides and iron pnictides). Since the late 1970's there has been an explosion in the number of known superconductors, and materials of particular current interest include strontium ruthenate (Sr_2RuO_4), ferromagnetic superconductors, non-centrosymmetric SCs, and multi-band SCs [27].

Most of the fundamental research currently focuses on the unconventional superconductors. Consequently, in the next subsection we will give an overview of the important concepts used to characterize the different pairing possibilities in these systems. Specifically, we discuss a two-particle wavefunction in which the Cooper pairs have zero center-of-mass momentum, but with a non-BCS pairing. Then, in Sec. 3, we will apply these symmetry insights to general nonuniform states in the many-body problem, to derive the Bogoliubov-de Gennes (BdG) equations for the quasiparticle excitation spectrum.

1.4 Unconventional pairing

In general, since electrons with opposite momenta $(\boldsymbol{k}, -\boldsymbol{k})$ sufficiently close to the Fermi surface form Cooper pairs, we can represent the wavefunction of a pair of electrons in the form $\Psi_{pair} = \langle \boldsymbol{k}, \boldsymbol{k}' | \Psi \rangle = \delta_{\boldsymbol{k}',-\boldsymbol{k}} \Psi(\boldsymbol{k})$, where $\Psi(\boldsymbol{k}) = g_{\uparrow\uparrow}(\boldsymbol{k}) | \uparrow\uparrow\rangle + g_{\uparrow\downarrow}(\boldsymbol{k}) | \uparrow\downarrow\rangle + g_{\downarrow\uparrow}(\boldsymbol{k}) | \downarrow\uparrow\rangle + g_{\downarrow\downarrow}(\boldsymbol{k}) | \downarrow\downarrow\rangle$. This expression can be reformulated in a short-hand matrix notation as follows:

$$\hat{g} = \begin{pmatrix} g_{\uparrow\uparrow}(\boldsymbol{k}) & g_{\uparrow\downarrow}(\boldsymbol{k}) \\ g_{\downarrow\uparrow}(\boldsymbol{k}) & g_{\downarrow\downarrow}(\boldsymbol{k}) \end{pmatrix}, \tag{1.103}$$

where we have explicitly renamed the matrix to stress that $\hat{g}$ is not *literally* the wavefunction of the pair. In a superconducting material with multiple Cooper pairs, the order parameter is related to the pair wavefunction, and will be mathematically introduced in Sec. 3.1. For now, we focus on the single-pair case to lay the foundation of our explanation of the spin-matrix basis functions $\hat{\phi}_a(\boldsymbol{k})$.

Since in the BCS theory only electrons near the Fermi surface with opposite momenta form Cooper pairs, exchanging particle momenta is equivalent to setting $\boldsymbol{k} \to -\boldsymbol{k}$. The exchange of particle labels is accomplished by interchanging both momenta (or position) and spin. Therefore to preserve the condition of anti-symmetry of the wavefunction, if the spin state (matrix) is anti-symmetric with respect to spin exchange (electrons that pair in the singlet ($S = 0$) spin state), then we must have $\hat{g}$ even in $\boldsymbol{k}$, i.e. $\hat{g}(-\boldsymbol{k}) = \hat{g}(\boldsymbol{k})$. In this case, $\hat{g}$ can be written in terms of the antisymmetric Pauli matrix: $\hat{g}^s = g(\boldsymbol{k}) i\hat{\sigma}_2$, where we have only one distinct function $g(\boldsymbol{k})$ since the weighting of the $| \uparrow\downarrow\rangle, | \downarrow\uparrow\rangle$ states must be equivalent for $S_z = 0$.

In an isotropic system, we can expand the functions $g(\boldsymbol{k})$ in terms of the spherical harmonics $Y_{\ell m}$ with orbital angular momentum ℓ and its z-projection m as $g(\boldsymbol{k}) = \sum_{m=-\ell}^{\ell} a_{\ell m} Y_{\ell m}$, and then $\hat{g}$ takes the form:

$$\hat{g}^s = \sum_{m=-\ell}^{\ell} a_{\ell m} Y_{\ell m}(\hat{\boldsymbol{k}}) i\hat{\sigma}_2. \tag{1.104}$$

Here $\ell = 0, 2, 4, ...$ corresponds to the traditional atomic states labelled by the letters $s, d, g, ...$, and $\hat{\boldsymbol{k}} = \boldsymbol{k}/k_F$ is a unit vector. The coefficients $a_{\ell m}$ represent the superconductor order parameter, and in non-uniform cases are functions of position. In the case of conventional singlet s-wave pairing, the order parameter is a single complex function, whereas for d-wave pairing the order parameter consists of five complex functions.

For electrons that pair in the symmetric spin-triplet state ($S = 1$), we can express $\hat{g}$ in terms of the basis of symmetric spin matrices $i\hat{\boldsymbol{\sigma}}\hat{\sigma}_2$ as $\hat{g}^t = i(\hat{\boldsymbol{\sigma}}\hat{\sigma}_2) \cdot \tilde{\boldsymbol{d}}(\boldsymbol{k}) = (\tilde{d}_x(\boldsymbol{k})\hat{\sigma}_1 + \tilde{d}_y(\boldsymbol{k})\hat{\sigma}_2 + \tilde{d}_z(\boldsymbol{k})\hat{\sigma}_3) i\hat{\sigma}_2$, where $\tilde{\boldsymbol{d}}(\boldsymbol{k})$ is the single-pair spin vector, and $\hat{\boldsymbol{\sigma}}$ is the vector of Pauli spin matrices. The single-pair spin vector must be odd in $\boldsymbol{k}$, $\tilde{\boldsymbol{d}}(-\boldsymbol{k}) = -\tilde{\boldsymbol{d}}(\boldsymbol{k})$, and it is related to the components of $\hat{g}$ as follows: $g_{\uparrow\uparrow} = -\tilde{d}_x + i\tilde{d}_y$, $g_{\uparrow\downarrow} = g_{\downarrow\uparrow} = \tilde{d}_z$, $g_{\downarrow\downarrow} = \tilde{d}_x + i\tilde{d}_y$.

As in the spin-singlet case, we can expand the components of the spin vector in terms of the spherical harmonics in an isotropic system: $\tilde{d}_\alpha(\boldsymbol{k}) = \sum_{m=-\ell}^{\ell} b_{\ell m}^{\alpha} Y_{\ell m}(\hat{\boldsymbol{k}})$, where the coefficients $b_{\ell m}^{\alpha}$ represent the superconductor order parameter for a given value of quantum number ℓ. We can then express the matrix $\hat{g}$ for the triplet pairing state as

$$\begin{aligned} \hat{g}^t &= \sum_{m=-\ell}^{\ell} Y_{\ell m}(\hat{\boldsymbol{k}})(\hat{\boldsymbol{\sigma}} \cdot \boldsymbol{b}_{\ell m}) i\hat{\sigma}_2 \\ &= \sum_{m=-\ell}^{\ell} Y_{\ell m}(\hat{\boldsymbol{k}})\,(b_{\ell m}^{x}\hat{\sigma}_1 + b_{\ell m}^{y}\hat{\sigma}_2 + b_{\ell m}^{z}\hat{\sigma}_3)\, i\hat{\sigma}_2, \end{aligned} \tag{1.105}$$

and for the odd spherical harmonics, one has $\ell = 1, 3, ...$, corresponding to $p, f, ...$-wave states. For the simplest triplet pairing (p-wave orbital), the order parameter is a set of nine complex functions, labelled by $\alpha = x, y, z$ and $m = -1, 0, 1$. This pairing state is realized in ^{3}He, see, for example, Refs. [28] and [18].

In general, the spin component of the wave function of a Cooper pair can be a superposition of the states with spin $S = 0$ and $S = 1$, and hence $\hat{g} = a_s\hat{g}^s + a_t\hat{g}^t$, where $a_{s/t}$ are arbitrary complex coefficients. This can happen if there is no inversion center in a crystal [18]; however in a centrosymmetric crystal only a definite spin state is realized.

In view of Eqs. (1.104) and (1.105), the choice of reference frame is arbitrary since the spherical harmonics obtained after a rotation of the reference frame in three-dimensional space are related to the spherical harmonics with the same orbital angular momentum ℓ as follows:

$$Y_{\ell m}(\hat{\boldsymbol{k}}') = \sum_{m'=-\ell}^{\ell} R_{mm'} Y_{\ell m'}(\hat{\boldsymbol{k}}), \tag{1.106}$$

i.e. it is simply a linear superposition, and here $R_{mm'}$ are components of a 3×3 matrix which characterizes the rotation. In general, a set of functions $\varphi_a(\boldsymbol{r})$ forms a basis of an irreducible representation (IREP) Γ of a certain spatial symmetry group G if any $\varphi_a(\boldsymbol{r})$ is transformed under any symmetry operation of G to a linear combination of the functions belonging to the set [18]:

$$\varphi_a(g\boldsymbol{r}) = \varphi_a(\boldsymbol{r}') = \sum_{b=1}^{d_\Gamma} c_{ab}\varphi_b(\boldsymbol{r}), \tag{1.107}$$

where in this last expression, $g\boldsymbol{r} \to \boldsymbol{r}'$ corresponds to reflections, rotations, inversions and combinations of these three operations, and d_Γ is the dimensionality of the set $\{\varphi_a\}$, i.e. of the irreducible representation Γ.

Recall that for an isotropic system, the matrix $\hat{g}$ can be expanded in terms of the spherical harmonics, Eqs. (1.104) and (1.105). Thus in the isotropic case, i.e. when the system is invariant under all spatial rotations, forming the group SO_3, Γ is labelled by the orbital angular momentum ℓ, and for each type of pairing (i.e. for each value of ℓ), there is a one-to-one correspondence with the IREPs of SO_3. Consequently, the dimensionality d_Γ is given by the degeneracy of the orbital angular momentum states, $d_\Gamma = 2\ell + 1$, and the basis functions are nothing but the spherical harmonics. For example, if $\Gamma = \ell = 1$ (p-wave pairing), then the basis functions are given by $Y_{1,1}(\theta, \varphi), Y_{1,0}(\theta, \varphi)$, and $Y_{1,-1}(\theta, \varphi)$, where θ, φ are the usual spherical polar angles of the unit vector $\hat{\boldsymbol{k}}$. Alternatively, we can take a linear combination of these spherical harmonics and use as the basis functions the components of the unit vector $\hat{\boldsymbol{k}}$: $\hat{k}_x, \hat{k}_y$, and $\hat{k}_z$.

One can still use this classification procedure when the normal state is anisotropic, which is generally the case in a crystal lattice. In this case, there is still a direct correspondence between the IREPs of the point group G of the crystal and the types of pairing states. In fact, superconducting states with different values of T_c are described by basis functions belonging to different IREPs Γ of the point symmetry group G of the solid, that is $T_c = T_c(\Gamma)$. It is the superconducting state corresponding to the highest critical temperature which is actually realized in the crystal [18].

In the anisotropic case, the components of the pair matrix $\hat{g}$ are expanded in terms of the basis functions of the irreducible representation Γ. In the case of singlet pairing, we have:

$$g(\boldsymbol{k}) = \sum_{a=1}^{d_\Gamma} \eta_a \varphi_a^{\Gamma_g}(\hat{\boldsymbol{k}}), \tag{1.108}$$

where η_a are complex coefficients, and superscript Γ_g denotes the fact that the basis functions are even in $\boldsymbol{k}$. Recall the form for the matrix $\hat{g}$ corresponding to a pair in the singlet state: $\hat{g}^s = g(\boldsymbol{k}) i\hat{\sigma}_2$. We introduce the spin-matrix basis functions for the singlet pairing $\hat{\phi}_a^s(\boldsymbol{k}) = (i\hat{\sigma}_2)\varphi_a^{\Gamma_g}(\hat{\boldsymbol{k}})$, and from Eq. (1.108), it then follows that

$$\hat{g}^s = \sum_{a=1}^{d_\Gamma} \eta_a \hat{\phi}_a^s(\boldsymbol{k}). \tag{1.109}$$

For the triplet pairing, we can expand the single-pair spin vector $\tilde{\boldsymbol{d}}(\boldsymbol{k})$ in terms of the odd basis functions of Γ, $\varphi_a^{\Gamma_u}(\hat{\boldsymbol{k}})$. In the case of negligible spin-orbit coupling, the appropriate expansion is given by

$$\tilde{\boldsymbol{d}}(\boldsymbol{k}) = \sum_{a=1}^{d_\Gamma} \boldsymbol{\eta}_a \varphi_a^{\Gamma_u}(\hat{\boldsymbol{k}}), \tag{1.110}$$

where $\boldsymbol{\eta}_a$ are complex vectors, and superscript Γ_u denotes the fact that the basis functions are odd in $\boldsymbol{k}$. In this limit, the pair states are degenerate with respect to rotation of spin vectors, i.e. they correspond to the same energy. Under a spin rotation, we have:

$$\eta_a^\alpha \to \tilde{\eta}_a^\alpha = \sum_{\beta=1}^{3} R_{\alpha\beta}^s \eta_a^\beta, \tag{1.111}$$

where $\alpha = 1, 2, 3$ label the vector components of $\boldsymbol{\eta}_a$, and here superscript s denotes the rotation in spin space characterized by the 3×3 matrix $\hat{R}^s$.

In the case of strong spin-orbit coupling, which occurs in materials containing chemical elements with large atomic numbers, it is convenient to expand $\tilde{\boldsymbol{d}}(\boldsymbol{k})$ in the following way:

$$\tilde{\boldsymbol{d}}(\boldsymbol{k}) = \sum_{a=1}^{d_\Gamma} \eta_a \boldsymbol{\varphi}_a^{\Gamma_u}(\hat{\boldsymbol{k}}), \tag{1.112}$$

where $\boldsymbol{\varphi}_a^{\Gamma_u}(\hat{\boldsymbol{k}}) = \varphi_a^x(\hat{\boldsymbol{k}})\hat{x} + \varphi_a^y(\hat{\boldsymbol{k}})\hat{y} + \varphi_a^z(\hat{\boldsymbol{k}})\hat{z}$ are the vector basis functions which are odd in $\boldsymbol{k}$. Due to the strong spin-orbit coupling, the basis in spin space is defined by the axial unit vectors $\hat{x}, \hat{y}, \hat{z}$ which are uniquely determined by the crystal axes [29, 18]. Although electron spin is not a "good" quantum number in the case of strong spin-orbit coupling, electron states are doubly degenerate as a result of the Kramer's degeneracy due to time reversal symmetry. This allows one to classify electrons in terms of a pseudospin, and so in this limit "spin-singlet" and "spin-triplet" should be understood in terms of this pseudospin.

We can use the expression introduced previously for $\hat{g}^t$ in terms of the spin vector, $\hat{g}^t = (i\hat{\boldsymbol{\sigma}}\hat{\sigma}_2) \cdot \tilde{\boldsymbol{d}}(\boldsymbol{k})$, along with Eq. (1.110) to obtain:

$$\hat{g}^t = \sum_{a=1}^{d_\Gamma} \varphi_a^{\Gamma_u}(\hat{\boldsymbol{k}})(i\hat{\boldsymbol{\sigma}}\hat{\sigma}_2) \cdot \boldsymbol{\eta}_a, \tag{1.113}$$

in the limit of weak spin-orbit coupling. Analogously, we obtain the following expression for $\hat{g}^t$:

$$\hat{g}^t = \sum_{a=1}^{d_\Gamma} \eta_a (i\hat{\boldsymbol{\sigma}}\hat{\sigma}_2) \cdot \boldsymbol{\varphi}_a^{\Gamma_u}(\hat{\boldsymbol{k}}), \tag{1.114}$$

in the limit of strong spin-orbit coupling. In this case, it is convenient to introduce a spin-matrix basis function for the triplet pairing given by $\hat{\phi}_a^t(\boldsymbol{k}) = (i\hat{\boldsymbol{\sigma}}\hat{\sigma}_2) \cdot \boldsymbol{\varphi}_a^{\Gamma_u}(\hat{\boldsymbol{k}})$, and then Eq. (1.114) takes the form:

$$\hat{g}^t = \sum_{a=1}^{d_\Gamma} \eta_a \hat{\phi}_a^t(\boldsymbol{k}). \tag{1.115}$$

The set of coefficients η_a or $\boldsymbol{\eta}_a$ in the expansions of $g(\boldsymbol{k})$ or $\tilde{\boldsymbol{d}}(\boldsymbol{k})$ play the role of the order parameter in crystalline superconductors. One can therefore conclude that it is possible to have states with one-component order parameters $\eta = |\eta|e^{i\phi}$ (with ϕ an arbitrary phase), as well as states described by multicomponent order parameters. The number of components in the order parameter is related to both the dimensionality of the particular IREP, d_Γ, as well as the structure of the complex coefficients (η_a or $\boldsymbol{\eta}_a$) themselves. For example, in the case of a scalar η_a and a two-dimensional irreducible representation one has a two-component order parameter. In the case of complex vector coefficients [Eq (1.113)] in a two-dimensional IREP, one has a six-component order parameter, since $\boldsymbol{\eta}_a$ is a vector in three spin dimensions. In this work we primarily focus on the pairing corresponding to the irreducible representation E_u of the group D_{4h}, in the strong spin-orbit coupling case. While there are different kinds of order parameter vectors, we assume that $\tilde{\boldsymbol{d}}(\boldsymbol{k}) = \eta_1(k_x/k_F)\hat{z} + \eta_2(k_y/k_F)\hat{z}$ (for a cylindrical Fermi surface characterized by the Fermi wavevector k_F). Due to the structure of the basis functions, the two-component complex order parameter vector $\boldsymbol{\eta} = (\eta_1, \eta_2)$ transforms like a vector in real space.

The symmetry group $\mathcal{G}$ of the normal state contains, in addition to the point symmetry group G, also the operation of time reversal R and the gauge transformations $U(1)$, i.e. $\mathcal{G} = G \times R \times U(1)$. Since the Cooper pairs exhibit phase coherence, the states with different phases are distinguishable, and this is often coined "breaking of gauge symmetry $U(1)$". Breaking of other symmetry properties of a system under the operations of $\mathcal{G}$ is also possible as a result of the transition into a particular superconducting state, and this additional symmetry breaking is the defining feature of unconventional superconductivity or superfluidity. Due to this additional symmetry breaking, only invariance under symmetry operations of the subgroup H (associated with the particular superconducting class) of the symmetry group $\mathcal{G}$ persist in the superconducting state, see Refs. [18] and [30].

We can therefore reduce the problem of determining all the possible superconducting states to the determination of the superconducting classes corresponding to different types of the normal-state symmetry breaking. The conventional superconducting state (singlet, s-wave pairing) has the full point symmetry of the crystal lattice, and therefore belongs to the identity representation A_{1g}. In other words, the wave function of the pair remains invariant under all operations of the point symmetry group. As a result, this type of superconductivity is described by trivial superconducting class $H = G \times R$, i.e. only the gauge symmetry is broken. For other superconducting states, which belong to non-identity representations (or odd identity representation A_{1u}), the point symmetry properties are broken, and these states are called nontrivial or unconventional superconducting states.

1.5 Chiral p-wave superconductivity

The s-wave superconducting state is appropriately called conventional because it is, in many senses, the simplest pairing state. As we have seen, there is a relationship between the binding state of the Cooper pairs and the symmetry-breaking properties of the condensate [31], and thus the order parameter of the superconducting phase transition is related to the gap function $\Delta(\boldsymbol{k})$. In the s-wave pairing, the phase of the order parameter is constant for all directions of $\boldsymbol{k}$; however, there may be anisotropy in the magnitude of the order parameter depending on $\boldsymbol{k}$ [31]. This is related to the gauge-symmetry breaking that occurs at the transition temperature, while no other symmetry is broken in the conventional state.

When the Cooper pairs have a finite orbital angular momentum (i.e. non s-wave SC), other symmetries of the system are necessarily broken, as briefly discussed in the previous subsection. Since the first experimental observation of superfluid phases of ^{3}He [32], which have p-wave ($\ell = 1$) pairing, interest in "unconventional pairing" has persisted as we continue to discover new exotic materials. This is because, in contrast to the conventional SCs, the mechanisms behind the Cooper pair formation in these systems are not well understood, despite considerable efforts from both theory and experiment. Currently, the most studied examples of unconventional superconductivity are the singlet d-wave pairing (found in the high-T_c SCs) and the triplet p-wave pairing. The triplet pairing, in particular the chiral p-wave state, is not only one of the simplest examples of unconventional pairing, but it also possesses nontrivial topological properties associated with interesting potential applications.

Recent years have seen an increase in interest in topological superconductors and superfluids from both experimental and theoretical facets. This is due to the fact that, while the fermionic excitations in the bulk are fully gapped, topological superconductors and superfluids support gapless quasiparticle excitations localized near inhomogeneities of the order parameter, such as Abrikosov vortices, domain walls, and sample boundaries [33]. Among other things, the quasiparticle excitations protected by topology determine the static and dynamical properties of topological defects, such as domain walls, in these systems. Specifically, the chiral p-wave state has received notable consideration because the quasiparticle excitations (Majorana fermions) and non-Abelian winding statistics associated with half-quantum vortices in this state are potentially useful as a route to quantum computing [34].

The chiral p-wave triplet state, whose order parameter is proportional to $k_x \pm ik_y$, is experimentally realized in the A-phase (Anderson-Brinkman-Morel, or ABM, state [35]) of superfluid ^{3}He, see Ref. [28], as well as the superconducting state of Sr_2RuO_4, see e.g. Refs. [31, 34]. The helium atoms are fermions since they contain an odd number of spin-1/2 particles. Thus, in contrast to the Bose-Einstein condensation, which is responsible for superfluidity in ^{4}He, the superfluidity in ^{3}He results from the formation of Cooper pairs of composite fermions (i.e. the helium atoms), which is largely mediated by van der Waals interactions. This is quite different from the formation of Cooper pairs in superconductors, which are comprised of point-like electrons, with zero orbital angular momentum in the conventional case. Consequently, this superfluid exhibits a rich array of physics, with many nontrivial properties.

The order parameter of a triplet fermionic superfluid is a 2×2 spin matrix which has the following form: $\hat{\Delta}(\boldsymbol{k}) = i\hat{\sigma}_2 \hat{\boldsymbol{\sigma}} \cdot \boldsymbol{d}(\boldsymbol{k})$, where $\hat{\boldsymbol{\sigma}}$ are the Pauli matrices and $\boldsymbol{d}$ is the spin vector (the derivation will be given below in Sec. 3.1). In superfluid ^{3}He, the spin vector $\boldsymbol{d}$ is expanded in terms of the spherical harmonics, or equivalently, the components of the wavevector $\boldsymbol{k}$ as follows: $d_\alpha(\boldsymbol{k}) = A_{\alpha,i}\hat{k}_i$, where $A_{\alpha,i}$ comprise a 3×3 complex matrix [18], and the Einstein summation convention is assumed. It is assumed that the basic ideas of the BCS theory, namely that the superfluidity is due to the formation of pairs of atoms with equal and opposite momenta $(\boldsymbol{k}, -\boldsymbol{k})$, can be applied to ^{3}He. We can see that in this system the order parameter is characterized by nine complex components, in contrast to the single-component order parameter that describes conventional pairing.

In an arbitrary reference frame, the A-phase of superfluid ^{3}He is described by the order parameter of the form $A_{\alpha,i} = V_\alpha(\Delta'_i + i\Delta''_i)$ [18, 28], where $\boldsymbol{V}$ is a unit vector in the spin space, and $\boldsymbol{\Delta}'$ and $\boldsymbol{\Delta}''$ are mutually orthogonal vectors in the coordinate space. Neglecting the weak spin-orbit interaction, in the absence of external magnetic field and far away from the container walls [28], the direction of the quantization axis of the orbital moment $\hat{\boldsymbol{\ell}} = \boldsymbol{\Delta}' \times \boldsymbol{\Delta}''$, and of the unit vector $\boldsymbol{V}$ are arbitrary. The simplest choice is $\boldsymbol{V} = (0,0,1)$, $\boldsymbol{\Delta}' = (1,0,0)$, and $\boldsymbol{\Delta}'' = (0,1,0)$, and then the spin vector has the form

$$\boldsymbol{d}(\boldsymbol{k}) \sim (0, 0, \hat{k}_x + i\hat{k}_y). \tag{1.116}$$

It is easy to see that in this case the orbital quantization axis is directed along $\hat{\boldsymbol{z}}$.

One can alternatively choose, for example, $\boldsymbol{\Delta}'' = (0,-1,0)$ and then the corresponding spin vector has the form

$$\boldsymbol{d}(\boldsymbol{k}) \sim (0, 0, \hat{k}_x - i\hat{k}_y). \tag{1.117}$$

In contrast to the previous choice, in this case the orbital quantization axis is directed along $-\hat{\boldsymbol{z}}$. It turns out that these spin vectors (1.116) and (1.117) correspond to opposite chiral states, which are obtained from each other by time reversal. Consequently, both states correspond to the same energy in the absence of an external field.

From the form of $\boldsymbol{d}$ it is clear that the neutral helium atoms in superfluid ^{3}He-A pair in a state with $S_z = 0$, and there is no nuclear magnetic moment associated with the spin of the Cooper pair. Interestingly enough, electronic-rotational coupling in the Cooper pairs in ^{3}He-A results in a charge distortion in the nucleus, leading to a weak orbital magnetic moment for each pair, which is of the order of 10^{-11} Bohr magnetons per atom [36]. Because the superfluid is in a coherent state described by the same $\hat{\boldsymbol{\ell}}$ for all pairs, there is a resulting weak macroscopic orbital magnetic moment, and this ferromagnetic behaviour has indeed been confirmed in experiments by Paulson and Wheatley [37]. In an external magnetic field, the two chiral states correspond to slightly different energies, and thus the "liquid ferromagnetic behaviour" lifts the energy degeneracy. While the charge distortion in the Cooper pairs leads to a weak ferromagnetic behaviour in this system, the Meissner screening is still absent, as one would expect in a neutral superfluid.

In contrast to the superfluid ^{3}He, it is the electron pairing which is responsible for the superconductivity in Sr_2RuO_4. This compound has a layered tetragonal crystal structure similar to high-T_c cuprates, as illustrated in Fig. 6. As measured by Bergemann *et al.*, strontium ruthenate is described by a quasi-two-dimensional, multiband Fermi surface [38]. The NMR Knight shift experiments, which measure the spin susceptibility, support the Cooper pair formation in the spin-triplet ($S = 1$) state with $S_z = 0$ in this compound [39, 40]. According to μSR measurements, at $T < T_c$ an internal magnetic field emerges, suggesting that in the superconducting state the time-reversal symmetry (TRS) is broken [41]. While there are conflicting experimental results from scanning Hall [42] and scanning SQUID measurements [43], the pairing state is believed to be described by the following parameters: $S = 1, S_z = 0, \ell = 1, \ell_z = \pm 1$, as illustrated in Fig. 7.

Of the allowed p-wave states on a cylindrical Fermi surface for a tetragonal crystal, there is only one triplet pairing state which is unitary (i.e. $\boldsymbol{d} \times \boldsymbol{d}^* = 0$) and also breaks time-reversal symmetry [34]. It is the chiral p-wave state, with $\boldsymbol{d} \sim \hat{\boldsymbol{z}}(k_x \pm i k_y)$, which is equivalent to the ABM state of superfluid ^{3}He. This state is fully gapped at the Fermi surface, as illustrated in Fig. 8. We see that the spin vector in this state is oriented along the z-axis, which is chosen to be the c-axis of the crystal, and this corresponds to the equal-spin pairing in the xy (or ab) plane. The two chiralities (positive and negative) correspond to the ± signs in the above expression for $\boldsymbol{d}$, and to the orbital angular momentum projection $\ell_z = \pm 1$, respectively. What makes Sr_2RuO_4 such an interesting compound is that it exhibits the same rich physics as the ABM state in ^{3}He-A, but with a charged superfluid in a crystalline material at temperatures 1000 times higher than for ^{3}He [34].

In the systems described above, the ground state is two-fold degenerate in the absence of an external magnetic field, and this gives rise to the possibility of superfluid or superconducting states with opposite chirality, separated by a domain wall (DW), to form in different parts of the system [30, 29]. There is in fact experimental evidence of the existence of DWs in Sr_2RuO_4 from Josephson measurements [44, 45], and also in thin films of ^{3}He-A from torsional oscillator measurements [46]. In general, pairing states in other unconventional superconductors can also exhibit discrete degeneracies of the ground state [30, 29], which leads to the possibility of DW formation in these systems.

The formation of a DW costs gradient energy to the system due to the spatial variation of the order parameter. Unlike in ferromagnets, which break up into domains in order to minimize the net magnetic moment, in a neutral superfluid there is no analogous energetic rationale behind the formation of DWs. One possible explanation is that the DWs are spontaneously formed due to sample inhomogeneities during cooling across

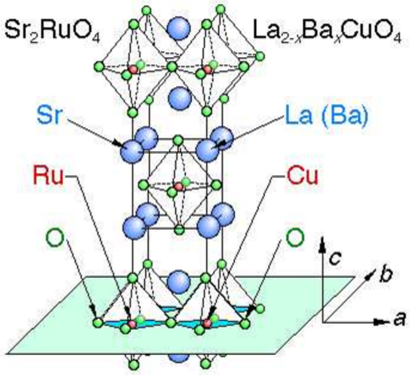
Sr_2RuO_4
$La_{2-x}Ba_xCuO_4$
Sr
La (Ba)
Ru
Cu
O
O
c
b
a

Figure 6: The tetragonal crystal structure of Sr_2RuO_4 compared to that of LBCO. Image reproduced from Ref. [31].

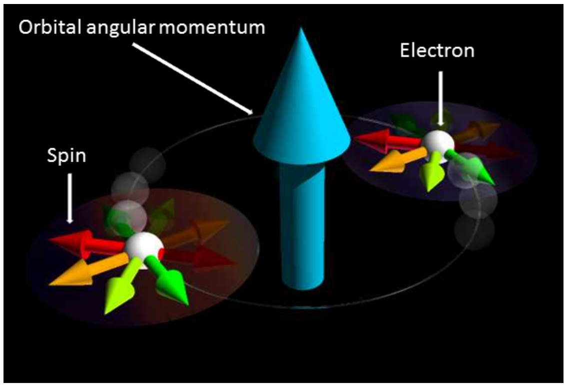
Orbital angular momentum
Electron
Spin

Figure 7: The electron pairing state in superconducting Sr_2RuO_4. The large arrow denotes the direction of $\hat{\boldsymbol{\ell}}$, and the small arrows the spins of the electrons in a pair. The spins lie in the xy plane, and all $\hat{\boldsymbol{\ell}}$ lie along the z-axis. Image reproduced from Ref. [31].

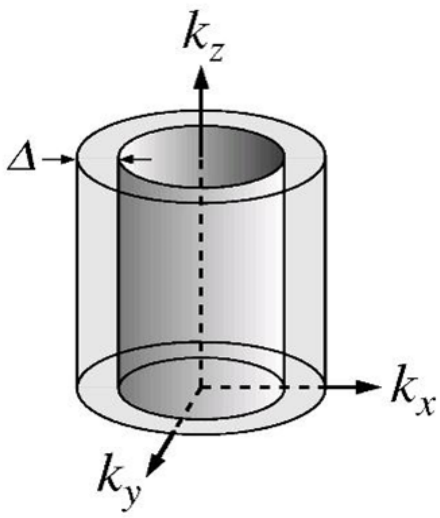

Figure 8: Isotropic excitation energy gap on a cylindrical Fermi surface [31].

the phase transition into the superfluid state. Alternatively, the creation of low-energy quasiparticles bound to the DW may compensate for the increase in gradient energy; this is expected to be particularly effective in one-dimensional systems [47].

In a charged superconductor, on the other hand, the intrinsic rotational motion of the Cooper pairs can result in a nonzero magnetic moment. In a p-wave superconductor, it is given by $\boldsymbol{M} \sim i(\boldsymbol{\eta}^* \times \boldsymbol{\eta})$, where $\boldsymbol{\eta}$ is the complex superconducting order parameter vector. It is easy to verify from this last expression that the two chiral p-wave states in $\mathrm{Sr_2RuO_4}$, $\boldsymbol{\eta} \propto (1, \pm i)$, correspond to opposite orbital magnetic moments, analogous to a uniaxial ferromagnet. Similar to a ferromagnet, domains are formed in zero external field to reduce the energy of the stray magnetic field outside the sample.

One can make progress in the theoretical treatment of superconducting DW textures using the Ginzburg-Landau formalism introduced in Sec. 1.1. The structure of a single DW was studied in Refs. [30, 48, 49, 50, 51, 52, 53, 54, 55]. From the GL calculation, see Appendix A, we have found that there are no stable two-DW solutions, and, consequently, there must be some form of interaction between the DWs. Therefore, either an attraction between two DWs must cause an effective collapse of the DWs to a single domain; or a repulsion between them pushes one of the DWs to infinity, leading to the effective formation of just two domains. It is this interaction which has stimulated our current work.

The purpose of this thesis is to develop a general formalism for calculating the interaction between superconducting DWs at an arbitrary temperature. We introduce the two-DW configuration in Sec. 2, for which we will ultimately determine the interaction energy. In Sec. 4.2 we compute the quasiparticle spectrum of this texture using the semiclassical (Andreev) approximation. Then, using the transfer matrix method, we relate the interaction energy to the scattering matrix of the Bogoliubov quasiparticles in Sec. 5. Finally, we obtain an analytical expression for the interaction energy in the limit of large DW separation. The method developed in this work can also be applied to any planar texture of the SC order parameter. To illustrate this, we apply it to the interaction between phase solitons in a two-band s-wave superconductor, such as MgB_2 [56, 57] or the iron pnictides [58], in Sec. 6. From this point on, we use the units in which $\hbar = k_B = 1$.

2 The model

We consider a neutral isotropic two-dimensional chiral p-wave superfluid. Any external fields and disorder are neglected. The order parameter of a triplet fermionic superfluid or superconductor is a 2×2 spin matrix which has the following form: $\hat{\Delta}(\boldsymbol{k}, \boldsymbol{r}) = i\hat{\sigma}_2 \hat{\boldsymbol{\sigma}} \cdot \boldsymbol{d}(\boldsymbol{k}, \boldsymbol{r})$, where $\hat{\boldsymbol{\sigma}}$ are the Pauli matrices and $\boldsymbol{d}$ is the spin vector, which for unitary states defines the normal to the plane in which electrons paired at $(\boldsymbol{k}, -\boldsymbol{k})$ are equal spin paired [31]. In our case, $\boldsymbol{d}$ has only $\hat{z}$-component, and its momentum dependence is given by [18]:

$$\boldsymbol{d} = \frac{\eta_1 k_x + \eta_2 k_y}{k_F} \hat{z}, \tag{2.1}$$

where η_1 and η_2 are components of a complex order parameter vector $\boldsymbol{\eta}$ and k_F is the Fermi wavevector.

We focus on planar superconducting textures describing one or more DWs perpendicular to the x axis, therefore only x-dependence is retained in the order parameter components. The DWs separate states of opposite chirality, and thus the order parameter alternates between $k_x + ik_y$ and $k_x - ik_y$ states. The spatial dependence of $\boldsymbol{\eta}$ can be studied using, e.g. the Ginzburg-Landau formalism, see Appendix A. There is no exact analytical solution for the DW structure, even in the case of a single DW, and a variety of approximations have been proposed in the literature (Refs. [30, 48, 49, 50, 51, 52, 53, 54, 55]). Most important qualitative features of the DW textures can be illustrated using the constant-amplitude model introduced by Volovik and Gor'kov in Ref. [30]. In this model the order parameter has the form $\boldsymbol{\eta}(x) = \Delta_0(1, e^{-i\gamma(x)})e^{i\phi(x)}$, where ϕ is the common phase, and γ is relative phase, of the order parameter components.

The phases ϕ and γ are not independent: conservation of current requires $\nabla_x j_x = 0$ and, since the transverse current is therefore constant and fixed by external sources, one may set $j_x = 0$, which results in a linear relationship between the gradients of ϕ and γ. Thus the DW texture can be described in terms of a single variable – a spatially-dependent relative phase $\gamma(x)$. Variational minimization of the Ginzburg-Landau free energy functional with respect to γ leads to a sine-Gordon equation, whose simplest nontrivial solution corresponding to a single DW has a kink-like form, connecting the asymptotics $\gamma(\pm\infty) = \pm\pi/2$ and varying within a region of thickness ξ_d (which has the meaning of the DW thickness).

In general, different models give different expressions for $\boldsymbol{\eta}(x)$, but the condition $\gamma(\pm\infty) = \pm\pi/2$ always holds without reference to a specific profile of the order parameter near the wall. Furthermore, the common phase difference between the two domains is fixed by the condition of vanishing supercurrent across the DW, see Appendix A for

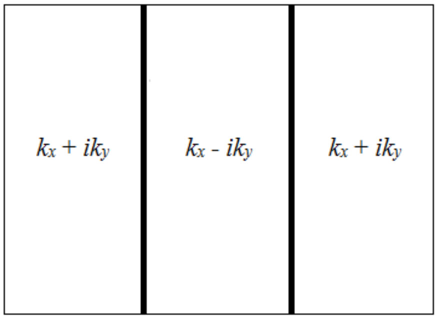

Figure 9: Alternating chirality states in the two-DW model.

details. Thus, one can write the order parameter asymptotics far from the single DW as follows:

$$\boldsymbol{\eta}(x) = \Delta_0(1, i), \tag{2.2a}$$

at $x \to -\infty$, and

$$\boldsymbol{\eta}(x) = \Delta_0 e^{i\chi}(1, -i), \tag{2.2b}$$

at $x \to +\infty$. Here χ is a parameter depending on the microscopic details of the system, satisfying the condition $0 \leq \chi \leq \pi$. One can make analytical progress by considering the sharp DW model, in which case $\xi_d \to 0$ and the order parameter changes abruptly at $x = 0$ between its asymptotic values. In accordance with Eq. (2.2), the domain in the region $x < 0$ corresponds to the $k_x + ik_y$ chiral state, while the $x > 0$ region is comprised of Cooper pairs in the $k_x - ik_y$ momentum state.

We now consider two DWs at fixed separation L, with the first DW positioned at $x = 0$, and the second at $x = L$. Using a similar setup as in the single DW case, now the chirality alternates between the three domains, and we analogously impose the constraint of vanishing supercurrent along the x axis, which leads to a non-zero common phase difference between the domains. The outer left region ($x < 0$), and the region on the far right ($x > L$), correspond to $k_x + ik_y$ state, while the middle domain ($0 < x < L$) corresponds to the $k_x - ik_y$ state, as shown in Fig. 9.

As in the single DW case, we focus on the sharp DW model to obtain an analytical solution for the interaction energy of the two DWs. Then the order parameter for both of the outer domains is given by the expression in Eq. (2.2a), and a non-zero global phase factor appears in the order parameter of the middle domain, which is given by the

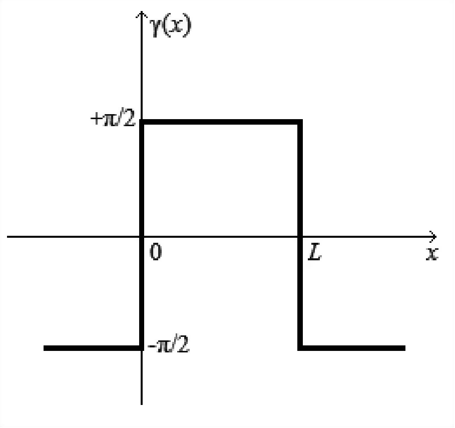

Figure 10: The relative phase between the order parameter components for two sharp DWs separated by distance L.

expression in Eq. (2.2b). In accordance with the sharp DW model, $\gamma(x)$ changes abruptly between its asymptotic values in the three domains, as illustrated in Fig. 10. The explicit expression for the order parameter for two DWs is discussed below in Sec. 3.2.

3 Derivation of the BdG and Andreev equations

In this thesis, we focus on the effects of the quasiparticle excitations in nonuniform textures in chiral p-wave superconductors. The spectrum of quasiparticle excitations can be found by solving the Bogoliubov-de Gennes (BdG) equations.

3.1 Derivation of BdG equations

We begin our derivation of the BdG equations for a centrosymmetric BCS-like superconductor by first considering the BCS Hamiltonian. This Hamiltonian can be written in the form $\hat{H}_{BCS} = \hat{H}_0 + \hat{H}_{int}$, where $\hat{H}_0$ is the non-interacting Hamiltonian, and $\hat{H}_{int}$ accounts for the interactions between electrons. Neglecting disorder and external magnetic field, in the second quantization formalism this Hamiltonian has the general form:

$$\hat{H}_{BCS} = \sum_{\boldsymbol{k},\sigma} \xi(\boldsymbol{k})\, \hat{a}^{\dagger}_{\boldsymbol{k},\sigma}\, \hat{a}_{\boldsymbol{k},\sigma} + \frac{1}{2\mathcal{V}} \sum_{\substack{\boldsymbol{k},\boldsymbol{k}',\boldsymbol{q},\\ \alpha,\beta,\gamma,\delta}} V_{\alpha\beta,\gamma\delta}(\boldsymbol{k},\boldsymbol{k}')\, \hat{a}^{\dagger}_{\boldsymbol{k}+\boldsymbol{q},\alpha}\, \hat{a}^{\dagger}_{-\boldsymbol{k},\beta}\, \hat{a}_{-\boldsymbol{k}',\gamma}\, \hat{a}_{\boldsymbol{k}'+\boldsymbol{q},\delta}, \tag{3.1}$$

where $\xi(\boldsymbol{k})$ is the kinetic energy measured with respect to the chemical potential (we neglect the difference between the chemical potential and the Fermi energy), $a_{\boldsymbol{k},\sigma}$ ($a^{\dagger}_{\boldsymbol{k},\sigma}$) is the single particle annihilation (creation) operator corresponding to momentum $\boldsymbol{k}$ and spin σ, and $\mathcal{V}$ is the system volume. In this last expression, $V_{\alpha\beta,\gamma\delta}(\boldsymbol{k},\boldsymbol{k}')$ is the pairing potential, which describes the scattering of a Cooper pair, mediated by, e.g., interactions with phonons or spin fluctuations [18]. In this mechanism, a Cooper pair in the arbitrary two-particle state $|\boldsymbol{k}+\boldsymbol{q},\alpha;-\boldsymbol{k},\beta\rangle$ is scattered to the state $\left|\boldsymbol{k}'+\boldsymbol{q},\gamma;-\boldsymbol{k}',\delta\right\rangle$, where $\boldsymbol{q}$ is the centre-of-mass momentum of the pair.

The Hamiltonian must be Hermitian and as such must be equal to its Hermitian conjugate. The first term in Eq. (3.1) is manifestly Hermitian, and so we check the Hermiticity of $\hat{H}_{int}$, whose adjoint is given by the following expression:

$$\hat{H}^{\dagger}_{int} = \frac{1}{2\mathcal{V}} \sum_{\substack{\boldsymbol{k},\boldsymbol{k}',\boldsymbol{q}\\ \alpha\beta\gamma\delta}} V^{*}_{\alpha\beta,\gamma\delta}(\boldsymbol{k},\boldsymbol{k}')\, \hat{a}^{\dagger}_{\boldsymbol{k}'+\boldsymbol{q},\delta}\, \hat{a}^{\dagger}_{-\boldsymbol{k}',\gamma}\, \hat{a}_{-\boldsymbol{k},\beta}\, \hat{a}_{\boldsymbol{k}+\boldsymbol{q},\alpha}. \tag{3.2}$$

We require that $\hat{H}_{int} = \hat{H}^{\dagger}_{int}$, and rename the variables in the previous equation as follows: $\boldsymbol{k} \leftrightarrow \boldsymbol{k}', \alpha \leftrightarrow \delta, \beta \leftrightarrow \gamma$. In this way, we obtain the Hermiticity condition for the pairing potential: $V_{\alpha\beta,\gamma\delta}(\boldsymbol{k},\boldsymbol{k}') = V^{*}_{\delta\gamma,\beta\alpha}(\boldsymbol{k}',\boldsymbol{k})$.

Using the anti-commutation relation that holds for single-fermion creation operators $\{\hat{a}^{\dagger}_i, \hat{a}^{\dagger}_j\} = 0$ (there is an analogous expression for the fermionic annihilation operators), we can rearrange the terms in $\hat{H}_{int}$, see Eq. (3.1), as follows:

$$\hat{H}_{int} = -\frac{1}{2\mathcal{V}} \sum_{\substack{\boldsymbol{k},\boldsymbol{k}',\boldsymbol{q} \\ \alpha\beta\gamma\delta}} V_{\alpha\beta,\gamma\delta}(\boldsymbol{k},\boldsymbol{k}')\, \hat{a}^{\dagger}_{-\boldsymbol{k},\beta}\, \hat{a}^{\dagger}_{\boldsymbol{k}+\boldsymbol{q},\alpha}\, \hat{a}_{-\boldsymbol{k}',\gamma}\, \hat{a}_{\boldsymbol{k}'+\boldsymbol{q},\delta}. \tag{3.3}$$

By renaming the summation variables $\alpha \leftrightarrow \beta$, and setting $-\boldsymbol{k} = \boldsymbol{p} + \boldsymbol{q} \Rightarrow \boldsymbol{k} + \boldsymbol{q} = -\boldsymbol{p}$, we find:

$$\hat{H}_{int} = -\frac{1}{2\mathcal{V}} \sum_{\substack{\boldsymbol{p},\boldsymbol{k}',\boldsymbol{q} \\ \alpha\beta\gamma\delta}} V_{\beta\alpha,\gamma\delta}(-\boldsymbol{p}-\boldsymbol{q},\boldsymbol{k}')\, \hat{a}^{\dagger}_{\boldsymbol{p}+\boldsymbol{q},\alpha}\, \hat{a}^{\dagger}_{-\boldsymbol{p},\beta}\, \hat{a}_{-\boldsymbol{k}',\gamma}\, \hat{a}_{\boldsymbol{k}'+\boldsymbol{q},\delta}, \tag{3.4}$$

and finally renaming $\boldsymbol{p} \to \boldsymbol{k}$, it immediately follows that

$$\hat{H}_{int} = -\frac{1}{2\mathcal{V}} \sum_{\substack{\boldsymbol{k},\boldsymbol{k}',\boldsymbol{q} \\ \alpha\beta\gamma\delta}} V_{\beta\alpha,\gamma\delta}(-\boldsymbol{k}-\boldsymbol{q},\boldsymbol{k}')\, \hat{a}^{\dagger}_{\boldsymbol{k}+\boldsymbol{q},\alpha}\, \hat{a}^{\dagger}_{-\boldsymbol{k},\beta}\, \hat{a}_{-\boldsymbol{k}',\gamma}\, \hat{a}_{\boldsymbol{k}'+\boldsymbol{q},\delta}. \tag{3.5}$$

By comparing this last expression with the interacting part of the Hamiltonian in Eq. (3.1), we have the condition $V_{\alpha\beta,\gamma\delta}(\boldsymbol{k},\boldsymbol{k}') = -V_{\beta\alpha,\gamma\delta}(-\boldsymbol{k}-\boldsymbol{q},\boldsymbol{k}')$.

To proceed with the derivation, we make the physical assumption that the typical values of the centre-of-mass momentum of Cooper pairs $\boldsymbol{q}$ are of the order of ξ^{-1}, the inverse correlation length. This assumption can be justified by considering the following argument. The wavefunction of the Cooper pair is modulated in the presence of nonzero $\boldsymbol{q}$: $\Psi_{pair}(\boldsymbol{r}) \sim \Psi_0 e^{i\boldsymbol{q}\cdot\boldsymbol{r}}$, which leads to a nonzero supercurrent. There is a maximum supercurrent at which superconductivity can be sustained, and this corresponds to $|\boldsymbol{q}_{max}| \sim \xi_0^{-1}$, where ξ_0 is the coherence length. In comparison, since the electrons involved in pairing have energies within a small shell around the Fermi surface, typical values of the momentum of individual electrons are $|\boldsymbol{k}| \sim k_F$. Taking the ratio of the two momenta, we see $|\boldsymbol{q}_{max}|/|\boldsymbol{k}| \sim (k_F\xi_0)^{-1}$, and since $\xi_0 \sim v_F/T_c$, it follows that $|\boldsymbol{q}_{max}|/|\boldsymbol{k}| \sim T_c/\epsilon_F$. However, typical values of the transition temperature $T_c \sim 1-100$K [12], while the Fermi energy $\epsilon_F \sim 10^4$K [59], and thus $|\boldsymbol{q}_{max}|/|\boldsymbol{k}| \ll 1$.

This allows us to neglect the argument $\boldsymbol{q}$ in the pairing potential, and then we have the relation $V_{\alpha\beta,\gamma\delta}(\boldsymbol{k},\boldsymbol{k}') = -V_{\beta\alpha,\gamma\delta}(-\boldsymbol{k},\boldsymbol{k}')$. Note that we have not completely neglected the center-of-mass momentum of the Cooper pairs, since it is still present in the single-particle creation/annihilation operators. Following an analogous procedure using the anticommutation relations of the particle annihilation operators, and appropriately renaming the summation variables, one finds: $V_{\alpha\beta,\gamma\delta}(\boldsymbol{k},\boldsymbol{k}') = -V_{\alpha\beta,\delta\gamma}(\boldsymbol{k},-\boldsymbol{k}'-\boldsymbol{q})$. For the reasons mentioned above, we can again neglect the centre-of-mass momentum of the Cooper pair here, and then we find that the pairing potential satisfies the following anti-commutation relations:

$$V_{\alpha\beta,\gamma\delta}(\boldsymbol{k},\boldsymbol{k}^{'}) = -V_{\beta\alpha,\gamma\delta}(-\boldsymbol{k},\boldsymbol{k}^{'}) = -V_{\alpha\beta,\delta\gamma}(\boldsymbol{k},-\boldsymbol{k}^{'}). \tag{3.6}$$

Now recall the discussion of the single-pair wavefunction given in Section 1.4. To derive the pairing interaction in the many-body problem, we use insight from the symmetry analysis of single-pair wavefunctions. In the case of strong spin-orbit coupling, the interaction potential can be expressed in terms of the 2 × 2 spin-matrix basis functions $\hat{\phi}_a(\boldsymbol{k})$ introduced in Section 1.4 as follows:

$$V_{\alpha\beta,\gamma\delta}(\boldsymbol{k},\boldsymbol{k}^{'}) = -\frac{V}{2}\sum_{a=1}^{d_\Gamma}\phi_{a,\alpha\beta}(\boldsymbol{k})\phi^{\dagger}_{a,\gamma\delta}(\boldsymbol{k}^{'}), \tag{3.7}$$

where $V > 0$ is the coupling constant in the Γ pairing channel. Here, Γ labels the irreducible representation (IREP) of the point group G of the crystal of dimensionality d_Γ. By inspection of this last expression, it is clear that the spin-matrix basis functions must satisfy certain conditions for the interaction potential to retain the necessary anti-commutation relations (3.6). It directly follows that:

$$\phi_{a,\alpha\beta}(\boldsymbol{k}) = -\phi_{a,\beta\alpha}(-\boldsymbol{k}) \;\;\Rightarrow\;\; -\hat{\phi}^T_a(-\boldsymbol{k}) = \hat{\phi}_a(\boldsymbol{k}). \tag{3.8}$$

Recall that in the limit of strong spin-orbit coupling, spin is not a "good" quantum number, and so any reference to spin from this point on should be understood in terms of the pseudospin introduced in Section 1.4.

For electrons that pair in the singlet ($S = 0$) spin state, the spin-matrix is antisymmetric with respect to particle exchange, i.e. $\{\alpha,\beta\} \to \{\beta,\alpha\}$, whereas the momentum exchange is symmetric: $\hat{\phi}^s_a(-\boldsymbol{k}) = \hat{\phi}^s_a(\boldsymbol{k})$. In this case, we find from Eq. (3.8) that the singlet spin-matrix basis functions satisfy the condition $\hat{\phi}^T_a(\boldsymbol{k}) = -\hat{\phi}_a(\boldsymbol{k})$, where we have dropped the superscript s. The spin-matrix basis functions for the singlet pairing were previously defined in Section 1.4, and have the form: $\hat{\phi}^s_a(\boldsymbol{k}) = (i\hat{\sigma}_2)\varphi^{\Gamma_g}_a(\hat{\boldsymbol{k}})$, where Γ_g denotes the fact that the basis functions of this IREP are even in $\boldsymbol{k}$. For the conventional singlet s-wave case, Γ corresponds to the identity representation A_{1g} for any point group, with dimensionality $d_\Gamma = 1$ and the basis function $\varphi(\hat{\boldsymbol{k}}) = \theta(\epsilon_c - |\xi_{\boldsymbol{k}}|)$, where $\theta(x)$ is the Heaviside step function and ϵ_c is the BCS cutoff energy. Thus, in this case we see that the pairing potential, Eq. (3.7), has the simple form

$$V_{\alpha\beta,\gamma\delta} = -\frac{V}{2}(i\sigma_2)_{\alpha\beta}(-i\sigma_2)_{\gamma\delta}\,\theta(\epsilon_c - |\xi_{\boldsymbol{k}}|)\theta(\epsilon_c - |\xi_{\boldsymbol{k}'}|).$$

In the case of triplet ($S = 1$) pairing, the spin-matrix is symmetric with respect to particle exchange, and so the exchange of momentum is therefore anti-symmetric: $\hat{\phi}^t_a(-\boldsymbol{k}) = -\hat{\phi}^t_a(\boldsymbol{k})$. From Eq. (3.8), it then follows that the triplet spin-matrix basis functions satisfy $\hat{\phi}^T_a(\boldsymbol{k}) = \hat{\phi}_a(\boldsymbol{k})$, dropping the superscript t. Recall from Section 1.4 that the triplet spin-matrix basis functions have the form

$$\hat{\phi}^t_a(\boldsymbol{k}) = (i\hat{\boldsymbol{\sigma}}\hat{\sigma}_2) \cdot \boldsymbol{\varphi}^{\Gamma_u}_a(\hat{\boldsymbol{k}}), \tag{3.9}$$

where Γ_u denotes the fact that the basis functions are odd in $\boldsymbol{k}$. For example, in the triplet p-wave case that occurs in $\mathrm{Sr_2RuO_4}$, described by point group $G = D_{4h}$, the two-dimensional ($d_\Gamma = 2$) IREP $\Gamma = E_u$, and the basis functions are given by

$$\boldsymbol{\varphi}_1(\boldsymbol{k}) = \hat{z}\frac{k_x}{k_F}, \qquad \boldsymbol{\varphi}_2(\boldsymbol{k}) = \hat{z}\frac{k_y}{k_F}. \tag{3.10}$$

Please note that we did not explicitly include the BCS cutoffs in these expressions. The cutoffs will be included in the final expressions as needed.

Due to the complexity of the interacting system described by Eq. (3.1) it cannot be solved exactly. In order to make progress, we apply the mean-field approximation to the BCS Hamiltonian. To this end, we introduce the bosonic pair fields:

$$\begin{aligned} \hat{B}_a(\boldsymbol{q}) &= \frac{1}{2\mathcal{V}} \sum_{\substack{\boldsymbol{k} \\ \alpha\beta}} \phi^{\dagger}_{a,\alpha\beta}(\boldsymbol{k})\, \hat{a}_{-\boldsymbol{k},\alpha}\, \hat{a}_{\boldsymbol{k}+\boldsymbol{q},\beta}, \\ \hat{B}^{\dagger}_a(\boldsymbol{q}) &= \frac{1}{2\mathcal{V}} \sum_{\substack{\boldsymbol{k} \\ \alpha\beta}} \phi_{a,\alpha\beta}(\boldsymbol{k})\, \hat{a}^{\dagger}_{\boldsymbol{k}+\boldsymbol{q},\alpha}\, \hat{a}^{\dagger}_{-\boldsymbol{k},\beta}, \end{aligned} \tag{3.11}$$

where $a = 1 \ldots d_\Gamma$, and then we can rewrite the interacting portion of the BCS Hamiltonian as follows:

$$\hat{H}_{int} = -V \sum_{a=1}^{d_\Gamma} \mathcal{V} \sum_{\boldsymbol{q}} \hat{B}^{\dagger}_a(\boldsymbol{q}) \hat{B}_a(\boldsymbol{q}). \tag{3.12}$$

The paired electrons form a condensate which leads to an average field, and this introduces a mean-field potential that is experienced by unpaired electrons. We evaluate $\hat{H}_{int}$ in terms of this mean field by setting $\hat{B}_a = \langle \hat{B}_a \rangle + \delta\hat{B}_a$ (and $\hat{B}^{\dagger}_a = \langle \hat{B}^{\dagger}_a \rangle + \delta\hat{B}^{\dagger}_a$), where $\delta\hat{B}_a$ and $\delta\hat{B}^{\dagger}_a$ are treated as small operators since the fluctuations away from the mean field are weak. After direct substitution, it follows that:

$$\hat{H}_{int} = -V \sum_{a=1}^{d_\Gamma} \mathcal{V} \sum_{\boldsymbol{q}} \left(\langle \hat{B}^{\dagger}_a \rangle + \delta\hat{B}^{\dagger}_a \right) \left(\langle \hat{B}_a \rangle + \delta\hat{B}_a \right), \tag{3.13}$$

and up to the linear order in $\delta\hat{B}_a$ and $\delta\hat{B}_a^\dagger$, we have:

$$\hat{H}_{int} = -V\sum_{a=1}^{d_\Gamma}\mathcal{V}\sum_{\boldsymbol{q}}\left[\langle\hat{B}_a\rangle^*\delta\hat{B}_a + \delta\hat{B}_a^\dagger\langle\hat{B}_a\rangle + \langle\hat{B}_a\rangle^*\langle\hat{B}_a\rangle\right]. \tag{3.14}$$

Next, we replace the small operators with their expressions in terms of the bosonic pair field operator $\hat{B}_a$ and its mean value, namely $\delta\hat{B}_a^\dagger = \hat{B}_a^\dagger - \langle\hat{B}_a\rangle^*$ and $\delta\hat{B}_a = \hat{B}_a - \langle\hat{B}_a\rangle$ and find:

$$\hat{H}_{int} = -V\sum_{a=1}^{d_\Gamma}\mathcal{V}\sum_{\boldsymbol{q}}\left[-\langle\hat{B}_a\rangle^*\langle\hat{B}_a\rangle + \langle\hat{B}_a\rangle^*\hat{B}_a + \hat{B}_a^\dagger\langle\hat{B}_a\rangle\right]. \tag{3.15}$$

The next step is to introduce complex functions $\eta_a(\boldsymbol{q})$, which physically play the role of the components of the order parameter. They are related to the expectation values of the bosonic pair field operators as follows:

$$\eta_a(\boldsymbol{q}) = -V\mathcal{V}\langle\hat{B}_a(\boldsymbol{q})\rangle, \quad \eta_a^*(\boldsymbol{q}) = -V\mathcal{V}\langle\hat{B}_a(\boldsymbol{q})\rangle^*. \tag{3.16}$$

The order parameter components $\eta_a(\boldsymbol{q})$ introduced above are proportional to the coefficients in the expressions (1.108, 1.112) for the single-pair wavefunctions. By substitution of this last expression into Eq. (3.15)), it is immediately clear that $\hat{H}_{int}$ takes the form

$$\hat{H}_{int} = \frac{1}{V}\sum_{a=1}^{d_\Gamma}\frac{1}{\mathcal{V}}\sum_{\boldsymbol{q}}|\eta_a(\boldsymbol{q})|^2 + \sum_{a=1}^{d_\Gamma}\sum_{\boldsymbol{q}}\left[\eta_a^*(\boldsymbol{q})\hat{B}_a(\boldsymbol{q}) + \hat{B}_a^\dagger(\boldsymbol{q})\eta_a(\boldsymbol{q})\right], \tag{3.17}$$

and after using the definitions of the pair field operators, see Eq. (3.11), in this last equation, we obtain the mean-field expression for the interacting part of the BCS Hamiltonian:

$$\begin{aligned}\hat{H}_{int} &= \frac{1}{V}\sum_{a=1}^{d_\Gamma}\frac{1}{\mathcal{V}}\sum_{\boldsymbol{q}}|\eta_a(\boldsymbol{q})|^2 \\ &+ \frac{1}{2}\sum_{a=1}^{d_\Gamma}\frac{1}{\mathcal{V}}\sum_{\substack{\boldsymbol{k},\boldsymbol{q}\\ \alpha\beta}}\left[\eta_a^*(\boldsymbol{q})\phi_{a,\alpha\beta}^\dagger(\boldsymbol{k})\,\hat{a}_{-\boldsymbol{k},\alpha}\,\hat{a}_{\boldsymbol{k}+\boldsymbol{q},\beta} + \eta_a(\boldsymbol{q})\phi_{a,\alpha\beta}(\boldsymbol{k})\,\hat{a}_{\boldsymbol{k}+\boldsymbol{q},\alpha}^\dagger\,\hat{a}_{-\boldsymbol{k},\beta}^\dagger\right].\end{aligned} \tag{3.18}$$

To proceed with the derivation of the BdG equations, we introduce the gap functions

$\Delta_{\alpha\beta}$, which are the entries of a 2×2 gap matrix $\hat{\Delta}$:

$$\begin{aligned}\Delta_{\alpha\beta}(\boldsymbol{k},\boldsymbol{q}) &= \sum_{a=1}^{d_\Gamma} \eta_a(\boldsymbol{q})\phi_{a,\alpha\beta}(\boldsymbol{k}),\\ \Delta^\dagger_{\alpha\beta}(\boldsymbol{k},\boldsymbol{q}) &= \sum_{a=1}^{d_\Gamma} \eta^*_a(\boldsymbol{q})\phi^\dagger_{a,\alpha\beta}(\boldsymbol{k}),\end{aligned} \tag{3.19}$$

where the second expression denotes the $\alpha\beta$-component of the Hermitian conjugate of $\hat{\Delta}$ in the 2×2 spin space. For example, in the singlet isotropic s-wave case (the original BCS case), the gap matrix has the following form:

$$\hat{\Delta}(\boldsymbol{k},\boldsymbol{q}) = \begin{pmatrix} 0 & \eta(\boldsymbol{q}) \\ -\eta(\boldsymbol{q}) & 0 \end{pmatrix}.$$

In this case the superconductivity is described by a single complex function η, which is the order parameter. For the triplet pairing, inserting Eq. (3.9) into Eq. (3.19), we obtain the following expression:

$$\begin{aligned}\hat{\Delta}(\boldsymbol{k},\boldsymbol{q}) &= \sum_{a=1}^{d_\Gamma} \eta_a(\boldsymbol{q})(i\hat{\boldsymbol{\sigma}}\hat{\sigma}_2)\cdot\boldsymbol{\varphi}_a^{\Gamma_u}(\boldsymbol{k})\\ &= (i\hat{\boldsymbol{\sigma}}\hat{\sigma}_2)\cdot\boldsymbol{d}(\boldsymbol{k},\boldsymbol{q}),\end{aligned} \tag{3.20}$$

where we have introduced the spin vector order parameter

$$\boldsymbol{d}(\boldsymbol{k},\boldsymbol{q}) = \sum_{a=1}^{d_\Gamma} \eta_a(\boldsymbol{q})\boldsymbol{\varphi}_a^{\Gamma_u}(\boldsymbol{k}). \tag{3.21}$$

This spin vector is similar in structure to the single-pair spin vector $\tilde{\boldsymbol{d}}$ defined by Eq. (1.112).

Using the definitions of the gap functions, see Eq. (3.19), we can further simplify the interacting part of the BCS Hamiltonian as follows:

$$\begin{aligned}\hat{H}_{int} &= \frac{1}{V}\frac{1}{\mathcal{V}}\sum_{\boldsymbol{q}}\sum_{a=1}^{d_\Gamma}|\eta_a(\boldsymbol{q})|^2\\ &+ \frac{1}{2}\frac{1}{\mathcal{V}}\sum_{\substack{\boldsymbol{k},\boldsymbol{q}\\ \alpha\beta}}\left[\Delta_{\alpha\beta}(\boldsymbol{k},\boldsymbol{q})\,\hat{a}^\dagger_{\boldsymbol{k}+\boldsymbol{q},\alpha}\,\hat{a}^\dagger_{-\boldsymbol{k},\beta} + \Delta^\dagger_{\alpha\beta}(\boldsymbol{k},\boldsymbol{q})\,\hat{a}_{-\boldsymbol{k},\alpha}\,\hat{a}_{\boldsymbol{k}+\boldsymbol{q},\beta}\right].\end{aligned} \tag{3.22}$$

From here we introduce the 4-component Nambu spinor operators:

$$\hat{A}_{\boldsymbol{k}} = \begin{bmatrix} \hat{a}_{\boldsymbol{k},\uparrow} \\ \hat{a}_{\boldsymbol{k},\downarrow} \\ \hat{a}^{\dagger}_{-\boldsymbol{k},\uparrow} \\ \hat{a}^{\dagger}_{-\boldsymbol{k},\downarrow} \end{bmatrix}, \quad \hat{A}^{\dagger}_{\boldsymbol{k}} = \begin{pmatrix} \hat{a}^{\dagger}_{\boldsymbol{k},\uparrow} & \hat{a}^{\dagger}_{\boldsymbol{k},\downarrow} & \hat{a}_{-\boldsymbol{k},\uparrow} & \hat{a}_{-\boldsymbol{k},\downarrow} \end{pmatrix}. \tag{3.23}$$

Below we will express the mean-field Hamiltonian in terms of these operators.

We begin with the non-interacting Hamiltonian $\hat{H}_0$, which in the general case can be written as follows:

$$\hat{H}_0 = \frac{1}{\mathcal{V}} \sum_{\substack{\boldsymbol{k}_1,\boldsymbol{k}_2 \\ \alpha\beta}} \hat{a}^{\dagger}_{\boldsymbol{k}_1,\alpha}\, \xi_{\alpha\beta}(\boldsymbol{k}_1,\boldsymbol{k}_2)\, \hat{a}_{\boldsymbol{k}_2,\beta}, \tag{3.24}$$

where $\xi_{\alpha\beta}(\boldsymbol{k}_1,\boldsymbol{k}_2) = \langle \boldsymbol{k}_1,\alpha|(\hat{h}-\epsilon_F)|\boldsymbol{k}_2,\beta\rangle$ comprise a 2×2 matrix $\hat{\xi}(\boldsymbol{k}_1,\boldsymbol{k}_2)$. Here, $\hat{h}$ is the single-particle Hamiltonian, which in general takes the form $\hat{h} = (\hbar^2/2m)\hat{\boldsymbol{k}}^2 + U(\boldsymbol{r}) + \mu_B \boldsymbol{B}\cdot\hat{\boldsymbol{\sigma}}$, where μ_B is the Bohr magneton, $\boldsymbol{B}$ is an arbitrary magnetic field, and $\hat{\boldsymbol{\sigma}}$ is the Pauli spin matrix vector.

Since the summation in Eq. (3.24) runs over all wavevectors (positive and negative), we can split it into two sums and rewrite the equation as follows:

$$\hat{H}_0 = \frac{1}{2\mathcal{V}} \sum_{\substack{\boldsymbol{k}_1,\boldsymbol{k}_2 \\ \alpha\beta}} \hat{a}^{\dagger}_{\boldsymbol{k}_1,\alpha}\, \xi_{\alpha\beta}(\boldsymbol{k}_1,\boldsymbol{k}_2)\, \hat{a}_{\boldsymbol{k}_2,\beta} + \frac{1}{2\mathcal{V}} \sum_{\substack{\boldsymbol{k}_1,\boldsymbol{k}_2 \\ \alpha\beta}} \hat{a}^{\dagger}_{-\boldsymbol{k}_2,\beta}\, \xi_{\beta\alpha}(-\boldsymbol{k}_2,-\boldsymbol{k}_1)\, \hat{a}_{-\boldsymbol{k}_1,\alpha}, \tag{3.25}$$

where we have interchanged the summation labels $\boldsymbol{k}_1 \leftrightarrow \boldsymbol{k}_2, \alpha \leftrightarrow \beta$. Using the anticommutation relation of the single-particle creation and annihilation operators $\{\hat{a}_i, \hat{a}^{\dagger}_j\} = \delta_{ij}$, and neglecting the constant resulting from the delta function, we find:

$$\hat{H}_0 = \frac{1}{2\mathcal{V}} \sum_{\substack{\boldsymbol{k}_1,\boldsymbol{k}_2 \\ \alpha\beta}} \left[\hat{a}^{\dagger}_{\boldsymbol{k}_1,\alpha}\, \xi_{\alpha\beta}(\boldsymbol{k}_1,\boldsymbol{k}_2)\, \hat{a}_{\boldsymbol{k}_2,\beta} - \hat{a}_{-\boldsymbol{k}_1,\alpha}\, \xi^{T}_{\alpha\beta}(-\boldsymbol{k}_2,-\boldsymbol{k}_1)\, \hat{a}^{\dagger}_{-\boldsymbol{k}_2,\beta} \right], \tag{3.26}$$

where we have invoked the identity for 2×2 matrix transposition, $\xi^{T}_{\alpha\beta} = \xi_{\beta\alpha}$. Using the Nambu operators introduced in Eq. (3.23), we can rewrite the expression (3.26) in a more compact form:

$$\hat{H}_0 = \frac{1}{2\mathcal{V}} \sum_{\boldsymbol{k}_1,\boldsymbol{k}_2} \hat{A}^{\dagger}_{\boldsymbol{k}_1} \begin{pmatrix} \hat{\xi}(\boldsymbol{k}_1,\boldsymbol{k}_2) & 0 \\ 0 & -\hat{\xi}^{T}(-\boldsymbol{k}_2,-\boldsymbol{k}_1) \end{pmatrix} \hat{A}_{\boldsymbol{k}_2}, \tag{3.27}$$

where the matrix in this last expression has the dimensionality 4×4, since $\hat{\xi}(\boldsymbol{k}_1,\boldsymbol{k}_2)$ is a 2×2 matrix.

We now focus our attention on the interacting part of the BCS Hamiltonian. First, we represent Eq. (3.22) as follows:

$$\hat{H}_{int} = \hat{H}^{(1)}_{int} + \hat{H}^{(2)}_{int}, \tag{3.28}$$

with

$$\hat{H}^{(1)}_{int} = \frac{1}{V}\frac{1}{\mathcal{V}}\sum_{\boldsymbol{q}}\sum_{a=1}^{d_\Gamma}\left|\eta_a(\boldsymbol{q})\right|^2, \tag{3.29}$$

and

$$\hat{H}^{(2)}_{int} = \frac{1}{2\mathcal{V}}\sum_{\substack{\boldsymbol{k},\boldsymbol{q}\\ \alpha\beta}}\left[\Delta_{\alpha\beta}(\boldsymbol{k},\boldsymbol{q})\,\hat{a}^\dagger_{\boldsymbol{k}+\boldsymbol{q},\alpha}\,\hat{a}^\dagger_{-\boldsymbol{k},\beta} + \Delta^\dagger_{\alpha\beta}(\boldsymbol{k},\boldsymbol{q})\,\hat{a}_{-\boldsymbol{k},\alpha}\,\hat{a}_{\boldsymbol{k}+\boldsymbol{q},\beta}\right]. \tag{3.30}$$

As in the non-interacting Hamiltonian, we wish to express the interactions in terms of a summation over $\boldsymbol{k}_1, \boldsymbol{k}_2$, and we do so in the following way:

$$\begin{aligned}\hat{H}^{(2)}_{int} &= \frac{1}{2\mathcal{V}}\sum_{\substack{\boldsymbol{k},\boldsymbol{q}\\ \alpha\beta}}\sum_{\boldsymbol{k}_1,\boldsymbol{k}_2}\Big[\Delta_{\alpha\beta}(\boldsymbol{k},\boldsymbol{q})\delta_{\boldsymbol{k}_1,\boldsymbol{k}+\boldsymbol{q}}\delta_{\boldsymbol{k}_2,\boldsymbol{k}}\,\hat{a}^\dagger_{\boldsymbol{k}_1,\alpha}\,\hat{a}^\dagger_{-\boldsymbol{k}_2,\beta} \\ &+ \Delta^\dagger_{\alpha\beta}(\boldsymbol{k},\boldsymbol{q})\delta_{\boldsymbol{k},\boldsymbol{k}_1}\delta_{\boldsymbol{k}+\boldsymbol{q},\boldsymbol{k}_2}\,\hat{a}_{-\boldsymbol{k}_1,\alpha}\,\hat{a}_{\boldsymbol{k}_2,\beta}\Big].\end{aligned} \tag{3.31}$$

We use the delta functions in this last expression to remove the summation over $\boldsymbol{k}, \boldsymbol{q}$, then $\hat{H}^{(2)}_{int}$ takes the form

$$\hat{H}^{(2)}_{int} = \frac{1}{2\mathcal{V}}\sum_{\substack{\boldsymbol{k}_1,\boldsymbol{k}_2\\ \alpha\beta}}\left[\Delta_{\alpha\beta}(\boldsymbol{k}_2,\boldsymbol{k}_1-\boldsymbol{k}_2)\,\hat{a}^\dagger_{\boldsymbol{k}_1,\alpha}\,\hat{a}^\dagger_{-\boldsymbol{k}_2,\beta} + \Delta^\dagger_{\alpha\beta}(\boldsymbol{k}_1,\boldsymbol{k}_2-\boldsymbol{k}_1)\,\hat{a}_{-\boldsymbol{k}_1,\alpha}\,\hat{a}_{\boldsymbol{k}_2,\beta}\right]. \tag{3.32}$$

Utilizing once again the Nambu spinor operators, Eq. (3.23), we have:

$$\hat{H}^{(2)}_{int} = \frac{1}{2\mathcal{V}}\sum_{\boldsymbol{k}_1,\boldsymbol{k}_2}\hat{A}^\dagger_{\boldsymbol{k}_1}\begin{pmatrix} 0 & \hat{\Delta}(\boldsymbol{k}_2,\boldsymbol{k}_1-\boldsymbol{k}_2) \\ \hat{\Delta}^\dagger(\boldsymbol{k}_1,\boldsymbol{k}_2-\boldsymbol{k}_1) & 0\end{pmatrix}\hat{A}_{\boldsymbol{k}_2}, \tag{3.33}$$

where the matrix in this last expression has dimensionality 4 × 4 since $\hat{\Delta}$ is a 2 × 2 matrix in spin space.

We are now in a position where we can express the BCS Hamiltonian $\hat{H}_{BCS} = \hat{H}_0 + \hat{H}_{int}$ in a compact form. From Eqs. (3.27, 3.29, 3.33) it follows that, in the mean-field approximation, the Hamiltonian can be expressed in the following form:

$$\hat{H}_{MF} = \frac{1}{V}\frac{1}{\mathcal{V}}\sum_{\boldsymbol{q}}\sum_{a=1}^{d_\Gamma}\left|\eta_a(\boldsymbol{q})\right|^2 + \frac{1}{2\mathcal{V}}\sum_{\boldsymbol{k}_1,\boldsymbol{k}_2}\hat{A}^\dagger_{\boldsymbol{k}_1}\hat{\mathcal{H}}(\boldsymbol{k}_1,\boldsymbol{k}_2)\hat{A}_{\boldsymbol{k}_2}, \tag{3.34}$$

where $\hat{\mathcal{H}}(\boldsymbol{k}_1, \boldsymbol{k}_2)$ is the 4×4 BdG Hamiltonian in momentum space, given by the expression:

$$\hat{\mathcal{H}}(\boldsymbol{k}_1, \boldsymbol{k}_2) = \begin{pmatrix} \hat{\xi}(\boldsymbol{k}_1, \boldsymbol{k}_2) & \hat{\Delta}(\boldsymbol{k}_2, \boldsymbol{k}_1 - \boldsymbol{k}_2) \\ \hat{\Delta}^\dagger(\boldsymbol{k}_1, \boldsymbol{k}_2 - \boldsymbol{k}_1) & -\hat{\xi}^T(-\boldsymbol{k}_2, -\boldsymbol{k}_1) \end{pmatrix}. \tag{3.35}$$

We wish to transform our expression for the mean-field Hamiltonian into position representation. Recall from Eq. (3.19) that the entries of the gap matrix are defined in terms of the order parameter components, and thus we must first transform the order parameter components into coordinate space. This amounts to the Fourier summation:

$$\eta_a(\boldsymbol{r}) = \frac{1}{\mathcal{V}} \sum_{\boldsymbol{q}} \eta_a(\boldsymbol{q}) e^{i\boldsymbol{q}\cdot\boldsymbol{r}}, \quad \eta_a(\boldsymbol{q}) = \int d\boldsymbol{r}\, \eta_a(\boldsymbol{r}) e^{-i\boldsymbol{q}\cdot\boldsymbol{r}}. \tag{3.36}$$

We see that a uniform order parameter $\eta_a(\boldsymbol{r}) = \eta_a$ has as its Fourier transform $\eta_a(\boldsymbol{q}) = \eta_a \int d\boldsymbol{r}\, e^{-i\boldsymbol{q}\cdot\boldsymbol{r}} = \mathcal{V}\eta_a \delta_{\boldsymbol{q},0}$.

We begin with the first term in $\hat{H}_{MF}$. Using expression (3.36), we have:

$$\begin{aligned} \frac{1}{V}\frac{1}{\mathcal{V}} \sum_{\boldsymbol{q}} \sum_{a=1}^{d_\Gamma} |\eta_a(\boldsymbol{q})|^2 &= \frac{1}{V}\frac{1}{\mathcal{V}} \sum_{\boldsymbol{q}} \sum_{a=1}^{d_\Gamma} \int d\boldsymbol{r}_1 \int d\boldsymbol{r}_2\, \eta_a^*(\boldsymbol{r}_1)\eta_a(\boldsymbol{r}_2) e^{i\boldsymbol{q}\cdot\boldsymbol{r}_1} e^{-i\boldsymbol{q}\cdot\boldsymbol{r}_2} \\ &= \frac{1}{V} \sum_{a=1}^{d_\Gamma} \int d\boldsymbol{r}_1 \int d\boldsymbol{r}_2\, \eta_a^*(\boldsymbol{r}_1)\eta_a(\boldsymbol{r}_2) \left[\frac{1}{\mathcal{V}} \sum_{\boldsymbol{q}} e^{i\boldsymbol{q}\cdot(\boldsymbol{r}_1 - \boldsymbol{r}_2)}\right], \end{aligned} \tag{3.37}$$

where the term in parentheses can be written as an integral over continuous variable $\boldsymbol{q}$,

$$\int \frac{d^n q}{(2\pi)^n} e^{i\boldsymbol{q}\cdot(\boldsymbol{r}_1 - \boldsymbol{r}_2)} = \delta(\boldsymbol{r}_1 - \boldsymbol{r}_2) \tag{3.38}$$

in the limit $\mathcal{V} \to \infty$, where n is the dimensionality of the momentum space. In this limit, Eq. (3.37) takes the following form:

$$\begin{aligned} \frac{1}{V}\frac{1}{\mathcal{V}} \sum_{\boldsymbol{q}} \sum_{a=1}^{d_\Gamma} |\eta_a(\boldsymbol{q})|^2 &= \frac{1}{V} \sum_{a=1}^{d_\Gamma} \int d\boldsymbol{r}_1 \int d\boldsymbol{r}_2\, \delta(\boldsymbol{r}_1 - \boldsymbol{r}_2) \eta_a^*(\boldsymbol{r}_1)\eta_a(\boldsymbol{r}_2) \\ &= \frac{1}{V} \sum_{a=1}^{d_\Gamma} \int d\boldsymbol{r}\, |\eta_a(\boldsymbol{r})|^2. \end{aligned} \tag{3.39}$$

To transform the second term of expression (3.34) into the coordinate representation, which we shall call $\hat{H} = \hat{H}_0 + \hat{H}_{int}^{(2)}$, we recall that a one-body operator $\hat{O} = \sum_i \hat{o}_i$ (with the summation over single-particle operators $\hat{o}$, e.g. $\hat{\boldsymbol{p}}^2/2m$) is represented in the second-quantized form as follows:

$$\hat{O} \to \sum_{\ell,\ell'} \langle \ell | \hat{o} | \ell' \rangle \hat{a}^\dagger_\ell \hat{a}_{\ell'}, \tag{3.40}$$

where $\hat{O}$ now acts in the Fock space for identical fermions $\mathcal{F}_f$. In this last expression $\{|\ell\rangle\}$ is an orthonormal basis in $\mathcal{H}^{(a)}_{N=1}$, $\langle \ell|\hat{o}|\ell'\rangle$ denote the matrix elements of $\hat{o}$ in this basis, and $\hat{a}^\dagger_\ell, \hat{a}_\ell$ are single-particle creation and annihilation operators, respectively, corresponding to the state ℓ. This form is analogous to the second term in Eq. (3.34) if we take the basis $\{|\ell\rangle\}$ to be $\{|\boldsymbol{k},\sigma\rangle\}$ (i.e. momentum-spin representation), but note that we have suppressed the summation over spin states via the Nambu spinors. Here, our single-particle operator is the BdG Hamiltonian $\hat{\mathcal{H}}$, and one can see from its matrix elements in $|\boldsymbol{k},\sigma\rangle$-space, Eq. (3.35), that it is a 4×4 matrix. In each of the 2×2 blocks of this matrix, $\{\sigma,\sigma'\} = \uparrow\uparrow, \uparrow\downarrow, \downarrow\uparrow, \downarrow\downarrow$, and the fact that there are a total of 16 entries is a reflection of the particle-hole symmetry of the Hamiltonian.

We will first perform the transformation into coordinate space using the bra-ket notation, then show that we obtain the equivalent expression by a direct Fourier transform of the Nambu operators. Inserting the resolution of unity in terms of the single-particle basis $\{|\boldsymbol{r}\rangle\}$, $\hat{1} = \int d\boldsymbol{r} |\boldsymbol{r}\rangle\langle\boldsymbol{r}|$, twice into $\hat{H}$, we obtain:

$$\hat{H} = \frac{1}{2\mathcal{V}} \int d\boldsymbol{r}_1 \int d\boldsymbol{r}_2 \sum_{\substack{\boldsymbol{k}_1,\boldsymbol{k}_2 \\ \sigma,\sigma'}} \hat{A}^\dagger_{\boldsymbol{k}_1,\sigma} \langle \boldsymbol{k}_1|\boldsymbol{r}_1\rangle \langle \boldsymbol{r}_1,\sigma|\hat{\mathcal{H}}|\boldsymbol{r}_2,\sigma'\rangle \langle \boldsymbol{r}_2|\boldsymbol{k}_2\rangle \hat{A}_{\boldsymbol{k}_2,\sigma'}, \tag{3.41}$$

where we have restored the summation over the spin states. Note that $\sigma = \uparrow,\downarrow,\uparrow,\downarrow$ labels the rows of the spin matrix, and $\sigma' = \uparrow,\downarrow,\uparrow,\downarrow$ labels the columns, which gives the 4×4 matrix. Rearranging slightly this last expression, we have:

$$\hat{H} = \frac{1}{2\mathcal{V}} \int d\boldsymbol{r}_1 \int d\boldsymbol{r}_2 \sum_{\sigma,\sigma'} \left(\sum_{\boldsymbol{k}_1} \hat{A}^\dagger_{\boldsymbol{k}_1,\sigma} \langle \boldsymbol{k}_1|\boldsymbol{r}_1\rangle \right) \langle \boldsymbol{r}_1,\sigma|\hat{\mathcal{H}}|\boldsymbol{r}_2,\sigma'\rangle \left(\sum_{\boldsymbol{k}_2} \langle \boldsymbol{r}_2|\boldsymbol{k}_2\rangle \hat{A}_{\boldsymbol{k}_2,\sigma'} \right), \tag{3.42}$$

where the terms in parentheses are simply the single-particle Nambu field operators: $\hat{\Psi}_\sigma(\boldsymbol{r}) = \sum_{\boldsymbol{k}} \langle \boldsymbol{k}|\boldsymbol{r}\rangle \hat{A}_{\boldsymbol{k},\sigma}$, $\hat{\Psi}^\dagger_\sigma(\boldsymbol{r}) = \sum_{\boldsymbol{k}} \langle \boldsymbol{k}|\boldsymbol{r}\rangle^* \hat{A}^\dagger_{\boldsymbol{k},\sigma}$, which annihilate or create a particle at position $\boldsymbol{r}$ with spin σ. We can then rewrite this last expression as:

$$\hat{H} = \frac{1}{2\mathcal{V}} \int d\boldsymbol{r}_1 \int d\boldsymbol{r}_2 \sum_{\sigma,\sigma'} \hat{\Psi}^\dagger_\sigma(\boldsymbol{r}_1) \langle \boldsymbol{r}_1,\sigma|\hat{\mathcal{H}}|\boldsymbol{r}_2,\sigma'\rangle \hat{\Psi}_{\sigma'}(\boldsymbol{r}_2), \tag{3.43}$$

and suppressing the spin indices we obtain:

$$\hat{H} = \frac{1}{2\mathcal{V}} \int d\boldsymbol{r}_1 \int d\boldsymbol{r}_2 \hat{\Psi}^\dagger(\boldsymbol{r}_1) \langle \boldsymbol{r}_1 | \hat{\mathcal{H}} | \boldsymbol{r}_2 \rangle \hat{\Psi}(\boldsymbol{r}_2). \tag{3.44}$$

An alternative way to arrive at this expression is to directly consider the Fourier transforms of the Nambu spinor operators, which are written as follows:

$$\begin{aligned} \hat{A}_{\boldsymbol{k}} &= \frac{1}{\sqrt{\mathcal{V}}} \int d\boldsymbol{r}\, \hat{\Psi}(\boldsymbol{r}) e^{-i\boldsymbol{k}\cdot\boldsymbol{r}}, \qquad \hat{A}^\dagger_{\boldsymbol{k}} = \frac{1}{\sqrt{\mathcal{V}}} \int d\boldsymbol{r}\, \hat{\Psi}^\dagger(\boldsymbol{r}) e^{i\boldsymbol{k}\cdot\boldsymbol{r}}; \\ \hat{\Psi}(\boldsymbol{r}) &= \frac{1}{\sqrt{\mathcal{V}}} \sum_{\boldsymbol{k}} \hat{A}_{\boldsymbol{k}} e^{i\boldsymbol{k}\cdot\boldsymbol{r}}, \end{aligned} \tag{3.45}$$

where $\hat{\Psi}(\boldsymbol{r}) = \left[\hat{\Psi}_\uparrow(\boldsymbol{r}), \hat{\Psi}_\downarrow(\boldsymbol{r}), \hat{\Psi}^\dagger_\uparrow(\boldsymbol{r}), \hat{\Psi}^\dagger_\downarrow(\boldsymbol{r})\right]^T$ are the 4-component Nambu field operators introduced previously. After substitution of these last expressions into the second term in Eq. (3.34), we find:

$$\begin{aligned} \hat{H} &= \frac{1}{2\mathcal{V}^2} \sum_{\boldsymbol{k}_1,\boldsymbol{k}_2} \int d\boldsymbol{r}_1 \int d\boldsymbol{r}_2\, \hat{\Psi}^\dagger(\boldsymbol{r}_1) e^{i\boldsymbol{k}_1\cdot\boldsymbol{r}_1} \hat{\mathcal{H}}(\boldsymbol{k}_1,\boldsymbol{k}_2) \hat{\Psi}(\boldsymbol{r}_2) e^{-i\boldsymbol{k}_2\cdot\boldsymbol{r}_2} \\ &= \frac{1}{2\mathcal{V}} \int d\boldsymbol{r}_1 \int d\boldsymbol{r}_2\, \hat{\Psi}^\dagger(\boldsymbol{r}_1) \hat{\mathcal{H}}(\boldsymbol{r}_1,\boldsymbol{r}_2) \hat{\Psi}(\boldsymbol{r}_2), \end{aligned} \tag{3.46}$$

where

$$\hat{\mathcal{H}}(\boldsymbol{r}_1,\boldsymbol{r}_2) = \frac{1}{\mathcal{V}} \sum_{\boldsymbol{k}_1,\boldsymbol{k}_2} e^{i\boldsymbol{k}_1\cdot\boldsymbol{r}_1 - i\boldsymbol{k}_2\cdot\boldsymbol{r}_2} \hat{\mathcal{H}}(\boldsymbol{k}_1,\boldsymbol{k}_2) \tag{3.47}$$

are the position-space matrix elements of the 4 × 4 BdG Hamiltonian $\hat{\mathcal{H}}$, which acts on functions of $\boldsymbol{r}_2$, see Eq. (3.44). We can arrive at the same result from Eq. (3.44) by inserting the resolution of unity in terms of the momentum eigenkets into the matrix elements of $\hat{\mathcal{H}}$ in coordinate space, since the eigenfunctions of the momentum operator in position space are "normalized" plane waves.

We now focus our attention on calculating the matrix elements of the 4 × 4 BdG Hamiltonian, Eq. (3.47), and to do this we first introduce a shorthand notation for the gap functions that appear in the momentum-space matrix elements of $\hat{\mathcal{H}}$:

$$\hat{\mathcal{D}}(\boldsymbol{k}_1,\boldsymbol{k}_2) = \hat{\Delta}(\boldsymbol{k}_2, \boldsymbol{k}_1 - \boldsymbol{k}_2), \qquad \hat{\mathcal{D}}^\dagger(\boldsymbol{k}_2,\boldsymbol{k}_1) = \hat{\Delta}^\dagger(\boldsymbol{k}_1, \boldsymbol{k}_2 - \boldsymbol{k}_1). \tag{3.48}$$

In this manner, expression (3.35) takes the form:

$$\hat{\mathcal{H}}(\boldsymbol{k}_1, \boldsymbol{k}_2) = \begin{pmatrix} \hat{\mathcal{H}}_{11} & \hat{\mathcal{H}}_{12} \\ \hat{\mathcal{H}}_{21} & \hat{\mathcal{H}}_{22} \end{pmatrix}, \tag{3.49}$$

where each of the entries in the above matrix are 2×2 matrices given by: $\hat{\mathcal{H}}_{11} = \hat{\xi}(\boldsymbol{k}_1, \boldsymbol{k}_2), \hat{\mathcal{H}}_{12} = \hat{\mathcal{D}}(\boldsymbol{k}_1, \boldsymbol{k}_2), \hat{\mathcal{H}}_{21} = \hat{\mathcal{D}}^{\dagger}(\boldsymbol{k}_2, \boldsymbol{k}_1)$, and $\hat{\mathcal{H}}_{22} = -\hat{\xi}^T(-\boldsymbol{k}_2, -\boldsymbol{k}_1)$. Here, the Hermitian conjugation and matrix transposition are taken in the 2×2 spin space.

In $\boldsymbol{k}$-space, the BdG Hamiltonian acts on 4-component Nambu spinor functions

$$\psi = [\psi_1(\boldsymbol{k}), \psi_2(\boldsymbol{k}), \psi_3(\boldsymbol{k}), \psi_4(\boldsymbol{k})]^T ,$$

and so the eigenvalue problem $\hat{\mathcal{H}}\psi_i = E_i\psi_i$, where i labels the eigenstates, takes the form $\sum_{\boldsymbol{k}_2,n} \mathcal{H}_{m,n}(\boldsymbol{k}_1, \boldsymbol{k}_2)\psi_{i,n}(\boldsymbol{k}_2) = E_i\psi_{i,m}(\boldsymbol{k}_1)$, where $m, n = 1 \ldots 4$. Similarly, the action of $\hat{\mathcal{H}}$ on some arbitrary single-particle state ket $|\psi\rangle$: $|\phi\rangle = \hat{\mathcal{H}}|\psi\rangle$ can be represented in the coordinate space as follows:

$$\phi(\boldsymbol{r}_1) \equiv \langle \boldsymbol{r}_1|\phi\rangle = \langle \boldsymbol{r}_1|\hat{\mathcal{H}}|\psi\rangle = \int d\boldsymbol{r}_2\langle \boldsymbol{r}_1|\hat{\mathcal{H}}|\boldsymbol{r}_2\rangle\psi(\boldsymbol{r}_2), \tag{3.50}$$

where the summation over the spin states is assumed, and has therefore been supressed in the above expression. Recall that the matrix elements of $\hat{\mathcal{H}}$ in the coordinate-spin space can be expressed in terms of the $\boldsymbol{k}$-space elements, see Eq. (3.47).

We look at the matrix elements of 2×2 blocks, see Eq. (3.49), and consider first the element $\hat{\mathcal{H}}_{11}$. Assuming that the single-particle Hamiltonian $\hat{H}_0$ is diagonal in $\boldsymbol{k}$ and σ, i.e. in the absence of external field and disorder, the kinetic energy operator has matrix elements $\xi_{\alpha\beta}(\boldsymbol{k}_1, \boldsymbol{k}_2) = \mathcal{V}\delta_{\boldsymbol{k}_1,\boldsymbol{k}_2}\delta_{\alpha,\beta}\xi(\boldsymbol{k}_2)$, and thus $\hat{\mathcal{H}}_{11}(\boldsymbol{k}_1, \boldsymbol{k}_2) = \mathcal{V}\delta_{\boldsymbol{k}_1,\boldsymbol{k}_2}\hat{\sigma}_0\xi(\boldsymbol{k}_2)$. Using Eq. (3.50) along with Eq. (3.47), we find:

$$\tilde{\phi}(\boldsymbol{r}_1) = \int d\boldsymbol{r}_2\hat{\mathcal{H}}_{11}(\boldsymbol{r}_1, \boldsymbol{r}_2)\tilde{\psi}(\boldsymbol{r}_2) = \frac{1}{\mathcal{V}}\sum_{\boldsymbol{k}_1,\boldsymbol{k}_2}\int d\boldsymbol{r}_2\mathcal{V}\delta_{\boldsymbol{k}_1,\boldsymbol{k}_2}\xi(\boldsymbol{k}_2)e^{i\boldsymbol{k}_1\cdot\boldsymbol{r}_1 - i\boldsymbol{k}_2\cdot\boldsymbol{r}_2}\tilde{\psi}(\boldsymbol{r}_2), \tag{3.51}$$

where $\tilde{\psi}(\boldsymbol{r}_2)$ is an arbitrary two-component function of $\boldsymbol{r}_2$ (labeled by $\sigma =\uparrow, \downarrow$). This last expression can be further simplified and manipulated as follows:

$$\begin{aligned}\tilde{\phi}(\boldsymbol{r}_1) &= \sum_{\boldsymbol{k}_1}\int d\boldsymbol{r}_2\,\xi(\boldsymbol{k}_1)e^{i\boldsymbol{k}_1\cdot(\boldsymbol{r}_1-\boldsymbol{r}_2)}\tilde{\psi}(\boldsymbol{r}_2)\\ &= \sum_{\boldsymbol{k}_1}\int d\boldsymbol{r}_2\,\xi\left(-i\frac{\partial}{\partial\boldsymbol{r}_1}\right)e^{i\boldsymbol{k}_1\cdot(\boldsymbol{r}_1-\boldsymbol{r}_2)}\tilde{\psi}(\boldsymbol{r}_2)\\ &= \int d\boldsymbol{r}_2\,\xi\left(-i\frac{\partial}{\partial\boldsymbol{r}_1}\right)\left[\sum_{\boldsymbol{k}_1}e^{i\boldsymbol{k}_1\cdot(\boldsymbol{r}_1-\boldsymbol{r}_2)}\right]\tilde{\psi}(\boldsymbol{r}_2),\end{aligned}\tag{3.52}$$

where the term in square parentheses in the final expression is simply $\mathcal{V}\delta(\boldsymbol{r}_1-\boldsymbol{r}_2)$, see Eq. (3.38). We can therefore write this last expression as follows:

$$\tilde{\phi}(\boldsymbol{r}_1) = \mathcal{V}\,\xi\left(-i\frac{\partial}{\partial\boldsymbol{r}_1}\right)\int d\boldsymbol{r}_2\delta(\boldsymbol{r}_1-\boldsymbol{r}_2)\tilde{\psi}(\boldsymbol{r}_2),\tag{3.53}$$

and carrying out the integration over $\boldsymbol{r}_2$, we have:

$$\tilde{\phi}(\boldsymbol{r}_1) = \int d\boldsymbol{r}_2\hat{\mathcal{H}}_{11}(\boldsymbol{r}_1,\boldsymbol{r}_2)\tilde{\psi}(\boldsymbol{r}_2) = \mathcal{V}\,\xi\left(-i\frac{\partial}{\partial\boldsymbol{r}_1}\right)\tilde{\psi}(\boldsymbol{r}_1).\tag{3.54}$$

From this we conclude that the matrix elements of $\hat{\mathcal{H}}_{11}$ in the coordinate representation are given by

$$\hat{\mathcal{H}}_{11}(\boldsymbol{r}_1,\boldsymbol{r}_2) = \mathcal{V}\hat{\sigma}_0\xi\left(-i\frac{\partial}{\partial\boldsymbol{r}_1}\right)\delta(\boldsymbol{r}_1-\boldsymbol{r}_2),\tag{3.55}$$

where we have restored the reference to spin indices in this last expression.

One can use this result to immediately find the 2 × 2 matrix $\hat{\mathcal{H}}_{22}(\boldsymbol{r}_1,\boldsymbol{r}_2)$. Since $\xi^T_{\alpha,\beta}(\boldsymbol{k}_1,\boldsymbol{k}_2) = \xi_{\beta,\alpha}(\boldsymbol{k}_1,\boldsymbol{k}_2)$, we have $-\xi^T_{\alpha,\beta}(-\boldsymbol{k}_2,-\boldsymbol{k}_1) = -\mathcal{V}\delta_{\boldsymbol{k}_1,\boldsymbol{k}_2}\delta_{\beta,\alpha}\xi(-\boldsymbol{k}_1)$. Taking into account the symmetry of the kinetic energy in $\boldsymbol{k}$, $\xi(-\boldsymbol{k}) = \xi(\boldsymbol{k})$, it follows that $\hat{\mathcal{H}}_{22}(\boldsymbol{k}_1,\boldsymbol{k}_2) = -\mathcal{V}\delta_{\boldsymbol{k}_1,\boldsymbol{k}_2}\hat{\sigma}_0\xi(\boldsymbol{k}_2) = -\hat{\mathcal{H}}_{11}(\boldsymbol{k}_1,\boldsymbol{k}_2)$. Consequently, it is clear that the matrix elements of $\hat{\mathcal{H}}_{22}$ in position space have the form

$$\hat{\mathcal{H}}_{22}(\boldsymbol{r}_1,\boldsymbol{r}_2) = -\mathcal{V}\hat{\sigma}_0\xi\left(-i\frac{\partial}{\partial\boldsymbol{r}_1}\right)\delta(\boldsymbol{r}_1-\boldsymbol{r}_2).\tag{3.56}$$

We can now consider the off-diagonal elements of the BdG Hamiltonian, beginning with $\hat{\mathcal{H}}_{12}$. Proceeding in the same fashion as above, we look at the action of $\hat{\mathcal{H}}_{12}$ on an arbitrary state in the coordinate space:

$$\tilde{\phi}(\boldsymbol{r}_1) = \int d\boldsymbol{r}_2\hat{\mathcal{H}}_{12}(\boldsymbol{r}_1,\boldsymbol{r}_2)\tilde{\psi}(\boldsymbol{r}_2) = \frac{1}{\mathcal{V}}\sum_{\boldsymbol{k}_1,\boldsymbol{k}_2}\int d\boldsymbol{r}_2e^{i\boldsymbol{k}_1\cdot\boldsymbol{r}_1-i\boldsymbol{k}_2\cdot\boldsymbol{r}_2}\hat{\mathcal{D}}(\boldsymbol{k}_1,\boldsymbol{k}_2)\tilde{\psi}(\boldsymbol{r}_2),\tag{3.57}$$

and using Eqs. (3.48) and (3.19), we have:

$$\tilde{\phi}(\boldsymbol{r}_1) = \frac{1}{\mathcal{V}} \sum_{\boldsymbol{k}_1,\boldsymbol{k}_2} \int d\boldsymbol{r}_2 \sum_{a=1}^{d_\Gamma} \eta_a(\boldsymbol{k}_1 - \boldsymbol{k}_2)\hat{\phi}_a(\boldsymbol{k}_2) e^{i\boldsymbol{k}_1\cdot\boldsymbol{r}_1 - i\boldsymbol{k}_2\cdot\boldsymbol{r}_2} \tilde{\psi}(\boldsymbol{r}_2). \tag{3.58}$$

Recall that $\hat{\phi}_a(\boldsymbol{k})$ are the spin-matrix basis functions, see Eq. (3.9). Renaming $\boldsymbol{k}_1 = \boldsymbol{k}_2 + \boldsymbol{q}$, it follows that

$$\tilde{\phi}(\boldsymbol{r}_1) = \frac{1}{\mathcal{V}} \sum_{a=1}^{d_\Gamma} \sum_{\boldsymbol{k}_2,\boldsymbol{q}} \int d\boldsymbol{r}_2\, \eta_a(\boldsymbol{q})\hat{\phi}_a(\boldsymbol{k}_2) e^{i\boldsymbol{k}_2\cdot(\boldsymbol{r}_1-\boldsymbol{r}_2)} e^{i\boldsymbol{q}\cdot\boldsymbol{r}_1} \tilde{\psi}(\boldsymbol{r}_2), \tag{3.59}$$

and then using the expression (3.36), we replace $\eta_a(\boldsymbol{q})$ by its Fourier transform to obtain:

$$\begin{aligned} \tilde{\phi}(\boldsymbol{r}_1) &= \sum_{a=1}^{d_\Gamma} \eta_a(\boldsymbol{r}_1) \sum_{\boldsymbol{k}_2} \int d\boldsymbol{r}_2\, \hat{\phi}_a(\boldsymbol{k}_2) e^{i\boldsymbol{k}_2\cdot(\boldsymbol{r}_1-\boldsymbol{r}_2)} \tilde{\psi}(\boldsymbol{r}_2) \\ &= \sum_{a=1}^{d_\Gamma} \eta_a(\boldsymbol{r}_1) \int d\boldsymbol{r}_2\, \hat{\phi}_a \left(-i\frac{\partial}{\partial \boldsymbol{r}_1}\right) \sum_{\boldsymbol{k}_2} e^{i\boldsymbol{k}_2\cdot(\boldsymbol{r}_1-\boldsymbol{r}_2)} \tilde{\psi}(\boldsymbol{r}_2). \end{aligned} \tag{3.60}$$

To obtain the second equality, we have used the facts that the derivative of the exponential function pulls down the constants in the exponent, and that $\hat{\phi}_a(\boldsymbol{k})$ is a 2×2 matrix comprised of analytic functions of $\boldsymbol{k}$. We can rewrite the summation over $\boldsymbol{k}_2$ in terms of a delta function, see Eq. (3.38), and then the above equation takes the form:

$$\begin{aligned} \tilde{\phi}(\boldsymbol{r}_1) &= \mathcal{V} \sum_{a=1}^{d_\Gamma} \eta_a(\boldsymbol{r}_1)\hat{\phi}_a \left(-i\frac{\partial}{\partial \boldsymbol{r}_1}\right) \int d\boldsymbol{r}_2\, \delta(\boldsymbol{r}_1 - \boldsymbol{r}_2) \tilde{\psi}(\boldsymbol{r}_2) \\ &= \mathcal{V} \sum_{a=1}^{d_\Gamma} \eta_a(\boldsymbol{r}_1)\hat{\phi}_a \left(-i\frac{\partial}{\partial \boldsymbol{r}_1}\right) \tilde{\psi}(\boldsymbol{r}_1). \end{aligned} \tag{3.61}$$

From the above expressions, it can be concluded that the matrix elements of $\hat{\mathcal{H}}_{12}$ in the coordinate space have the following form:

$$\hat{\mathcal{H}}_{12}(\boldsymbol{r}_1, \boldsymbol{r}_2) = \mathcal{V} \sum_{a=1}^{d_\Gamma} \eta_a(\boldsymbol{r}_1)\hat{\phi}_a \left(-i\frac{\partial}{\partial \boldsymbol{r}_1}\right) \delta(\boldsymbol{r}_1 - \boldsymbol{r}_2). \tag{3.62}$$

We now consider the remaining element of the BdG Hamiltonian, $\hat{\mathcal{H}}_{21}$, via its action on an arbitrary two-component function in coordinate-spin space:

$$\tilde{\phi}(\boldsymbol{r}_1) = \int d\boldsymbol{r}_2 \hat{\mathcal{H}}_{21}(\boldsymbol{r}_1, \boldsymbol{r}_2)\tilde{\psi}(\boldsymbol{r}_2) = \frac{1}{\mathcal{V}} \sum_{\boldsymbol{k}_1,\boldsymbol{k}_2} \int d\boldsymbol{r}_2 e^{i\boldsymbol{k}_1\cdot\boldsymbol{r}_1 - i\boldsymbol{k}_2\cdot\boldsymbol{r}_2} \hat{\mathcal{D}}^\dagger(\boldsymbol{k}_2, \boldsymbol{k}_1)\tilde{\psi}(\boldsymbol{r}_2). \tag{3.63}$$

Using Eqs. (3.48) and (3.19), it follows that

$$\tilde{\phi}(\boldsymbol{r}_1) = \frac{1}{\mathcal{V}} \sum_{\boldsymbol{k}_1,\boldsymbol{k}_2} \int d\boldsymbol{r}_2 \sum_{a=1}^{d_\Gamma} \eta_a^*(\boldsymbol{k}_2 - \boldsymbol{k}_1)\hat{\phi}_a^\dagger(\boldsymbol{k}_1) e^{i\boldsymbol{k}_1\cdot\boldsymbol{r}_1 - i\boldsymbol{k}_2\cdot\boldsymbol{r}_2}\tilde{\psi}(\boldsymbol{r}_2). \tag{3.64}$$

Renaming again $\boldsymbol{k}_1 = \boldsymbol{k}_2 + \boldsymbol{q}$, we find:

$$\tilde{\phi}(\boldsymbol{r}_1) = \frac{1}{\mathcal{V}} \sum_{a=1}^{d_\Gamma} \sum_{\boldsymbol{k}_2,\boldsymbol{q}} \int d\boldsymbol{r}_2\, \eta_a^*(-\boldsymbol{q})\hat{\phi}_a^\dagger(\boldsymbol{k}_2 + \boldsymbol{q}) e^{i(\boldsymbol{k}_2+\boldsymbol{q})\cdot\boldsymbol{r}_1 - i\boldsymbol{k}_2\cdot\boldsymbol{r}_2}\tilde{\psi}(\boldsymbol{r}_2). \tag{3.65}$$

Since the derivative of the exponential function pulls down the constants in the exponent, and $\hat{\phi}_a^\dagger(\boldsymbol{k})$ is a 2×2 matrix comprised of analytic functions of $\boldsymbol{k}$, this last expression can be written as

$$\tilde{\phi}(\boldsymbol{r}_1) = \frac{1}{\mathcal{V}} \sum_{a=1}^{d_\Gamma} \hat{\phi}_a^\dagger \left(-i\frac{\partial}{\partial \boldsymbol{r}_1}\right) \sum_{\boldsymbol{k}_2,\boldsymbol{q}} \int d\boldsymbol{r}_2\, \eta_a^*(-\boldsymbol{q}) e^{i(\boldsymbol{k}_2+\boldsymbol{q})\cdot\boldsymbol{r}_1 - i\boldsymbol{k}_2\cdot\boldsymbol{r}_2}\tilde{\psi}(\boldsymbol{r}_2). \tag{3.66}$$

We can reformulate this last equation as follows:

$$\tilde{\phi}(\boldsymbol{r}_1) = \frac{1}{\mathcal{V}} \sum_{a=1}^{d_\Gamma} \hat{\phi}_a^\dagger \left(-i\frac{\partial}{\partial \boldsymbol{r}_1}\right) \int d\boldsymbol{r}_2 \sum_{\boldsymbol{q}} \eta_a^*(-\boldsymbol{q}) e^{i\boldsymbol{q}\cdot\boldsymbol{r}_1} \sum_{\boldsymbol{k}_2} e^{i\boldsymbol{k}_2\cdot(\boldsymbol{r}_1-\boldsymbol{r}_2)}\tilde{\psi}(\boldsymbol{r}_2), \tag{3.67}$$

and then it becomes apparent that we can replace $\eta_a^*(-\boldsymbol{q})$ by its Fourier transform, see Eq. (3.36), and the summation over $\boldsymbol{k}_2$ with a delta function, to obtain:

$$\begin{aligned} \tilde{\phi}(\boldsymbol{r}_1) &= \mathcal{V} \sum_{a=1}^{d_\Gamma} \hat{\phi}_a^\dagger \left(-i\frac{\partial}{\partial \boldsymbol{r}_1}\right) \eta_a^*(\boldsymbol{r}_1) \int d\boldsymbol{r}_2\, \delta(\boldsymbol{r}_1 - \boldsymbol{r}_2)\tilde{\psi}(\boldsymbol{r}_2) \\ &= \mathcal{V} \sum_{a=1}^{d_\Gamma} \hat{\phi}_a^\dagger \left(-i\frac{\partial}{\partial \boldsymbol{r}_1}\right) \eta_a^*(\boldsymbol{r}_1)\tilde{\psi}(\boldsymbol{r}_1). \end{aligned} \tag{3.68}$$

From the last expression, we conclude that the matrix elements of $\hat{\mathcal{H}}_{21}$ in coordinate space have the following form:

$$\hat{\mathcal{H}}_{21}(\boldsymbol{r}_1,\boldsymbol{r}_2)=\mathcal{V}\sum_{a=1}^{d_\Gamma}\hat{\phi}_a^\dagger\left(-i\frac{\partial}{\partial\boldsymbol{r}_1}\right)\eta_a^*(\boldsymbol{r}_1)\delta(\boldsymbol{r}_1-\boldsymbol{r}_2). \tag{3.69}$$

Now we collect everything together, and from Eqs. (3.44, 3.55, 3.56, 3.62, 3.69), it follows that Eq. (3.34) takes the form:

$$\begin{aligned}\hat{H}_{MF} &= \frac{1}{V}\frac{1}{\mathcal{V}}\sum_{\boldsymbol{q}}\sum_{a=1}^{d_\Gamma}|\eta_a(\boldsymbol{q})|^2 \qquad (3.70)\\ &+ \frac{1}{2}\int d\boldsymbol{r}_1\int d\boldsymbol{r}_2\hat{\Psi}^\dagger(\boldsymbol{r}_1)\begin{bmatrix}\hat{\sigma}_0\xi\left(-i\frac{\partial}{\partial\boldsymbol{r}_1}\right) & \sum_{a=1}^{d_\Gamma}\eta_a(\boldsymbol{r}_1)\hat{\phi}_a\left(-i\frac{\partial}{\partial\boldsymbol{r}_1}\right)\\ \sum_{a=1}^{d_\Gamma}\hat{\phi}_a^\dagger\left(-i\frac{\partial}{\partial\boldsymbol{r}_1}\right)\eta_a^*(\boldsymbol{r}_1) & -\hat{\sigma}_0\xi\left(-i\frac{\partial}{\partial\boldsymbol{r}_1}\right)\end{bmatrix}\\ &\quad\times\delta(\boldsymbol{r}_1-\boldsymbol{r}_2)\hat{\Psi}(\boldsymbol{r}_2),\end{aligned}$$

which can be written in the more condensed form:

$$\hat{H}_{MF}=\frac{1}{V}\frac{1}{\mathcal{V}}\sum_{\boldsymbol{q}}\sum_{a=1}^{d_\Gamma}|\eta_a(\boldsymbol{q})|^2+\frac{1}{2}\int d\boldsymbol{r}\hat{\Psi}^\dagger(\boldsymbol{r})\hat{\mathcal{H}}\hat{\Psi}(\boldsymbol{r}). \tag{3.71}$$

In this expression, we have renamed $\boldsymbol{r}_1=\boldsymbol{r}$, and

$$\hat{\mathcal{H}}=\begin{pmatrix}\hat{\xi} & \hat{\Delta}\\ \hat{\Delta}^\dagger & -\hat{\xi}\end{pmatrix} \tag{3.72}$$

is the 4×4 BdG Hamiltonian, which is a Hermitian differential operator. In Eq. (3.72),

$$\hat{\xi}=\hat{\sigma}_0\xi\left(-i\frac{\partial}{\partial\boldsymbol{r}}\right)$$

and

$$\hat{\Delta}=\sum_{a=1}^{d_\Gamma}\eta_a(\boldsymbol{r})\hat{\phi}_a\left(-i\frac{\partial}{\partial\boldsymbol{r}}\right). \tag{3.73}$$

We should point out that the matrix elements of the gap function operator $\hat{\Delta}$ in Eq. (3.72) in $\{\boldsymbol{k},\sigma\}$-space were first introduced in Eq. (3.19). For singlet pairing, the ath spin-matrix basis function has the form $\hat{\phi}_a(\boldsymbol{k})=(i\hat{\sigma}_2)\varphi_a(\hat{\boldsymbol{k}})$, where $\varphi_a(\hat{\boldsymbol{k}})$ is an even basis function of Γ. In particular, for the conventional singlet s-wave pairing, $d_\Gamma=1$ and $\varphi(\hat{\boldsymbol{k}})$ is independent of $\hat{\boldsymbol{k}}$, i.e. $\varphi(\hat{\boldsymbol{k}})=1$ (neglecting cutoffs), thus $\hat{\Delta}=i\hat{\sigma}_2\eta(\boldsymbol{r})$. Recall that for triplet pairing with strong spin-orbit coupling, $\hat{\phi}_a(\boldsymbol{k})=(i\hat{\boldsymbol{\sigma}}\hat{\sigma}_2)\cdot\boldsymbol{\varphi}_a(\hat{\boldsymbol{k}})$, where $\boldsymbol{\varphi}_a(\hat{\boldsymbol{k}})$

is a vector basis function belonging to Γ which is odd in $\boldsymbol{k}$. In the p-wave case, $d_\Gamma = 2$ and the basis functions are given by $\boldsymbol{\varphi}_1(\hat{\boldsymbol{k}}) = \hat{z}k_x/k_F$ and $\boldsymbol{\varphi}_2(\hat{\boldsymbol{k}}) = \hat{z}k_y/k_F$. Since in the coordinate space the arguments of the basis functions take the form $\boldsymbol{k} \to -i\boldsymbol{\nabla}$, the gap function operator for the p-wave pairing is given by

$$\hat{\Delta} = \eta_1(\boldsymbol{r})\hat{\sigma}_1\frac{-i\nabla_x}{k_F} + \eta_2(\boldsymbol{r})\hat{\sigma}_1\frac{-i\nabla_y}{k_F}. \tag{3.74}$$

Next, we will relate the energy of quasiparticle excitations to the eigenvalues of $\hat{\mathcal{H}}$, and this is accomplished by performing a Bogoliubov transformation on the mean-field Hamiltonian, Eq. (3.71). To facilitate the transformation, we first prove an important property of the BdG Hamiltonian:

$$\hat{\mathcal{H}}^* = -\hat{K}\hat{\mathcal{H}}\hat{K}, \tag{3.75}$$

where

$$\hat{K} = \begin{pmatrix} 0 & 0 & 1 & 0 \\ 0 & 0 & 0 & 1 \\ 1 & 0 & 0 & 0 \\ 0 & 1 & 0 & 0 \end{pmatrix} = \left(\begin{array}{c:c} 0 & \hat{\sigma}_0 \\ \hdashline \hat{\sigma}_0 & 0 \end{array}\right), \tag{3.76}$$

where the dashed lines separate 2×2 blocks. The second equality in this last expression allows us to easily calculate the right-hand side of Eq. (3.75), which is given by

$$\begin{aligned} -\hat{K}\hat{\mathcal{H}}\hat{K} &= -\begin{pmatrix} 0 & \hat{\sigma}_0 \\ \hat{\sigma}_0 & 0 \end{pmatrix}\begin{pmatrix} \hat{\xi} & \hat{\Delta} \\ \hat{\Delta}^\dagger & -\hat{\xi} \end{pmatrix}\begin{pmatrix} 0 & \hat{\sigma}_0 \\ \hat{\sigma}_0 & 0 \end{pmatrix} \\ &= \begin{pmatrix} \hat{\xi} & -\hat{\Delta}^\dagger \\ -\hat{\Delta} & -\hat{\xi} \end{pmatrix}. \end{aligned} \tag{3.77}$$

To prove that Eq. (3.75) holds true, one must therefore show that

$$\hat{\xi}^* = \hat{\xi}, \tag{3.78a}$$

$$\hat{\Delta}^* = -\hat{\Delta}^\dagger, \tag{3.78b}$$

$$\hat{\Delta}^{\dagger,*} = -\hat{\Delta}. \tag{3.78c}$$

Relation (3.78c) follows directly from relation (3.78b), since $\hat{\Delta} = (\hat{\Delta}^*)^* = (-\hat{\Delta}^\dagger)^* = -\hat{\Delta}^{\dagger,*}$. To prove equation (3.78a) we consider the following argument: the kinetic energy operator is given by $\hat{\xi} = \hat{\sigma}_0\xi(-i\boldsymbol{\nabla})$, so $\hat{\xi}^* = \hat{\sigma}_0\xi^*(i\boldsymbol{\nabla})$. Since the kinetic energy must be real, it follows that $\hat{\xi}^* = \hat{\sigma}_0\xi(i\boldsymbol{\nabla})$, and furthermore because $\xi(\boldsymbol{k}) = \xi(-\boldsymbol{k})$, one has $\hat{\xi}^* = \hat{\sigma}_0\xi(-i\boldsymbol{\nabla}) = \hat{\xi}$.

To prove the relation (3.78b), we consider Eq. (3.73), whose complex conjugate is given by $\hat{\Delta}^* = \sum_a \eta_a^*(\boldsymbol{r})\hat{\phi}_a^*(i\boldsymbol{\nabla})$. Furthermore, it follows from the complex conjugate of Eq. (3.8) that $\hat{\phi}_a^*(i\boldsymbol{\nabla}) = -\hat{\phi}_a^\dagger(-i\boldsymbol{\nabla})$, and thus one has

$$\hat{\Delta}^* = -\sum_a \eta_a^*(\boldsymbol{r})\hat{\phi}_a^\dagger(-i\boldsymbol{\nabla}). \tag{3.79}$$

From Eq. (3.70), it is clear that $\hat{\Delta}^\dagger = \sum_a \hat{\phi}_a^\dagger(-i\boldsymbol{\nabla})\eta_a^*(\boldsymbol{r})$, and, using the product rule of differentiation, this last expression takes the form

$$\hat{\Delta}^\dagger = \sum_a \left[\left(\hat{\phi}_a^\dagger(-i\boldsymbol{\nabla})\eta_a^*(\boldsymbol{r})\right) + \eta_a^*(\boldsymbol{r})\hat{\phi}_a^\dagger(-i\boldsymbol{\nabla})\right]. \tag{3.80}$$

The central assumption in the theory of superconductivity is that only electrons sufficiently close to the Fermi surface are involved in pairing. Consequently, in the interacting part of the Hamiltonian, Eq. (3.2), the summation is taken over wavevectors such that $|\boldsymbol{k}|, |\boldsymbol{k}'| \simeq k_F$, and thus the typical values of $\boldsymbol{q}$ are much smaller than $|\boldsymbol{k}|, |\boldsymbol{k}'|$. In the coordinate space this translates into a slowly varying order parameter, i.e. $\eta_a(\boldsymbol{r})$ varies on the scale of $|\boldsymbol{q}|^{-1} \sim \xi$, where ξ is the correlation length. Since the Nambu field operators vary on the scale of $|\boldsymbol{k}|^{-1} \sim k_F^{-1}$, the terms containing the derivatives of $\eta_a(\boldsymbol{r})$, see Eq. (3.80), can be neglected compared to the derivatives of $\hat{\Psi}(\boldsymbol{r})$ in the mean-field Hamiltonian. As a result, the adjoint of the gap function operator takes the following form:

$$\hat{\Delta}^\dagger = \sum_a \eta_a^*(\boldsymbol{r})\hat{\phi}_a^\dagger(-i\boldsymbol{\nabla}), \tag{3.81}$$

and thus it immediately follows from Eq. (3.79) that $\hat{\Delta}^* = -\hat{\Delta}^\dagger$, and we can therefore conclude that Eq. (3.75) holds true.

An important symmetry of the spectrum of the BdG Hamiltonian follows from Eq. (3.75). To obtain this symmetry we consider the eigenfunctions of this Hamiltonian. If $\psi(\boldsymbol{r}) = [u_\uparrow(\boldsymbol{r}), u_\downarrow(\boldsymbol{r}), v_\uparrow(\boldsymbol{r}), v_\downarrow(\boldsymbol{r})]^T$ is an eigenfunction of $\hat{\mathcal{H}}$ corresponding to eigenvalue E, then $\tilde{\psi}(\boldsymbol{r}) = \hat{K}\psi^*(\boldsymbol{r}) = \left[v_\uparrow^*(\boldsymbol{r}), v_\downarrow^*(\boldsymbol{r}), u_\uparrow^*(\boldsymbol{r}), u_\downarrow^*(\boldsymbol{r})\right]^T$ is also an eigenfunction of $\hat{\mathcal{H}}$ corresponding to the eigenvalue $-E$. This can be proven by considering the BdG equation $\hat{\mathcal{H}}\psi = E\psi$. We have $\hat{\mathcal{H}}\tilde{\psi} = \hat{\mathcal{H}}(\hat{K}\psi^*) = (\hat{\mathcal{H}}\hat{K})\psi^*$. Using Eq. (3.75), along with the fact that $\hat{K}^2 = \hat{1}$, it follows that $\hat{\mathcal{H}}\hat{K} = -\hat{K}\hat{\mathcal{H}}^*$, and thus $\hat{\mathcal{H}}\tilde{\psi} = -\hat{K}(\hat{\mathcal{H}}\psi)^*$. Furthermore, because the energy eigenvalues are real, we have $\hat{\mathcal{H}}\tilde{\psi} = -E(\hat{K}\psi^*) = -E\tilde{\psi}$.

We use the fact that the energy eigenvalues of the BdG Hamiltonian always come in pairs $(E, -E)$ to proceed with the Bogoliubov transformation of the mean-field Hamiltonian, via focusing on the upper half of the energy spectrum. We associate fermionic operators $\hat{\gamma}_i$ and $\hat{\gamma}_i^\dagger$ with each state from the upper half of the spectrum, i.e. with $E_i \geq 0$. We can now introduce the Bogoliubov transformation, where we take the components of the Nambu field operators, see Eq. (3.45), to have the following form:

$$\begin{aligned}
\hat{\Psi}_\uparrow(\boldsymbol{r}) &= \sum_i \left[u_\uparrow^i(\boldsymbol{r})\hat{\gamma}_i + v_\uparrow^{i,*}(\boldsymbol{r})\hat{\gamma}_i^\dagger\right], \\
\hat{\Psi}_\downarrow(\boldsymbol{r}) &= \sum_i \left[u_\downarrow^i(\boldsymbol{r})\hat{\gamma}_i + v_\downarrow^{i,*}(\boldsymbol{r})\hat{\gamma}_i^\dagger\right], \\
\hat{\Psi}_\uparrow^\dagger(\boldsymbol{r}) &= \sum_i \left[v_\uparrow^i(\boldsymbol{r})\hat{\gamma}_i + u_\uparrow^{i,*}(\boldsymbol{r})\hat{\gamma}_i^\dagger\right], \\
\hat{\Psi}_\downarrow^\dagger(\boldsymbol{r}) &= \sum_i \left[v_\downarrow^i(\boldsymbol{r})\hat{\gamma}_i + u_\downarrow^{i,*}(\boldsymbol{r})\hat{\gamma}_i^\dagger\right],
\end{aligned} \tag{3.82}$$

where the sum runs over the upper half of the energy spectrum only. By writing this in a vector form, it becomes apparent that the 4-component Nambu spinors are transformed as follows:

$$\begin{aligned}
\hat{\Psi}(\boldsymbol{r}) &= \sum_i \left[\psi_i(\boldsymbol{r})\hat{\gamma}_i + \tilde{\psi}_i(\boldsymbol{r})\hat{\gamma}_i^\dagger\right], \\
\hat{\Psi}^\dagger(\boldsymbol{r}) &= \sum_i \left[\tilde{\psi}_i^\dagger(\boldsymbol{r})\hat{\gamma}_i + \psi_i^\dagger(\boldsymbol{r})\hat{\gamma}_i^\dagger\right].
\end{aligned} \tag{3.83}$$

in terms of the eigenfunctions of the BdG Hamiltonian, $\psi(\boldsymbol{r})$ and $\tilde{\psi}(\boldsymbol{r})$, which were introduced above.

Substituting expression (3.83) for the Nambu field operators into the second term of Eq. (3.71), we obtain:

$$\begin{aligned}
\frac{1}{2}\int d\boldsymbol{r}\hat{\Psi}^\dagger(\boldsymbol{r})\hat{\mathcal{H}}\hat{\Psi}(\boldsymbol{r}) &= \frac{1}{2}\int d\boldsymbol{r}\sum_{i,j}\left[\psi_i^\dagger(\boldsymbol{r})\hat{\gamma}_i^\dagger + \tilde{\psi}_i^\dagger(\boldsymbol{r})\hat{\gamma}_i\right]\hat{\mathcal{H}}\left[\psi_j(\boldsymbol{r})\hat{\gamma}_j + \tilde{\psi}_j(\boldsymbol{r})\hat{\gamma}_j^\dagger\right], \\
&= \frac{1}{2}\sum_{i,j}\left[\hat{\gamma}_i^\dagger\hat{\gamma}_j\int d\boldsymbol{r}\psi_i^\dagger(\boldsymbol{r})\hat{\mathcal{H}}\psi_j(\boldsymbol{r}) + \hat{\gamma}_i^\dagger\hat{\gamma}_j^\dagger\int d\boldsymbol{r}\psi_i^\dagger(\boldsymbol{r})\hat{\mathcal{H}}\tilde{\psi}_j(\boldsymbol{r})\right. \\
&+ \left.\hat{\gamma}_i\hat{\gamma}_j\int d\boldsymbol{r}\tilde{\psi}_i^\dagger(\boldsymbol{r})\hat{\mathcal{H}}\psi_j(\boldsymbol{r}) + \hat{\gamma}_i\hat{\gamma}_j^\dagger\int d\boldsymbol{r}\tilde{\psi}_i^\dagger(\boldsymbol{r})\hat{\mathcal{H}}\tilde{\psi}_j(\boldsymbol{r})\right].
\end{aligned} \tag{3.84}$$

Due to the orthonormality of the eigenfunctions of $\hat{\mathcal{H}}$, it follows that the integrals in the second and third terms in this last expression are identically zero (since the eigenfunctions ψ_i and $\tilde{\psi}_i$ correspond to different eigenvalues). Evaluating the remaining two integrals, we arrive at the following expression:

$$\begin{aligned}\frac{1}{2}\int d\boldsymbol{r}\hat{\Psi}^{\dagger}(\boldsymbol{r})\hat{\mathcal{H}}\hat{\Psi}(\boldsymbol{r}) &= \frac{1}{2}\sum_{i,j}E_j\delta_{ij}\left(\hat{\gamma}_i^{\dagger}\hat{\gamma}_j-\hat{\gamma}_i\hat{\gamma}_j^{\dagger}\right), \\ &= \frac{1}{2}\sum_i E_i\left(\hat{\gamma}_i^{\dagger}\hat{\gamma}_i-\hat{\gamma}_i\hat{\gamma}_i^{\dagger}\right).\end{aligned} \tag{3.85}$$

Using the anti-commutation relation for the fermionic operators, $\{\hat{\gamma}_i,\hat{\gamma}_i^{\dagger}\}=1$, it follows that this last equation takes the final form:

$$\frac{1}{2}\int d\boldsymbol{r}\hat{\Psi}^{\dagger}(\boldsymbol{r})\hat{\mathcal{H}}\hat{\Psi}(\boldsymbol{r}) = -\frac{1}{2}\sum_i E_i+\sum_i E_i\hat{\gamma}_i^{\dagger}\hat{\gamma}_i. \tag{3.86}$$

Therefore, we can rewrite the mean-field Hamiltonian, Eq. (3.71), after the Bogoliubov transformation as follows:

$$\hat{H}_{MF} = (c\text{-number})+\sum_i E_i\hat{\gamma}_i^{\dagger}\hat{\gamma}_i. \tag{3.87}$$

Here we recall that the sum is taken over the “upper half” of the energy spectrum of the BdG Hamiltonian, where $E_i \geq 0$.

From the Hamiltonian (3.87), we can see that $E_i \geq 0$ are the energies of the elementary excitations in the superconductor. Physically this means that at zero temperature, all states with energies in the lower half of the BdG spectrum ($E_i \leq 0$) are filled, and all of the states in the upper half of the spectrum are empty. At nonzero temperature, quasiparticles with energies $E_i \geq 0$ will be thermally excited, resulting in these states being filled according to the Fermi-Dirac distribution. These excitations become important when considering thermodynamic quantities, such as the specific heat, spin susceptibility, or thermal conductivity [29, 18].

One can obtain the eigenenergies E_i by solving the BdG equation $\hat{\mathcal{H}}\psi = E\psi$. However, even for the simplest kinetic energy in the effective mass approximation, $\xi(\boldsymbol{k}) = (\boldsymbol{k}^2-k_F^2)/2m^*$, the differential equations are of second order, and there is no standard method to solve these equations. Luckily there is a more practical option for obtaining the eigenenergies, provided by the semiclassical, or Andreev, approximation. In this approach, the second-order BdG differential equations are reduced to a set of two linear first-order differential equations. In the following section we will apply this approximation, and derive the corresponding Andreev equations for the quasiparticle spectrum.

3.2 Semiclassical (Andreev) approximation

Since in this work we consider a neutral superfluid, the interaction between the DWs can only be due to their effect on the Bogoliubov fermionic quasiparticles. Recall from the previous subsection that the quasiparticle spectrum for a non-uniform superconductor is determined by the BdG equations, with the 4×4 BdG Hamiltonian given by Eq. (3.72).

In this work, we focus on the quasiparticle properties in the chiral p-wave states, in which the gap function operator has the form given by Eq. (3.74). This form for $\hat{\Delta}$ allows the BdG Hamiltonian in Eq. (3.72), which operates on a four-component quasiparticle wavefunction, to be written as a direct sum of two identical 2×2 matrices, denoted by $\hat{H}_{BdG}$. The four-component wavefunction is thus decoupled into 2 two-component wavefunctions, which satisfy $\hat{H}_{BdG}\Psi_\sigma = E\Psi_\sigma$, where $\sigma = \pm$, and $\hat{H}_{BdG}$ is given by

$$\hat{H}_{BdG} = \begin{pmatrix} \xi(-i\boldsymbol{\nabla}) & d_z \\ d_z^\dagger & -\xi(-i\boldsymbol{\nabla}) \end{pmatrix}, \tag{3.88}$$

with

$$d_z = \eta_1(\boldsymbol{r})\frac{-i\nabla_x}{k_F} + \eta_2(\boldsymbol{r})\frac{-i\nabla_y}{k_F}.$$

We should point out that σ does not denote the spin projection of the two-component wavefunction; in fact, the components of both spinors have mixed spin projections. From this point, we may drop the label σ and restore it where necessary in final expressions.

As mentioned in Sec. 2, we consider superconducting textures in two dimensions in which the order parameter depends only on x. For a DW parallel to the y-axis, the y-dependence of the quasiparticle wavefunction is equivalent to that of a free particle (i.e. plane wave). It can be written as $e^{ik_y y}\Psi(x)$, where $\Psi(x)$ satisfies the two-component BdG equations for a given k_y:

$$\begin{pmatrix} \dfrac{\hat{k}_x^2 - k_0^2}{2m^*} & \Delta(x) \\ \Delta^\dagger(x) & -\dfrac{\hat{k}_x^2 - k_0^2}{2m^*} \end{pmatrix} \Psi = E\Psi, \tag{3.89}$$

with $\hat{k}_x = -i\nabla_x$, $k_0 = \sqrt{k_F^2 - k_y^2}$, and $\Delta(x) = d_z(x) = \eta_1(x)(\hat{k}_x/k_F) + \eta_2(x)(k_y/k_F)$. To obtain Eq. (3.89), we made the assumption that the band dispersion is isotropic and given by $\xi(\boldsymbol{k}) = (\boldsymbol{k}^2 - k_F^2)/2m^*$, where m^* is the effective mass. Note that k_y is not an operator here, and this reflects the fact that the system contains only x-dependence.

The DW order parameter $\Delta(x)$ varies slowly on the scale of $1/k_F$. Consequently, we can apply the semiclassical (Andreev) approximation [60] and seek solutions of Eq. (3.89) in the form $\Psi(x) = e^{ik_x x}\psi(x)$, where $\psi(x) = (u, v)^T$ is a slowly varying "envelope" function with electron-like (u) and hole-like (v) components. Due to the circular symmetry of the Fermi surface in the xy plane, we have $k_x = \pm k_0$ for a given k_y. It thus follows that $\hat{k}_x\Psi(x) = \exp(\pm ik_0x)(\pm k_0 - i\nabla_x)\psi(x)$, and also $\hat{k}_x^2\Psi(x) = \exp(\pm ik_0x)(-i\nabla_x \pm k_0)^2\psi(x)$. Substituting $\Psi(x)$ into Eq. (3.89), from the first row of the Hamiltonian we obtain the following equation:

$$\begin{aligned}&\frac{1}{2m^*}e^{\pm ik_0x}\left[(-i\nabla_x \pm k_0)^2 - k_0^2\right]u(x)\\ &+\eta_1\frac{\hat{k}_x}{k_F}\left[e^{\pm ik_0x}v(x)\right] + \eta_2\frac{k_y}{k_F}\left[e^{\pm ik_0x}v(x)\right] = Ee^{\pm ik_0x}u(x),\end{aligned}$$

and there is an analogous expression that follows from the second row of the Hamiltonian. Simplifying this last expression by performing the differentiation and canceling the exponentials, we obtain:

$$\frac{\nabla_x}{2m^*}\left[-2ik_xu(x) - \nabla_xu(x)\right] + \left(\eta_1\frac{k_x}{k_F} + \eta_2\frac{k_y}{k_F}\right)v(x) - i\eta_1\frac{(\nabla_xv(x))}{k_F} = Eu(x), \qquad (3.90)$$

where we have used the fact that $k_x = \pm k_0$.

As a consequence of the cylindrical symmetry of the Fermi surface, the direction of semiclassical propagation of quasiparticles is defined by the Fermi wavevector $\boldsymbol{k}_F \equiv (k_x, k_y) = k_F(\cos\theta, \sin\theta)$. It follows that $k_x/k_F = \cos\theta$ and $k_y/k_F = \sin\theta$, and since $\cos\theta, \sin\theta \sim 1$ and $\psi(x)$ is a slowly varying function, $|\nabla_x\psi(x)|/k_F \ll k_x\psi(x)/k_F$. This allows us to neglect the terms containing the gradients of $\psi(x)$, and then Eq. (3.90) takes the form:

$$-iv_{F,x}\nabla_xu(x) + (\eta_1\cos\theta + \eta_2\sin\theta)\,v(x) = Eu(x), \qquad (3.91)$$

where $v_{F,x} = v_F\cos\theta$ and $v_F = k_F/m^*$. A similar manipulation of the equation obtained from the second row of the 2×2 reduced BdG Hamiltonian, Eq. (3.89), will show that $\psi(x)$ satisfies the Andreev equations:

$$\begin{pmatrix} -iv_{F,x}\nabla_x & \Delta_{\boldsymbol{k}_F}(x) \\ \Delta^*_{\boldsymbol{k}_F}(x) & iv_{F,x}\nabla_x \end{pmatrix}\psi = E\psi, \qquad (3.92)$$

where $\Delta_{\boldsymbol{k}_F}(x)$ is the DW order parameter for a given $\boldsymbol{k}_F$, which has the form

$$\Delta_{\boldsymbol{k}_F} = \eta_1(x)\cos\theta + \eta_2(x)\sin\theta = |\Delta_{\boldsymbol{k}_F}(x)|e^{i\Phi(x)}. \qquad (3.93)$$

In this last expression, $|\Delta_{\boldsymbol{k}_F}(x)|$ is the magnitude, and $\Phi(x)$ is the phase, of the semiclassical order parameter.

The asymptotics of $\Delta_{\boldsymbol{k}_F}$ for the chiral p-wave state are fixed by Eqs. (2.2a) and (2.2b); however, different models for the DW structure (see Sec. 2) lead to different forms for the order parameter in the vicinity of the DW. While the exact shape is unknown, the chiral p-wave order parameter far from the DW can be written as

$$\begin{aligned} \Delta_- &\equiv \Delta_{\boldsymbol{k}_F}(x \ll -\xi_d) = \Delta_0 e^{i\theta}, \\ \Delta_+ &\equiv \Delta_{\boldsymbol{k}_F}(x \gg \xi_d) = \Delta_0 e^{i\chi} e^{-i\theta}. \end{aligned} \tag{3.94}$$

In the single sharp DW model, the order parameter is uniform within the domains of opposing chirality, changing abruptly at the boundary $x = 0$. Thus we have the following form for $\Delta_{\boldsymbol{k}_F}$ in terms of its asymptotic values above:

$$\Delta_{\boldsymbol{k}_F} = \Delta_-\Theta(-x) + \Delta_+\Theta(x), \tag{3.95}$$

where $\Theta(x)$ is the Heaviside step function. For two DWs, we have

$$\Delta_{\boldsymbol{k}_F}(x) = \Delta_-\Theta(-x) + \Delta_+\Theta(x)\Theta(L-x) + \Delta_-\Theta(x-L). \tag{3.96}$$

There are two types of solutions supported by the Andreev equations: discrete bound states (Andreev bound states, or ABS's), for which $|E| \leq \Delta_0$; as well as a continuum of scattering states, where $|E| > \Delta_0$. In the next subsection we will discuss the formal properties of the Andreev scattering states. Subsequently, in Sec. 4, we will analyze the bound and scattering states for the DW configurations introduced above.

3.2.1 Formal properties of the Andreev scattering states

We consider a single-DW setup as described in Sec. 2, with a DW of thickness ξ_d, whose order parameter asymptotics are given by $\Delta_{\boldsymbol{k}_F}(x \to \pm\infty) = \Delta_\pm$. At given energy, there are two solutions $\psi_L(x)$ and $\psi_R(x)$, corresponding to left- and right-incident scattering, respectively, which have the following asymptotic form:

$$\begin{aligned} \psi_L(x) &= C(E)\begin{cases} \alpha_L e^{iqx} + r_L\beta_L e^{-iqx}, & x \ll -\xi_d \\ t_L\gamma_L e^{iqx}, & x \gg \xi_d \end{cases} \\ \psi_R(x) &= C(E)\begin{cases} t_R\gamma_R e^{-iqx}, & x \ll -\xi_d \\ \alpha_R e^{-iqx} + r_R\beta_R e^{iqx}, & x \gg \xi_d \end{cases}, \end{aligned} \tag{3.97}$$

where $\alpha_p, \beta_p, \gamma_p$ $(p = L, R)$ are two-component constants which depend on energy, $q = \sqrt{E^2 - \Delta_0^2}/|v_{F,x}| \geq 0$, and $C(E)$ is the normalization coefficient.

We see that there are two sets of the Andreev equations, corresponding to $\psi_{R(L)} = [u_{R(L)}, v_{R(L)}]^T$, i.e. two directions of scattering. Let us temporarily rename $\Delta_{\boldsymbol{k}_F}(x) = \Delta$, and then substitution of ψ_{p_1} $(p_1 = R, L)$ into Eq. (3.92) gives

$$-iv_{F,x}\frac{du_{p_1}}{dx} + \Delta v_{p_1} = Eu_{p_1}, \tag{3.98a}$$

$$\Delta^* u_{p_1} + iv_{F,x}\frac{dv_{p_1}}{dx} = Ev_{p_1}. \tag{3.98b}$$

We take the complex conjugates of the analogous expressions for ψ_{p_2} to obtain:

$$iv_{F,x}\frac{du^*_{p_2}}{dx} + \Delta^* v^*_{p_2} = Eu^*_{p_2}, \tag{3.99a}$$

$$\Delta u^*_{p_2} - iv_{F,x}\frac{dv^*_{p_2}}{dx} = Ev^*_{p_2}. \tag{3.99b}$$

Subsequently, we multiply Eq. (3.98a) from the left by $u^*_{p_2}$, and subtract from the resulting expression Eq. (3.99b) multiplied from the right by v_{p_1}, to obtain:

$$-iv_{F,x}\left(u^*_{p_2}\frac{du_{p_1}}{dx} - \frac{dv^*_{p_2}}{dx}v_{p_1}\right) = E(u^*_{p_2}u_{p_1} - v^*_{p_2}v_{p_1}). \tag{3.100}$$

In a similar manner, we multiply Eq. (3.98b) from the left by $v^*_{p_2}$, and subtract from the result Eq. (3.99a) multiplied from the right by u_{p_1}, to find:

$$iv_{F,x}\left(v^*_{p_2}\frac{dv_{p_1}}{dx} - \frac{du^*_{p_2}}{dx}u_{p_1}\right) = E(v^*_{p_2}v_{p_1} - u^*_{p_2}u_{p_1}). \tag{3.101}$$

Adding together Eqs. (3.100) and (3.101), it becomes evident that there is a conserved quantity, i.e.

$$\frac{d}{dx}\left(u^*_{p_2}u_{p_1} - v^*_{p_2}v_{p_1}\right) = 0. \tag{3.102}$$

We define a new quantity $\mathcal{W}_{p_1,p_2}(x)$, which plays the role of the Wronskian of states $|E, p_1\rangle$ and $|E, p_2\rangle$, where $\langle x|E, p\rangle = \psi_p(x)$:

$$\mathcal{W}_{p_1,p_2} = u^*_{p_1}u_{p_2} - v^*_{p_1}v_{p_2} = \mathrm{tr}\left(\psi^\dagger_{p_1}\hat{\sigma}_3\psi_{p_2}\right), \tag{3.103}$$

and since, according to Eq. (3.102), $d\mathcal{W}_{p_1,p_2}/dx = 0$, it follows that $\mathcal{W}_{p_1,p_2}$ does not depend on x. Furthermore, since $\mathcal{W}_{p_1,p_2} = \text{const}$ for all values of x, continuity of $\mathcal{W}_{p_1,p_2}$ on either side of the DW for the four possible combinations of p_1, p_2 leads to a set of conditions for the reflection and transmission coefficients.

The exact expressions for $\alpha_p, \beta_p, \gamma_p$ in terms of $\alpha_q^{(\pm)}$ are derived below, see Eqs. (4.5) and (4.6) and the discussion thereafter. To facilitate the calculation of the four elements of $\mathcal{W}_{p_1,p_2}$, we impose an additional factor of $1/\sqrt{2}$ on the vector coefficients $\alpha_p, \beta_p, \gamma_p$. After calculating the expressions (3.103) for all combinations of p_1, p_2, we have:

$$\mathcal{W}_{L,L}(x) = C^2(E)\frac{v_{F,x}q}{E}\begin{cases}1-|r_L|^2, & x \ll -\xi_d \\ |t_L|^2, & x \gg \xi_d\end{cases}; \tag{3.104a}$$

$$\mathcal{W}_{R,R}(x) = C^2(E)\frac{v_{F,x}q}{E}\begin{cases}-|t_R|^2, & x \ll -\xi_d \\ |r_R|^2-1, & x \gg \xi_d\end{cases}; \tag{3.104b}$$

$$\mathcal{W}_{L,R}(x) = C^2(E)\frac{v_{F,x}q}{E}\begin{cases}-r_L^* t_R, & x \ll -\xi_d \\ t_L^* r_R, & x \gg \xi_d\end{cases}; \tag{3.104c}$$

$$\mathcal{W}_{R,L}(x) = C^2(E)\frac{v_{F,x}q}{E}\begin{cases}-t_R^* r_L, & x \ll -\xi_d \\ r_R^* t_L, & x \gg \xi_d\end{cases}. \tag{3.104d}$$

Since $\mathcal{W}_{p_1,p_2}$ is constant for all x, we now invoke continuity across the DW in each of the above four expressions to obtain:

$$\begin{aligned}|r_L|^2 + |t_L|^2 &= 1,\\ |r_R|^2 + |t_R|^2 &= 1,\\ r_L^* t_R + t_L^* r_R &= 0,\\ t_R^* r_L + r_R^* t_L &= 0,\end{aligned} \tag{3.105}$$

where there is a direct correspondence between the order of the expressions in Eq. (3.104) and this last set of relations. It is clear that these relations are satisfied if $|t_L| = |t_R| = t, |r_L| = |r_R| = r = \sqrt{1-t^2}$, and thus the scattering matrix defined by

$$S = \begin{pmatrix} t_L & r_R \\ r_L & t_R \end{pmatrix} \tag{3.106}$$

is unitary, i.e. $S^\dagger = S^{-1}$.

Further manipulation of the Andreev equations for the left- and right-incident scattering states reveals that there is another conserved quantity. We take the complex conjugate of Eq. (3.99a), then multiply it from the left by v_{p_1}, and finally subtract it from Eq. (3.98a) multiplied from the right by v_{p_2}, to obtain:

$$iv_{F,x}\left(v_{p_1}\frac{du_{p_2}}{dx}-\frac{du_{p_1}}{dx}v_{p_2}\right)=E(u_{p_1}v_{p_2}-v_{p_1}u_{p_2}). \tag{3.107}$$

Similarly, we multiply Eq. (3.98b) from the right by u_{p_2} and subtract from it Eq. (3.99b) complex conjugated and multiplied by u_{p_1}:

$$iv_{F,x}\left(\frac{dv_{p_1}}{dx}u_{p_2}-u_{p_1}\frac{dv_{p_2}}{dx}\right)=E(v_{p_1}u_{p_2}-u_{p_1}v_{p_2}). \tag{3.108}$$

After adding Eqs. (3.107) and (3.108) together, the other conserved quantity presents itself:

$$\frac{d}{dx}\left(u_{p_1}v_{p_2}-v_{p_1}u_{p_2}\right)=0. \tag{3.109}$$

Consequently, we introduce

$$\tilde{\mathcal{W}}_{p_1,p_2}(x)=u_{p_1}v_{p_2}-v_{p_1}u_{p_2}=i\mathrm{tr}\left(\psi_{p_1}^T\hat{\sigma}_2\psi_{p_2}\right), \tag{3.110}$$

and since $d\tilde{\mathcal{W}}_{p_1,p_2}/dx=0$, this new quantity is constant for all values of x. Note that because u_p, v_p are just functions, their order can be interchanged in Eq. (3.110), and thus $\tilde{\mathcal{W}}_{p_1,p_2}$ is by definition the Wronskian of the vector states $|E,p_1\rangle$ and $|E,p_2\rangle$. Quick inspection of Eq. (3.110) reveals that $\tilde{\mathcal{W}}_{R,L}(x)=-\tilde{\mathcal{W}}_{L,R}(x)$, and furthermore $\tilde{\mathcal{W}}_{L,L}(x)=\tilde{\mathcal{W}}_{R,R}(x)=0$, since the state $|E,p_1\rangle$ is itself linearly dependent, necessitating a Wronskian which is zero for all values of x.

We calculate the element $\tilde{\mathcal{W}}_{R,L}$ on both sides of the DW to find:

$$\tilde{\mathcal{W}}_{R,L}=-C^2(E)\frac{v_{F,x}q}{E}\,\mathrm{sgn}\,(E)\begin{cases}\dfrac{\Delta_-}{\Delta_0}t_R, & x\ll-\xi_d\\ \dfrac{\Delta_+}{\Delta_0}t_L, & x\gg\xi_d\end{cases}, \tag{3.111}$$

and since $\tilde{\mathcal{W}}_{R,L}(x\ll-\xi_d)=\tilde{\mathcal{W}}_{R,L}(x\gg\xi_d)$, we recover another property for the transmission coefficients:

$$\frac{t_R}{t_L}=\frac{\Delta_+}{\Delta_-}. \tag{3.112}$$

We note that while relations (3.105) hold for an arbitrary DW configuration, this last identity holds only in the case of a DW configuration with an even number of domains, i.e. one with $\Delta_{\boldsymbol{k}_F}(x \to \pm\infty) = \Delta_\pm$, where $\Delta_\pm$ are defined in Eq. (3.94). For the two-DW configuration considered in Sec. 2, for example, this exact identity does not hold because $\Delta_{\boldsymbol{k}_F}(x \to \pm\infty) = \Delta_-$. As a second note we point out that the identities (3.105) and (3.112) are independent of the exact profile for the DW in the region $-\xi_d < x < \xi_d$, i.e. of the model considered. In particular, these relations hold for the sharp DW models considered in subsequent sections throughout the work.

4 Quasiparticle properties of DWs

4.1 Quasiparticle spectrum for a single DW

In this section we apply the general results from Sec. 3 to obtain the quasiparticle spectrum of a single planar defect in the semiclassical approximation. We will calculate both the bound state spectrum and the properties of the scattering states.

4.1.1 ABS energies for a DW

For a single DW the semiclassical order parameter in Eq. (3.92) is given by the expression (3.95). The solution of this equation corresponding to the bound states is given by:

$$\psi(x) = \sqrt{\frac{\Omega}{2|v_{F,x}|}} e^{-\Omega|x|/|v_{F,x}|} \begin{pmatrix} \dfrac{\Delta_\pm}{E \mp i\Omega \operatorname{sgn} v_{F,x}} \\ 1 \end{pmatrix}, \tag{4.1}$$

where $\Omega = \sqrt{\Delta_0^2 - E^2}$, the upper (lower) sign corresponds to $x > 0$ ($x < 0$), $\Delta_\pm$ are defined in Eq. (3.94), and the coefficient in this last expression arises from the normalization condition:

$$\int_{-\infty}^{\infty} \operatorname{tr}[\psi^\dagger(x)\psi(x)]dx = 1.$$

By equating the wave functions at the boundary between the two domains, we obtain the characteristic equation for the bound state energy:

$$\frac{E + i\Omega \operatorname{sgn} v_{F,x}}{E - i\Omega \operatorname{sgn} v_{F,x}} = \frac{\Delta_-}{\Delta_+}. \tag{4.2}$$

To solve this last equation, we first introduce $\tilde{E} = E \operatorname{sgn} v_{F,x}$. Now $\tilde{E}^2 + \Omega^2 = \Delta_0^2$ (a constant), and we use this identity to seek solutions for the energy in the following form: $\tilde{E} = \Delta_0 \cos\Theta$ and $\Omega = \Delta_0 \sin\Theta$. We also impose the restriction on the values of Θ such that Ω is real and $\Omega \geq 0$. From Eq. (4.2), one can see that Θ satisfies $e^{2i\Theta} = e^{i(2\theta-\chi)}$, and consequently $\Theta = \theta - \chi/2 + \pi n$, where n is an integer. Thus we have $\tilde{E} = \Delta_0(-1)^n \cos(\theta - \chi/2)$, and the value of n is found from the condition mentioned above ($\Omega \geq 0$), which yields

$$\operatorname{sgn}(\sin\Theta) = 1 = (-1)^n \operatorname{sgn}\left[\sin(\theta - \chi/2)\right].$$

Taking everything into consideration, we obtain the following expression for the ABS energy [61]:

$$E_0(\theta) = \Delta_0 s(\theta) \cos\left(\theta - \frac{\chi}{2}\right), \tag{4.3}$$

with $s(\theta) = \operatorname{sgn}[\sin(\theta - \chi/2)\cos\theta]$. This expression is valid for an arbitrary phase difference across the DW and it should be noted that, in general, the ABS energy is not a continuous function of θ. There are certain directions of semiclassical propagation at which discontinuities occur: at $\theta = \pm\pi/2$, corresponding to a "grazing trajectory" where the quasiparticles move parallel to the DW (in this case the Andreev approximation is actually not applicable); and also at $\theta = \chi/2$ and $\theta = \chi/2 + \pi$, in which case the quasiparticles do not "see" the DW, since $\Delta_+ = \Delta_-$.

Fig. 11 depicts the structure of the ABS energy for several values of the common phase difference χ. In particular, if $\chi = \pi$, then Eq. (4.3) yields $E = -\Delta_0 \sin\theta = -\Delta_0 k_y/k_F$ (see also Ref. [49]), which vanishes at $k_y = 0$. The presence of zero modes is in fact generic: the ABS energy vanishes at $\theta = (\chi \pm \pi)/2$, resulting in low-energy quasiparticles bound to the DW. Taking the spin into account, we have two pairs of spin-degenerate zero mode branches.

4.1.2 Andreev scattering states for a DW

We proceed in the standard fashion to obtain the reflection/transmission coefficients for the Andreev scattering states in the sharp DW model. We consider the general form of the quasiparticle wavefunctions on each side of the single DW:

$$\begin{aligned} \psi_-(x) &= A_+^{(-)} \begin{pmatrix} \alpha_{1-} \\ \beta_{1-} \end{pmatrix} e^{iqx} + A_-^{(-)} \begin{pmatrix} \alpha_{2-} \\ \beta_{2-} \end{pmatrix} e^{-iqx}, \\ \psi_+(x) &= A_+^{(+)} \begin{pmatrix} \alpha_{1+} \\ \beta_{1+} \end{pmatrix} e^{iqx} + A_-^{(+)} \begin{pmatrix} \alpha_{2+} \\ \beta_{2+} \end{pmatrix} e^{-iqx}, \end{aligned} \tag{4.4}$$

where the subscripts on the coefficients correspond to directions of propagation (left or right), and the subscripts on the wavefunctions and the superscripts on the coefficients "$-$" ($+$) correspond to the region $x < 0$ ($x > 0$). After substitution of these expressions into the Andreev equations (3.92), we find that the quasiparticle wavefunctions take the form:

$$\begin{aligned} \psi_-(x) &= A_+^{(-)} \alpha_q^{(-)} e^{iqx} + A_-^{(-)} \alpha_{-q}^{(-)} e^{-iqx}, \\ \psi_+(x) &= A_+^{(+)} \alpha_q^{(+)} e^{iqx} + A_-^{(+)} \alpha_{-q}^{(+)} e^{-iqx}, \end{aligned} \tag{4.5}$$

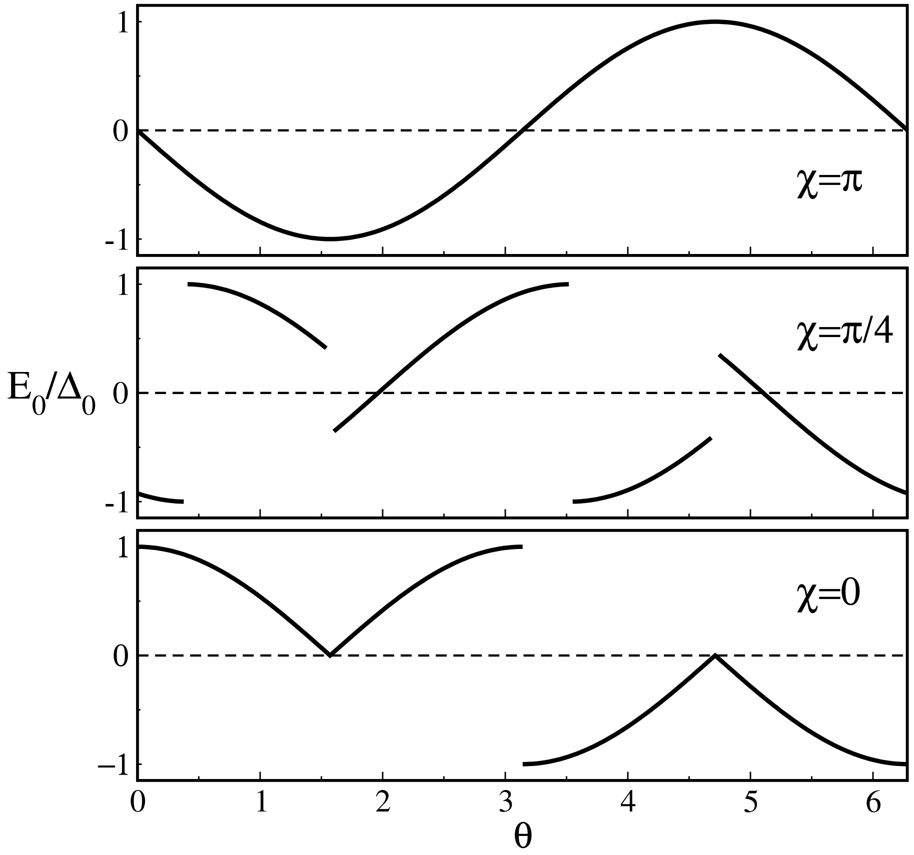

Figure 11: The ABS energy for a sharp DW as a function of the direction of the quasiparticle propagation θ, for selected values of the phase difference across the DW: $\chi = \pi$ (top), $\chi = \pi/4$ (middle), and $\chi = 0$ (bottom).

where $q = \sqrt{E^2 - \Delta_0^2}/|v_{F,x}| \geq 0$,

$$\alpha_q^{(\pm)} = \begin{pmatrix} \frac{\Delta_\pm}{\Delta_0}\left(1 + \frac{qv_{F,x}}{E}\right)^{1/2} \operatorname{sgn}(E) \\ \left(1 - \frac{qv_{F,x}}{E}\right)^{1/2} \end{pmatrix}, \tag{4.6}$$

and $\alpha_{-q}^{(\pm)}$ results from replacing $q \to -q$ in this last expression.

Inspection of Eq. (4.5) reveals that the amplitudes of the waves incident on the DW correspond to coefficients $A_+^{(-)}$ and $A_-^{(+)}$, while the outgoing wave amplitudes are given by $A_-^{(-)}$ and $A_+^{(+)}$. Thus in the case of left-incident scattering, it follows that $A_+^{(-)} = 1$, $A_-^{(-)} = r_L$, $A_+^{(+)} = t_L$, and $A_-^{(+)} = 0$, where r_L is the left-incident reflection coefficient and t_L is the corresponding transmission coefficient. For the right-incident scattering, one has $A_+^{(-)} = 0$, $A_-^{(-)} = t_R$, $A_+^{(+)} = r_R$, and $A_-^{(+)} = 1$, where t_R and r_R are the right-incident transmission and reflection coefficients, respectively. By equating the wavefunctions at the boundary $x = 0$ (i.e. the location of the sharp domain wall) separately for each of these cases, we find that the reflection and transmission coefficients have the following form [61]:

$$\begin{aligned} t_L &= \frac{\Delta_-}{\Delta_+} t_R = \frac{2\Delta_- q v_{F,x}}{(\Delta_+ + \Delta_-) q v_{F,x} + (\Delta_+ - \Delta_-)E}, \\ r_L &= r_R = -\frac{\Delta_0(\Delta_+ - \Delta_-)\operatorname{sgn}(E)}{(\Delta_+ + \Delta_-) q v_{F,x} + (\Delta_+ - \Delta_-)E}. \end{aligned} \tag{4.7}$$

It's easy to see that these coefficients satisfy the general properties (3.105), which are independent of the DW configuration.

4.2 Quasiparticle spectrum for two DWs

It will be shown below that all quantities of interest, including the interaction between the DWs and also the ABS spectrum, can be expressed in terms of the properties of the bulk scattering states, encoded in the scattering matrix $\hat{S}$. Accordingly, we begin the analysis of the quasiparticle spectrum for the two DWs with the calculation of the scattering matrix.

4.2.1 Scattering matrix for the two DWs

The scattering matrix $\hat{S}$ relates the amplitudes of the incident wavefunctions to the outgoing amplitudes, i.e. the amplitudes of the waves that are reflected/transmitted by the DW configuration. To facilitate the calculation of $\hat{S}$, we perform a gauge transformation on the wavefunctions $\psi(x)$ to remove the phase in the order parameter $\Delta_{\boldsymbol{k}_F}$, see Eq. (3.93), that appears in the off-diagonal elements of the Andreev Hamiltonian. For the two-DW setup described in Sec. 2, we can adopt a more convenient notation to describe the order parameter in each of the three domains:

$$\Delta_{\boldsymbol{k}_F}(x) = \begin{cases} \Delta_0 e^{i\varphi_1}, & x < 0,\ x > L \\ \Delta_0 e^{i\varphi_2}, & 0 < x < L \end{cases}, \tag{4.8}$$

which can be further simplified to $\Delta_{\boldsymbol{k}_F}(x) = \Delta_0 e^{i\Phi(x)}$, with $\Phi(x) = \varphi_2 = \chi - \theta$ in the middle domain and $\Phi(x) = \varphi_1 = \theta$ in the outer two domains.

We denote the gauge-transformed wavefunctions by $\tilde{\psi}$ and define $\psi = \hat{U}\tilde{\psi}$, where $\hat{U}$ is given by

$$\hat{U} = e^{i\Phi(x)\hat{\sigma}_3/2} = \begin{pmatrix} e^{i\Phi/2} & 0 \\ 0 & e^{-i\Phi/2} \end{pmatrix}. \tag{4.9}$$

Note that this choice for the gauge-transformed wavefunctions is consistent with the order parameter asymptotics far from the DW, i.e. $\psi(+\infty) = \psi(-\infty)$, in accordance with the gap equation since $\Delta_{\boldsymbol{k}_F}(+\infty) = \Delta_{\boldsymbol{k}_F}(-\infty)$, and it is easy to show from this boundary condition that $\tilde{\psi}(+\infty) = \tilde{\psi}(-\infty)$.

Continuity of the original wavefunctions at the boundaries $x = 0, L$ implies that $\psi(+0) = \psi(-0)$ and $\psi(L+0) = \psi(L-0)$; however, removing the phase from the order parameter causes the gauge-transformed wavefunctions $\tilde{\psi}$ to suffer a discontinuity in the phase at the boundaries. In fact, one can easily verify that $\tilde{\psi}$ satisfy the following boundary conditions:

$$\begin{aligned} \tilde{\psi}(+0) &= e^{-i\delta\hat{\sigma}_3}\tilde{\psi}(-0) \\ \tilde{\psi}(L+0) &= e^{i\delta\hat{\sigma}_3}\tilde{\psi}(L-0), \end{aligned} \tag{4.10}$$

where $\delta = \Delta\varphi/2$, with $\Delta\varphi = \varphi_2 - \varphi_1 = \chi - 2\theta$.

Although we have removed the phase Φ from the off-diagonal terms in the Andreev Hamiltonian, its derivative Φ' appears in the diagonal elements after the gauge transformation, so that $\tilde{\psi}$ satisfies the equation

$$\begin{pmatrix} -iv_{F,x}\nabla_x + v_{F,x}\Phi'(x)/2 & \Delta_0 \\ \Delta_0 & iv_{F,x}\nabla_x + v_{F,x}\Phi'(x)/2 \end{pmatrix} \tilde{\psi} = E\tilde{\psi}, \tag{4.11}$$

with the same energy eigenvalues as the original wavefunctions. Due to the delta-function singularities of Φ' at $x = 0, L$, we apply the gauge transformation separately in each region (i.e. at all $x \neq 0, L$, where $\Phi' = 0$), and obtain:

$$\begin{pmatrix} -iv_{F,x}\nabla_x & \Delta_0 \\ \Delta_0 & iv_{F,x}\nabla_x \end{pmatrix} \tilde{\psi} = E\tilde{\psi} \tag{4.12}$$

in each domain. This last equation has the form of the Andreev equation in a uniform superconductor, and as such can easily be solved. The solution must satisfy the "twisted" matching conditions given by Eq. (4.10).

We focus on the scattering states, and for now we drop the tilde on the gauge-transformed wavefunctions. For the continuum of scattering states, the quasiparticle wavefunctions are linear combinations of plane waves:

$$\psi(x) = \sum_{\alpha=\pm} A_\alpha e^{\alpha iqx} \begin{pmatrix} u_\alpha \\ 1 \end{pmatrix}, \tag{4.13}$$

where

$$u_\pm = \frac{\Delta_0}{E \mp qv_{F,x}}, \tag{4.14}$$

and $q = \sqrt{E^2 - \Delta_0^2}/|v_{F,x}| \geq 0$. The subscript on the amplitudes of the wavefunction in Eq. (4.13) corresponds to the direction of quasiparticle propagation (i.e. left or right). We also introduce a superscript on the amplitudes of the wavefunctions in the outer two domains ($x < 0, x > L$) to identify each particular region. Let the "$-$" superscript denote the region $x < 0$, and the "+" superscript correspond to the $x > L$ region. Then the amplitudes of the waves incident on the DW configuration are given by $A_+^{(-)}$ and $A_-^{(+)}$, while the outgoing (reflected and transmitted) waves have the amplitudes $A_+^{(+)}$ and $A_-^{(-)}$. We then define the scattering matrix $\hat{S}$ as follows:

$$\begin{pmatrix} A_+^{(+)} \\ A_-^{(-)} \end{pmatrix} = \hat{S} \begin{pmatrix} A_+^{(-)} \\ A_-^{(+)} \end{pmatrix}. \tag{4.15}$$

The scattering matrix is calculated by using the matching conditions in Eq. (4.10) to eliminate the wave amplitudes in the region $0 < x < L$ and relate the amplitudes of incident waves to those of the outgoing waves. In this way we find that our scattering matrix has the following entries:

$$\begin{aligned} S_{11} = S_{22} &= \frac{(E^2 - \Delta_0^2)}{(E^2 - \Delta_0^2) - \Delta_0^2 (e^{2iqL} - 1)\sin^2\delta}, \\ S_{12} &= \frac{(E^2 - \Delta_0^2)\left[\sin\delta(i\cos\delta - \varrho\sin\delta)(\varrho - 1)\right](e^{-2iqL} - 1)}{(E^2 - \Delta_0^2) - \Delta_0^2 (e^{2iqL} - 1)\sin^2\delta}, \\ S_{21} &= \frac{(E^2 - \Delta_0^2)\left[\sin\delta(i\cos\delta + \varrho\sin\delta)(\varrho + 1)\right](e^{2iqL} - 1)}{(E^2 - \Delta_0^2) - \Delta_0^2 (e^{2iqL} - 1)\sin^2\delta}, \end{aligned} \tag{4.16}$$

with q, L, and δ defined previously, and $\varrho = E/qv_{F,x}$.

From the Andreev equations it immediately follows that $\psi^\dagger \hat{\sigma}_3 \psi$ is conserved, see Eq. (3.102), and so this combination plays the role of the probability current density in our time-independent system. Using the wavefunctions in Eq. (4.13), we can calculate the probability current density in the outer two domains ($x < 0$, $x > L$), and imposing the condition of continuity across each region, we find that our scattering matrix $\hat{S}$ satisfies the following relation: $\hat{S}^\dagger \hat{W} \hat{S} = \hat{W}$, where $\hat{W}$ is given by

$$\hat{W} = \begin{pmatrix} 1 - u_+^2 & 0 \\ 0 & u_-^2 - 1 \end{pmatrix},$$

with $u_\pm$ defined in Eq. (4.14).

To conclude this subsection we note that, by considering scattering from the left and right separately, one can relate the scattering matrix to the reflection and transmission coefficients of the Bogoliubov quasiparticles in the presence of the order parameter texture. If, for example, there is a wave incident on the DW located at $x = 0$ from the left, then we can set the incident amplitude $A_+^{(-)} = 1$, and we must have $A_-^{(+)} = 0$, $A_+^{(+)} = t_L$ and $A_-^{(-)} = r_L$, where t_L and r_L represent the left-incident transmission and reflection coefficients, respectively. The right-incident transmission and reflection coefficients t_R and r_R can be introduced in a similar way, by considering right-incident scattering on the DW at $x = L$. Then one can relate the scattering matrix to the reflection and transmission coefficients as follows:

$$\hat{S} = \begin{pmatrix} t_L & r_R \\ r_L & t_R \end{pmatrix}. \tag{4.17}$$

We should point out that since we have applied the gauge transformation to the quasiparticle wavefunction before calculating the scattering matrix, the reflection and transmission coefficients obtained by this method are not equivalent to the ones obtained from the direct Andreev calculation (without the gauge transformation).

4.2.2 Reflection and transmission coefficients from direct Andreev calculation

In this section we calculate the reflection and transmission coefficients by directly solving the Andreev equations, without gauge transformation, analogous to the calculation in Sec. 4.1.2 for the single sharp-DW model. The sharp two-DW configuration considered here was introduced in Sec. 2, and has the order parameter distribution given in Eq. (3.96).

We proceed as in Sec. 4.1.2 to determine the scattering states ($|E| > \Delta_0$) for the two-DW configuration, and find that the quasiparticle wavefunctions in each of the three domains have the analogous form of Eq. (4.5):

$$\begin{aligned}
\psi_1(x) &= A_+^{(-)}\alpha_q^{(-)}e^{iqx} + A_-^{(-)}\alpha_{-q}^{(-)}e^{-iqx},\\
\psi_2(x) &= B_+\alpha_q^{(+)}e^{iqx} + B_-\alpha_{-q}^{(+)}e^{-iqx},\\
\psi_3(x) &= A_+^{(+)}\alpha_q^{(+)}e^{iqx} + A_-^{(+)}\alpha_{-q}^{(+)}e^{-iqx},
\end{aligned} \tag{4.18}$$

where subscripts $1, 2, 3$ correspond to the domains $x < 0$, $0 < x < L$, and $x > L$, respectively. The subscripts on the coefficients correspond to the directions of propagation (left or right), and the coefficients are labelled by superscripts "$-$" ("$+$") in the regions $x < 0$ ($x > L$) to denote their relation to the reflection and transmission coefficients as in Secs. 4.1.2 and 4.2.1. In Eq. (4.18), $q = \sqrt{E^2 - \Delta_0^2}/|v_{F,x}| \geq 0$, and $\alpha_q^{(\pm)}$ are two-component functions given by Eq. (4.6).

We consider again the left- and right-incident scattering separately to arrive at a matrix equation for the reflection and transmission coefficients in both of these cases. For the left-incident scattering, we have $A_+^{(-)} = 1$, $A_-^{(-)} = r_L$, $A_-^{(+)} = 0$, and $A_+^{(+)} = t_L$. Using the matching conditions $\psi_1(0) = \psi_2(0)$, $\psi_2(L) = \psi_3(L)$ for continuity of the quasiparticle wavefunction, we obtain a set of four equations for the four unknowns r_L, t_L, B_+, and B_-. These equations can be written in the matrix form as follows:

$$\begin{pmatrix}
-1 & \dfrac{\Delta_+}{\Delta_-}\dfrac{\sqrt{1+\gamma}}{\sqrt{1-\gamma}} & \dfrac{\Delta_+}{\Delta_-} & 0\\
-1 & \dfrac{\sqrt{1-\gamma}}{\sqrt{1+\gamma}} & 1 & 0\\
0 & \dfrac{\Delta_+}{\Delta_-} & \dfrac{\Delta_+}{\Delta_-}\dfrac{\sqrt{1-\gamma}}{\sqrt{1+\gamma}}e^{-2iqL} & -1\\
0 & 1 & \dfrac{\sqrt{1+\gamma}}{\sqrt{1-\gamma}}e^{-2iqL} & -1
\end{pmatrix}
\begin{pmatrix} r_L \\ B_+ \\ B_- \\ t_L \end{pmatrix}
=
\begin{pmatrix} \dfrac{\sqrt{1+\gamma}}{\sqrt{1-\gamma}} \\ \dfrac{\sqrt{1-\gamma}}{\sqrt{1+\gamma}} \\ 0 \\ 0 \end{pmatrix}, \tag{4.19}$$

where $\gamma = qv_{F,x}/E$. We solve this linear system using the mathematical software Maple, and find that the amplitudes of the left-incident reflected and transmitted waves are given by the following expressions:

$$\begin{aligned} r_L &= \frac{\Delta_0}{|E|}\frac{(e^{-2iqL}-1)(\Delta_- - \Delta_+)\left[\Delta_-(1+\gamma) - \Delta_+(1-\gamma)\right]}{D}, \\ t_L &= \frac{4\Delta_+\Delta_-\gamma^2 e^{-2iqL}}{D}, \end{aligned} \tag{4.20}$$

where

$$D = \left[(\Delta_+ + \Delta_-)^2\gamma^2 - (\Delta_+ - \Delta_-)^2\right] e^{-2iqL} + (\Delta_+ - \Delta_-)^2(1-\gamma^2).$$

Substituting the definition of q into γ, we see $\gamma = \operatorname{sgn} v_{F,x}\sqrt{E^2 - \Delta_0^2}/E$. Consequently, for large values of the energy, $|E| \gg \Delta_0$, $\gamma \to \operatorname{sgn} v_{F,x}\sqrt{E^2}/E = \operatorname{sgn} v_{F,x} \operatorname{sgn} E$, and $\sqrt{1-\gamma^2} = \Delta_0/|E| \to 0$. As a result, the numerator of r_L goes to zero, and since $D \to [(\Delta_+ + \Delta_-)^2\gamma^2 - (\Delta_+ - \Delta_-)^2]\, e^{-2iqL}$, which is nonzero, it follows that $r_L \to 0$ as $E \to \infty$. This is intuitively expected since in the limit $|E| \gg \Delta_0$, the quasiparticle is moving so quickly that it does not "see" the DW configuration.

For the right-incident scattering, it follows that $A_+^{(-)} = 0$, $A_-^{(-)} = t_R$, $A_-^{(+)} = 1$, and $A_+^{(+)} = r_R$. Using the matching conditions at the boundaries $x = 0$ and $x = L$, we obtain again four equations for the unknown amplitudes r_R, t_R, B_+, and B_-, which can be arranged in a matrix form as follows:

$$\begin{pmatrix} 0 & -\dfrac{\Delta_+}{\Delta_-}\dfrac{\sqrt{1+\gamma}}{\sqrt{1-\gamma}} & -\dfrac{\Delta_+}{\Delta_-} & 1 \\ 0 & \dfrac{\sqrt{1-\gamma}}{\sqrt{1+\gamma}} & 1 & -1 \\ -1 & \dfrac{\Delta_+}{\Delta_-} & \dfrac{\Delta_+}{\Delta_-}\dfrac{\sqrt{1-\gamma}}{\sqrt{1+\gamma}}e^{-2iqL} & 0 \\ -1 & 1 & \dfrac{\sqrt{1+\gamma}}{\sqrt{1-\gamma}}e^{-2iqL} & 0 \end{pmatrix} \begin{pmatrix} r_R \\ B_+ \\ B_- \\ t_R \end{pmatrix} = \begin{pmatrix} 0 \\ 0 \\ \dfrac{\sqrt{1-\gamma}}{\sqrt{1+\gamma}}e^{-2iqL} \\ \dfrac{\sqrt{1+\gamma}}{\sqrt{1-\gamma}}e^{-2iqL} \end{pmatrix}. \tag{4.21}$$

The solution to this last equation was again obtained using Maple, and the corresponding right-incident reflection and transmission coefficients are given by:

$$\begin{aligned} r_R &= -\frac{\Delta_0}{|E|}\frac{e^{-2iqL}(e^{-2iqL}-1)(\Delta_- - \Delta_+)\left[\Delta_+(1+\gamma) - \Delta_-(1-\gamma)\right]}{D}, \\ t_R &= t_L, \end{aligned} \tag{4.22}$$

where D is defined above. It can be shown that these scattering coefficients satisfy the formal properties in Sec. 3.2.1, namely, the relations in Eq. (3.105). Furthermore, we note that $t_R/t_L = \Delta_-/\Delta_- = 1$, in accordance with the order parameter asymptotics at $x \to \pm\infty$, see Eq. (3.112) and discussion thereafter in Sec. 3.2.1. One can further check that $|r_R|^2 = |r_L|^2$.

4.2.3 Bound state spectrum from the scattering matrix

We now proceed with the calculation of the bound state energies in the two-DW model. Rather than using the direct Andreev calculation similar to that performed for the single-DW case, we begin with the scattering matrix for the two-DW setup, see Eq. (4.16). This expression will ultimately be used to evaluate the interaction energy between the DWs in Sec. 5.3. The ABS energies are obtained from the poles in the scattering matrix entries, after analytical continuation to the real energy axis within the interval $|E| \leq \Delta_0$.

Consequently, we begin by determining the poles of the entries in the scattering matrix to recover the bound state energy for our two-DW setup. We must analytically continue q in the complex energy plane to the energies in the subgap region $|E| \leq \Delta_0$. Defining the dimensionless energy $\epsilon = E/\Delta_0$, we rewrite

$$q = \frac{\Delta_0}{|v_{F,x}|}\sqrt{\epsilon^2 - 1} = \frac{\Delta_0}{v_F|\cos\theta|}\sqrt{\epsilon^2 - 1}. \tag{4.23}$$

We also introduce the correlation length $\xi = v_F/\Delta_0$ (recall that we use the units in which $\hbar = 1$) and define dimensionless distance $\tilde{L} = L/\xi$ to rewrite $qL = \tilde{L}\sqrt{\epsilon^2 - 1}/|\cos\theta|$. For the bound state energies with $|\epsilon| \leq 1$, we have $qL = \pm i\tilde{L}\sqrt{1 - \epsilon^2}/|\cos\theta|$, and so we have to choose the correct branch of q before proceeding further. To this end, we consider the function $w(z) = \sqrt{z^2 - 1}$, which has two branch points: one at $z = 1$, and the other at $z = -1$. We choose the branch to ensure that $w(z)$ is real and $w(z) \geq 0$ if z is real and $|z| > 1$, in accordance with the definition of q, see Eq. (4.23). One can select the branch cuts to run parallel to the imaginary axis, from $\pm\Delta_0$ to $\pm\Delta_0 \mp i\infty$, and then the correct choice is $w(z) = +i\sqrt{1 - z^2}$ for z along the real axis within the interval $[-1, 1]$.

To simplify the denominator in Eq. (4.16), we define a new variable $\tilde{\alpha}(\epsilon) = e^{2iqL} = e^{-2\tilde{L}\sqrt{1-\epsilon^2}/|\cos\theta|}$. Then from the poles in the scattering matrix entries we derive the following equation for the bound state energies:

$$\epsilon^2 - \cos^2\delta - \tilde{\alpha}\sin^2\delta = 0. \tag{4.24}$$

The presence of ϵ in $\tilde{\alpha}$ makes obtaining an analytical solution for the energy nearly impossible. Consequently, we solve this equation numerically to obtain a profile for the ABS energies. To illustrate the effect of $\tilde{L}$ on the spectrum, we present the results for $\chi = \pi$ in Fig. 12.

To make analytical progress, we can consider Eq. (4.24) for small values of $\tilde{\alpha}$, which physically corresponds to large DW separation. Expanding this equation in powers of $\tilde{\alpha}$ up to linear order, we obtain the following result:

$$\epsilon = \pm|\cos\delta|\left(1 + \frac{\tilde{\alpha}}{2}\tan^2\delta\right). \tag{4.25}$$

The two DWs become decoupled at $\tilde{\alpha} \to 0$, which occurs for either the grazing trajectory $\theta = \pm\pi/2$, or for the DW separation $\tilde{L} \to \infty$. This is because, if a particle travels on a path which is nearly tangential to the first DW or if the DWs are infinitely separated, by the time the particle reaches the second DW it will have no memory of the first one. In this case, we recover the same shape for the ABS energy $E_0(\theta)$ associated with the single DW configuration, see Eq. (4.3), but the dependence on $s(\theta)$ has been lost. The DW located at $x = 0$ is associated with bound state energies corresponding to $E_0(\theta)$, while the anti-wall at $x = L$ corresponds to $-E_0(\theta)$, and consequently, our energy curves for the two DWs have two branches, as shown in Fig. 12.

4.2.4 Bound states from the direct Andreev solution

We briefly review the DW configuration under consideration in this section. Recall that in the semiclassical approximation the order parameter can be written as $\Delta_{\boldsymbol{k}_F}(x) = \Delta_-\Theta(-x) + \Delta_+\Theta(x)\Theta(L-x) + \Delta_-\Theta(x-L)$, where $\Theta(x)$ is the Heaviside step function. We consider the bound state wavefunctions separately in each of the three domains: (1) $x < 0$, (2) $0 < x < L$, and (3) $x > L$. The total x-dependence of the quasiparticle wavefunction in this approximation takes the form $\Psi(x) = e^{ik_x x}\psi(x)$, where $k_x = \pm k_0$ and $\psi(x) = (u, v)^T$ is a slowly varying two-component envelope function which satisfies the Andreev equations (3.92). In region (1) with $\Delta_{\boldsymbol{k}_F} = \Delta_- = \Delta_0 e^{i\theta}$, we seek solutions which are bound to the DW: $\psi_1(x) = C_1(\alpha_1, \beta_1)^T e^{ik_1 x}$, where C_1 is an energy-dependent normalization constant, α_1 and β_1 are components of a constant spinor, and $k_1 = i\kappa_1$, where $\kappa_1 < 0$. Solving the Andreev equations for this expression, we find that the quasiparticle wavefunction is given by:

$$\begin{pmatrix} u_1(x) \\ v_1(x) \end{pmatrix} = C_1 \begin{pmatrix} \dfrac{\Delta_0 e^{i\theta}}{E + i\Omega \operatorname{sgn} v_{F,x}} \\ 1 \end{pmatrix} e^{-\Omega|x|/|v_{F,x}|}, \tag{4.26}$$

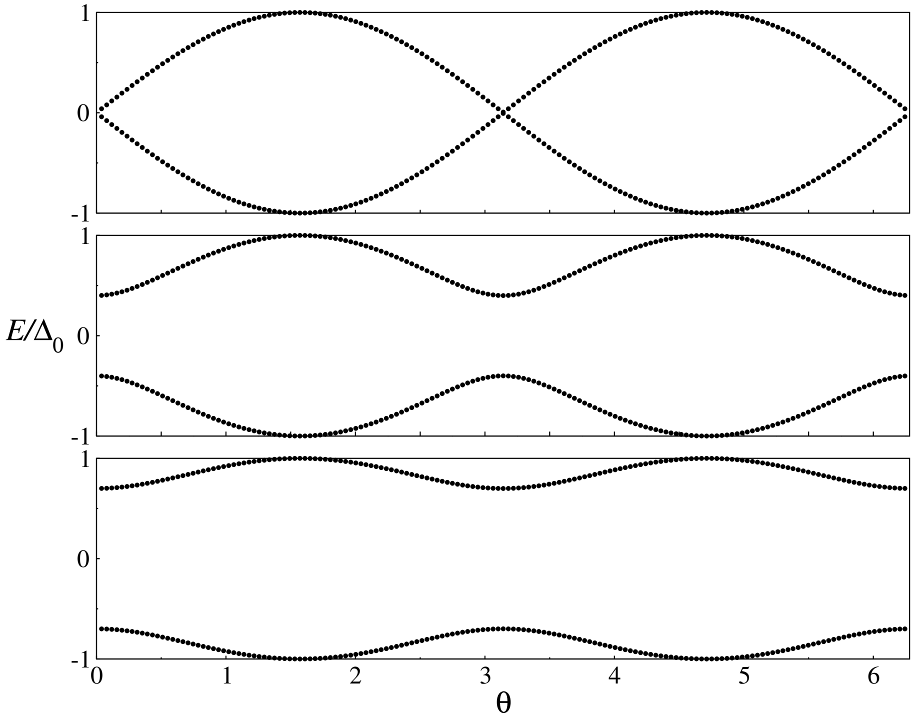

Figure 12: Bound state energy for the sharp two-DW model with $\chi = \pi$, for varying dimensionless DW separation $\tilde{L} = L/\xi$. From the top: $\tilde{L} = 5$, 1, 0.5.

where $\Omega = \sqrt{\Delta_0^2 - E^2} \geq 0$, and thus $\kappa_1 = -\Omega/|v_{F,x}|$.

In the second region $0 < x < L$, we do not have to worry about the quasiparticle wavefunction blowing up, and we can therefore seek solutions to the Andreev equations which are linear combinations of positive and negative exponentials ($e^{\pm ik_2 x}$). Solving the Andreev equations in this region with $\Delta_{\boldsymbol{k}_F} = \Delta_+ = \Delta_0 e^{i\chi} e^{-i\theta}$, we find that the wavefunctions have the form

$$\begin{aligned} \begin{pmatrix} u_2(x) \\ v_2(x) \end{pmatrix} &= C_{2,1} \begin{pmatrix} \dfrac{\Delta_0 e^{i\chi} e^{-i\theta}}{E - i\Omega \,\mathrm{sgn}\, v_{F,x}} \\ 1 \end{pmatrix} e^{-\Omega x/|v_{F,x}|} \\ &+ C_{2,2} \begin{pmatrix} \dfrac{\Delta_0 e^{i\chi} e^{-i\theta}}{E + i\Omega \,\mathrm{sgn}\, v_{F,x}} \\ 1 \end{pmatrix} e^{\Omega x/|v_{F,x}|}, \end{aligned} \tag{4.27}$$

where $C_{2,1}$ and $C_{2,2}$ are energy-dependent constants.

In region (3), we again seek a solution comprised of a single exponential function to keep the quasiparticle localized to the DW. In this region we find

$$\begin{pmatrix} u_3(x) \\ v_3(x) \end{pmatrix} = C_3 \begin{pmatrix} \dfrac{\Delta_0 e^{i\theta}}{E - i\Omega \,\mathrm{sgn}\, v_{F,x}} \\ 1 \end{pmatrix} e^{-\Omega|x|/|v_{F,x}|}. \tag{4.28}$$

Now we are in a position to discuss the bound state energies. In the sharp-DW model we consider here, the DW thickness $\xi_d \to 0$ and thus the order parameter changes abruptly at the boundary between the domains, i.e. at $x = 0, L$. Therefore, for the quasiparticle wavefunction to be continuous across all of the domains, we must have the following conditions hold:

$$\begin{aligned} \psi_1(0) &= \psi_2(0) \to \begin{cases} u_1(0) = u_2(0) \\ v_1(0) = v_2(0) \end{cases}, \\ \psi_2(L) &= \psi_3(L) \to \begin{cases} u_2(L) = u_3(L) \\ v_2(L) = v_3(L) \end{cases}. \end{aligned} \tag{4.29}$$

Substituting the wavefunctions (4.26), (4.27), and (4.28) into this last set of relations, we obtain four equations for the bound state energy, which can be arranged in a matrix form as follows:

$$\begin{pmatrix} e^{i(2\theta-\chi)} & -\dfrac{E + i\Omega \,\mathrm{sgn}\, v_{F,x}}{E - i\Omega \,\mathrm{sgn}\, v_{F,x}} & -1 & 0 \\ 1 & -1 & -1 & 0 \\ 0 & 1 & \dfrac{E - i\Omega \,\mathrm{sgn}\, v_{F,x}}{E + i\Omega \,\mathrm{sgn}\, v_{F,x}} e^{2\Omega L/|v_{F,x}|} & -e^{i(2\theta-\chi)} \\ 0 & 1 & e^{2\Omega L/|v_{F,x}|} & -1 \end{pmatrix} \begin{pmatrix} C_1 \\ C_{2,1} \\ C_{2,2} \\ C_3 \end{pmatrix} = 0. \tag{4.30}$$

To obtain a nontrivial solution of this last equation, the determinant of the matrix must be zero. To facilitate the calculation of the determinant, we introduce a shorthand notation:

$$\begin{aligned} \varepsilon &= \frac{E + i\Omega \,\mathrm{sgn}\, v_{F,x}}{E - i\Omega \,\mathrm{sgn}\, v_{F,x}}, \\ \alpha &= e^{2\Omega L/|v_{F,x}|}, \\ \beta &= e^{i(2\theta-\chi)}, \end{aligned} \tag{4.31}$$

and then the matrix in Eq. (4.30) takes the form:

$$M(E) = \begin{pmatrix} \beta & -\varepsilon & -1 & 0 \\ 1 & -1 & -1 & 0 \\ 0 & 1 & \dfrac{\alpha}{\varepsilon} & -\beta \\ 0 & 1 & \alpha & -1 \end{pmatrix}. \tag{4.32}$$

By setting the determinant of $M(E)$ to zero, we find that the ABS energy satisfies the following equation:

$$(\beta - 1)^2 + \alpha\left(\frac{\beta}{\varepsilon} - \beta^2 - 1 + \beta\varepsilon\right) = 0. \tag{4.33}$$

In the limit of large domain wall separation $L \to \infty$, we have $\alpha \to \infty$ and so the first term in Eq. (4.33) can be neglected. Consequently, in this limit we recover the following equation for the bound state energy:

$$\left(\beta - \frac{1}{\varepsilon}\right)(\varepsilon - \beta) = 0, \tag{4.34}$$

which has two solutions: one for each single domain wall, as the two DWs are essentially decoupled at $L \to \infty$. The first solution, $\varepsilon = \beta$, is equivalent to the equation obtained for the bound state energy of a single DW located at $x = 0$, see Eq. (4.2), and the other solution corresponds to the anti-wall located at $x = L$, and is given by $\varepsilon = 1/\beta$. We can further employ an analogous approach to the one used in obtaining Eq. (4.2), to find that the bound state energy for the second DW is indeed given by $E = -E_0(\theta)$, where $E_0(\theta)$ is defined in Eq. (4.3).

We now consider the case of arbitrary L and introduce a new variable $\tilde{\alpha} = 1/\alpha$. Rearranging Eq. (4.33), we then arrive at a quadratic equation for ε:

$$\beta\varepsilon^2 - \left[(1 + \beta^2) - \tilde{\alpha}(1 - \beta)^2\right]\varepsilon + \beta = 0, \tag{4.35}$$

and applying the quadratic formula, we find

$$\varepsilon = y \pm i\sqrt{1 - y^2}, \tag{4.36}$$

where $y = \left[(1 + \beta^2) - \tilde{\alpha}(1 - \beta)^2\right]/2\beta$. Recall that ε is a function of E and as such, we use Maple to isolate E in the left-hand side of this last equation, to obtain the following implicit expression:

$$E = \pm\, \mathrm{sgn}\,(v_{F,x}) \frac{\Delta_0}{\sqrt{2}} \left[(1+\tilde{\alpha}) + (1-\tilde{\alpha})\cos(2\theta - \chi)\right]^{1/2}. \tag{4.37}$$

As in Sec. 4.2.3, we introduce a dimensionless notation by defining $\epsilon = E/\Delta_0$, as well as a characteristic length scale $\xi = v_F/\Delta_0$, which determines the spatial extent of pair correlation. We can then introduce the dimensionless distance between the DWs, $\tilde{L} = L/\xi$, and so $\tilde{\alpha}$ takes the form:

$$\tilde{\alpha} = e^{-2\tilde{L}\sqrt{1-\epsilon^2}/|\cos\theta|}. \tag{4.38}$$

Due to the presence of $\tilde{\alpha}$ in Eq. (4.37), obtaining an analytical expression for the bound state energy is not feasible, and consequently we use Maple to solve it numerically. The results are equivalent to those obtained in Sec. 4.2.3 (see Fig. 12 for the effects of $\tilde{L}$ on the bound state spectrum in the case $\chi = \pi$), which is not surprising given the fact that expressions (4.24) and (4.35), each obtained through different approaches, are the same.

By appropriately manipulating Eq. (4.35), i.e. substituting the definition of ε in terms of E and carefully rearranging thereafter, we find that this implicit expression can be written as follows:

$$\epsilon^2 - \frac{(1+\beta)^2}{4\beta} + \tilde{\alpha}\frac{(1-\beta)^2}{4\beta} = 0, \tag{4.39}$$

where we recall that ϵ is the dimensionless energy. From the definition of β, Eq. (4.31), it is easy to show that $(1+\beta)^2/4\beta = \cos^2(\theta - \chi/2)$, and $(1-\beta)^2/4\beta = -\sin^2(\theta - \chi/2)$. Thus we recover the same equation for the bound state energy as the one obtained from the poles in the scattering matrix entries, Eq. (4.24).

5 Interaction between DWs

In this section we calculate the interaction between domain walls, which is mediated by the scattering of quasiparticle excitations. The free energy of an arbitrary nonuniform superconducting texture can be expressed in terms of the Fredholm determinant of the BdG Hamiltonian, and for a system with a two-component order parameter in zero magnetic field, it has the following form:

$$\mathcal{F} = -T\sum_n \ln \operatorname{Det}\left(\frac{i\omega_n - \hat{H}_{BdG}}{i\omega_n - \hat{H}_N}\right) + \frac{1}{V}\int \left(|\eta_1|^2 + |\eta_2|^2\right) d^2r, \tag{5.1}$$

where $\mathcal{F}$ is the total free energy of the system measured with respect to the normal state with $\Delta(x) = 0$, $\hat{H}_{BdG}$ is the BdG Hamiltonian defined by Eqs. (3.88) and (3.89), $\hat{H}_N$ is the normal-state BdG Hamiltonian, $\omega_n = (2n+1)\pi T$ is the fermionic Matsubara frequency, and V is the coupling constant in the chiral p-wave channel. The derivation of Eq. (5.1) is presented in Ref. [62].

We introduce the free energy difference between the nonuniform and uniform superconducting states $\delta\mathcal{F} = \mathcal{F}_{nonuniform} - \mathcal{F}_{uniform}$, where the nonuniform state has two DWs. From Eq. (5.1), we have:

$$\delta\mathcal{F} = -T\sum_n \ln \operatorname{Det}\left[\frac{i\omega_n - \hat{H}_{BdG}}{i\omega_n - \hat{H}^{(0)}_{BdG}}\right] + \frac{1}{V}\int \left(|\boldsymbol{\eta}|^2 - |\boldsymbol{\eta}^{(0)}|^2\right) d^2r, \tag{5.2}$$

where $\boldsymbol{\eta}^{(0)}$ and $\hat{H}^{(0)}_{BdG}$ denote the order parameter and the BdG Hamiltonian corresponding to the uniform chiral state. The total free energy in the two-DW system depends on the separation between the DWs L via the eigenvalues of $\hat{H}_{BdG}$, and thus the expression (5.2) varies with L. Since the DWs are decoupled at infinite separation, $\delta\mathcal{F}(L \to \infty)$ gives the self-energy of two DWs, measured with respect to the uniform superconducting state. We are now in a position to introduce the interaction energy between the two DWs, $\mathcal{F}_{int}$, which is simply the difference between the free energy at arbitrary DW separation L and the self-energy of the two-DW configuration, i.e. $\mathcal{F}_{int} = \delta\mathcal{F}(L) - \delta\mathcal{F}(L \to \infty)$.

For the sharp two-DW model introduced in Sec. 2, we have $|\boldsymbol{\eta}|^2 = 2\Delta_0^2$ in each of the three domains. Furthermore, the order parameter for the uniform state $\boldsymbol{\eta}^{(0)}$ is also independent of the DW separation, and consequently the second term on the right hand side of Eq. (5.2) vanishes. Then the interaction energy takes the form

$$\mathcal{F}_{int} = \tilde{\mathcal{F}}(L) - \tilde{\mathcal{F}}(\infty), \tag{5.3}$$

where

$$\tilde{\mathcal{F}}(L) = -T\sum_n \ln \mathrm{Det}\left[\frac{i\omega_n - \hat{H}_{BdG}(L)}{i\omega_n - \hat{H}^{(0)}_{BdG}}\right]. \tag{5.4}$$

The logarithm of each of the Fredholm determinants in Eq. (5.3) can be written as follows:

$$\ln \mathrm{Det}\left[\frac{i\omega_n - \hat{H}_{BdG}}{i\omega_n - \hat{H}^{(0)}_{BdG}}\right] = \sum_i \ln\left[\frac{i\omega_n - E_i}{i\omega_n - E_i^{(0)}}\right], \tag{5.5}$$

where i is a set of quantum numbers labelling the eigenstates of the 2×2 BdG Hamiltonian, see Eq. (3.89), at given DW separation L, E_i are the corresponding eigenvalues, and $E_i^{(0)}$ are the eigenvalues for the uniform chiral state.

The sum over the BdG spectrum in Eq. (5.5) can be expressed in the semiclassical approximation as a sum over the eigenvalues of the Andreev Hamiltonian $\hat{H}_A$, defined by Eq. (3.92), as follows:

$$\sum_i(\cdots) = 2\pi N_F \ell_y \int \frac{d\hat{\boldsymbol{k}}_F}{2\pi}|v_{F,x}|\sum_j(\cdots), \tag{5.6}$$

where $N_F = m^*/2\pi$ is the density of states at the Fermi level in two dimensions per one spin projection, ℓ_y is the length of the DW, $\hat{\boldsymbol{k}}_F$ defines the direction of semiclassical propagation of the quasiparticles, and j labels the eigenstates of the Andreev Hamiltonian at given $\hat{\boldsymbol{k}}_F$. Recall from Sec. 4.2.1 that the quasiparticle wavefunctions satisfy $\psi(+\infty) = \psi(-\infty)$ in accordance with the gap equation, so we have appropriately placed our system in a box of dimensions $\ell_x = \ell$ and ℓ_y (with $\ell \to \infty$), and imposed the periodic boundary conditions.

It follows from Eqs. (5.3, 5.4, 5.5, 5.6) that the interaction energy per unit DW length is given by:

$$F_{int}(L) = -2\pi N_F T\sum_n \int_0^{2\pi}\frac{d\theta}{2\pi}|v_{F,x}|\left[\ln D(i\omega_n; L) - \ln D(i\omega_n;\infty)\right], \tag{5.7}$$

with

$$D(z) = \prod_j \frac{z - E_j}{z - E_j^{(0)}}, \tag{5.8}$$

where E_j are the eigenvalues of the Andreev Hamiltonian at given $\hat{\boldsymbol{k}}_F$ for given DW separation L, and $E_j^{(0)}$ are the eigenvalues of this Hamiltonian corresponding to the uniform chiral state.

As in Sec. 4.2.1, we perform a gauge transformation on the Andreev wavefunctions to remove the phase $\Phi(x)$ from the order parameter, with the corresponding eigenvalues unaffected. After the transformation, the Andreev Hamiltonian can be written as $\hat{H}_A = \hat{H}_A^{(0)} + \delta\hat{H}$, where $\hat{H}_A^{(0)} = -iv_{F,x}\nabla_x\hat{\sigma}_3 + \Delta_0\hat{\sigma}_1$ is the Andreev Hamiltonian for the uniform chiral state, which now has $\Delta_{\boldsymbol{k}_F}(x) = \Delta_0$, and $\delta\hat{H} = v_{F,x}\Phi'(x)\hat{\sigma}_0/2$ is a localized perturbation, see Eq. (4.11). Adiabatically switching on the perturbation, there is a one-to-one correspondence between the eigenvalues of $\hat{H}_A$ and $\hat{H}_A^{(0)}$.

We should note that the gauge-transformed wavefunctions satisfy $\tilde{\psi}(\infty) = \tilde{\psi}(-\infty)$, which is consistent with the periodic boundary conditions imposed above. Furthermore, these boundary conditions are compatible with the Hermiticity condition for the gauge-transformed Hamiltonian $\hat{H}_A$. To illustrate this, we consider the matrix element $(\hat{H}_A)_{12}$ in some arbitrary basis $|\psi\rangle$ (not necessarily the eigenkets of the Andreev Hamiltonian), which can be written as follows:

$$\left\langle \psi_1 \middle| \hat{H}_A \middle| \psi_2 \right\rangle = \int_{-\ell/2}^{\ell/2} dx\, (u_1^* \;\; v_1^*) \left[\begin{pmatrix} -iv_{F,x}\nabla_x & 0 \\ 0 & iv_{F,x}\nabla_x \end{pmatrix} + \hat{w}(x) \right] \begin{pmatrix} u_2 \\ v_2 \end{pmatrix}, \tag{5.9}$$

where $\hat{w}(x)$ is a Hermitian matrix which contains no derivatives. Multiplying through the matrices, this last expression takes the form:

$$(\hat{H}_A)_{12} = \int_{-\ell/2}^{\ell/2} dx \left[-iv_{F,x}u_1^*(\nabla_x u_2) + iv_{F,x}v_1^*(\nabla_x v_2) + (u_1^* \;\; v_1^*)\, \hat{w}(x) \begin{pmatrix} u_2 \\ v_2 \end{pmatrix} \right],$$

and after integrating by parts we obtain:

$$\begin{aligned} (\hat{H}_A)_{12} = &- iv_{F,x}\,(u_1^* u_2 - v_1^* v_2)\,\Big|_{-\ell/2}^{\ell/2} + iv_{F,x}\int_{-\ell/2}^{\ell/2} dx\, (u_2\nabla_x u_1^* - v_2\nabla_x v_1^*) \\ &+ \langle \psi_1 | \hat{w} | \psi_2 \rangle . \end{aligned} \tag{5.10}$$

Equation (5.10) can be further simplified as follows:

$$\left\langle \psi_1 \middle| \hat{H}_A \middle| \psi_2 \right\rangle = \mathcal{S} + \int_{-\ell/2}^{\ell/2} dx\, (u_2 \;\; v_2)\, \hat{H}_A^T \begin{pmatrix} u_1^* \\ v_1^* \end{pmatrix}, \tag{5.11}$$

where $\mathcal{S} = -iv_{F,x}\,(u_1^* u_2 - v_1^* v_2)\,\Big|_{-\ell/2}^{\ell/2}$. If $\hat{H}_A$ is to be Hermitian, then $\left\langle \psi_1 \middle| \hat{H}_A \middle| \psi_2 \right\rangle^* = \left\langle \psi_2 \middle| \hat{H}_A \middle| \psi_1 \right\rangle$, and since $\hat{w}$ is Hermitian this can hold only if $\mathcal{S} = \mathcal{S}^* = 0$. Thus we have the property $\mathrm{tr}\left(\psi_1^\dagger \hat{\sigma}_3 \psi_2\right)\Big|_{-\ell/2}^{\ell/2} = 0$ for any ψ_1, ψ_2. Then it follows that the periodic boundary conditions are consistent with the Hermiticity property of the Andreev Hamiltonian.

Now we will evaluate the Fredholm determinants in Eq. (5.7). To this end, we introduce the 2×2 transfer matrix $\hat{M}(x;E)$ which acts as an x-evolution operator for the quasiparticle wavefunctions at given energy E: $\psi(x) = \hat{M}(x;E)\psi(-\ell/2)$. We define the transfer matrix to satisfy the following conditions:

$$\begin{aligned} \left(\hat{H}_A - E\right)\hat{M}(x;E) &= 0, \\ \hat{M}\left(-\ell/2;E\right) &= \hat{\sigma}_0. \end{aligned} \tag{5.12}$$

These conditions hold for arbitrary values of E. It follows from the periodic boundary conditions that the quasiparticle wavefunctions satisfy $[\hat{\sigma}_0 - \hat{M}(\ell/2;E)]\psi(-\ell/2) = 0$, and this quantization condition leads to the characteristic equation for the eigenvalues of $\hat{H}_A$, given by $\det\left[\hat{\sigma}_0 - \hat{M}\left(\ell/2;E\right)\right] = 0$, where $\det(\cdots)$ is a 2×2 determinant.

We also define another transfer matrix $\hat{M}_0(x;E)$, and this matrix satisfies the same conditions as $\hat{M}(x;E)$ in Eq. (5.12), but for the uniform state Hamiltonian $\hat{H}_A^{(0)}$. From here we can introduce a new quantity $d(z)$, which is defined by the following expression:

$$d(z) = \frac{\det\left[\hat{\sigma}_0 - \hat{M}(\ell/2;z)\right]}{\det\left[\hat{\sigma}_0 - \hat{M}_0(\ell/2;z)\right]}. \tag{5.13}$$

Both $D(z)$ and $d(z)$ have zeros at $z = E_j$, as well as poles at $z = E_j^{(0)}$. For $|z| \to \infty$, which physically corresponds to large values of E, the quasiparticles are not affected by the superconducting order parameter. Consequently, $\hat{H}_A \to \hat{H}_A^{(0)}$, and both $D(z)$ and $d(z) \to 1$. Due to these properties, we have

$$D(z) = d(z), \tag{5.14}$$

see, for example, Ref. [63] for review. This is a significant result because we have been able to express an infinite dimensional Fredholm determinant in terms of the determinant of a 2×2 matrix.

5.1 Relating the determinants

To present a general derivation of Eq. (5.14) we start with the general Andreev Hamiltonian, given by

$$\hat{H}_A = \begin{pmatrix} -iv_{F,x}\nabla_x & \Delta(x) \\ \Delta^*(x) & iv_{F,x}\nabla_x \end{pmatrix}. \tag{5.15}$$

Note that, compared to Eq. (3.92), we have dropped the subscript in the semiclassical order parameter in the above Hamiltonian, i.e. $\Delta_{\boldsymbol{k}_F}(x) \to \Delta(x)$. Applying a gauge transformation as in Sec. 4.2.1 with $\hat{U} = e^{i\Phi(x)\hat{\sigma}_3/2}$, the gauge-transformed Hamiltonian takes the form $\tilde{\hat{H}} = \hat{U}^{-1}\hat{H}\hat{U}$. Since the matrix $\hat{U}$ is unitary, $\hat{U}^\dagger = \hat{U}^{-1}$, it follows that $\tilde{\hat{H}} = \hat{U}^\dagger\hat{H}\hat{U}$. From now on we drop the tildes, and after the gauge transformation, we can rewrite the Andreev Hamiltonian as $\hat{H}_A = \hat{H}_A^{(0)} + \delta\hat{H}$, where $\hat{H}_A^{(0)} = -iv_{F,x}\hat{\sigma}_3\nabla_x + \Delta_0\hat{\sigma}_1$ is the uniform-state Andreev Hamiltonian, and $\delta\hat{H} = v_{F,x}\Phi'(x)\hat{\sigma}_0/2 + (|\Delta(x)| - \Delta_0)\hat{\sigma}_1$ is a perturbation. This expression holds without reference to a particular profile for a configuration of planar defects running parallel to the y-axis. Since $|\Delta(x)| \to \Delta_0$ for $|x| \to \infty$ regardless of the model considered, $\delta\hat{H}$ is indeed a localized perturbation. Furthermore, $\Phi(x)$ changes only in the vicinity of the defect, and for a physically realistic profile of the DW, it is a smooth continuous function without singularities. In the sharp two-DW model, $\delta\hat{H} = v_{F,x}\Phi'(x)\hat{\sigma}_0/2$, and $\Phi'(x)$ takes the form of a delta function centered on the DW, where the phase of the order parameter changes abruptly.

To proceed with the derivation, we now introduce the following Green's functions:

$$\hat{G}(z) = \left(z - \hat{H}_A\right)^{-1}, \;\; \hat{G}_0(z) = \left(z - \hat{H}_A^{(0)}\right)^{-1}, \tag{5.16}$$

and we will show that these functions can be related to the Fredholm determinant $D(z)$ and to $d(z)$. The Green's function is a 2×2 matrix in the electron-hole space, whose matrix elements in the x-representation have the following form:

$$G_{\alpha\beta}(x, x'; z) \equiv \langle x, \alpha|\hat{G}|x', \beta\rangle = \sum_i \frac{\langle x, \alpha|i\rangle\,\langle i|x', \beta\rangle}{z - E_i}. \tag{5.17}$$

Here $\alpha, \beta = 1, 2$ label the electron and hole components and $\langle x, \alpha|i\rangle \equiv \psi_{i,\alpha}(x)$ are the two-component eigenfunctions of the Andreev Hamiltonian, satisfying $\hat{H}_A|i\rangle = E_i|i\rangle$, with $\psi_{i,1}$ being the electron-like (u) component, and $\psi_{i,2}$ the hole-like (v) component. The expression (5.17) can be written as follows:

$$G_{\alpha\beta}(x, x'; z) = \sum_i \frac{\psi_{i,\alpha}(x)\psi^\dagger_{i,\beta}(x')}{z - E_i}. \tag{5.18}$$

We are now in a position to make the connection between the matrix Green's function and the Fredholm determinant $D(z)$. The trace of the Green's function is simply the sum of the diagonal entries given in Eq. (5.18) for all values of x:

$$\mathrm{Tr}\,\hat{G} = \int_{-\ell/2}^{\ell/2} dx \sum_{\alpha} G_{\alpha\alpha}(x,x;z) = \sum_i \frac{1}{z-E_i} \int_{-\ell/2}^{\ell/2} dx \sum_{\alpha} \psi_{i,\alpha}(x)\psi_{i,\alpha}^{\dagger}(x). \tag{5.19}$$

By imposing a standard normalization condition on the quasiparticle wavefunctions

$$\int_{-\ell/2}^{\ell/2} dx\, \mathrm{tr}\left[\psi_i^{\dagger}(x)\psi_i(x)\right] = 1,$$

we find

$$\mathrm{Tr}\,\hat{G} = \sum_i \frac{1}{z-E_i}, \tag{5.20}$$

and the trace of $\hat{G}_0$ is given by an analogous expression, in terms of the eigenvalues of the uniform-state Andreev Hamiltonian $\hat{H}_A^{(0)}$.

Now we consider the Fredholm determinant, Eq. (5.8), noting that

$$\ln D(z) = \sum_i \left[\ln(z-E_i) - \ln\left(z-E_i^{(0)}\right)\right],$$

and therefore

$$\frac{\partial}{\partial z}\ln D(z) = \sum_i \left[\frac{1}{z-E_i} - \frac{1}{z-E_i^{(0)}}\right]. \tag{5.21}$$

From this last equation, and in view of Eq. (5.20), it immediately follows that

$$\frac{\partial}{\partial z}\ln D(z) = \mathrm{Tr}\,\left(\hat{G}-\hat{G}_0\right). \tag{5.22}$$

We are now in a position to relate the Green's functions to $d(z)$, which reduces the calculation of an infinite determinant to the determinant of a 2×2 matrix. From the definition of $\hat{G}(z)$, Eq. (5.16), it is clear that $(z-\hat{H}_A)\hat{G} = 1$. Using the spectral form of the Green's function, given by

$$\hat{G} = \sum_i \frac{|i\rangle\,\langle i|}{z-E_i},$$

one can easily see that $(z-\hat{H}_A)\hat{G}$ acts as the identity operator in the coordinate and electron-hole spaces, and therefore it follows that

$$\langle x,\alpha|(z-\hat{H}_A)\hat{G}|x',\beta\rangle = \delta(x-x')\delta_{\alpha\beta}. \tag{5.23}$$

Inserting the resolution of unity $\int dx'' \sum_\gamma |x'',\gamma\rangle\langle x'',\gamma| = 1$ into Eq. (5.23), we find

$$\int dx'' \sum_\gamma \langle x,\alpha|(z-\hat{H}_A)|x'',\gamma\rangle G_{\gamma\beta}(x'',x';z) = \delta(x-x')\delta_{\alpha\beta}. \tag{5.24}$$

The first matrix element on the left-hand side can be written as follows:

$$\langle x,\alpha|(z-\hat{H}_A)|x'',\gamma\rangle = z\delta(x-x'')\delta_{\alpha\gamma} - \langle x,\alpha|\hat{H}_A|x'',\gamma\rangle = z\delta(x-x'')\delta_{\alpha\gamma} - \langle x|\hat{H}_{A,\alpha\gamma}|x''\rangle,$$

where $|x\rangle$ are the eigenkets of the position operator and $\hat{H}_{A,\alpha\gamma}$ are the matrix elements of the Andreev Hamiltonian. The latter form the following 2×2 matrix:

$$\langle x|\hat{H}_A|x'\rangle = \begin{pmatrix} v_{F,x}\langle x|\hat{p}_x|x'\rangle + \frac{1}{2}v_{F,x}\langle x|\Phi'(x)|x'\rangle & \langle x||\Delta(x)||x'\rangle \\ \langle x||\Delta(x)||x'\rangle & -v_{F,x}\langle x|\hat{p}_x|x'\rangle + \frac{1}{2}v_{F,x}\langle x|\Phi'(x)|x'\rangle \end{pmatrix}. \tag{5.25}$$

For the matrix element of the momentum operator, we insert the resolution of unity in terms of the momentum eigenstates $|p\rangle$ twice into the expression to find

$$\begin{aligned} \langle x|\hat{p}_x|x'\rangle &= \int dp \int dp' \langle x|p\rangle\langle p|\hat{p}_x|p'\rangle\langle p'|x'\rangle \\ &= \int dp_x e^{ip_x(x-x')} p_x \\ &= -i\frac{\partial}{\partial x}\int dp_x e^{ip_x(x-x')} = -i\frac{\partial}{\partial x}\delta(x-x'). \end{aligned} \tag{5.26}$$

Similarly, for a function which depends only on the position operator, such as $V(\hat{x})$, it can be written in the spectral form $V(\hat{x}) = \int dx V(x)|x\rangle\langle x|$, where $|x\rangle$ are the eigenstates of the position operator. Thus we have

$$\begin{aligned} \langle x'|V(\hat{x})|x''\rangle &= \int dx V(x)\delta(x'-x)\delta(x-x'') \\ &= V(x')\delta(x'-x''), \end{aligned} \tag{5.27}$$

and therefore $\langle x|\Phi'(x)|x'\rangle = \Phi'(x)\delta(x-x')$ and $\langle x||\Delta(x)||x'\rangle = |\Delta(x)|\delta(x-x')$.

Using the above expressions for the matrix elements of $\hat{H}_A$, Eq. (5.24) takes the following form:

$$\int dx'' \begin{pmatrix} z + iv_{F,x}\nabla_x - \frac{1}{2}v_{F,x}\Phi'(x) & -|\Delta(x)| \\ -|\Delta(x)| & z - iv_{F,x}\nabla_x - \frac{1}{2}v_{F,x}\Phi'(x) \end{pmatrix} \delta(x - x'') \times G(x'', x'; z) = \hat{\sigma}_0 \delta(x - x'). \tag{5.28}$$

We perform the integration in this last equation and obtain:

$$\begin{pmatrix} z + iv_{F,x}\nabla_x - \frac{1}{2}v_{F,x}\Phi'(x) & -|\Delta(x)| \\ -|\Delta(x)| & z - iv_{F,x}\nabla_x - \frac{1}{2}v_{F,x}\Phi'(x) \end{pmatrix} G(x, x'; z) = \hat{\sigma}_0 \delta(x - x'). \tag{5.29}$$

Using a similar treatment with the uniform-state Andreev Hamiltonian yields an analogous result:

$$\begin{pmatrix} z + iv_{F,x}\nabla_x & -\Delta_0 \\ -\Delta_0 & z - iv_{F,x}\nabla_x \end{pmatrix} G_0(x, x'; z) = \hat{\sigma}_0 \delta(x - x'). \tag{5.30}$$

We then conclude that the matrix elements of the Green's functions satisfy the following identities:

$$\begin{aligned} (z - \hat{H}_A)G(x, x'; z) &= \hat{\sigma}_0\, \delta(x - x'), \\ (z - \hat{H}_A^{(0)})G_0(x, x'; z) &= \hat{\sigma}_0\, \delta(x - x'). \end{aligned} \tag{5.31}$$

From the periodic boundary conditions, along with Eq. (5.18), it follows that the matrix Green's function satisfies the condition

$$G(\ell/2, x'; z) = G(-\ell/2, x'; z), \tag{5.32}$$

and so does the Green's function for the uniform-state Andreev Hamiltonian, $G_0(x, x'; z)$. Of course, this periodicity holds for x' as well, but we focus on the x-dependence only.

From Eq. (5.31), it becomes apparent that one can seek $G(x, x'; z)$ in the form

$$G(x, x'; z) = \begin{cases} \hat{M}(x; z)\hat{A}(x'; z), & x < x' \\ \hat{M}(x; z)\hat{B}(x'; z), & x > x', \end{cases} \tag{5.33}$$

where $\hat{M}(x; z)$ is the transfer matrix defined in Eq. (5.12). We seek an analogous expression for the uniform-state Green's function. In this way, we satisfy the condition

$(z - \hat{H}_A)G(x, x'; z) = 0$ for all $x \neq x'$. Note that because of the delta-function in Eq. (5.31), it follows that $G(x, x'; z)$ is discontinuous at $x = x'$, and this discontinuity must be addressed.

Substituting the gauge-transformed Andreev Hamiltonian into Eq. (5.31), we obtain the expression

$$\left[z + iv_{F,x}\hat{\sigma}_3\frac{\partial}{\partial x} - \Delta_0\hat{\sigma}_1 - \delta\hat{H}\right] G(x, x'; z) = \hat{\sigma}_0\delta(x - x'), \tag{5.34}$$

with $\delta\hat{H}$ defined earlier in this section. We can write this last equation as

$$\left[\frac{\partial}{\partial x} - \frac{i\hat{\sigma}_3}{v_{F,x}}\left(z - \Delta_0\hat{\sigma}_1 - \delta\hat{H}\right)\right] G(x, x'; z) = -\frac{i\hat{\sigma}_3}{v_{F,x}}\delta(x - x'), \tag{5.35}$$

and integrate over the discontinuity to determine the nature of the singularity in $G(x, x'; z)$ as follows:

$$\begin{aligned}\int_{x'-\epsilon}^{x'+\epsilon} dx \left[\frac{\partial}{\partial x}G(x, x'; z)\right] - \frac{i\hat{\sigma}_3}{v_{F,x}}\int_{x'-\epsilon}^{x'+\epsilon} dx \left[z - \Delta_0\hat{\sigma}_1 - \delta\hat{H}\right] G(x, x'; z) = \\ - \frac{i\hat{\sigma}_3}{v_{F,x}}\int_{x'-\epsilon}^{x'+\epsilon} dx\, \delta(x - x').\end{aligned} \tag{5.36}$$

This last expression can be simplified to

$$G(x' + \epsilon, x'; z) - G(x' - \epsilon, x'; z) + \int_{x'-\epsilon}^{x'+\epsilon} dx \left[\cdots\right] G(x, x'; z) = -\frac{i}{v_{F,x}}\hat{\sigma}_3, \tag{5.37}$$

where the terms in parentheses in the above integral are nonsingular. Taking the limit $\epsilon \to 0$, the integral on the left-hand side vanishes, and we find that the discontinuity in $G(x, x'; z)|_{x=x'}$ is given by:

$$G(x' + 0, x'; z) - G(x' - 0, x'; z) = -\frac{i}{v_{F,x}}\hat{\sigma}_3. \tag{5.38}$$

Note that while $G(x, x'; z)$ is discontinuous at $x = x'$, $\operatorname{tr} G(x', x'; z)$ is continuous since $\operatorname{tr} \hat{\sigma}_3 = 0$.

We would like to quickly address the vanishing integral in Eq. (5.37), in the sharp two-DW model. In this case, the integrand is in fact singular due to the delta-function behaviour of $\Phi'(x)$ in $\delta\hat{H}$ at $x = 0, L$. We therefore apply the gauge transformation to the Andreev Hamiltonian for all $x \neq 0, L$, i.e. where $\Phi'(x) = 0$. Consequently, we assume both $x, x' \neq 0, L$ when evaluating the integral and taking the limit $\epsilon \to 0$ in this calculation.

Now that we have addressed the discontinuity in $G(x, x'; z)$, we can proceed with the remainder of the derivation. Using the boundary condition, Eq. (5.32), we can relate $\hat{A}(x'; z)$ to $\hat{B}(x'; z)$ in Eq. (5.33) in the following manner. First, we consider the Green's function at the boundaries of the system:

$$\begin{aligned} G(-\ell/2, x'; z) &= \hat{M}(-\ell/2; z)\hat{A}(x'), \\ G(+\ell/2, x'; z) &= \hat{M}(+\ell/2; z)\hat{B}(x'), \end{aligned} \tag{5.39}$$

where we have suppressed the energy argument z in $\hat{A}$ and $\hat{B}$. Recalling that $\hat{M}(-\ell/2; z) = \hat{\sigma}_0$, and introducing a shorthand notation for the transfer matrix from $-\ell/2$ to $\ell/2$, $\hat{M}(\ell/2; z) = \hat{m}$, we arrive at the relations

$$\hat{A}(x') = \hat{m}\hat{B}(x'),\ \hat{B}(x') = \hat{m}^{-1}\hat{A}(x'), \tag{5.40}$$

using Eq. (5.39) in the boundary condition (5.32).

From the expressions for $G(x, x'; z)$ in terms of the transfer matrix, Eq. (5.33), we can rewrite the expression for the discontinuity in the matrix elements of $\hat{G}$, Eq. (5.38), as

$$\hat{M}(x')\hat{B}(x') - \hat{M}(x')\hat{A}(x') = -\frac{i}{v_{F,x}}\hat{\sigma}_3, \tag{5.41}$$

where we have suppressed the argument z in $\hat{M}(x; z)$. The relations between $\hat{B}$ and $\hat{A}$, Eq. (5.40), can now be used with this last expression to obtain the following results:

$$\begin{aligned} \hat{A}(x') &= -\frac{i}{v_{F,x}}(1 - \hat{m})^{-1}\hat{m}\hat{M}^{-1}(x')\hat{\sigma}_3, \\ \hat{B}(x') &= -\frac{i}{v_{F,x}}(1 - \hat{m})^{-1}\hat{M}^{-1}(x')\hat{\sigma}_3. \end{aligned} \tag{5.42}$$

Since one can write

$$(1 - \hat{m})^{-1}\hat{m} = \frac{1}{2}\left[(1 - \hat{m})^{-1}(1 + \hat{m}) - 1\right]$$

and

$$(1 - \hat{m})^{-1} = \frac{1}{2}\left[(1 - \hat{m})^{-1}(1 + \hat{m}) + 1\right],$$

we substitute Eq. (5.42) into Eq. (5.33), arriving at an expression for the matrix elements of the Green's function in terms of the transfer matrix which is valid at all x, x':

$$\begin{aligned} G(x,x';z) &= -\frac{i}{2v_{F,x}}\hat{M}(x;z)\left\{[1-\hat{m}(z)]^{-1}[1+\hat{m}(z)]+\operatorname{sgn}(x-x')\right\} \\ &\quad \times\hat{M}^{-1}(x';z)\hat{\sigma}_3, \end{aligned} \tag{5.43}$$

where we have explicitly restored the z-dependence. We should note that from the presence of the signum function, this last expression is not defined for $x = x'$.

It is now possible to express the trace of the matrix elements of $\hat{G}$ in terms of the transfer matrix in the following way:

$$\begin{aligned} \operatorname{tr} G(x,x';z) = &-\frac{i}{2v_{F,x}}\operatorname{tr}\left\{\hat{M}(x;z)\left[1-\hat{m}(z)\right]^{-1}\left[1+\hat{m}(z)\right]\hat{M}^{-1}(x';z)\hat{\sigma}_3\right\} \\ &-\frac{i}{2v_{F,x}}\operatorname{tr}\left\{\hat{M}(x;z)\hat{M}^{-1}(x';z)\hat{\sigma}_3\right\}\operatorname{sgn}(x-x'), \end{aligned} \tag{5.44}$$

and one can again see that the trace is continuous at $x = x'$, since

$$\operatorname{tr}\left\{\hat{M}(x;z)\hat{M}^{-1}(x;z)\hat{\sigma}_3\right\} = \operatorname{tr}\hat{\sigma}_3 = 0.$$

We can therefore represent Eq. (5.44) as follows:

$$\operatorname{tr} G(x,x;z) = -\frac{i}{2v_{F,x}}\operatorname{tr}\left\{\hat{M}(x;z)\left[1-\hat{m}(z)\right]^{-1}\left[1+\hat{m}(z)\right]\hat{M}^{-1}(x;z)\hat{\sigma}_3\right\}, \tag{5.45}$$

and using the cyclic invariance of the trace this last equation becomes

$$\operatorname{tr} G(x,x;z) = -\frac{i}{2v_{F,x}}\operatorname{tr}\left\{\hat{M}^{-1}(x;z)\hat{\sigma}_3\hat{M}(x;z)\left[1-\hat{m}(z)\right]^{-1}\left[1+\hat{m}(z)\right]\right\}. \tag{5.46}$$

We have an identical expression for $\operatorname{tr} G_0(x,x;z)$ in terms of the uniform-state transfer matrix $\hat{M}_0(x;z)$.

Using Eq. (5.46), the relation (5.22) can be written in the form:

$$\begin{aligned} \frac{\partial}{\partial x}\ln D(z) = &-\frac{i}{2v_{F,x}}\int_{-\ell/2}^{\ell/2}dx\left[\operatorname{tr}\left\{\hat{M}^{-1}(x;z)\hat{\sigma}_3\hat{M}(x;z)\left[1-\hat{m}(z)\right]^{-1}\left[1+\hat{m}(z)\right]\right\}\right. \\ &\left.-\operatorname{tr}\left\{\hat{M}_0^{-1}(x;z)\hat{\sigma}_3\hat{M}_0(x;z)\left[1-\hat{m}_0(z)\right]^{-1}\left[1+\hat{m}_0(z)\right]\right\}\right], \end{aligned} \tag{5.47}$$

where we have introduced another shorthand notation, for the uniform-state transfer matrix from $-\ell/2$ to $\ell/2$: $\hat{M}_0(\ell/2;z) = \hat{m}_0$.

Now we can relate Eq. (5.47) to $d(z)$. To do this, we consider again the equation defining the transfer matrix: $(z-\hat{H}_A)\hat{M}(x;z)=0$. For now we suppress the arguments of $\hat{M}(x;z)$, and then differentiation of this expression with respect to z gives

$$\hat{M}+\left(z-\hat{H}_A\right)\frac{\partial\hat{M}}{\partial z}=0. \tag{5.48}$$

After manipulating this last equation, in particular, inserting unity in the form of $\hat{M}\hat{M}^{-1}$, we find

$$\left(z-\hat{H}_A\right)\hat{M}\hat{M}^{-1}\frac{\partial\hat{M}}{\partial z}=-\hat{M}. \tag{5.49}$$

Substituting the Andreev Hamiltonian into this last expression, we obtain:

$$\left(z+iv_{F,x}\hat{\sigma}_3\frac{\partial}{\partial x}-\Delta_0\hat{\sigma}_1-\delta\hat{H}\right)\hat{M}\hat{M}^{-1}\frac{\partial\hat{M}}{\partial z}=-\hat{M}, \tag{5.50}$$

and a quick calculation will show that this can be written as follows:

$$\left[\left(z-\hat{H}_A\right)\hat{M}\right]\hat{M}^{-1}\frac{\partial\hat{M}}{\partial z}+iv_{F,x}\hat{\sigma}_3\frac{\partial}{\partial x}\left[\hat{M}^{-1}\frac{\partial\hat{M}}{\partial z}\right]=-\hat{M}. \tag{5.51}$$

Invoking the definition of the transfer matrix, the first term in this last expression is identically zero, and therefore

$$iv_{F,x}\hat{\sigma}_3\hat{M}\frac{\partial}{\partial x}\left[\hat{M}^{-1}\frac{\partial\hat{M}}{\partial z}\right]=-\hat{M}, \tag{5.52}$$

which can be manipulated into the following form:

$$\frac{\partial}{\partial x}\left[\hat{M}^{-1}\frac{\partial\hat{M}}{\partial z}\right]=\frac{i}{v_{F,x}}\hat{M}^{-1}\hat{\sigma}_3\hat{M}. \tag{5.53}$$

From the right-hand side of Eq. (5.53), we begin to see a relation to our most recent expression for $D(z)$, Eq. (5.47). Integrating both sides of this last equation and restoring the arguments in the transfer matrix, we find:

$$\begin{aligned}\frac{i}{v_{F,x}}\int_{-\ell/2}^{\ell/2}dx\,\hat{M}^{-1}(x;z)\hat{\sigma}_3\hat{M}(x;z)&=\int_{-\ell/2}^{\ell/2}dx\left[\frac{\partial}{\partial x}\left(\hat{M}^{-1}\frac{\partial\hat{M}}{\partial z}\right)\right]\\&=\hat{M}^{-1}(x;z)\left.\frac{\partial\hat{M}(x;z)}{\partial z}\right|_{-\ell/2}^{\ell/2}.\end{aligned} \tag{5.54}$$

Recall from the definition of the transfer matrix that $\hat{M}(-\ell/2;z) = \hat{\sigma}_0 = \text{const}$, and thus:

$$\frac{i}{v_{F,x}} \int_{-\ell/2}^{\ell/2} dx\, \hat{M}^{-1}(x;z)\hat{\sigma}_3\hat{M}(x;z) = \hat{m}^{-1}\frac{\partial \hat{m}}{\partial z}, \tag{5.55}$$

where we have used the shorthand notation introduced earlier in this section. Since $\hat{m}$ and $\hat{m}_0$ are independent of x, we can immediately evaluate the integral in Eq. (5.47) using Eq. (5.55) and an analogous expression with $\hat{M}_0(x;z)$. In this way, the equation for $D(z)$ takes the form

$$\begin{aligned} \frac{\partial}{\partial z}\ln D(z) = -\frac{1}{2}\Bigg\{ &\text{tr}\left[\hat{m}^{-1}\frac{\partial \hat{m}}{\partial z}\left(1-\hat{m}\right)^{-1}\left(1+\hat{m}\right)\right] \\ &- \text{tr}\left[\hat{m}_0^{-1}\frac{\partial \hat{m}_0}{\partial z}\left(1-\hat{m}_0\right)^{-1}\left(1+\hat{m}_0\right)\right]\Bigg\}. \end{aligned} \tag{5.56}$$

Using the cyclic invariance of the trace we have

$$\text{tr}\left[\hat{m}^{-1}\frac{\partial \hat{m}}{\partial z}\left(1-\hat{m}\right)^{-1}\left(1+\hat{m}\right)\right] = \text{tr}\left[\frac{\partial \hat{m}}{\partial z}\left(1-\hat{m}\right)^{-1}\left(1+\hat{m}\right)\hat{m}^{-1}\right],$$

and since $\left(1-\hat{m}\right)^{-1}\left(1+\hat{m}\right)\hat{m}^{-1} = \hat{m}^{-1} + 2\left(1-\hat{m}\right)^{-1}$, Eq. (5.56) becomes

$$\begin{aligned} \frac{\partial}{\partial z}\ln D(z) = -\frac{1}{2}\Bigg\{ &\text{tr}\left[\frac{\partial \hat{m}}{\partial z}\hat{m}^{-1}\right] + 2\text{tr}\left[\frac{\partial \hat{m}}{\partial z}\left(1-\hat{m}\right)^{-1}\right] \\ &- \text{tr}\left[\frac{\partial \hat{m}_0}{\partial z}\hat{m}_0^{-1}\right] - 2\text{tr}\left[\frac{\partial \hat{m}_0}{\partial z}\left(1-\hat{m}_0\right)^{-1}\right]\Bigg\}. \end{aligned} \tag{5.57}$$

From Eq. (5.55), using again cyclic invariance of the trace, it immediately follows that

$$\text{tr}\left[\frac{\partial \hat{m}}{\partial z}\hat{m}^{-1}\right] = \frac{i}{v_{F,x}}\int_{-\ell/2}^{\ell/2} dx\,\text{tr}\,\hat{\sigma}_3 = 0, \tag{5.58}$$

and thus we can eliminate two terms from the expression (5.57) to obtain:

$$\frac{\partial}{\partial z}\ln D(z) = -\text{tr}\left[\frac{\partial \hat{m}}{\partial z}\left(1-\hat{m}\right)^{-1}\right] + \text{tr}\left[\frac{\partial \hat{m}_0}{\partial z}\left(1-\hat{m}_0\right)^{-1}\right]. \tag{5.59}$$

Lemma 1. *The following property holds for any matrix function $F(\hat{m})$:*

$$\frac{d}{dz}\text{tr}\,F(\hat{m}) = \text{tr}\left[F'(\hat{m})\frac{d\hat{m}}{dz}\right]. \tag{5.60}$$

Proof. Since $\hat{m}$ is a 2×2 square matrix, we begin with diagonalizing it : $\hat{m} = \hat{R}\,[\mathrm{diag}\,(\hat{m})]\,\hat{R}^{-1}$, and then we can rewrite the above equation as follows:

$$\begin{aligned}\frac{d}{dz}\mathrm{tr}\,F(\hat{m}) &= \frac{d}{dz}\mathrm{tr}\left[\hat{R}\,[\mathrm{diag}\,(F(\hat{m}))]\,\hat{R}^{-1}\right]\\ &= \sum_i \frac{dF(m_i)}{dz}\\ &= \sum_i F'(m_i)\frac{dm_i}{dz}.\end{aligned} \tag{5.61}$$

On the other hand, one can rewrite the right-hand side of Eq. (5.60) as

$$\begin{aligned}\mathrm{tr}\left[F'(\hat{m})\frac{d\hat{m}}{dz}\right] &= \mathrm{tr}\left[\hat{R}\,[\mathrm{diag}\,(F'(\hat{m}))]\,\hat{R}^{-1}\frac{d\hat{m}}{dz}\right]\\ &= \sum_i F'(m_i)\left[\hat{R}^{-1}\frac{d\hat{m}}{dz}\hat{R}\right]_{ii},\end{aligned} \tag{5.62}$$

where we have used the cyclic invariance of the trace. By considering the diagonal term in parentheses in the last expression, we find

$$\begin{aligned}\hat{R}^{-1}\frac{d\hat{m}}{dz}\hat{R} &= \hat{R}^{-1}\frac{d}{dz}\left[\hat{R}(\mathrm{diag}(\hat{m}))\hat{R}^{-1}\right]\hat{R}\\ &= \hat{R}^{-1}\frac{d\hat{R}}{dz}\mathrm{diag}(\hat{m}) + \frac{d}{dz}[\mathrm{diag}(\hat{m})] + \mathrm{diag}(\hat{m})\frac{d\hat{R}^{-1}}{dz}\hat{R}.\end{aligned} \tag{5.63}$$

Now from the definition of matrix multiplication, it follows that

$$\begin{aligned}\left[\mathrm{diag}(\hat{m})\frac{d\hat{R}^{-1}}{dz}\hat{R}\right]_{ii} &= \sum_j [\mathrm{diag}(\hat{m})]_{ij}\left[\frac{d\hat{R}^{-1}}{dz}\hat{R}\right]_{ji}\\ &= m_i\left[\frac{d\hat{R}^{-1}}{dz}\hat{R}\right]_{ii},\end{aligned} \tag{5.64}$$

since $[\mathrm{diag}(\hat{m})]_{ij} = m_i\delta_{ij}$. Furthermore, because m_i and $\left[(d\hat{R}^{-1}/dz)\hat{R}\right]_{ii}$ are just numbers, we can interchange their order in Eq. (5.64), and then expression (5.63) takes the form:

$$\left[\hat{R}^{-1}\frac{d\hat{m}}{dz}\hat{R}\right]_{ii} = \left[\hat{R}^{-1}\frac{d\hat{R}}{dz}\right]_{ii} m_i + \frac{dm_i}{dz} + \left[\frac{d\hat{R}^{-1}}{dz}\hat{R}\right]_{ii} m_i. \tag{5.65}$$

> To simplify this last equation, we use the fact that $\hat{R}^{-1}\hat{R} = 1$, and hence $d(\hat{R}^{-1}\hat{R})/dz = 0$. Invoking the product rule in this identity, one can eliminate the two terms containing $\hat{R}$ and $\hat{R}^{-1}$ in Eq. (5.65), and then Eq. (5.62) immediately takes the form:
>
> $$\operatorname{tr}\left[F'(\hat{m})\frac{d\hat{m}}{dz}\right] = \sum_i F'(m_i)\frac{dm_i}{dz} = \frac{d}{dz}\operatorname{tr} F(\hat{m}), \tag{5.66}$$
>
> where we have used Eq. (5.61) to obtain the final equality in this last expression. □

From the definition of the matrix inverse, it follows that $(1-\hat{m})^{-1}(1-\hat{m}) = 1$. If we consider the Taylor expansion of function $1/(1-\hat{m}) = 1 + \hat{m} + \hat{m}^2 + \cdots = \sum_{n=0}^{\infty} \hat{m}^n$ (the geometric series), quick inspection reveals that $(1 + \hat{m} + \hat{m}^2 + \cdots)(1-\hat{m}) = 1$, since all powers of $\hat{m}$ higher than zero vanish, and thus the matrix inverse $(1-\hat{m})^{-1}$ is identically equivalent to $1/(1-\hat{m})$. We can now apply identity (5.60) to Eq. (5.59) with $F'(\hat{m}) = -1/(1-\hat{m})$, and therefore $F(\hat{m}) = \ln(1-\hat{m}) + c$, with an arbitrary constant c. This choice for the antiderivative becomes clear from a comparison of the Taylor expansion of $\ln(1-\hat{m}) = -\hat{m} - \hat{m}^2/2 - \hat{m}^3/2 + \cdots = -\sum_{n=1}^{\infty} \hat{m}^n/n!$ with the one for $-1/(1-\hat{m})$, and differentiating term by term. It then follows that

$$\begin{aligned}\frac{\partial}{\partial z}\ln D(z) &= \frac{d}{dz}\operatorname{tr}\left[\ln(1-\hat{m}) - \ln(1-\hat{m}_0) + c\right] \\ &= \frac{d}{dz}\left[\ln\prod_i(1-m_i) - \ln\prod_i(1-m_{0,i})\right] \\ &= \frac{d}{dz}\ln\left[\frac{\det(1-\hat{m})}{\det(1-\hat{m}_0)}\right].\end{aligned} \tag{5.67}$$

In view of Eq. (5.13), we immediately find:

$$\ln D(z) = \ln d(z) + \text{const.} \tag{5.68}$$

Since $D(z)$ and $d(z)$ have the same asymptotic behaviour at $|z| \to \infty$, the constant on the right-hand side of this last equation is zero. Indeed, as mentioned in the introduction of this section, $|z| \to \infty$ physically corresponds to large values of the quasiparticle energy, where the quasiparticles are not affected by the superconducting order parameter. In this case, $H_A \to H_A^{(0)}$ and therefore $D(z) = d(z) \to 1$. From here we conclude that conjecture

(5.14) has been rigorously proven, and thus

$$D(z) = \frac{\det[\hat{\sigma}_0 - \hat{M}(\ell/2; z)]}{\det[\hat{\sigma}_0 - \hat{M}_0(\ell/2; z)]}. \tag{5.69}$$

In the following subsection we use the transfer matrix method, in particular Eq. (5.69), to relate the interaction energy to the scattering matrix entries. Subsequently, we evaluate the sum over the Matsubara frequencies and the integral over semiclassical directions of propagation in Eq. (5.7) to obtain an analytical expression for the interaction energy in the limit of large DW separation.

5.2 Calculation of the Fredholm determinant

To facilitate the calculation of the Fredholm determinant, we first define a matrix $\hat{\tau}$, which relates the amplitudes of the gauge-transformed quasiparticle wavefunctions on the left-hand side of the DW configuration to those on the right-hand side, see Sec. 4.2.1, as follows:

$$\begin{pmatrix} A_+^{(+)} \\ A_-^{(+)} \end{pmatrix} = \hat{\tau} \begin{pmatrix} A_+^{(-)} \\ A_-^{(-)} \end{pmatrix}. \tag{5.70}$$

It can therefore be expressed in terms of the scattering matrix $\hat{S}$ in the following way:

$$\hat{\tau} = \frac{1}{S_{22}} \begin{pmatrix} \det \hat{S} & S_{12} \\ -S_{21} & 1 \end{pmatrix}. \tag{5.71}$$

As in the previous subsection, we introduce a shorthand notation for the transfer matrix from $-\ell/2$ to $+\ell/2$, $\hat{M}(\ell/2; z) = \hat{m}$, and using Eq. (5.70) and the wavefunctions defined by Eq. (4.13), we find that $\hat{m} = \hat{V}_+ \hat{\tau} \hat{V}_-^{-1}$, where

$$\hat{V}_\pm = \begin{pmatrix} u_+ e^{\pm iq\ell/2} & u_- e^{\mp iq\ell/2} \\ e^{\pm iq\ell/2} & e^{\mp iq\ell/2} \end{pmatrix},$$

and $u_\pm$ and q are defined in Sec. 4.2.1. We introduce a similar notation for the uniform-state transfer matrix $\hat{M}_0(\ell/2; z) = \hat{m}_0$, and since in the absence of DWs $\hat{\tau} = \hat{S} = \hat{\sigma}_0$, it immediately follows that $\hat{m}_0 = \hat{V}_+ \hat{V}_-^{-1}$. We can now rewrite the expression for the

Fredholm determinant, see Eq. (5.69), as

$$D(z) = \frac{\det\left(\hat{\sigma}_0 - \hat{V}_+ \hat{\tau} \hat{V}_-^{-1}\right)}{\det\left(\hat{\sigma}_0 - \hat{V}_+ \hat{V}_-^{-1}\right)}, \tag{5.72}$$

and after multiplying the matrices we find that the numerator in this last equation takes the form

$$\det\left(\hat{\sigma}_0 - \hat{m}\right) = 1 + \det\hat{\tau} - \left(\tau_{11} e^{iq\ell} + \tau_{22} e^{-iq\ell}\right), \tag{5.73}$$

which reduces to $\det\left(\hat{\sigma}_0 - \hat{m}_0\right) = 2(1 - \cos q\ell)$ for the uniform superconducting state.

According to Eq. (5.7), to calculate the interaction energy we must evaluate $D(z)$ at discrete imaginary points $z = i\omega_n$, and since q in Eq. (5.73) is defined for real values of E such that $|E| > \Delta_0$ only, we must analytically continue q in the complex energy plane to the imaginary energy axis. Using the same procedure as in Sec. 4.2.3 we find that the appropriate expression for q is $q(E = i\omega_n) = i\varkappa$, with $\varkappa = \sqrt{\omega_n^2 + \Delta_0^2}/|v_{F,x}|$. Therefore the exponential terms in Eq. (5.73) take the form $e^{\pm iq\ell} = e^{\mp\varkappa\ell}$, and in the thermodynamic limit $\ell \to \infty$, we keep only the last term as the others are small in comparison. In this limit, we obtain the following expression for the Fredholm determinant in Eq. (5.72):

$$D(z = i\omega_n) = \tau_{22}(i\omega_n) = \frac{1}{S_{22}(i\omega_n)}, \tag{5.74}$$

where we have used the relation between $\hat{\tau}$ and $\hat{S}$ given in Eq. (5.71). We see that the calculation of the Fredholm determinant has thus been reduced to finding the properties of the scattering states.

Since q appears in the scattering matrix coefficient S_{22}, see Eq. (4.16), and we must evaluate this coefficient at imaginary energies $E = i\omega_n$, we must once again choose the correct branch for q. We use the expression $q(i\omega_n) = i\varkappa$, see above, and rewrite the scattering matrix coefficient $S_{22}(i\omega_n)$ as follows:

$$D(i\omega_n) = \frac{1}{S_{22}(i\omega_n)} = 1 - \frac{\Delta_0^2 \sin^2\delta}{\omega_n^2 + \Delta_0^2}\left(1 - e^{-2\varkappa L}\right), \tag{5.75}$$

where $\delta = \chi/2 - \theta$.

5.3 Interaction energy

From Eqs. (5.7) and (5.75), it follows that the interaction energy per unit DW length at given DW separation has the following form:

$$F_{int} = -v_F N_F T \sum_n \int_0^{2\pi} d\theta |\cos\theta| \ln\left(1 + \frac{\Delta_0^2 \sin^2\delta}{\omega_n^2 + \Delta_0^2 \cos^2\delta} e^{-2\varkappa L}\right). \tag{5.76}$$

The overall sign of the interaction energy is negative, so we see that the nature of the interaction is attractive at all temperatures, which means there is an effective collapse of the walls to a single uniform domain. Qualitatively, from the structure of expression (5.76), it is clear that the attraction is exponentially weak in the limit of large separation. To make analytical progress, we focus on the case of zero temperature and $\chi = 0$. The results for other values of the common phase difference are expected to be qualitatively similar.

In the zero temperature case, the summation over the discrete Matsubara frequencies ω_n becomes an integral over continuous variable ω: $T\sum_n(\cdots) \to \int(\cdots)d\omega/2\pi$. In the limit of large DW separation, one can expand the logarithm in Eq. (5.76), then the interaction energy takes the form:

$$F_{int} = -\frac{N_F \Delta_0 v_F}{2\pi} \int_0^{2\pi} d\theta |\cos\theta| \int_{-\infty}^{+\infty} d\tilde{\omega} \frac{\sin^2\theta}{\tilde{\omega}^2 + \cos^2\theta} e^{-2\tilde{L}\sqrt{\tilde{\omega}^2+1}/|\cos\theta|}, \tag{5.77}$$

where $\tilde{\omega} = \omega/\Delta_0$, and the dimensionless distance $\tilde{L}$ was introduced in Sec. 4.2.3. In the limit $\tilde{L} \gg 1$, one can further neglect the $\tilde{\omega}$-dependence of the pre-exponential factor in the integral over $\tilde{\omega}$, and evaluate it by the steepest descent method. In this way, we can represent Eq. (5.77) in the following form:

$$F_{int} = -\frac{2N_F \Delta_0 v_F}{\sqrt{\pi \tilde{L}}} \tilde{I}(\tilde{L}), \tag{5.78}$$

where

$$\tilde{I}(\tilde{L}) = \int_0^{\pi/2} d\theta \frac{\sin^2\theta}{\sqrt{|\cos\theta|}} e^{-2\tilde{L}/|\cos\theta|}, \tag{5.79}$$

and we have invoked the symmetry of the angular integral to reduce the region of integration.

Next, we make a change of variable $\rho = 1/\cos\theta$ in Eq. (5.79) and obtain:

$$\tilde{I} = \int_1^{\infty} d\rho (\rho^2 - 1)^{\frac{1}{2}} \rho^{-\frac{5}{2}} e^{-2\tilde{L}\rho}.$$

This last integral can be calculated exactly, with the following result:

$$\begin{aligned}\tilde{I} \;=\;& \frac{1}{3}\sqrt{\frac{2a^3}{\pi}}\left\{\frac{a^4-6a^2+9}{a^3}\left[K_{3/4}\left(\frac{a}{2}\right)\right]^2+\frac{1-a^2}{a}\left[K_{7/4}\left(\frac{a}{2}\right)\right]^2\right.\\ &\left.+\frac{5a^2-6}{a^2}\left[K_{3/4}\left(\frac{a}{2}\right)\right]\left[K_{7/4}\left(\frac{a}{2}\right)\right]\right\},\end{aligned} \tag{5.80}$$

where $a = 2\tilde{L}$ and $K_n(z)$ are the modified Bessel functions of the second kind of order n [64].

For large values of the argument $z \gg 1$, corresponding to large DW separation, we have $K_{3/4}(z) = K_{7/4}(z) \approx \sqrt{\pi/2z}\, e^{-z}$. Keeping only the leading term in Eq. (5.80) $\propto a^0$, we find:

$$\tilde{I} = \frac{10}{3}\sqrt{\pi\tilde{L}}e^{-2\tilde{L}}.$$

Using this result in Eq. (5.78), and restoring the dimensional quantities, we arrive at our final expression for the interaction energy per unit DW length, in the limit of large DW separation [65]:

$$F_{int} = -\frac{20}{3}N_F\Delta_0 v_F \exp\left(-\frac{2\Delta_0 L}{v_F}\right). \tag{5.81}$$

Thus, the interaction between the DWs is attractive and, as expected, it is exponentially weak in the limit of large separation between the walls.

6 Phase solitons in two-band superconductors

In this section, we apply the concepts and results of the previous sections, with a minimal modification, to a different type of topological defect, namely phase solitons in two-band SCs. We assume a two-band superconductor with isotropic s-wave singlet pairing, described by two order parameters $\eta_1(\boldsymbol{r}) = |\eta_1(\boldsymbol{r})|e^{i\varphi_1(\boldsymbol{r})}$ and $\eta_2(\boldsymbol{r}) = |\eta_2(\boldsymbol{r})|e^{i\varphi_2(\boldsymbol{r})}$, in the absence of magnetic field. The free energy difference between the superconducting and normal states is given by $\mathcal{F}_s - \mathcal{F}_n = \int f_{GL}\, d^3\boldsymbol{r}$, where

$$f_{GL} = \sum_{a=1,2}\left[\alpha_a|\eta_a|^2 + \frac{\beta_a}{2}|\eta_a|^4 + K_a|\boldsymbol{\nabla}\eta_a|^2\right] + \gamma(\eta_1^*\eta_2 + \eta_2^*\eta_1). \tag{6.1}$$

The intraband terms have the usual Ginzburg-Landau form, while the last term describes the interband “Josephson coupling”, i.e. the Cooper pair tunneling between the bands.

The stable uniform states are obtained by minimizing the interband term with respect to the relative phase $\theta = \varphi_1 - \varphi_2$. We have $|\eta_a| = \Delta_a$ and $\theta = \theta_0$, where $\theta_0 = 0$, if $\gamma < 0$, and $\theta_0 = \pi$, if $\gamma > 0$. The first possibility (interband attraction) is realized in MgB_2, where both gaps have the same phase [66], while the second possibility (interband repulsion) is likely realized in the iron pnictides, where, according to the most popular model, the gap function reverses its sign between different sheets of the Fermi surface, corresponding to the so-called $s_\pm$ pairing [67]. Without any loss of generality below we assume $\gamma < 0$, therefore, the two bands have the same phase in the uniform state.

In addition to the uniform states, the GL equations (supplemented by the condition of vanishing supercurrent, see Appendix B) have topologically nontrivial solutions, in which $\theta(+\infty) - \theta(-\infty) = \pm 2\pi$. Here the positive (negative) sign corresponds to a phase soliton (anti-soliton). An explicit expression for the phase soliton can be obtained in the London approximation [68], when the order parameter amplitudes are assumed constant everywhere, i.e. $|\eta_a(x)| = \Delta_a$. The minimization of Eq. (B.1) then yields a static sine-Gordon equation for the relative phase, whose soliton solution has the form $\theta(x) = \pi + \theta_s(x)$, where $\theta_s(x) = 2\arcsin[\tanh(x/\xi_s)]$ and

$$\xi_s = \sqrt{\frac{K_1K_2\Delta_1\Delta_2}{(K_1\Delta_1^2 + K_2\Delta_2^2)|\gamma|}}$$

has the meaning of the soliton width. Thus the phase soliton connects the states with $\theta = 0$ at $x \to -\infty$ and $\theta = 2\pi$ at $x \to +\infty$.

The presence of a soliton texture in the relative phase implies that each of the two phases φ_1 and φ_2 are also spatially nonuniform and attain different values at $x = +\infty$

and $x = -\infty$, see Ref. [69]. The phase textures in the bands are given by the following expressions (up to a uniform rotation of the common phase):

$$\varphi_1(x) = \frac{1}{1+\rho_0}\theta_s(x), \qquad \varphi_2(x) = -\frac{\rho_0}{1+\rho_0}\theta_s(x) - \pi, \tag{6.2}$$

where $\rho_0 = K_1\Delta_1^2/K_2\Delta_2^2$. The phase winding parameters across the soliton are given by $\chi_1 = \Phi$ and $\chi_2 = \Phi - 2\pi$, where $\Phi = 2\pi/(1+\rho_0)$, see Appendix B.

The same argument used in Appendix A for the absence of two-DW solutions applies to the phase solitons. The fact that there are no stable two-soliton solutions implies there must be some form of interaction between the solitons. If this interaction is attractive, it will cause a collapse of the solitons into a uniform state. If it is repulsive, then one of the solitons will be pushed to infinity, leaving just a single-soliton state. The periodic solution for $\theta(x)$ can also be understood in terms of this interaction, as a mutual attraction or repulsion between neighbouring solitons could potentially lead to a stable periodic configuration.

To make analytical progress in the calculation of the interaction between solitons, we use a model similar to the one for the DWs. Namely, we consider two planar solitons at separation L. The phase solitons divide the superconductor into three domains, separated by two "domain walls", whose thickness is of the order of ξ_s. We assume that $L \gg \xi_s$. We will focus on the sharp-soliton model in which the gap magnitudes are assumed constant everywhere and the soliton thickness $\xi_s \to 0$, so that the relative phase of the order parameters changes abruptly at the boundaries, as illustrated in Fig. 13. This variation of the relative phase implies that the order parameter phases in each of the two bands are also spatially-nonuniform, so that the gap functions are given by the following expressions:

$$\eta_a(x) = \begin{cases} \Delta_a & , \quad x < 0,\ x > L \\ \Delta_a e^{i\chi_a} & , \quad 0 < x < L \end{cases} . \tag{6.3}$$

Here the phase winding parameters in the two bands are given by

$$\chi_1 = \Phi, \qquad \chi_2 = \Phi - 2\pi, \tag{6.4}$$

where Φ is a non-universal fraction of 2π, determined by the microscopic details. One can rotate both phases uniformly throughout the system by adding an arbitrary constant in the right-hand side of Eq. (6.3), without affecting the final results.

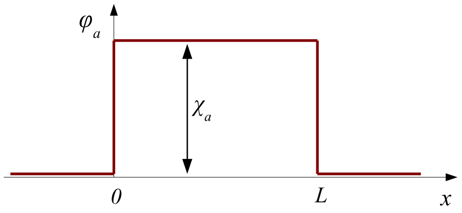

Figure 13: The order parameter phase in the ath band for two sharp solitons with a fixed separation L.

6.1 Quasiparticle spectrum in the two-soliton texture

Our goal is to calculate the interaction between the phase solitons, which is due to their effect on the Bogoliubov quasiparticles. Here we consider a three-dimensional system, and the bands are assumed to be isotropic, with the dispersions $\xi_a(\boldsymbol{k}) = (\boldsymbol{k}^2 - k_{F,a}^2)/2m_a$, characterized by the effective masses m_a and the Fermi wavevectors $k_{F,a}$. Since the order parameters vary slowly on the length scales $k_{F,a}^{-1}$, one can calculate the quasiparticle spectrum using the semiclassical, or Andreev, approximation [60]. An important point is that the slow perturbation due to the phase solitons cannot cause quasiparticle transitions between the bands, therefore one can solve the Andreev equations independently in each band. The calculation is very similar to the one in Sec. 4.2 for the two DWs.

In the rest of this section we will drop the band index for brevity. Quasiparticles propagating along the semiclassical trajectory directed along the unit vector $\hat{\boldsymbol{k}}_F$ are described by the wavefunction ψ, which varies slowly compared to k_F^{-1}. The quasiparticle spectrum at given $\hat{\boldsymbol{k}}_F$ is determined by the equation $\hat{H}\psi = E\psi$, where the Andreev Hamiltonian is given by

$$\hat{H} = \begin{pmatrix} -iv_{F,x}\nabla_x & \eta(x) \\ \eta^*(x) & iv_{F,x}\nabla_x \end{pmatrix}. \tag{6.5}$$

Here $\boldsymbol{v}_F = \boldsymbol{k}_F/m$ is the Fermi velocity and $\eta = |\eta|e^{i\varphi}$. The gap magnitude approaches its bulk mean-field value, $|\eta| \to \Delta_0$, far from the solitons. To make the eigenvalue problem for the Hamiltonian (6.5) well-defined, we put the system in a box of length ℓ, such that $\ell \gg L \gg \xi_s$, and use periodic boundary conditions for the quasiparticle wavefunctions, $\psi(+\ell/2) = \psi(-\ell/2)$, which are consistent with the phase winding of the order parameter. When safe to do so, we will take the limit $\ell \to \infty$. The band index a will be restored in the end by making the following replacements: $\boldsymbol{v}_F \to \boldsymbol{v}_{F,a} = (k_{F,a}/m_a)\hat{\boldsymbol{k}}_F$, $\Delta_0 \to \Delta_a$, $\varphi(x) \to \varphi_a(x)$, and $\chi \to \chi_a$.

Our calculation of the quasiparticle spectrum generalizes the procedure developed in Ref. [69] for a single-soliton texture. As in Sec. 4.2.1, it is convenient to represent the phase variation as a localized perturbation, which is achieved by applying a gauge transformation: $\psi = \hat{U}\tilde{\psi}$ and $\hat{U}^\dagger \hat{H} U = \hat{\tilde{H}}$, where

$$\hat{U}(x) = \exp\left[\frac{i}{2}\varphi(x)\hat{\sigma}_3\right]. \tag{6.6}$$

We can drop the tildas and write the transformed Hamiltonian in the form

$$\hat{H} = \hat{H}_0 + \delta\hat{H}, \tag{6.7}$$

where

$$\hat{H}_0 = -iv_{F,x}\hat{\sigma}_3\nabla_x + \Delta_0\hat{\sigma}_1 \tag{6.8}$$

describes the Bogoliubov quasiparticles in the uniform superconducting state, while

$$\delta\hat{H} = \frac{1}{2}v_{F,x}\varphi'(x)\hat{\sigma}_0 + [|\eta(x)| - \Delta_0]\,\hat{\sigma}_1$$

represents a perturbation which is nonzero only in the vicinity of the solitons. One can show that the gauge-transformed eigenfunctions satisfy the periodic boundary conditions. We note that there is a one-to-one correspondence between the spectra of $\hat{H}$ and $\hat{H}_0$: the eigenvalues of the operator $\hat{H}_\lambda = \hat{H}_0 + \lambda\delta\hat{H}$ evolve smoothly between those of $\hat{H}_0$ and $\hat{H}$ as the parameter λ varies between 0 and 1.

At given $\hat{\boldsymbol{k}}_F$, the spectrum of the Andreev Hamiltonian, Eq. (6.7), consists of scattering states with the energies $|E| \geq \Delta_0$ and bound states with $|E| < \Delta_0$. Below we examine the properties of the scattering states for the sharp two-soliton texture.

6.1.1 Scattering states for the two-soliton texture

Since the Hamiltonian is equal to $\hat{H}_0$ at $|x| \to \infty$, the scattering eigenstates in those regions are just the superpositions of plane waves:

$$\psi(x)\big|_{x\to\pm\infty} = C_R^\pm \begin{pmatrix} w_R \\ 1 \end{pmatrix} e^{iqx} + C_L^\pm \begin{pmatrix} w_L \\ 1 \end{pmatrix} e^{-iqx}, \tag{6.9}$$

where $q = \sqrt{E^2 - \Delta_0^2}/|v_{F,x}| > 0$, $w_{R(L)} = \Delta_0/(E \mp v_{F,x}q)$, and the subscripts R, L refer to the direction of propagation of the corresponding waves. The coefficients in these asymptotics are not independent, and it is convenient to introduce a 2×2 scattering matrix, or the S-matrix, which expresses the amplitudes of the outgoing waves in terms of the amplitudes of the incoming waves:

$$\begin{pmatrix} C_R^+ \\ C_L^- \end{pmatrix} = \hat{S} \begin{pmatrix} C_R^- \\ C_L^+ \end{pmatrix}. \tag{6.10}$$

The elements of the S-matrix depend on the energy and are determined by the details of the order parameter texture.

We note that, by considering scattering from the left and right separately, one can relate the scattering matrix to the reflection and transmission coefficients of the Bogoliubov quasiparticles. If, for example, there is a wave incident on the soliton located at $x = 0$ from the left, then we can set the incident amplitude $C_R^- = 1$, and we must have $C_L^+ = 0$, $C_R^+ = t_L$, and $C_L^- = r_L$, where t_L and r_L represent the left-incident transmission and reflection coefficients, respectively. The right-incident transmission and reflection coefficients t_R and r_R can be introduced in a similar way, by considering right-incident scattering on the soliton at $x = L$. Then one can relate the scattering matrix entries to the transmission and reflection coefficients as follows: $t_L = S_{11}$, $r_L = S_{21}$, $t_R = S_{22}$, and $r_R = S_{12}$.

Similarly to Sec. 5.2, one can also introduce the τ-matrix, which relates the scattering wave amplitudes at $x \to +\infty$ to those at $x \to -\infty$:

$$\begin{pmatrix} C_R^+ \\ C_L^+ \end{pmatrix} = \hat{\tau} \begin{pmatrix} C_R^- \\ C_L^- \end{pmatrix}. \tag{6.11}$$

Comparing Eqs. (6.11) and (6.10), we find that the τ-matrix can be expressed in terms of the S-matrix in the same way as in Eq. (5.71). In the absence of the phase solitons, there is no scattering and thus $\hat{S} = \hat{\tau} = \hat{\sigma}_0$.

We note that the S-matrix can also be used to obtain the bound states, following the analytical continuation procedure described in Sec. 4.2.3. In this way, it was found in Ref. [69] that a single phase soliton can "trap" quasiparticles in its vicinity, creating a subgap bound state, whose energy depends on the phase winding across the soliton.

The scattering matrix for the quasiparticles in each band can be calculated analytically in the sharp two-soliton model, defined by Eq. (6.3). After the gauge transformation, see Eq. (6.6), we obtain the following matching conditions for the gauge-transformed wavefunction: $\psi(+0) = e^{-i\chi\hat{\sigma}_3/2}\psi(-0)$ and $\psi(L+0) = e^{i\chi\hat{\sigma}_3/2}\psi(L-0)$.

The scattering matrix is calculated by using the matching conditions to eliminate the wave amplitudes in the region $0 < x < L$ and relate the amplitudes of incident waves to those of the outgoing waves. The final result has the following form:

$$\begin{aligned} S_{11} = S_{22} = \frac{1}{P}, \\ S_{12} = \frac{R_-}{P}, \quad S_{12} = \frac{R_+}{P}, \end{aligned} \tag{6.12}$$

where

$$\begin{aligned} P &= 1 - \frac{\Delta_0^2}{E^2 - \Delta_0^2}(e^{2iqL} - 1)\sin^2\left(\frac{\chi}{2}\right), \\ R_\pm &= (\varrho \pm 1)\left[i\cos\left(\frac{\chi}{2}\right) \pm \varrho\sin\left(\frac{\chi}{2}\right)\right]\left(e^{\pm 2iqL} - 1\right)\sin\left(\frac{\chi}{2}\right), \end{aligned}$$

and $\varrho = E/qv_{F,x}$, Now we can restore the band index, and in the ath band, we have $v_{F,x} \to v_{F,x,a}$, $\Delta_0 \to \Delta_a$, and $\chi \to \chi_a$, see Eq. (6.4).

6.2 Interaction between solitons

The microscopic derivation of the energy in the superconducting state starts with a two-band generalization of the BCS Hamiltonian:

$$\hat{\mathcal{H}} = \sum_{\boldsymbol{k},a} \xi_a(\boldsymbol{k})\hat{c}^\dagger_{\boldsymbol{k},a,\alpha}\hat{c}_{\boldsymbol{k},a,\alpha} - \frac{1}{\mathcal{V}}\sum_{\boldsymbol{k}\boldsymbol{k}'\boldsymbol{q},ab} V_{ab}\hat{c}^\dagger_{\boldsymbol{k}+\boldsymbol{q},a,\uparrow}\hat{c}^\dagger_{-\boldsymbol{k},a,\downarrow}\hat{c}_{-\boldsymbol{k}',b,\downarrow}\hat{c}_{\boldsymbol{k}'+\boldsymbol{q},b,\uparrow}, \tag{6.13}$$

where $\hat{c}^\dagger$, $\hat{c}$ are fermionic creation and annihilation operators, $a, b = 1, 2$ is the band index, $\alpha =\uparrow, \downarrow$ is the spin projection (the spin indices that appear twice are summed over), and $\mathcal{V}$ is the system volume. The second term in the Hamiltonian describes singlet s-wave pairing interactions: the intraband pairing, characterized by the coupling constants V_{11} and V_{22}, and the interband "tunneling" of the pairs, described by V_{12} and V_{21}.

Using a straightforward generalization of the standard effective bosonic action formalism, see, e.g., Ref. [62], one can derive an expression for the energy of an arbitrary nonuniform superconducting texture in a two-band superconductor [69]. For a planar state with $\eta_a(x) = |\eta_a(x)|e^{i\varphi_a(x)}$, in particular, for the phase solitons, the free energy difference per unit area between the uniform state and the soliton state can be represented as follows: $F_s = F_1 + F_2$. The first term explicitly depends on the quasiparticle spectrum and has the form

$$F_1 = -2\pi T\sum_n\sum_a N_{F,a}\int\frac{d\hat{\boldsymbol{k}}_F}{4\pi}|v_{F,a,x}|\,\ln D_{a,\hat{\boldsymbol{k}}_F}(i\omega_n), \tag{6.14}$$

where $N_{F,a}$ is the Fermi-level density of states ($N_{F,a} = m_a k_{F,a}/2\pi^2$ in a parabolic band),

$\boldsymbol{v}_{F,a}$ is the Fermi velocity in the ath band,

$$D_{a,\hat{\boldsymbol{k}}_F}(z)=\frac{\det[z-\hat{H}(a,\hat{\boldsymbol{k}}_F)]}{\det[z-\hat{H}_0(a,\hat{\boldsymbol{k}}_F)]} \tag{6.15}$$

is the ratio of the functional (Fredholm) determinants of the Andreev Hamiltonians in the nonuniform and uniform states, see Eqs. (6.7) and (6.8), for a given direction of the semiclassical propagation on the Fermi surface in the ath band, and $\omega_n=(2n+1)\pi T$ is the fermionic Matsubara frequency. The second term in the free energy is given by

$$F_2=\int dx\sum_{ab}(\hat{V}^{-1})_{ab}\left(\eta_a^*\eta_b-\eta_{a,0}^*\eta_{b,0}\right), \tag{6.16}$$

where V_{ab} are the coupling constants in the Hamiltonian (6.13).

In the sharp two-soliton model, $F_2=0$, so the interaction between the solitons is entirely determined by the quasiparticle contribution F_1. The ratio of the Fredholm determinants can be calculated using the same transfer matrix method as in Sec. 5.2, with the following result:

$$F_1=2\pi T\sum_n\sum_a N_{F,a}\int\frac{d\hat{\boldsymbol{k}}_F}{4\pi}|v_{F,a,x}|\,\ln S_{22}(i\omega_n;a,\hat{\boldsymbol{k}}_F). \tag{6.17}$$

Thus, the problem of evaluating the free energy of a nonuniform order parameter texture has been reduced to the calculation of the semiclassical scattering matrix of the Bogoliubov quasiparticles, analytically continued to the complex energies.

6.2.1 Interaction energy

The energy of the soliton texture depends on the separation L, and is given by $F_s(L)=F_1$ for two sharp solitons. Since the solitons are decoupled at infinite separation, $F_s(L\to\infty)$ gives the self-energy of two solitons, measured with respect to the uniform superconducting state. The interaction energy per unit area, F_{int}, is simply the difference between the free energy at arbitrary separation L and the self-energy of the two-soliton configuration, i.e. $F_{int}=F_s(L)-F_s(L\to\infty)$.

Using the same analytical continuation procedure as in Sec. 5.2, it follows from Eqs. (6.17) and (6.12) that the interaction energy per unit soliton area at given separation has the following form:

$$F_{int} = -2\pi T \sum_n \sum_a N_{F,a} \int \frac{d\hat{\boldsymbol{k}}_F}{4\pi} |v_{F,a,x}| \ln \left[1 + \frac{\Delta_a^2 \sin^2(\chi_a/2)}{\omega_n^2 + \Delta_a^2 \cos^2(\chi_a/2)} e^{-2\kappa_a L} \right], \tag{6.18}$$

where $\kappa_a = \sqrt{\omega_n^2 + \Delta_a^2}/|v_{F,x,a}|$. The overall sign of the interaction energy is negative as in the DW case, and therefore the soliton interaction mediated by the Bogoliubov quasiparticles is attractive at all temperatures, causing an effective collapse of the soliton texture into a uniform superconducting state. Qualitatively it is evident from Eq. (6.18) that the attraction depends exponentially on the distance between the solitons. We note that the integrand in Eq. (6.18) has the same form as in Eq. (5.76) if one makes the replacement $\delta \to \chi_a/2$, $\Delta_0 \to \Delta_a$, and $\varkappa \to \kappa_a$ in the ath band.

To make analytical progress, we focus on the case of zero temperature, where the sum over the discrete Matsubara frequencies ω_n becomes an integral over a continuous variable ω: $T\sum_n(\cdots) \to \int(\cdots)d\omega/2\pi$. In the limit of large soliton separation, one can expand the logarithm in Eq. (6.18), and then the interaction energy takes the form:

$$\begin{aligned} F_{int} &= -\frac{1}{2}\sum_a N_{F,a} v_{F,a} \Delta_a \int_0^\pi d\theta \sin\theta |\cos\theta| \\ &\quad \times \int_{-\infty}^{+\infty} d\tilde{\omega} \frac{\sin^2(\Phi/2)}{\tilde{\omega}^2 + \cos^2(\Phi/2)} \exp\left(-\frac{2\tilde{L}_a \sqrt{\tilde{\omega}^2+1}}{|\cos\theta|} \right), \end{aligned} \tag{6.19}$$

where $\tilde{L}_a = L\Delta_a/v_{F,a}$ and $\tilde{\omega} = \omega/\Delta_a$. Here we have used the expression (6.4) for the phase winding parameters. In the limit $\tilde{L}_a \gg 1$, one can further neglect the $\tilde{\omega}$-dependence of the pre-exponential factor in the integral over $\tilde{\omega}$, and evaluate this integral by the steepest descent method. In this way, we can represent Eq. (6.19) in the following form:

$$F_{int} = -\tan^2\left(\frac{\Phi}{2}\right) \sum_a N_{F,a} v_{F,a} \Delta_a \sqrt{\frac{\pi}{\tilde{L}_a}} I(\tilde{L}_a), \tag{6.20}$$

where

$$I(\tilde{L}_a) = \int_0^{\pi/2} d\theta \sin\theta \cos^{3/2}\theta e^{-2\tilde{L}_a/\cos\theta} = \int_1^\infty \frac{d\rho}{\rho^{7/2}} e^{-2\tilde{L}_a \rho}, \tag{6.21}$$

and we have invoked the symmetry of the angular integral to reduce the region of integration and also made a change of variable $\rho = 1/\cos\theta$.

The integral in Eq. (6.21) can be expressed in terms of the complementary error function [64], and in the limit $\tilde{L}_a \gg 1$, it has the form $I = e^{-2\tilde{L}_a}/2\tilde{L}_a$. Using this result in Eq. (6.20), we obtain the following form for the interaction energy per unit area:

$$F_{int} = -\tan^2\left(\frac{\Phi}{2}\right)\sum_a N_{F,a}v_{F,a}\Delta_a\sqrt{\pi}(\tilde{L}_a)^{-3/2}e^{-2\tilde{L}_a}.$$

Finally, we restore the dimensional quantities and arrive at our final expression for the soliton interaction energy per unit area:

$$F_{int} = -\tan^2\left(\frac{\Phi}{2}\right)\sqrt{\frac{\pi}{L^3}}\sum_a N_{F,a}v_{F,a}^{5/2}\Delta_a^{-1/2}\exp\left(-\frac{2\Delta_a L}{v_{F,a}}\right). \qquad (6.22)$$

We see that the interaction between the solitons is attractive and, as expected, it is exponentially weak in the limit of large separation between the solitons. Note that the interaction energy is zero when the phase difference is zero, corresponding to the absence of phase solitons. This is different from the chiral p-wave case, since even in the absence of a global phase difference between the domains, there are still different degenerate chiral states separated by DWs.

7 Conclusions

In this work, we studied the interaction between two DWs separating states of opposite chirality in a triplet p-wave superconductor, and found that it is attractive for arbitrary DW separation, at all temperatures. Furthermore, we found that the interaction energy is exponentially weak for large separation between the DWs. We used the transfer matrix method to relate the interaction energy of the DWs to the scattering matrix of the Bogoliubov quasiparticles, and the latter was calculated in the semiclassical approximation.

This method can be applied to any planar superconducting texture. The expression for the free energy will take the same form; however, the scattering matrix of the Bogoliubov quasiparticles will be sensitive to the order parameter of the texture, and can be determined from the Andreev equations. To illustrate the utility of the method developed in this work, we have applied it to the interaction between phase solitons in two-band s-wave SCs, to find a similar result as in the chiral p-wave DW system under the same limits.

Our results are immediately applicable to the neutral case. In a charged superconductor, there will be another contribution to the DW interaction coming from the Meissner screening currents and the magnetic fields associated with them. Investigation of these effects on the interaction energy is left for the future work, and there are, in fact, quite a few additional effects on the interaction energy that one can consider. In the next subsection, we will discuss some more possible avenues of future research into this field.

7.1 Future work

Throughout the work we considered the sharp-DW (sharp-soliton) model, in which the width of the DW (phase soliton) is zero, and the DW separation is large. Consequently, the order parameter changes abruptly at the boundaries between the neighbouring domains. It would be interesting to consider the situation of finite DW thickness and smooth, more realistic profiles for the DW, with arbitrary DW separation. More generally, one can apply the transfer matrix method to characterize the interaction between DWs in a variety of other unconventional superconducting states with degenerate ground states.

One can further extend this research to investigate the quasiparticle properties of DWs in different geometries, for example, the circular DWs that can form in chiral p-wave superconductors [70]. Additionally, one can consider how the DWs are affected by the presence of sample boundaries [71]; and perhaps consider the the dynamical properties of these textures and how they are affected by the quasiparticles. Other possibilities include the effects of external fields, external currents, and disorder, and perhaps even going beyond the semiclassical approximation. The interacting DWs also seem like interesting candidates for computational simulation. In particular, it would be interesting to study the dynamics of the DW interaction, to investigate what happens as the DWs become closer and closer to each other, and perhaps model the nature of the collapse of the DWs to a single domain.

A Ginzburg-Landau description of a domain wall

To gain insight into the structure of the DW, particularly the origin of the nonzero phase difference between the domains, we use the Ginzburg-Landau free energy functional. For the neutral non-uniform superfluid it is a sum of uniform (F_u) and gradient (F_g) energy densities. For the superconducting state with a two-component complex order parameter $\boldsymbol{\eta} = (\eta_1, \eta_2)$ we have

$$F_u = \alpha|\boldsymbol{\eta}|^2 + \beta_1|\boldsymbol{\eta}|^4 + \beta_2|\boldsymbol{\eta}\cdot\boldsymbol{\eta}|^2 + \beta_3(|\eta_1|^4 + |\eta_2|^4), \tag{A.1}$$

where $\beta_3 = 0$ in systems with isotropic Fermi surface, and

$$F_g = K_1(\nabla_i\eta_j)^*(\nabla_i\eta_j) + K_2(\nabla_i\eta_i)^*(\nabla_j\eta_j) + K_3(\nabla_i\eta_j)^*(\nabla_j\eta_i), \tag{A.2}$$

where the Einstein summation convention is assumed. We find that the minimum of the uniform free energy density for an isotropic system corresponds to the chiral states $\boldsymbol{\eta} = \Delta_0(1, \pm i)$ with $\Delta_0 = \sqrt{|\alpha|/4\beta_1}$, for the case β_1, $\beta_2 > 0$.

The structure of the DW, see Sec. 2, can be expressed in the following form:

$$\eta_1(x) = \Delta_0 f_1(x)e^{i\phi(x)}, \qquad \eta_2(x) = \Delta_0 f_2(x)e^{i\phi(x)-i\gamma(x)}, \tag{A.3}$$

where $f_{1,2}$ are the dimensionless amplitudes of the order parameter components, whose asymptotics are fixed by Eq. (2.2).

The nonzero phase difference χ, which arises between domains of opposing chirality, emerges from the condition of vanishing supercurrent across the DW. It follows from Eq. (A.2) that the supercurrent is given by the expression $j_i = 2\,\mathrm{Im}\,(K_1\eta_j^*\nabla_i\eta_j + K_2\eta_i^*\nabla_j\eta_j + K_3\eta_j^*\nabla_j\eta_i)$, in particular, the transverse current has the form

$$j_x = 2\,\mathrm{Im}\,(K_{123}\,\eta_1^*\nabla_x\eta_1 + K_1\eta_2^*\nabla_x\eta_2),$$

with $K_{123} = K_1 + K_2 + K_3$. Using the expressions for the order parameter components in Eq. (A.3), we find:

$$j_x = 2\Delta_0^2(K_{123}f_1^2 + K_1f_2^2)(\nabla_x\phi) - 2K_1\Delta_0^2f_2^2(\nabla_x\gamma), \tag{A.4}$$

with K_{123} as defined above.

In our work we focus on the static case, so conservation of current requires $\nabla_x j_x = 0$, and therefore $j_x = \text{const}$. Since external sources fix the value of the transverse current, we can set $j_x = 0$, and we recover a linear relation between the gradients of ϕ and γ. After substituting the expressions (A.3) into Eqs. (A.1) and (A.2), we use this linear relation to eliminate the common phase $\phi(x)$ from the gradient energy, and we have the following simplified expressions for the free energy densities:

$$\begin{aligned} F_u &= \alpha\Delta_0^2(f_1^2+f_2^2)+\beta_1\Delta_0^4(f_1^2+f_2^2)^2+\beta_2\Delta_0^4(f_1^4+f_2^4+2f_1^2f_2^2\cos 2\gamma), \\ F_g &= K_{123}\Delta_0^2(\nabla_x f_1)^2+K_1\Delta_0^2(\nabla_x f_2)^2+\frac{K_1K_{123}f_1^2f_2^2}{K_{123}f_1^2+K_1f_2^2}\Delta_0^2(\nabla_x\gamma)^2. \end{aligned} \tag{A.5}$$

Variational minimization of these expressions with respect to $f_{1,2}$ and γ gives rise to three coupled differential equations, which are subject to the boundary conditions $f_{1,2}(\pm\infty) = 1$ and $\gamma(\pm\infty) = \pm\pi/2$, in accordance with the order parameter asymptotics. Using the solutions to these equations, along with the relation between the gradients of ϕ and γ that emerges from current conservation, we can compute the phase difference between two arbitrary points x_1 and x_2:

$$\phi(x_2)-\phi(x_1)=\int_{x_1}^{x_2}\frac{K_1f_2^2}{K_{123}f_1^2+K_1f_2^2}\frac{d\gamma}{dx}\,dx. \tag{A.6}$$

We see that whenever there is a gradient of γ, the value of the common phase difference is nonzero, and it is evidently sensitive to the microscopic details of the system [61]. While we have imposed the condition of zero transverse current to obtain Eq. (A.6), we should note that the current along the DW is necessarily nonzero.

Obtaining an exact analytical solution for the DW structure is not possible due to the complexity of the differential equations obtained from variational minimization of the expressions in Eq. (A.5). However, we can make analytical progress by considering the constant-amplitude model [30], in which case $f_{1,2}(x) = 1$ for all x. Then from Eq. (A.5), the total free energy density $F = F_u + F_g$ is given by the expression:

$$F=(\cdots)+\tilde{K}\Delta_0^2(\nabla_x\gamma)^2+2\beta_2\Delta_0^4\cos 2\gamma, \tag{A.7}$$

where $\tilde{K} = K_1K_{123}/(K_{123} + K_1)$. The first term (in parentheses) of this last expression contains only γ-independent terms. It is immediately clear that variational minimization of F with respect to $\gamma(x)$ leads to an expression which has the form of a sine-Gordon equation:

$$\tilde{K}\nabla_x^2\gamma+2\beta_2\Delta_0^2\sin 2\gamma=0. \tag{A.8}$$

The simplest nontrivial solution to this last equation, which satisfies the boundary conditions mentioned above, is a kink-like solution given by $\sin\gamma(x) = \tanh(x/\xi_d)$, which corresponds to a single DW. The parameter $\xi_d = \sqrt{\tilde{K}/4\beta_2\Delta_0^2}$ has the physical meaning of the DW thickness. Using this expression for $\gamma(x)$ in Eq. (A.6) we obtain for the common phase difference:

$$\chi \equiv \phi(+\infty) - \phi(-\infty) = \frac{K_1}{2K_1 + K_2 + K_3}\pi. \tag{A.9}$$

In the weak coupling model, $K_1 = K_2 = K_3$ (Ref. [18]), and χ has the value $\pi/4$.

There are no stable two-kink (or two-DW) solutions to Eq. (A.8); the other non-trivial solution to the variational equation for γ corresponds to a periodic arrangement of DWs. This can be understood by considering a simple pendulum with $2\gamma \to \Theta$ (the angular displacement of the pendulum), and $x \to t$ (a time coordinate). Consider first the one-kink solution to $\gamma(x)$, where initially $t \to -\infty$, and we have $\Theta = -\pi$. After a sufficient amount of time has elapsed (i.e. at $t \to +\infty$) the pendulum has just enough energy to complete one full revolution, approaching an angular displacement of $\Theta = +\pi$. There can be no two-kink solutions because if the pendulum has enough energy to surpass the limit $\Theta = +\pi$ and complete one more revolution, it will have enough energy to do this an infinite number of times. This explains the origin of the second solution to the variational equation for γ, a periodic arrangement of DWs.

The fact that there are no stable two-DW solutions implies there must be some form of interaction between the walls. If we consider a two-DW configuration which separates states of alternating chirality, this interaction will cause either an effective collapse of the DWs to a single domain (if it is attractive), or the effective formation of a single DW which separates two domains of opposite chirality (if it is repulsive). The periodic solution for $\gamma(x)$ can also be understood in terms of this interaction, as a mutual attraction or repulsion between neighbouring DWs could potentially lead to a stable periodic configuration.

B Ginzburg-Landau description of a phase soliton

We assume a clean superconductor with two isotropic bands, labeled by $a = 1, 2$, and isotropic s-wave singlet pairing, described by two order parameters $\eta_1(\boldsymbol{r})$ and $\eta_2(\boldsymbol{r})$, in the absence of a magnetic field. The difference between the free energies in the superconducting and normal states is given by $\mathcal{F}_s - \mathcal{F}_n = \int f_{GL}\, d^3\boldsymbol{r}$, where

$$f_{GL} = \sum_a \left[\alpha_a|\eta_a|^2 + \frac{\beta_a}{2}|\eta_a|^4 + K_a|\boldsymbol{\nabla}\eta_a|^2\right] + \gamma(\eta_1^*\eta_2 + \eta_2^*\eta_1). \tag{B.1}$$

The intraband terms have the usual Ginzburg-Landau form, while the last term describes the interband “Josephson coupling”, i.e. the Cooper pair tunneling between the bands.

Using the amplitude-phase representation of the order parameter, $\eta_a(\boldsymbol{r}) = |\eta_a(\boldsymbol{r})|e^{i\varphi_a(\boldsymbol{r})}$, the free energy density can be written as

$$f_{GL} = \sum_a \left[\alpha_a|\eta_a|^2 + \frac{\beta_a}{2}|\eta_a|^4 + K_a(\boldsymbol{\nabla}|\eta_a|)^2 + K_a|\eta_a|^2(\boldsymbol{\nabla}\varphi_a)^2\right] + 2\gamma|\eta_1||\eta_2|\cos(\varphi_1 - \varphi_2). \tag{B.2}$$

In a uniform state, the minimum energy corresponds to $|\eta_a| = \Delta_a$ and $\varphi_1 - \varphi_2 = \theta_0 (\mathrm{mod}\, 2\pi)$, where

$$\theta_0 = 0, \quad \text{if } \gamma < 0, \qquad \theta_0 = \pi, \quad \text{if } \gamma > 0. \tag{B.3}$$

The first possibility (interband attraction) is realized in $\mathrm{MgB_2}$, in which both gaps have the same phase [66], while the second possibility (interband repulsion) is likely realized in the iron pnictides, in which, according to the most popular model, the gap function reverses its sign between different sheets of the Fermi surface, corresponding to the so-called $s_\pm$ pairing [67].

It follows from Eq. (B.2) that the supercurrent is a sum of independent contributions from individual bands: $\boldsymbol{j} = -(4e/c)\sum_a K_a|\eta_a|^2(\boldsymbol{\nabla}\varphi_a)$ (e is the absolute value of electron charge). For a planar texture perpendicular to the x axis, the current conservation implies that $\boldsymbol{j} = j\hat{\boldsymbol{x}}$, where j is a constant. The value of the current is set by external sources and can be assumed to be zero. In order for the supercurrent contributions from bands 1 and 2 to cancel each other, the two order parameter phases must vary in a counterphase fashion, with $\nabla_x\varphi_2 = -\rho(x)\nabla_x\varphi_1$, where $\rho = K_1|\eta_1|^2/K_2|\eta_2|^2$. This allows one to express the free energy (B.2) in terms of the relative phase $\theta = \varphi_1 - \varphi_2$:

$$f_{GL} = \sum_a \left[\alpha_a|\eta_a|^2 + \frac{\beta_a}{2}|\eta_a|^4 + K_a(\boldsymbol{\nabla}|\eta_a|)^2\right] + \frac{K_1K_2|\eta_1|^2|\eta_2|^2}{K_1|\eta_1|^2 + K_2|\eta_2|^2}(\nabla_x\theta)^2 + 2\gamma|\eta_1||\eta_2|\cos\theta, \tag{B.4}$$

Variational minimization of this expression yields a system of three coupled nonlinear differential equations for $|\eta_1(x)|$, $|\eta_2(x)|$, and $\theta(x)$, with the asymptotics $|\eta_a(\pm\infty)| = \Delta_a$ and $\theta(\pm\infty) = \theta_0 (\mathrm{mod}\, 2\pi)$.

In addition to the uniform solutions, the order parameter equations have various nonuniform ones, connecting different degenerate minima of $\cos\theta$. The simplest topologically nontrivial solutions are those with $\theta(+\infty) - \theta(-\infty) = \pm 2\pi$, where the positive (negative) sign corresponds to a phase soliton (anti-soliton). The presence of a soliton texture in the relative phase implies that each of the two phases φ_1 and φ_2 is also spatially nonuniform and attains different values at $x = +\infty$ and $x = -\infty$ [69]. We define the phase winding parameter as

$$\chi \equiv \varphi_1(+\infty) - \varphi_1(-\infty) = \int_{-\infty}^{+\infty} dx \frac{\nabla_x \theta}{1 + \rho(x)}, \tag{B.5}$$

then $\varphi_2(+\infty) - \varphi_2(-\infty) = \chi \mp 2\pi$ for the soliton (anti-soliton).

An explicit expression for the phase soliton can be obtained in the London approximation, when the order parameter amplitudes are constant everywhere, i.e. $|\eta_a(x)| = \Delta_a$ (Ref. [68]). The minimization of Eq. (B.4) then yields a static sine-Gordon equation for the relative phase, whose soliton solution has the form $\theta(x) = \theta_s(x) + (\pi - \theta_0)$, where $\theta_s(x) = 2 \arcsin[\tanh(x/\xi_s)]$ and

$$\xi_s = \sqrt{\frac{K_1 K_2 \Delta_1 \Delta_2}{(K_1 \Delta_1^2 + K_2 \Delta_2^2)|\gamma|}}$$

has the meaning of the soliton width. The phase textures in the bands are then given by the following expressions:

$$\varphi_1(x) = \frac{1}{1 + \rho_0} \theta_s(x), \qquad \varphi_2(x) = -\frac{\rho_0}{1 + \rho_0} \theta_s(x) - (\pi - \theta_0), \tag{B.6}$$

where $\rho_0 = K_1 \Delta_1^2 / K_2 \Delta_2^2$. We further note that in this approximation the phase winding parameter, see Eq. (B.5), takes the form $\chi = 2\pi/(1 + \rho_0)$.

References

[1] H. Kamerlingh Onnes, Commun. Phys. Lab. Univ. Leiden, **120b**, **122b**, **124c** (1911).

[2] P. Hofmann, *Solid State Physics* (Wiley-VCH Verlag GmbH & Co. KGaA, Weinheim, 2008).

[3] W. Meissner and R. Ochsenfeld, Naturwissenschaften **21**, 787 (1933).

[4] High School Teachers at CERN, *Superconductivity*- Temperature-dependence of the resistance of a superconductor (2012). Digital image. Web. Retrieved from http://teachers.web.cern.ch/teachers/archiv/HST2001/accelerators/superconductivity/superconductivity.htm, 2013.

[5] Piotr Jaworski (selfmade), Meissner-Ochsenfeld effect (2005). Wikipedia. Digital image. Web. Retrieved from http://en.wikipedia.org/wiki/Meissner_effect, 2013.

[6] Helsinki University of Technology (webpage maintained by A. Hakola), *High-Temperature Superconductivity*- Phase diagrams of type-I and type-II superconductors (2008). Digital image. Web. Retrieved from http://tfy.tkk.fi/aes/AES/projects/prlaser/supercond.htm, 2013.

[7] A. A. Abrikosov, Sov. Phys.-JETP **5**, 1174 (1957).

[8] Author unknown, Abrikosov vortices in type-II superconductors. Digital image. Web. Retrieved from http://govuadocs.com.ua/docs/index-18221090.html, 2013.

[9] F. London and H. London, Proc. Roy. Soc. (London) **A149**, 71 (1935).

[10] M. Tinkham, *Introduction to Superconductivity* (McGraw-Hill, USA, 1996).

[11] A. B. Pippard, Proc. Roy. Soc. (London) **A216**, 547 (1953).

[12] C. Kittel, *Introduction to Solid State Physics* (John Wiley & Sons, USA, 2005).

[13] T. E. Faber and A. B. Pippard, Proc. Roy. Soc. (London) **A231**, 336 (1955).

[14] V. L. Ginzburg and L. D. Landau, Zh. Eksp. Teor. Fiz. **20**, 1064 (1950).

[15] B. Deaver and W. Fairbank, Phys. Rev. Lett. **7**, 43 (1961); R. Doll and M. Näbauer, Phys. Rev. Lett. **7**, 51 (1961).

[16] L. P. Gor'kov, Sov. Phys.-JETP **9**, 1364 (1959).

[17] W. Corak, B. Goodman, C. Satterthwaite, and A. Wexler, Phys. Rev. **96**, 1442 (1954); **102**, 656 (1956).

[18] V. P. Mineev and K. V. Samokhin, *Introduction to Unconventional Superconductivity* (Gordon and Breach, London, 1999).

[19] R. Glover and M. Tinkham, Phys. Rev. **104**, 844 (1956); *ibid.* **108**, 243 (1957).

[20] L. Cooper, Phys. Rev. **104**, 1189 (1956).

[21] J. Annett, *Superconductivity, Superfluids and Condensates* (Oxford University Press, New York, 2004).

[22] E. Maxwell, Phys. Rev. **78**, 477 (1950); C. Reynolds, B. Serin, W. Wright, and L. Nesbitt, Phys. Rev. **78**, 487 (1950).

[23] J. Bardeen, L. Cooper, and J. Schrieffer, Phys. Rev. **108**, 1175 (1957).

[24] *Handbook of Superconductivity*, ed. by C. Poole, Jr. (Academic Press, 2000).

[25] N. Bogoliubov, Nuovo Cimento **7**, 794 (1958); Sov. Phys.-JETP **7**, 41 (1958).

[26] J. Valatin, Nuovo Cimento **7**, 843 (1958).

[27] K. V. Samokhin, Physics in Canada **67**, 69 (2011).

[28] D. Vollhardt and P. Wölfle, *The Superfluid Phases of Helium 3* (Taylor and Francis, London, 2002).

[29] M. Sigrist and K. Ueda, Rev. Mod. Phys. **63**, 239 (1991).

[30] G. E. Volovik and L. P. Gor'kov, Sov. Phys.-JETP **61**, 843 (1985).

[31] A. P. Mackenzie and Y. Maeno, Rev. Mod. Phys. **75**, 657 (2003).

[32] D. D. Osheroff, R. C. Richardson, and D. M. Lee, Phys. Rev. Lett. **28**, 885 (1972).

[33] C. Kallin, Physics in Canada **67**, 113 (2011).

[34] C. Kallin and A. J. Berlinsky, J. Phys.: Condensed Matter **21**, 164210 (2009).

[35] W. F. Brinkman, and P. W. Anderson, Phys. Rev. A **8**, 2732 (1973).

[36] A. J. Leggett, Nature **270**, 585 (1977).

[37] D. N. Paulson and J. C. Wheatley, Phys. Rev. Lett. **40**, 557 (1978).

[38] C. Bergemann, S. R. Julian, A. P. Mackenzie, S. NishiZaki, and Y. Maeno, Phys. Rev. Lett. **84**, 2662 (2000).

[39] K. Ishida et al., Nature **396**, 658 (1998).

[40] K. Fossheim and A. Sudbø, *Superconductivity Physics and Applications* (John Wiley & Sons, England, 2004).

[41] G. M. Luke et al., Nature **394**, 558 (1998).

[42] P. G. Björnsson, Y. Maeno, M. E. Huber, and K. A. Moler, Phys. Rev. B **72**, 012504 (2005).

[43] J. R. Kirtley, C. Kallin, C. W. Hicks, E.-A. Kim, Y. Liu, K. A. Moler, Y. Maeno, and K. D. Nelson, Phys. Rev. B **76**, 014526 (2007).

[44] H. Kambara, S. Kashiwaya, H. Yaguchi, Y. Asano, Y. Tanaka, and Y. Maeno, Phys. Rev. Lett. **101**, 267003 (2008).

[45] F. Kidwingira, J. D. Strand, D.J. Van Harlingen, and Y. Maeno, Science **314**, 1267 (2006).

[46] P. M. Walmsley, I. J. White, and A. I. Golov, Phys. Rev. Lett. **93**, 195301 (2004).

[47] H.-J. Kwon and V. M. Yakovenko, Phys. Rev. Lett. **89**, 017002 (2002).

[48] T. L. Ho, J. R. Fulco, J. R. Schrieffer, and F. Wilczek, Phys. Rev. Lett. **52**, 1524 (1984).

[49] L. I. Burlachkov and N. B. Kopnin, JETP Lett. **47**, 48 (1988).

[50] N. Read and D. Green, Phys. Rev. B **61**, 10267 (2000).

[51] M. Nakahara, J. Phys. C **19**, L195 (1986).

[52] M. Sigrist and D. F. Agterberg, Prog. Theor. Phys. **102**, 965 (1999).

[53] W. V. Liu, Phys. Rev. A **72**, 053613 (2005).

[54] N. A. Logoboy and E. B. Sonin, Phys. Rev. B **79**, 094511 (2009).

[55] A. Bouhon and M. Sigrist, New. J. Phys. **12**, 043031 (2010).

[56] J. Nagamatsu, N. Nakagawa, T. Muranaka, Y. Zenitani, and J. Akimitsu, Nature (London) **410**, 63 (2001).

[57] Review issue on MgB_2, edited by G. Crabtree, W. Kwok, P. C. Canfield, and S. L. Bud'ko, Physica C **385**, 1 (2003).

[58] M. R. Norman, Physics **1**, 21 (2008).

[59] D. Yoshioka, *Statistical Physics: An Introduction* (Springer-Verlag, Berlin/Heidelberg, 2007).

[60] A. F. Andreev, Sov. Phys.-JETP **19**, 1228 (1964).

[61] K. V. Samokhin, Phys. Rev. B **85**, 014515 (2012).

[62] V. N. Popov, *Functional Integrals and Collective Excitations* (Cambridge University Press, 1991).

[63] G.V. Dunne, J. Phys. A **41**, 1 (2008).

[64] M. Abramowitz and I. A. Stegun, *Handbook of Mathematical Functions* (Dover, New York, 1965).

[65] M. A. Przedborski and K. V. Samokhin, J. Low Temp. Phys. (in press, 2013).

[66] A. A. Golubov, J. Kortus, O. V. Dolgov, O. Jepsen, Y. Kong, O. K. Andersen, B. J. Gibson, K. Ahn, and R. K. Kremer, J. Phys.: Condens. Matter **14**, 1353 (2002).

[67] I. I. Mazin, D. J. Singh, M. D. Johannes, and M. H. Du, Phys. Rev. Lett. **101**, 057003 (2008).

[68] Y. Tanaka, Phys. Rev. Lett. **88**, 017002 (2001).

[69] K. V. Samokhin, Phys. Rev. B **86**, 064513 (2012).

[70] V. Vakaryuk, Phys. Rev. B. **84**, 214524 (2011).

[71] M. Matsumoto and M. Sigrist, J. Phys. Soc. Jpn. **68**, 994 (1999).